ABSTRACT

Title of Dissertation: MUTANT IL-7R-ALPHA DEVELOPMENTAL EFFECTS AND ONCOGENIC COLLABORATIONS

Sarah Delia Cramer, Doctor of Philosophy, 2017

Dissertation directed by: Professor Siba Samal
Department of Veterinary Medicine

Acute lymphoblastic leukemia is the most common cancer of children. Individual cases of leukemia may have multiple genetic lesions, and identifying those that drive leukemogenesis will be important in the development of targeted therapy. Approximately 10% of pediatric T-cell acute lymphoblastic leukemia (T-ALL) cases have a mutation in *IL-7Rα*. These mutations are thought to be oncogenic, but little is known about the effects of the mutation on T-cell development. In addition, the mutation does not seem to induce leukemia in the absence of other genetic lesions, suggesting that collaborative mutations are required for leukemogenesis. Based on patient data, potential collaborators include *TLX3* expression, *HOXA* gene cluster overexpression, and *NRAS* mutation.

Given the current state of knowledge regarding mutant *IL-7Rα*, this project was developed with two specific aims. The first was to investigate the effects of mutant *IL-7Rα* gain-of-function (*IL-7Rα-GOF*) on T-cell development *in vitro* and *in vivo*. The second was to determine whether candidate collaborative genetic lesions would drive T-ALL formation when

combined with mutated *IL-7Rα*. To address these aims, immature murine thymocytes were cultured on an OP9-DL4 stromal cell system, transduced with retroviral vectors, and injected into sub-lethally irradiated *Rag1*$^{-/-}$ mice. Resultant diseases were analyzed using a variety of techniques including flow cytometry, histology, immunohistochemistry, ligation-mediated PCR, TCRβ clonality assessment, RNA-sequencing, serial passage, and limiting dilution assay.

Studies showed that *IL-7Rα-GOF* mutation caused an increase of $CD8^+$ cells *in vitro*. When thymocytes transduced with *IL-7Rα-GOF* mutation were injected into mice, animals developed a multi-systemic inflammatory disease. This inflammation was not due to imbalance in populations of T_{reg} and Th17 cells, as had been hypothesized.

Assessing collaborations with *TLX3* expression, *HOXA* overexpression, and *NRAS* mutation showed that combination of these genetic lesions with *IL-7Rα-GOF* mutation caused different neoplastic diseases. The combination of *IL-7Rα-GOF* mutation and *TLX3* expression caused low-penetrance, late-onset T-cell lymphoma. Thymocytes overexpressing the *HOXA* gene cluster and transduced with *IL-7Rα-GOF* mutation caused a rapid-onset myeloid leukemia. Combination of *IL-7Rα-GOF* mutation with mutant *NRAS* yielded rapid-onset, full-penetrance T-cell lymphoblastic leukemia, suggesting that this combination of mutations was sufficient to induce T-ALL. These experimental results may help to lay the foundation for the development of targeted therapy for pediatric T-ALL.

MUTANT *IL-7R-ALPHA* DEVELOPMENTAL EFFECTS AND ONCOGENIC COLLABORATIONS

by

Sarah Delia Cramer

Dissertation submitted to the Faculty of the Graduate School of the
University of Maryland, College Park, in partial fulfillment
of the requirements for the degree of
Doctor of Philosophy
2017

Advisory Committee:
Professor Siba Samal, Chair
Dr. Scott Durum
Professor David Mosser
Dr. Mark Simpson
Professor Xiaoping Zhu

Acknowledgements

Thank you, Scott Durum, Wenqing Li, Julie Hixon, Caroline Andrews, Emilee Senkevitch, Ross Porter, and Gisele Rodrigues! I have learned so much and had so much fun! What a fantastic lab!

Thank you Tim Back, Kelli Czarra, Roberta Matthai, and Kathleen Noer for your conscientious care, your dedication to our experiments, and your good humor!

Thank you, Siba Samal, Xiaoping Zhu, and David Mosser for being wonderful guides on this pathway to a PhD!

Thank you Mark Simpson, Bih Wei, Shelley Hoover, Jen Dwyer, Josh Webster, and my fellow CBSTP fellows for unerring support!

Thank you, Jonathon Wiest, Kathleen Moore, Peter Aplan, Howard Young, and especially Katie Stagliano for helping me to succeed!

Most of all, thank you Tunie Cramer, Michael Cramer, Becky Cramer, Otto Kelley, Lena Kelley, and Kip Kelley for unreal patience, love, and encouragement!!!

Table of Contents

List of Tables

List of Figures

Chapter 1: Introduction to targeted therapy for the treatment of mutant *IL-7Rα*-associated pediatric acute lymphoblastic leukemia

Portions of this chapter have been published in Blood (Cramer et al., 2016).

Scope of human disease: Communicable and non-communicable diseases

Anyone who has ever been sick knows that it is hard to enjoy life or to be productive when you don't feel good. Health is vital. Unfortunately, human and animal health can be impacted by many different diseases, including communicable diseases and non-communicable diseases. Many diseases are shared between species, and often human health is dependent on the health of animals used for draft, food, or protection. Such zoonoses and anthropozoonoses include influenza virus, Lyme disease, Toxoplasmosis, and many others. Diseases impacting health vary, depending on location. Globally, communicable diseases that incur huge human costs include malaria, tuberculosis, human acquired immunodeficiency virus (HIV), dengue fever, and many others (Baxter and Abdool Karim, 2016; Castro et al., 2017; Dondorp et al., 2017; McBryde et al., 2017; Mendenhall et al., 2017). Work in many biomedical laboratories worldwide focuses on combating these communicable diseases, either by developing vaccines or working towards prevention or eradication.

Non-communicable diseases also weigh heavily on society. Common non-communicable diseases with significant health impacts include malnutrition, diabetes, heart disease, hypertension, depression, and cancer (Cuschieri et al., 2016; Higashiguchi et al., 2017; Mendenhall et al., 2017). Of the non-communicable diseases, cancer causes

some of the highest rates of morbidity. Globally in 2012, there were approximately 14 million new cases of cancer, and, 1 in 6 deaths is due to cancer according to the World Health Organization (WHO). The GLOBOCAN project seeks to estimate the incidence, prevalence, and mortality of major cancers across the world under the auspices of the WHO (globocan.iarc.fr). Cancer is the second leading cause of death in the United States, and 8.5% of American adults have been diagnosed with the disease, according to the National Center for Health Statistics.

While cancer burden is high across the world, specific cancer types may have differential impacts in certain areas, particularly in the case of those cancers that arise in association with infectious disease. Examples of such cancers include cervical cancer caused by human papillomavirus and liver cancer caused by hepatitis B or C virus (Plummer et al., 2016). In the United States, the top ten sites of cancer include the breast, prostate, lung, colon, uterus, skin, urinary bladder, kidney, and thyroid as well as non-Hodgkin lymphoma according to Center for Disease Control and Prevention (CDC) statistics.

Health as social justice

Health can be considered a social justice and global justice issue, and moral questions surrounding health care are fascinating and vast. The United Nations lists "good health and well-being" as one of 17 sustainable development goals (Rozendo et al., 2017). Within this goal, targets include reducing maternal mortality, ending preventable childhood deaths, ending AIDs, tuberculosis, and malaria epidemics, fighting against hepatitis, reducing deaths attributed to traffic accidents, enabling family planning access,

and protecting against pollution, as well as other goals (www.un.org). Other interesting global social justice issues include access to childhood vaccinations containing thimersol and HIV infection in different populations (Anderson et al., 2017; King et al., 2013; Rubenstein et al., 2016).

In the United States, there are many potential social justice issues intermingled with health. Racial health disparities plague the United States, and these may be rooted in "structural racism" (Bailey et al., 2017). Provision of mental health support and treatment of individuals who are addicted to drugs are also social justice issues (Dickey and Singh, 2017; Cumming et al., 2016). Currently, access to quality, affordable health care has been a pivotal political issue in the United States with rigorous debate regarding the Affordable Care Act, a law passed in 2010 with the goal of enabling greater numbers of Americans to access affordable health care. The law has become a major political flashpoint in recent years, and currently repeal of the law has been threatened. It is said that a society should be judged in part on how it treats its most vulnerable members, and it seems likely that such judgement should include the availability of affordable and quality health care.

With this in mind, I am proud to have worked on this project with the aim of improving the quality of therapy for some of our most vulnerable citizens: children with acute lymphoblastic leukemia. This project seeks to improve the way that we treat children that have acute lymphoblastic leukemia to reduce treatment side effects and to potentially cure children when current therapy fails. While this is an important and noble goal, it should, of course, be pursued at the same time as efforts to address other health issues affecting children globally. According to U.N. statistics, every year six million

children under the age of five die, and four out of five of these children are in sub-Saharan Africa and South Asia. While these figures are staggering and deeply troubling, continued efforts to improve the health care available to children globally can help. For example, the U.N. cites that measles vaccines have prevented the deaths of 15.6 million individuals since 2000. We must continue to expand our efforts to vaccinate, engage in preventative health care, and treat children around the world as well as to improve the way we treat children with leukemia and other childhood cancers. These are moral imperatives.

Cancer: Definition and pathogenesis

Cancer typically develops when cells within the body begin to proliferate uncontrollably. Some cancers stay localized to the organ of origin, but many cancers spread, or metastasize, to distant organs. Local spread and metastasis cause organ dysfunction leading to morbidity and mortality. For cancer cells to develop and metastasize, the cells must undergo many changes from normal cells. Identifying the changes necessary for malignant behavior has led to the development of a well-known, ever-evolving model, the ten "Hallmarks of Cancer." Based on this model, malignancy requires: "1) Sustaining proliferative signaling; 2) Evading growth suppressors; 3) Avoiding immune destruction; 4) Enabling replicative immortality; 5) Tumor-promoting inflammation; 6) Activating invasion and metastasis; 7) Inducing angiogenesis; 8) Genome instability and mutation; 9) Resisting cell death; and 10) Deregulating cellular energetics" (Hanahan and Weinberg, 2011).

Pediatric acute lymphoblastic leukemia

While cancer causes significant disease around the world, it usually impacts adults, often in the later stages of life. According to statistics from the American Cancer Society, pediatric cancers make up less than 1% of the global cancer burden. While pediatric cancer is, thankfully, not common, there are several types of cancer that more commonly arise in children. Pediatric solid tumors include neuroblastoma, renal tumors, retinoblastoma, hepatoblastoma, rhabdomyosarcoma, soft tissue sarcoma, osteosarcoma, germ cell tumors, and pediatric brain tumors. Hematologic malignancies include myeloid leukemia, lymphoma, and acute lymphoblastic leukemia (ALL). Of all pediatric cancers, ALL is the most common (Orkin et al., 2015).

Acute lymphoblastic leukemia arises from hematopoietic progenitor cells in the bone marrow, or thymus. In the United States, there are approximately 3,250 new cases of ALL every year. Unlike adult ALL, which is associated with human T-cell leukemia virus type I (HTLV-1) infection, pediatric ALL is not associated with infectious disease (Watanabe, 2017). Though the disease originates in the bone marrow or thymus, leukemic cells typically begin circulating and proliferating in the blood stream. Cells can also infiltrate organs including the spleen, liver, brain, testes, kidneys, lungs, and eye (Gutierrez and Silverman, 2015). Bone marrow involvement can impact developing blood cell precursors leading to anemia, thrombocytopenia, and leukocytopenias, though the total white blood cell count is typically elevated. Reductions in normal white blood cells can predispose children to infections which may be life-threatening (Gutierrez and Silverman, 2015). Untreated ALL is fatal with a median survival of 2 months (Frei, 1984). Acute lymphoblastic leukemia can be subdivided according to cell of origin,

including B-cell precursor ALL (BCP-ALL), T-cell ALL (T-ALL), and early T-cell precursor ALL (ETP-ALL) (Gutierrez and Silverman, 2015; Zhang et al., 2012).

Based on conventional approaches for genetic analysis, it has been thought that pediatric ALL cases have a relatively low mutational burden compared to most adult cancers. However, newer technologies are enabling identification of thousands of genetic lesions in pediatric ALL cases, including copy number variations as well as genetic mutations (Mullighan and Downing, 2009; Oshima et al., 2016). It is unclear whether these mutations play a role in disease development, though this suggests that we may be only beginning to understand the tangle of genetic lesions that cause ALL.

Based on current knowledge, cases of T-ALL can be subdivided into several groups based on gene expression patterns. These gene expression patterns are typically due to aberrant expression of an oncogenic transcription factor. Commonly identified subgroups include the TAL/LMO, TLX1, TLX3, NKX2-1/NKX2-2, MEF2C, and HOXA subgroups (Brandimarte et al., 2013; Homminga et al., 2011; Zenatti et al., 2011). Individual cases of ALL may have genetic lesions in multiple pathways including, most commonly, those involved in lymphoid development, growth factor signaling, epigenetic regulations, tumor suppression, and cell cycle regulation (Gutierrez and Silverman, 2015; Mullighan, 2013). Common chromosomal translocations in ALL include those that form the *ETV6-RUNX1* fusions, *MLL* fusions, *BCR-ABL* fusions, and translocations involving *MYC* and *TCRβ* (Ferrando and Look, 2000; Harrison, 2001). Recurrent genetic mutations include activating *NOTCH1* mutations, as well as *PTEN* and *CDKN2A* deletions (Carrasco Salas et al., 2016; Gutierrez et al., 2009; Gutierrez and Silverman, 2015). New technology continues to enable identification of new genetic lesions. Further

understanding which of these mutations are driving disease formation as well as those that are associated with disease relapse is a major focus of pediatric ALL research (Mullighan, 2013; Oshima et al., 2016).

The need for targeted therapy in ALL

Understanding the genetic lesions that drive All formation is fundamental to better treating the cancers. Current treatment of pediatric ALL is a major success of modern medicine. Fifty years ago, children diagnosed with ALL survived a median of two months (Gutierrez and Silverman, 2015). Today, the five-year overall survival rate is over 90% in some series (Pui et al., 2009). However, survival rates are much lower in children that experience relapse, varying between 21-39% (Freyer et al., 2011; Nguyen et al., 2008). In addition, while this overall improvement in outcome is staggering, it comes at a cost. To achieve remission, patients typically undergo 2-3 years of chemotherapy (Gutierrez and Silverman, 2015). Acute side effects include infections, allergic reactions, thrombosis, pancreatitis, and neurologic impairment. Chronic side effects include osteonecrosis, obesity, secondary malignancies, and neurocognitive deficits (Gutierrez and Silverman, 2015).

As we characterize the pathophysiology of ALL, we must use our improved understanding to develop targeted therapies (Mullighan and Hunger, 2013). Targeting molecular lesions in specific patients may enable reduced intensity chemotherapy and may help to rescue children that current protocols fail to cure. While there are many potential targets for therapy, here we describe the role of the IL-7Rα signaling pathways in normal T-cell development and leukemia with a focus on its potential as a therapeutic target.

IL-7 signaling supports survival and proliferation

IL-7Rα signaling is vital to normal T-cell and B-cell development

In health, the IL-7Rα chain forms two heterodimeric cytokine receptors (Tal et al., 2014). IL-7Rα forms the receptor for IL-7 by pairing with γc, and forms the receptor for TSLP by pairing with TSLPR (encoded by the *CRLF2* gene) (Tal et al., 2014). The γ_c is used by multiple cytokine receptors, including IL-2, IL-4, IL-9, and IL-15 (Giri et al., 1994; Kimura et al., 1995; Kondo et al., 1993; Russell et al., 1993). Binding of IL-7 or TSLP to their respective receptors is thought to enable transphosphorylation of the JAK proteins with subsequent activation of the JAK/STAT and PI3K/AKT/mTOR pathways (Corcoran et al., 1996; Dadi et al., 1994; Jiang et al., 2004; Li et al., 2004; Tal et al., 2014; van der Plas et al., 1996; Venkitaraman and Cowling, 1994). The MAPK cascade can also be activated with normal TSLP signaling and with IL-7 signaling in immature B and T-cells (Barata et al., 2004b; Johnson et al., 2008; van Bodegom et al., 2012). However, MAPK signaling does not seem to play a role in IL-7 signaling in normal T-cells (Barata et al., 2004b; Crawley et al., 1996). Since the JAK/STAT and PI3K/AKT/mTOR intracellular signaling cascades seem to be the major players in IL-7Rα signaling, we will focus on them.

TSLP signaling is involved in stimulation of growth and differentiation of B1 B-cell progenitors (Montecino-Rodriguez et al., 2006). In addition, TSLP is involved with $CD4^+$ T-cell homeostasis, regulatory T-cell development, and dendritic cell activation (Liu et al., 2007). Lastly, TSLP plays a prominent role in the pathogenesis of allergy and asthma (Ziegler and Artis, 2010). In comparison, IL-7Rα signaling promotes both T-cell proliferation and survival, and IL-7 signaling is vital for normal T-cell development and

survival of most mature T-cells (Mazzucchelli et al., 2012). Proliferative effects of IL-7 signaling appear to be mediated through its effects on regulating the cyclin-dependent kinase inhibitor $p27^{Kip1}$. Withdrawal of IL-7 from a dependent cell line induces cell cycle arrest that is associated with upregulation of $p27^{Kip1}$ (Li et al., 2006). In addition, the phosphatase Cdc25A appears to play a major role in mediating proliferative effects of IL-7 signaling (Khaled et al., 2005).

Pro-survival effects of IL-7 are mediated through regulation of apoptosis. IL-7 induces synthesis of the anti-apoptotic protein Bcl-2, as shown in the IL-7 dependent murine thymocyte cell line D1 (Jiang et al., 2004; Kim et al., 2003). It also induces the anti-apoptotic protein Mcl-1 (Opferman et al., 2003). Removal of IL-7 induces activation of the pro-apoptotic protein Bax by increasing intracellular pH, leading to Bax conformational change and translocation to the mitochondria (Khaled et al., 1999). IL-7 stimulation also induces inactivating phosphorylation of the pro-apoptotic protein Bad, preventing its translocation to the mitochondria (Jiang et al., 2004; Li et al., 2004).

In human patients, loss-of-function mutations in *IL-7Rα* may cause severe combined immunodeficiency with reduced T-cell numbers, but normal B-cell and NK cell numbers. Affected patients developed chronic viral and protozoal infections (Puel et al., 1998; Roifman et al., 2000). Similarly, *JAK3* mutations cause autosomal recessive SCID with lack of T-cells and NK cells, but presence of B-cells (Macchi et al., 1995; Russell et al., 1995). Mutation in γ_c leads to X-linked severe combined immunodeficiency with reductions in T-cell numbers (Noguchi et al., 1993). Using transgenic mice, knock-out of *IL-7*, *IL-7Rα*, γ_c, or *JAK3* leads to deficiencies of T-cells and, variably, NK cells and B-cells (Cao et al., 1995; DiSanto et al., 1995; Nosaka et al., 1995; Park et al., 1995;

Peschon et al., 1994; von Freeden-Jeffry et al., 1995). T-cell development halts at the $CD3^-CD4^-CD8^-$ stage (von Freeden-Jeffry et al., 1995). In addition to being necessary for T-cell development, IL-7 signaling is necessary for maintenance of peripheral $CD8^+$ T-cells and generation of $CD8^+$ memory T-cells (Schluns et al., 2000). This may be due, in part, to IL-7-induced post-translational inhibition of the pro-apoptotic protein Bim (Li et al., 2010).

IL-7 signaling is supportive of T-ALL cells

In addition to promoting normal T-cell development, IL-7 signaling can also support survival and proliferation of neoplastic T-cells and B-cells (Barata et al., 2004a; Karawajew et al., 2000; Makrynikola et al., 1991; Silva et al., 2011; Touw et al., 1990). IL-7 signaling effects in malignant T-cells are similar to its effects in normal T-cells. Malignant T-cells may express the IL-7R, and levels of expression correlate with responsiveness to IL-7 (Karawajew et al., 2000). As with normal cells, stimulation of the receptor activates the PI3K/AKT/mTOR pathway leading to anti-apoptotic and pro-survival effects (Barata et al., 2004b). Pathway activation inhibits spontaneous apoptosis of neoplastic T-cells by upregulating *Bcl-2* (Barata et al., 2001; Karawajew et al., 2000). IL-7 signaling does not seem to impact Bax regulation as significantly as it does in normal T-cells (Karawajew et al., 2000). Proliferation of primary patient T-ALL cells is encouraged by IL-7 induced downregulation of $p27^{Kip1}$ which enables cell cycle progression (Barata et al., 2001; Barata et al., 2004a). Assessing the impact of IL-7 signaling *in vivo*, patient T-ALL xenografts did not grow as well in IL-7 deficient mice. Similar to *in vitro* effects, IL-7 signaling led to upregulation of *Bcl-2* and downregulation

of *p27^{Kip1}* (Silva et al., 2011). Further supporting the importance of IL-7 signaling in T-ALL, IL-7 overexpressing transgenic mice may develop lymphoid cancers (Rich et al., 1993; Uehira et al., 1993). Targeting the IL-7Rα pathways may be useful for many T-ALL patients, regardless of the genetic lesions driving the disease (Barata et al., 2001).

IL-7 signaling and IL-7Rα mutations act to drive formation of ALL

IL-7Rα signaling can be hijacked by T-ALL associated mutations

While it appears that IL-7R signaling pathways support growth and proliferation of most T-ALL cells, a subset of leukemias have mutations that co-opt IL-7R signaling, likely playing a role in driving leukemogenesis. The zinc finger transcription factor *ZEB2* has increased expression in some cases of early thymic precursor ALL (ETP-ALL) as a result of the recurrent translocation t(2;14)(q22;q23) (Goossens et al., 2015). Supporting a role of *ZEB2* mutation as a driver in leukemia development, *Zeb2* gain-of-function mice developed T-cell lymphoblastic leukemia (Goossens et al., 2015). Chromatin immunoprecipitation demonstrated that Zeb2 bound to the *IL-7Rα* promoter, and upregulation of *IL-7Rα* by ZEB2, promoted survival of leukemic cells. Blockade of IL-7R signaling led to increased survival in mice carrying a *Zeb2* overexpressing cell line (Goossens et al., 2015). In both human ETP-ALL and the *Zeb2* gain-of-function mouse model, there was strong correlation between *ZEB2* mRNA levels and *IL-7Rα* mRNA levels. Knockdown of *ZEB2* in the ETP-ALL-like cell line LOUCY using siRNA led to downregulation of IL-7Rα mRNA levels (Goossens et al., 2015). Taken together, these data suggest that the driver effect of *ZEB2* mutation may be due, at least in part, to its induction of IL-7Rα signaling.

Mutations in Dynamin 2 (*DNM2),* a protein that regulates endocytosis, have been identified in approximately 20% of ETP-ALL cases (Zhang et al., 2012). In a mouse model, mutation in *DNM2* enhanced leukemogenesis of the *Lmo2* oncogene by impairing IL-7Rα endocytosis, leading to an increase of the receptor on leukemic cell surfaces and enhanced IL-7Rα signaling (Tremblay et al., 2016). From this, it seems likely that IL-7Rα signaling contributes to the oncogenicity of *DNM2* mutations.

Genetic lesions in the IL-7Rα signaling pathways in T-ALL

In addition to mutations that activate IL-7Rα signaling to drive leukemogenesis, multiple recent studies have identified mutations in *IL-7Rα* in T-ALL, B-ALL, and ETP-ALL (Figure 1) (Roberts et al., 2012; Shochat et al., 2011; Zenatti et al., 2011; Zhang et al., 2012). Our lab has been instrumental in identifying and characterizing these mutations in T-ALL (Zenatti et al., 2011). These mutations occurred in about 10% of T-ALL patients (Shochat et al., 2011; Zenatti et al., 2011). The mutations were typically large insertions in exon 6 of the extracellular juxtamembrane-transmembrane domain of the protein and usually contained a cysteine and a proline with additional amino acids possible (Shochat et al., 2011; Zenatti et al., 2011). Mutations in the extracellular domain of the receptor have also been identified, though these were far less common (Shochat et al., 2011). The insertions altered the structure of the receptor to enable homodimerization by the formation of disulfide bonds between unpaired cysteine residues, and the mutant receptor signaled constitutively in the absence of the typical signaling partners, IL-7, JAK3 and γ_c (Shochat et al., 2011; Zenatti et al., 2011). *IL-7Rα* mutations seem to be more prevalent in HOXA, TLX3, and early T-cell precursor (ETP-ALL) patient

subgroups (Zenatti et al., 2011; Zhang et al., 2012). The mutation does not seem to have prognostic implications (Zenatti et al., 2011). However, *in vitro*, these mutations improved cell viability, enabled growth factor independence, and encouraged proliferation (Zenatti et al., 2011).

While mutations in *IL-7Rα* occur in approximately 10% of pediatric patients, mutations in an upstream regulator of *IL-7Rα*, *NOTCH1*, occurred in over 50% of T-ALL cases (Weng et al., 2004). *NOTCH1* is the most commonly mutated gene in T-ALL and is known to regulate *IL-7Rα* transcription and expression. NOTCH1-promoted IL-7R signaling may play a role in *NOTCH1* mutation oncogenicity (Gonzalez-Garcia et al., 2009).

Mutations downstream of IL-7R also occur in T-ALL. The JAK/STAT pathway can be activated by several genetic lesions. Activating mutations in *JAK1* and *JAK3* are reported, and a *TEL-JAK2* fusion has also been described (Asnafi et al., 2010; Bains et al., 2012; Cante-Barrett et al., 2016b; Flex et al., 2008; Jeong et al., 2008; Kalender Atak et al., 2012; Lacronique et al., 1997; Zhang et al., 2012). Notably, *JAK2* mutations generally seem to be more associated with BCP-ALL than T-ALL. Further downstream, T-ALL patients may also have mutations in *STAT5B* (Bandapalli et al., 2014; Kontro et al., 2014). In addition, a negative regulator of JAK-STAT signaling, *PTPN2*, is deleted in some cases of T-ALL (Kleppe et al., 2010).

Activation of the PI3K/AKT/mTOR pathway also occurs in T-ALL secondary to genetic lesions, and an estimated 47.7% of pediatric cases have deletion or mutation of *PTEN*, *PI3K*, or *AKT* (Gutierrez et al., 2009). Mutations in *PI3K* and *AKT* have been described (Gutierrez et al., 2009; Remke et al., 2009). The PI3K/AKT/mTOR negative

regulator *PTEN* is mutated in an estimated 8.7-22% of T-ALL cases and deleted in 27.3% (Gutierrez et al., 2009; Remke et al., 2009). PTEN activity can also be decreased by post-translational effects such as casein kinase 2 (CK2) overexpression, high levels of reactive oxygen species (ROS), or miRNAs (Mavrakis et al., 2011; Silva et al., 2008).

Genetic lesions in the IL-7Rα signaling pathways in BCP-ALL

In BCP-ALL patients, IL-7Rα pathway perturbations are most commonly caused by genetic aberrations affecting the *CRLF2* gene. In most cases, chromosomal translocations, rearrangements, or gene duplications cause overexpression of *CRLF2*. Translocation leads to *IGH-CRLF2* fusion, while interstitial deletion causes *P2RY8-CRLF2* fusion (Mullighan et al., 2009a; Russell et al., 2009; Yano et al., 2014). *P2RY8-CRLF2* fusions are found at a much higher rate (53%) in patients with Down's syndrome-associated ALL (DS-ALL) (Mullighan et al., 2009a). Other chromosomal abnormalities can also lead to *CRLF2* deregulation (Russell et al., 2009; Yano et al., 2014). It appears that rearranged TSLP receptors signal conventionally through JAK/STAT and PI3K/AKT/mTOR pathways (Tasian et al., 2012). Less commonly, the *CRLF2* gene can have a F232C mutation that enables constitutive activation of TSLPR in the absence of IL-7Rα (Chapiro et al., 2010; Yoda et al., 2010). Mutant TSLPR may not signal through the same kinases as wild type TSLPR, particularly with regards to MAPK which is downregulated in response to mutant TSLPR/mutant JAK2 signaling (van Bodegom et al., 2012).

Notably, *CRLF2* overexpression is not always attributable to structural rearrangement involving the *CRLF2* gene (Bugarin et al., 2015; Chen et al., 2012). In all,

approximately 15% of patients with BCP-ALL have *CRLF2* overexpression (excluding those with *MLL, TCF3, TEL,* and *BCR/ABL* rearrangements) (Roberts et al., 2012; Yano et al., 2014; Yoda et al., 2010). Genetic aberrations of *CRLF2* seem to confer a poorer prognosis in most studies (Chen et al., 2012; Harvey et al., 2010; Palmi et al., 2012; Yoda et al., 2010). Fusion type may be associated with prognosis (Palmi et al., 2012). However, not all studies support a poorer prognosis associated with *CRLF2* lesions (van der Veer et al., 2013; Yano et al., 2014).

Patients with *CRLF2* lesions often have additional genetic abnormalities including deletion/mutation of *IKZF1* (encoding IKAROS) and mutation or translocation of *JAK2*. Of note, *CRLF2* aberrations can also be paired with concurrent mutations in *IL-7Rα* as well as *JAK1, JAK3,* and *SH2B3* (which encodes the JAK2 negative regulator LNK) (Chen et al., 2012; Roberts et al., 2012; Yoda et al., 2010). In Philadelphia chromosome-like B-ALL, as well as other cases of B-ALL, transmembrane in-frame insertions in *IL-7Rα* have also been identified (Roberts et al., 2014; Roberts et al., 2012). Those patients with combined *CRLF2* and *IKZF1* aberrations often have gene expression profiles similar to patients with the *BCR-ABL* fusion protein, leading them to be considered "Philadelphia chromosome-like" (along with other genetic lesions inducing similar gene expression profiles). Patients with a Ph-like gene expression profile have a poor prognosis (Mullighan et al., 2009b; Yoda et al., 2010). Mutation or translocation of *JAK2* also occurs independently of *CRLF2* mutations in BCP-ALL (Bercovich et al., 2008; Mullighan et al., 2009b; Yano et al., 2015). In B-ALL, some mutations in *IL-7Rα* were associated with aberrant overexpression of *CRLF2*, and the two combined to form a functional TSLPR (Shochat et al., 2011).

Genetic lesions in the IL-7Rα signaling pathways in ETP-ALL

A subset of ETP-ALL patients also have mutations in *IL-7Rα*, and these were in-frame insertions or substitutions in the transmembrane domain between residues I241-V253. Similar to the T-ALL mutations, the insertions included cysteine insertion into the transmembrane domain and led to receptor homodimerization with activation of downstream signaling. As in the case of T-ALL mutations, mutations found in ETP-ALL were able to transform the cytokine dependent BaF3 and MOHITO cell lines (Zhang et al., 2012).

IL-7Rα signaling pathway is a potential therapeutic target

Receptor Targeting

The mutant IL-7Rα homodimers found in T-ALL depend on formation of disulfide bonds for stability. These bonds could potentially be targeted therapeutically using the reducing agent N-acetylcysteine (Nac). In T-ALL cell lines, Nac disrupts homodimerization, and it slows progression of disease in a xenograft model. While Nac is inexpensive, it may require frequent dosing (Mansour et al., 2015). In addition to using Nac, development of antibodies against IL-7Rα and/or against mutant homodimers would be a potential therapeutic (Tal et al., 2014). A mutant-specific antibody would reduce potential off-target effects on normal T-cells. For treating CRLF2 genetic aberrations in BCP-ALL, T-cells engineered to express chimeric antigen receptors (CAR-T-cells) against TSLPR have been shown to be effective in treating multiple xenograft models of BCP-ALL (Qin et al., 2015). In addition, antibodies against TSLPR have been developed,

though these have mostly focused on applications in allergy/asthma to date (Borowski et al., 2013).

NOTCH1 Targeting

In T-ALL, mutated NOTCH1 could potentially be targeted using gamma secretase inhibitors, but these have shown significant side effects in a T-ALL clinical trial (Tosello and Ferrando, 2013). Alternative approaches to targeting NOTCH1 include using antibodies and proteasome inhibitors which are currently in varying stages of pharmaceutical development (Agnusdei et al., 2014; Koyama et al., 2014; Tosello and Ferrando, 2013). NOTCH1 targeting has caused significant side effects to date, suggesting that it may not be an ideal target, and it may be better to focus on development of other targets.

JAK/STAT Targeting

Efforts investigating JAK inhibitors to treat cancer have focused mainly on the effects of blocking JAK2 in myeloproliferative neoplasms (MPN), polycythemia vera, and myelofibrosis (Santos and Verstovsek, 2011). In ALL, most studies of JAK inhibition have explored its effects on BCP-ALL. These studies have used primary patient samples or cell lines, including CRLF2-overexpressing cells and Ph-like cells with *IL7Rα* activating mutation and *SH2B3* mutation. Results from these *in vitro* and *in vivo* experiments suggest JAK inhibition may have some efficacy against BCP-ALL (Bercovich et al., 2008; Maude et al., 2012; Roberts et al., 2012; Tasian et al., 2012; Treanor et al., 2014; Yoda et al., 2010). A recent Phase I clinical trial of the JAK1/2

inhibitor ruxolitinib suggests that the drug is well-tolerated in children (Loh et al., 2015). Fewer experimental studies have focused on JAK inhibition in experimental models of T-ALL and ETP-ALL, though results from these studies are promising (Maude et al., 2015).

Experience with MPN suggests that resistance to JAK inhibition may develop, fueled by additional mutations in JAK proteins, increased JAK2 expression, or shifting transphosphorylation partners; resistance has been identified in both MPN and T-ALL (Koppikar et al., 2012; Springuel et al., 2014). There are several potential approaches to overcoming resistance to JAK inhibition. New generations of JAK inhibitors are being developed to bind inactive forms of JAK to overcome resistance (Meyer and Levine, 2014). Alternatively, JAK inhibitors may be combined with histone deacetylase (HDAC) inhibitors or heat shock protein 90 (HSP90) inhibitors (Wang et al., 2009; Weigert et al., 2012). HDAC inhibitors induce hyperacetylation of HSP90, block its chaperone function, and promote JAK2 degradation (Wang et al., 2009). Inhibition of HSP90 increases degradation of both wild type and mutant JAK2 and shows some efficacy against xenograft models of CRLF2-overexpressing BCP-ALL (Weigert et al., 2012). However, both HSP90 inhibitors and HDAC inhibitors have multiple side effects (Hong et al., 2013). Phase I clinical trials of the HDAC inhibitor panobinostat included patients with myeloid and lymphoid malignancies, though none with ALL (DeAngelo et al., 2013).

STAT5B targeting is less advanced than JAK targeting (Dorritie et al., 2014). The drug pimozide targets STAT5B and induces apoptosis in cultures of chronic myelogenous leukemia (CML) cells. Alternative efforts to target STAT5B include the use of decoy oligonucleotides in CML and potentially the use of siRNA (Wang et al., 2011b;

Zhang et al., 2013). In an experimental model of BCP-ALL, *STAT5B* gene expression has also been targeted by epigenetics-based therapy using BET bromodomain inhibitors. Bromodomain inhibition induces apoptosis *in vitro*, improves survival in a xenograft model, and promotes downregulation of *IL-7Rα* (Ott et al., 2012). In addition, use of a pan-BCL-2 inhibitor, navitoclax, demonstrated efficacy against STAT5B-mutated cells *in vitr*o (Kontro et al., 2014).

PI3K/AKT/mTOR Targeting

The PI3K/AKT/mTOR pathway can be targeted by inhibitors of PI3K, AKT, and mTOR, dual inhibitors targeting both PI3K and mTOR, or inhibition of other components of the pathway including eukaryotic translation initiation factor 4E and phosphoinositide-dependent protein kinase I (Rodon et al., 2013). Studies of PI3K and AKT inhibition have focused on effects in experimental models of T-ALL. PI3K inhibitor NVP-BKM120 induces apoptosis in cell lines and primary T-ALL cells and synergizes with vincristine and doxorubicinin *in vitro* and *in vivo* (Lonetti et al., 2014). Conversely, while the PI3K inhibitor AS605240 synergizes with glucocorticoids, it antagonizes methotrexate and daunorubicin activity in cell lines, primary T-ALL cells, and murine xenograft models (Silveira et al., 2015). Dual PI3K and mTOR inhibitors are also effective against T-ALL cell lines and patient samples *in vitro* and are more effective than individual inhibition of PI3K, AKT, or mTOR (Chiarini et al., 2010). Dual inhibitor BEZ235 synergizes with dexamethasone *in vitro* and *in vivo* suggesting that targeting the PI3K/AKT/mTOR pathway could modulate glucocorticoid resistance in T-ALL (Hall et al., 2015). However, dual inhibitor PI-103 has been shown to cause upregulation of

NOTCH1 and *c-myc*; combining PI-103 with c-myc or short-term NOTCH1 inhibition is synergistic and leads to increased death of T-ALL cell lines (Shepherd et al., 2013). In addition, inhibition of the PI3K pathway can led to activation of the FAK/NFKB/Bcl-2 pathway, suggesting that inhibition of PI3K may be paired with FAK inhibition for greater efficacy (You et al., 2015).

AKT inhibition by GSK690693 is effective against both T-ALL and BCP-ALL cell lines *in vitro* (Levy et al., 2009). AKT inhibitor MK-2206 decreases T-ALL cell viability and induces apoptosis in leukemia-initiating cell populations (Simioni et al., 2012). Combining three AKT inhibitors with different mechanisms of action led to synergistic effects against T-ALL cell lines (Cani et al., 2015). AKT inhibition can also lead to reversal of T-ALL glucocorticoid resistance as demonstrated in cell lines and primografts *in vitro* as well as in several mouse models (Piovan et al., 2013).

Inhibition of mTOR has included studies in both T-ALL and BCP-ALL. Rapamycin, the first mTOR inhibitor, is an allosteric inhibitor which does not fully inhibit the mTORC1 and mTORC2 enzymes (Janes et al., 2013). Rapamycin shows efficacy against xenografted BCP-ALL with mutated *IL-7Rα* and altered *CRLF2* expression as well as Ph-like BCP-ALL and a transgenic model of BCP-ALL (Brown et al., 2003; Maude et al., 2012). However, treatment with rapamycin alone is not considered highly effective against T-ALL (Chiarini et al., 2010).

To improve on the efficacy of rapamycin, several other drug types have been developed to target mTOR. Drugs targeting the active site of mTOR are effective against both T-ALL and BCP-ALL cell lines (Evangelisti et al., 2011; Simioni et al., 2014). More specific targeting of mTORC1 also induces apoptosis and autophagy in BCP-ALL

cell lines and synergizes with AKT inhibitor MK-2206 (Neri et al., 2014; Simioni et al., 2014). Alternatively, mTORC1 activity can be targeted with metformin, an activator of LKB1/AMPK which down-modulates mTORC1 activity. Metformin was effective *in vitro* against T-ALL cell lines, primary cells, and leukemia-initiating cells. There is currently a clinical trial recruiting pediatric patients with relapsed ALL for treatment with a combination of metformin and chemotherapy (NCT01324180) (Grimaldi et al., 2012).

In both T-ALL and BCP-ALL cell lines, inhibition of mTOR synergizes with methotrexate and vincristine, potentially targeting leukemia-initiating cells (Evangelisti et al., 2011; Teachey et al., 2008). In addition, inhibition of mTOR may synergize with NOTCH1 or Bcl-2 inhibition as demonstrated in murine xenografts and T-ALL cell lines and primary samples, respectively (Cullion et al., 2009; Iacovelli et al., 2015).
In those T-ALL cases where PTEN inhibition by CK2 or ROS leads to activation of the PI3K/AKT/mTOR pathway, antagonists of CK2 or ROS scavengers may help to increase PTEN activity as suggested by results in T-ALL cell lines and primary cells (Buontempo et al., 2014; Silva et al., 2008).

Conclusion: IL-7Rα signaling pathways are ideal therapeutic targets

In the search for targeted ALL therapies, genetic aberrations in the IL-7Rα signaling pathways offer many potential opportunities for therapeutic intervention (Figure 1). We believe that targeting the IL-7Rα signaling pathways could currently be utilized as adjunctive, non-specific therapies for many leukemia patients, based on their potential to reduce cellular proliferation and survival. However, the real promise of these therapies lies in the (hopefully) near future, when each new case of pediatric leukemia

will be sequenced. This will enable clinicians to target an individual leukemia's specific genetic lesions with specific IL-7Rα-targeted therapies. The appropriate therapy or therapies will vary depending on the location of the genetic lesion within the signaling pathway. For example, a BCP-ALL patient with over-expressed *CRLF2* might be treated by targeting multiple levels of the signaling pathway, including use of anti-TSLPR CAR T-cells, monoclonal antibodies, JAK inhibitors, and/or dual PI3K/mTOR inhibitors. A patient with AKT mutation might benefit from AKT or mTOR inhibition. As we move forward, we will need to determine the best use of these therapies to minimize side effects and maximize patient benefit. Perhaps someday, targeted therapy will enable patients with IL-7Rα signaling pathway mutations to be treated with less intensive chemotherapy, and relapsed patients or those patients that current therapies fail will be successfully treated.

Figure 1. IL-7 pathway mutations provide potential targets for acute lymphoblastic leukemia. In both T-ALL and BCP-ALL, mutations can occur at many points within the IL-7Ra signaling pathways (A). Aberrant signaling through these pathways offers multiple potential therapeutic targets (B) (Cramer et al., 2016).

Figure 1. IL-7 Pathway Mutations Provide Potential Targets for Acute Lymphoblastic Leukemia

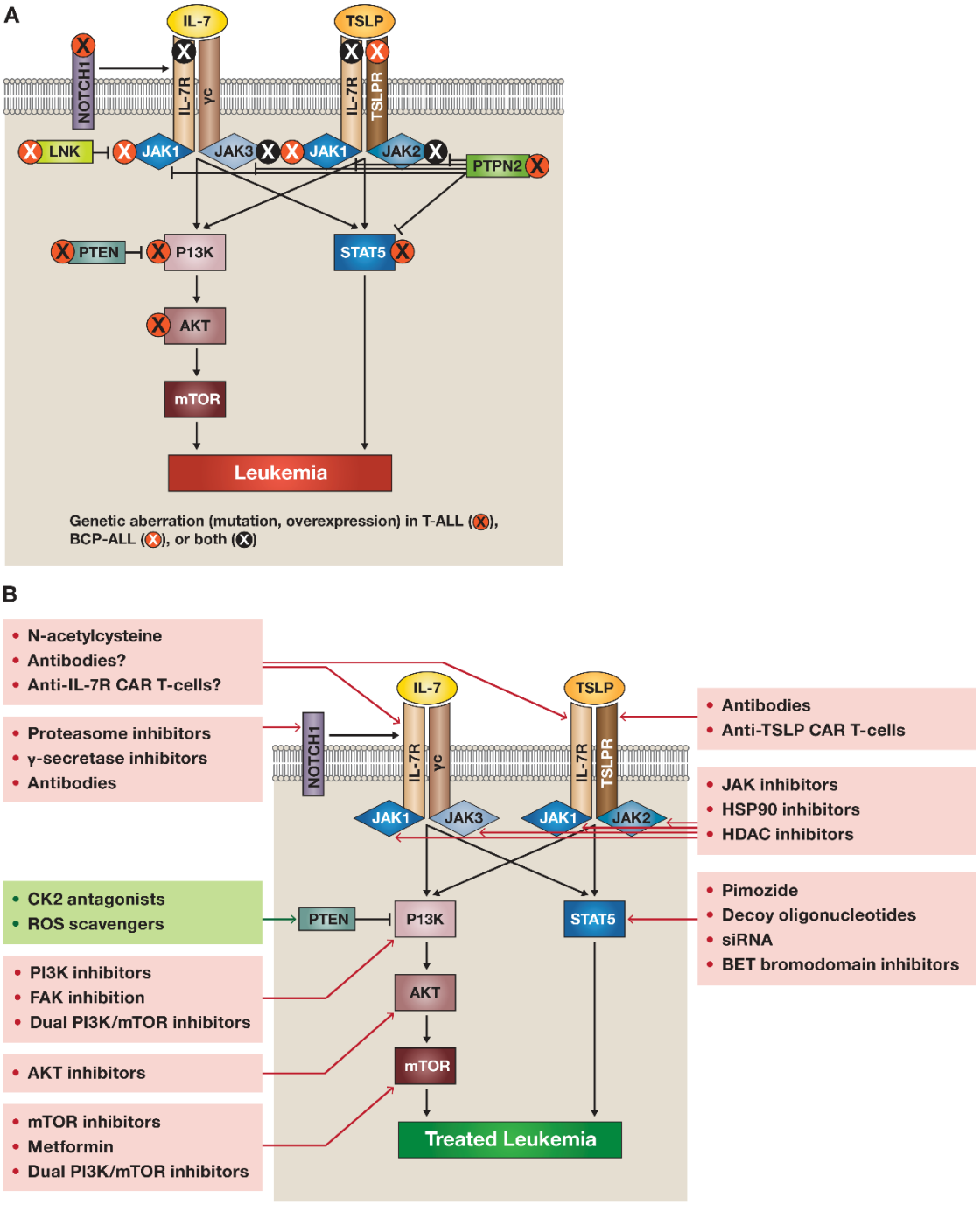

Chapter 2: Mutations that collaborate with IL-7Rα signaling to drive ALL

Mutant IL-7Rα is insufficient to drive T-ALL alone

It seems clear that IL-7R signaling plays an important role in normal lymphocyte development and in supporting survival and proliferation of T-ALL cells, including those cells without a genetic lesion in the signaling pathway. This makes the signaling pathways ideal therapeutic targets. However, sole mutation in IL-7Rα does not seem sufficient to drive leukemia formation on its own. The mutation did confer cytokine independent growth to immortalized BaF3 and MOHITO cell lines (Shochat et al., 2011; Zhang et al., 2012). When introduced to the immortalized thymocyte cell line D1, the mutation caused leukemia/lymphoma (Zenatti et al., 2011). However, similar to work shown in our laboratory, a study using bone marrow progenitors as well as common lymphoid precursors demonstrated that T-ALL did not result when these cells were transduced with mutant human *IL-7Rα* (Yokoyama et al., 2013). This is consistent with a model of clonal evolution wherein mutations in the IL-7Rα signaling pathways are considered a late event in the development of leukemia. The *IL-7Rα* mutations play a role in clonal proliferation and survival, but they must be combined with other genetic lesions that enable aberrant self-renewal for fulminant leukemia to develop (Tremblay and Curtis, 2014). Based on these data, we hypothesized that mutant *IL-7Rα* requires additional genetic mutations/ aberrations to induce T-ALL.

Genes known to collaborate with mutant IL-7Rα to induce T-ALL

In the search for mutations that collaborate with mutant *IL-7Rα*, there were multiple mutations that were known or likely collaborators (Table 1). Evidence from patient data and/or experimental studies suggested that collaboration may occur between mutant *IL-7Rα* and *NRAS*, *TLX3*, *HOXA*, *Notch1*, *Arf*, *PHF6*, *WT1*, and the *PRC2* complex.

GTP binding protein: *NRAS*

NRAS is a GTPase that mediates effects of growth factor receptors by activating multiple intracellular signaling pathways including the MAPK and PI3K pathways. RAS proteins are one of the most commonly mutated genes across human cancers (Ward et al., 2012). *NRAS* mutations have been reported to occur in 2/57 (4%) of pediatric patients and 4/18 (22%) of T-ALL cell lines (Kawamura et al., 1999). In another study, *NRAS* and *KRAS* mutations together were shown to be present in 15% of ALL patients, including B-ALL and T-ALL patients (Perentesis et al., 2004). With newer technologies, higher rates of *NRAS* mutation are reported, around 25% (Kalender Atak et al., 2012; Oshima et al., 2016). In patients with Downs syndrome, 15/42 (35.7%) had a mutation in *NRAS* or *KRAS* (Nikolaev et al., 2014). *RAS* pathway mutations had a high prevalence in cases of high-risk, relapsed ALL, and *RAS* mutations showed heterogeneous clonal evolution (Oshima et al., 2016). From a collaborative standpoint, mutations in *NRAS* may enable proliferation, survival, and aberrant self-renewal (Li et al., 2013).

Table 1: Patient and experimental data supporting collaboration between mutant *IL-7Rα* and other genes

Potential Collaborative Genes	**Expected Vital Collaborative Role**	**Evidence for collaboration in patients**	**Evidence for collaboration in experiments**
GTP binding protein: *NRAS*	Self-renewal	Concurrent mutations in *NRAS* and *IL-7Rα* signaling pathways occurred in a subset of T-ALL patients	None known
Homeobox transcription factors: *HOXA* and *TLX3 (HOX11L2)*	Self-renewal	Patients with mutant *IL-7Rα* were more likely to be in HOXA or TLX3 genetic subgroups	None known
Developmental regulator: *NOTCH1*	Self-renewal	None known	Combination of activated *Notch1* with mutant *hIL-7Rα* in bone marrow progenitor cells led to T-ALL in mice
Cell cycle regulator: *ARF*$^{-/-}$ (*CDKN2A* locus)	Self-renewal	Concurrent *CDKN2A* deletion and IL-7Rα signaling pathway mutations occurred in a subset of ETP-ALL patients	Transduction of *Arf-/-* primary immature murine thymocytes with mutant *hIL-7Rα* caused ETP-ALL in mice
Epigenetic regulators: *PHF6/ WT1/PRC2*	Enhanced *STAT5* binding	Patients with mutant *IL-7Rα* were more likely to have mutations in *PHF6*, *WT1*, or *PRC2*	None known

Evidence of collaboration with IL-7Rα signaling pathway

Analysis of T-ALL patient samples showed that 10/24 patients with mutations in N-Ras/K-Ras/NF1 had concurrent mutations in the IL-7Rα signaling pathway. Using a

combination of MEK inhibition and PI3K/AKT/mTOR inhibition had synergistic effects *in vitro* (Cante-Barrett et al., 2016a). Concurrent mutations in *NRAS* have also been identified in 2/15 Philadelphia chromosome-like B-ALL patients with mutations in *IL-7Rα* (Roberts et al., 2014). Prior experiments to assess the effects of combining mutant *NRAS* and mutant *IL-7Rα* have not been performed to our knowledge.

Homeobox transcription factors: *HOXA* and *TLX3*

The *HOXA* gene cluster is a group of class I homeobox genes containing four gene clusters located on four separate chromosomes, while *TLX3* is a class II, NKL homeobox gene that is isolated and non-clustered (Argiropoulos and Humphries, 2007; Homminga et al., 2012). In general, homeobox genes encode transcription factors that are involved in many facets of development (Argiropoulos and Humphries, 2007). Members of the *HOXA* gene cluster are normally expressed during early T-cell development (Argiropoulos and Humphries, 2007; Lawrence et al., 1997; Taghon et al., 2003). *TLX3* is not expressed in normal hematopoietic cells (Ballerini et al., 2002; Dadi et al., 2012; Nagel et al., 2017). Dysregulation of these homeobox genes leads to distinct gene expression patterns that can be used to subgroup T-ALL patients (Meijerink, 2010). Interestingly, dysregulation of the *HOXA* gene cluster and *TLX3* caused relatively similar gene expression profiles (Soulier et al., 2005; Zenatti et al., 2011).

The *HOXA* gene cluster is activated by translocation in less than 10% of T-ALL patients (Meijerink, 2010). Translocations may lead to overexpression by juxtaposing the gene cluster with *TCRβ* or *BCL11B* (Cauwelier et al., 2007; Speleman et al., 2005; Su et al., 2006b). In addition, *HOXA* gene cluster dysregulation may occur in T-ALL cases

with *MLL*, *CALM-AF10*, or *SET-NUP214* fusions (Bergeron et al., 2006; Soulier et al., 2005; Van Vlierberghe et al., 2008b). *TLX3* dysregulation occurs in approximately 15-25% of pediatric T-ALL patients, typically in association with the cryptic translocation t(5;14)(q35;q32.2) that juxtaposes *TLX3* with *BCL11B* (Ballerini et al., 2002; Bernard et al., 2001; Cave et al., 2004; MacLeod et al., 2003; Noronha et al., 2016; Su et al., 2006b). Other chromosomal translocations leading to overexpression of *TLX3* have been identified, including t(5;7)(q35;q21), t(2;5)(p21;q35), and t(5;10)(q35;q21) (Su et al., 2004). Expression of *TLX3* has been shown in up to 60% of pediatric T-ALL patients (Mauvieux et al., 2002). As to the potential collaborative role of the *HOXA* gene cluster and *TLX3*, dysregulation of these genes has been postulated to enable self-renewal, contributing to the formation of pre-leukemic stem cells (Argiropoulos and Humphries, 2007; Tremblay and Curtis, 2014).

Evidence of collaboration with IL-7Rα signaling pathway

In patients with mutant *IL-7Rα*, the HOXA and TLX3 subgroups were over-represented, with 5/17 patients in the HOXA oncogenetic group and 4/17 in the TLX3 subgroup. The increased representation was more striking for the HOXA subgroup than the TLX3 subgroup (Zenatti et al., 2011). A second study analyzing the genetic sequences of 155 T-ALL patients confirmed that *IL-7Rα* mutation was more common in both the HOXA and TLX3 subgroups (Vicente et al., 2015). A third study showed that TLX patients had a high prevalence of *IL-7Rα* mutation (Cante-Barrett et al., 2016a).

From an experimental standpoint, murine bone marrow cells transduced with retroviral vectors expressing *TLX3* did not survive *in vivo* (Su et al., 2006a). However,

prior experiments assessing collaboration between *TLX3* expression or *HOXA* gene cluster overexpression with mutant *IL-7Rα* have not been performed to our knowledge.

Developmental gene: *NOTCH1*

NOTCH1 is a member of the NOTCH family of cell surface receptors that have multiple developmental roles. In the thymus, *Notch1* signaling drives commitment to the T-cell lineage (Bray, 2016; Gonzalez-Garcia et al., 2012). Activating mutations in *NOTCH1* have been identified in more than 50% of T-ALL patients, making it one of the most commonly mutated genes in T-ALL (Breit et al., 2006; Weng et al., 2004). *NOTCH1* activation leads to transcriptional activation of multiple target genes, and *IL-7Rα* is notably one of its transcriptional targets (Garcia-Peydro et al., 2006). Active *NOTCH1* induces the IL-7Rα signaling pathway by binding to the *IL7Rα* promoter, regulating its transcription (Gonzalez-Garcia et al., 2009). *NOTCH1* mutation is used experimentally to drive T-ALL formation (Chiang et al., 2008; Oshima et al., 2016; Yokoyama et al., 2013). Collaboratively, *NOTCH1* mutation would be expected to encourage cell growth, proliferation, and differentiation, and it may encourage self-renewal in early T-cells (Gerby et al., 2014; Palomero et al., 2006; Yuan et al., 2011).

Evidence of collaboration with IL-7Rα signaling pathway

To our knowledge, studies have not been performed that focus on assessing the coincidence of mutations in *NOTCH1* and *IL-7Rα* signaling pathway members in patients with ALL. However, experiments in mice suggest that the two mutations act collaboratively. Injection of lineage negative bone marrow cells transduced with a

combination of *IL-7Rα* mutant and active *NOTCH1* into congenic recipient mice led to development of $CD4^+CD8^+$ leukemia/lymphoma. The combination of mutations caused more rapid disease onset than active *NOTCH1* alone, suggesting that mutant *IL-7Rα* enhanced the leukemogenic activity of *NOTCH1* (Yokoyama et al., 2013).

Cell cycle regulator: *Arf*

The *CDKN2A* locus is vital in cell cycle regulation as it produces both *p16INK4* and *p14ARF* (*p19ARF* in mice). The cell cycle regulator *p14ARF* acts as a tumor suppressor by activating p53 and binding MDM2 to stabilize p53, enabling cell cycle arrest (Carrasco Salas et al., 2016). Deletion of the chromosomal region 9p21 occurs in a high percentage of T-ALL cases with resultant loss of the *CDKN2A/B* locus (Bertin et al., 2003; Hebert et al., 1994; Vicente et al., 2015). Further supporting the role of *Arf* as a tumor suppressor, $Arf^{-/-}$ mice developed a variety of spontaneous cancers including thymoma, lymphoma, fibrosarcoma, and carcinoma within six months of age (Kamijo et al., 1997). Thymocytes from $Arf^{-/-}$ mice had increased self-renewal capacity suggesting that loss of *Arf* may enable self-renewal as a collaborative mutation (Treanor et al., 2011).

Evidence of collaboration with IL-7Rα signaling pathway

A screen of genetic aberrations in pediatric human cases of ETP-ALL showed that, of 54 total patients, 5 had activating *IL-7Rα* mutations, and two of these five had concurrent *CDKN2A/B* deletion (Zhang et al., 2012).

Experimentally, loss of *Arf* combined with expression of mutant *hIL-7Rα* has been shown to induce early thymic precursor ALL (ETP-ALL). Immature double negative (CD4-CD8-) $Arf^{-/-}$ thymocytes were transduced with retroviral vectors containing mutant *hIL-7Rα*. After 20 days of culture on OP9-DL1 stromal cells, cells were blocked at the double negative 2 stage and showed high expression of the leukemia-associated transcription factor LMO2 (Treanor et al., 2014). When these thymocytes were injected into mice, recipient animals developed leukemia with variable phenotypes. A subset of mice developed leukemia with a myeloid morphology that expressed the myeloid markers Gr1 and myeloperoxidase. Another subset had leukemia with erythroid morphology that expressed the erythroid marker CD71. In both cases, the leukemic cells also expressed intracellular CD3, suggestive of an ETP-ALL-like phenotype (Treanor et al., 2014). Assessment of T-cell receptor rearrangements showed that the resultant leukemias were monoclonal, suggesting that additional collaborating mutation(s) may have encouraged outgrowth of a single clone. Similar to cultured cells, leukemic cells expressed high levels of LMO2, as well as decreased levels of BCL11B; alterations in the expression of these transcription factors may have caused developmental block enabling development of the ETP-ALL phenotype from immature thymocytes. Assessment of human pediatric cases of ETP-ALL showed similar gene expression differences (Treanor et al., 2014).

Epigenetic regulators: *PHF6*/ *WT1*/ *PRC2* complex

PHF6

PHF6 is a chromatin adaptor protein that is thought to act as an epigenetic regulator with a role in regulating gene transcription (reviewed by Todd et al.) (Liu et al., 2015; Todd MA1, 2015; Todd and Picketts, 2012). Multiple studies have identified mutations in *PHF6* in pediatric T-ALL and ETP-ALL (Chao et al., 2010; Huether et al., 2014; Kalender Atak et al., 2012; Van Vlierberghe et al., 2010; Wang et al., 2011a; Yoo et al., 2012; Zhang et al., 2012). In pediatric T-ALL, the frequency of *PHF6* mutations was between 5.4 and 16%; mutations were more frequent in adult T-ALL (Kalender Atak et al., 2012; Van Vlierberghe et al., 2010; Wang et al., 2011a). *PHF6* is an X-linked gene, and mutations have been reported to be more common in males, though results of one study did not show a sex difference in mutation incidence (Van Vlierberghe et al., 2010; Wang et al., 2011a). The mutations seemed to be more common in patients with the TLX3 and TLX1 subtypes of T-ALL (Van Vlierberghe et al., 2010). *PHF6* mutation is not thought to impact prognosis (Wang et al., 2011a). Consistent with a role as tumor suppressor gene, mutations were most commonly loss-of function and included nonsense, frameshift, truncating, and missense mutations; *PHF6* deletions were less common (Huether et al., 2014; Van Vlierberghe et al., 2010; Wang et al., 2011a). Expression of *PHF6* may also be impacted by miRNA and DNA methylation (Kraszewska et al., 2012; Mavrakis et al., 2011; Mets et al., 2014).

WT1

Wilms' tumor-1 protein (WT1) is a transcription factor thought to have both oncogenic and tumor suppressor effects, dependent on context. Recently, WT1 has been

shown to have a role in epigenetic modification in AML, and it may also impact cell cycle progression (Rampal and Figueroa, 2016; Shandilya and Roberts, 2015). *WT1* mutations and deletions have been identified in T-ALL and ETP-ALL (Tosello et al., 2009; Van Vlierberghe et al., 2008a; Zhang et al., 2012). Genetic aberrations effecting *WT1* occurred in 13.2% of pediatric patients with T-ALL and were significantly more common in TLX1, TLX3, and HOXA subgroups of patients, with 85% of *WT1* cases having aberrant expression of a *HOX* gene (Tosello et al., 2009). *WT1* mutation did not appear to impact prognosis (Tosello et al., 2009). Loss-of-function mutations identified include frameshift, missense, and nonsense mutations as well as deletions, and *WT1* genetic lesions were often heterozygous (Tosello et al., 2009).

PRC2 Complex (*EZH2*, *SUZ12*, and *EED*)

Polycomb repressive complexes (PRC) are chromatin repressor complexes that regulate gene expression across many developmental pathways. There are two separate complexes, PRC1 and PRC2, and PRC2 contains the genes *EZH2*, *SUZ12*, and *EED* as well as others (Schwartz and Pirrotta, 2008). Most studies suggest that *PRC2* genes act as tumor suppressors in T-ALL. Mutations in *PRC2* genes were identified in 25% of T-ALL cases and a high proportion of ETP-ALL cases (Ntziachristos et al., 2012; Zhang et al., 2012). Another study showed much lower rates of *EZH2* mutations (1.3%) in pediatric ALL cases, though single nucleotide polymorphisms were identified in a higher percentage of patients (17.1%), and *EZH2* promoter hypermethylation was present in 60% of samples (Schafer et al., 2016). In T-ALL, loss-of-function mutations in *EZH2* and *SUZ12* included truncating, missense, substitution, and frameshift mutations as well as

recurrent deletions (Huether et al., 2014; Ntziachristos et al., 2012). Transgenic mice with deletion of *Ezh2* (enhancer of zeste homolog 2) in hematopoietic cells develop T-ALL (Simon et al., 2012). Mice with hypomorphic *eed* expression are more susceptible to N-methyl-N-nitrosourea-induced thymic lymphoma (Richie et al., 2002).

The actual role of epigenetic regulators such as *PHF6*, *WT1*, and the *PRC2* complex in T-ALL oncogenic collaboration is not known. However, it has been hypothesized that these mutations may result in altered chromatin conformation, increasing availability of *STAT5* for mutant IL-7Rα pathway signaling (Vicente et al., 2015).

Evidence of collaboration with IL-7Rα signaling pathway

Mutational profile analysis of T-ALL and ETP-ALL cases showed significant association between IL-7Rα pathway mutations and mutations in the epigenetic regulators *PHF6*, *WT1*, and the *PRC2* complex (Vicente et al., 2015; Wang et al., 2011a; Zhang et al., 2012). One study used PCR and sequencing to analyze 96 patients (pediatric and adult) with T-ALL, assessing frequency of *PHF6* mutation/deletion as well as frequency of several other T-ALL-associated mutations. There was a significant association between *PHF6* mutation and mutations in the IL-7Rα signaling pathway member, *JAK1* (Wang et al., 2011a). In a later study, samples from 111 children and 44 adults with T-ALL were analyzed using Haloplex enrichment to sequence the coding regions of 115 known or candidate T-ALL driver genes. From this analysis, patients with a mutation in the IL-7Rα signaling pathway were significantly more likely to also have

mutations in *PHF6* (34.9% vs 13.4% with wild type IL-7Rα pathway), *WT1* (30.2% vs 8.9% WT IL-7Rα), and *PRC2* complex (27.9% vs 13.4% with WT IL-7Rα). Whole genome or whole exome sequencing of patients with ETP-ALL and T-ALL showed several examples of concurrent mutations within the IL-7Rα signaling pathway and *PHF6*, *WT1*, and the *PRC2* complex (Oshima et al., 2016; Zhang et al., 2012).

To our knowledge, successful *in vitro* and *in vivo* experiments have not been performed to assess the interaction of these genes with mutant *IL-7Rα* (Holmfeldt and Mullighan, 2010).

Reviewing the roles of known collaborative partners

Evidence from *in vitro* and *in vivo* studies suggests that IL-7Rα signaling supports both normal and malignant lymphocytes by inducing cell proliferation and survival. However, collaborating genetic lesions seem to be required to drive leukemia formation. Collaborative partners would be anticipated to include genetic lesions that enable aberrant self-renewal and/or those that alter epigenetic regulation (Tremblay and Curtis, 2014). Consistent with this model, experimental data support collaboration between mutant *hIL-7Rα* and mutations supporting self-renewal including *NOTCH1*, and *Arf*. Patient data support collaborations with self-renewal-inducing *TLX3*, *HOXA*, and *NRAS* as well as the epigenetic regulators *PHF6*, *WT1*, and the *PRC2* complex.

Exploring mutant IL-7Rα oncogenic collaboration: Project outline and goals

This overview of known collaborative genes highlighted several genetic lesions which patient data suggested might collaborate with mutant *IL-7Rα*, but for which supportive experimental evidence was lacking. These genetic lesions included *TLX3* expression, *HOXA* overexpression, and *NRAS* mutation, as well as loss of the epigenetic regulators *PHF6*, *WT1*, and *PRC2*. The need for experimental evaluation of these potential collaborators combined with the lack of knowledge regarding the effects of mutant *IL-7Rα* signaling on T-cell development led to the construction of this project. In our focus on collaboration, we chose to focus on those genes that would be expected to behave as oncogenes (*TLX3*, *HOXA*, and *NRAS*). From this, we developed two specific aims:

1. Evaluate the effect of human *IL-7Rα* gain-of-function mutation (*IL-7Rα GOF*) on T-cell development and differentiation
2. Explore genetic lesions that may collaborate with mutated *IL-7Rα* to cause T-cell acute lymphoblastic leukemia formation

Results of experiments addressing the first specific aim are described in Chapter 3. Results from experiments addressing the second specific aim are addressed in Chapters 4 and 5.

We believe that understanding the effects of mutant *IL-7Rα* signaling on normal T-cell development might help to better understand its oncogenic effects. Furthermore, experimental investigation of potential oncogenic collaborations is vital to the

development of targeted therapies. We considered induction of leukemia would be the best indicator as to whether a certain combination of genes was sufficient to drive neoplastic transformation. This approach does not take into account our current understanding of the natural history of leukemia development, which is that fulminant leukemia likely evolves from pre-leukemic stem cells over time. Our studies have focused on the relevance of IL-7Rα mutation to T-ALL. However, mutations in IL-7Rα have also been found in B-ALL and ETP-ALL (Chapter 1), suggesting that the results from our experiments may have implications for these diseases as well. Understanding collaborative networks will enable clinicians to target driver mutations and tailor therapy to the genetic lesions present in each leukemia (Cramer et al., 2016; Hunger and Mullighan, 2015; Mullighan and Hunger, 2013).

Chapter 3: Effects of mutant *IL-7Rα* on T-cell development

Introduction

The effects of normal IL-7Rα signaling in T-cells have been well-characterized, with signaling supporting survival and proliferation of both developing and mature T-cells (see Chapter 1). The effects of mutant IL-7Rα signaling on T-cell development are less well understood. Work in our lab has shown that the mutant *IL-7Rα-GOF* found in pediatric T-ALL has constitutively active signaling in the absence of normal signaling partners JAK3 and γ_c in leukemic cells (Zenatti et al., 2011). The effect of this constitutive activation in normal immature T-cells is unknown. Another laboratory has investigated the effects of *IL-7Rα-GOF* mutation in progenitor cells by using bone marrow stem cells that were grown on OP9-DL1 stromal cells to an early T-cell progenitor stage of development. When these cells were transduced with mutant *IL-7Rα* and injected into BALB/c mice, recipient animals did not develop disease (Yokoyama et al., 2013). When bone marrow cells were transduced without first maturing on OP9-DL1 stromal cells, cells caused myeloproliferative disease in recipient mice (Yokoyama et al., 2013). In other studies of the effects of mutant *IL-7Rα* on development, it is only when the mutation is combined with other genetic lesions that it induces disease, as reviewed in Chapter 2 (Treanor et al., 2014; Yokoyama et al., 2013). Better understanding of the developmental effects of mutant IL-7Rα on T-cell development could help to explain the role of the mutation in leukemogenesis.

Establishing techniques

Before addressing the hypothesis and specific aims of this project, experimental techniques needed to be established. Since T-ALL is thought to arise from immature thymocytes, a reasonable approach seemed to be transducing primary murine cells with retroviral vectors to assess the developmental and collaborative effects of genetic lesions. However, cells would need to be cultured to enable transduction, and transduction of primary cells can be difficult. Experiments were performed to compare two culture systems, the OP9-DL4 stromal cell system and the cell-free DL4 protein system. OP9-DL4 cells originated from murine bone marrow stromal cells were created by the Zuniga-Pflucker laboratory (shared under a material transfer agreement). These stromal cells were engineered to express the NOTCH1 ligand DL4 to drive T-cell differentiation in the presence of media containing IL-7 and FLT-3L. The culture system has been used successfully for multiple years (Holmes and Zuniga-Pflucker, 2009). The DL4 protein cell-free system relies on recombinant DL4 protein bound to the culture well to drive T-cell differentiation. This technique was shared by the Rolink laboratory, and has only recently been published (Gehre et al., 2015).

We also compared three preparations of lineage-depleted murine thymocytes and one lineage-depleted murine bone marrow cell preparation to determine the ideal starting cell preparation. While transduction of primary cells required *in vitro* techniques, we planned to perform the majority experiments *in vivo*. *In vivo* work would be performed by injecting transduced cells into sub-lethally irradiated *Rag1*$^{-/-}$ mice. This is an immunocompromised strain that would not be expected to mount an effective immune response against injected cells. *In vivo* experiments were expected to give insights into

the developmental effects of mutant *IL-7Rα* and were considered the best method to determine the leukemogenic capacity of mutation combinations.

Normal T-cell development

In health, T-cells develop in the thymus from progenitor cells that originate in the bone marrow and travel hematogenously to the thymus. Initially, cells do not express the maturation markers CD4 or CD8 (double negative, hereafter abbreviated DN). These DN populations can be further subdivided into four developmental stages based on expression of CD25 and CD44. The most immature cells are $CD25^{-}CD44^{+}$ (DN1). Cells then become $CD25^{+}CD44^{+}$ (DN2) before losing CD44 expression (DN3). Loss of CD25 expression defines the DN4 stage ($CD25^{-}CD44^{-}$). Cells then progress through an immature $CD4^{+}$ or $CD8^{+}$ stage to a $CD4^{+}CD8^{+}$ (double positive/ DP) stage. Lastly, cells become mature $CD4^{+}$ or $CD8^{+}$ cells (Hong et al., 2012). T-cell dependence on IL-7 signaling is stage-specific. Cells express IL-7Rα at the DN2 and DN3 stages, then lose receptor expression in the DN4 and DP stage. Upon maturation into $CD4^{+}$ or $CD8^{+}$ cells, the receptor is again expressed (Hong et al., 2012). It is thought that down-regulation of the receptor at the double positive stage is important in enabling apoptosis of T-cells that do not undergo successful positive selection (Hong et al., 2012). Once thymocytes have matured through positive selection, IL-7 signaling also appears to play a role in differentiation of T-cells into single positive cells. Signaling appears to favor development of $CD8^{+}$ cells rather than $CD4^{+}$ cells. $CD4^{+}$ cells undergoing lineage commitment do not respond to IL-7 signaling, and signaling has been shown to induce silencing of CD4 genes (Hong et al., 2012; Park et al., 2010; Yu et al., 2003). Based on

this, we hypothesized that constitutive signaling by the mutant IL-7Rα might drive CD8 lineage commitment in immature thymocytes.

Given that earlier experiments had shown that BALB/c mice injected with mutant *IL-7Rα* T-cell progenitors did not develop disease, it was not clear whether *in vivo* experiments would yield results (Yokoyama et al., 2013). However, our experimental approach differed from those experiments in the cell of origin and the strain of mice used as recipients. To generate hypotheses as to the *in vivo* effects of mutant *IL-7Rα* signaling on T-cell development, a search of the literature revealed that IL-7 signaling can be important in regulating the balance between T_{reg} cells and Th17 cells. Both cell populations arise from $CD4^+$ cells, and development of one population seems to be balanced by development of the other in health (Diller et al., 2016; Joller et al., 2014). Th17 cells may incite inflammation and autoimmunity, while T_{reg} cells typically act to limit the immune response (Diller et al., 2016; Rodriguez-Perea et al., 2016). A mouse model of recurrent pregnancy loss showed that IL-7 signaling was important in the development of Th17-associated inflammation and dampened T_{reg} responses (Wu et al., 2016). In a model of ocular autoimmune disease, IL-7 signaling was important for maintaining Th17 populations (Chen et al., 2016). Similarly, in experimental autoimmune encephalitis, IL-7 signaling is important in maintaining Th17 cell survival (Liu et al., 2010). From this, we hypothesized that mutant IL-7Rα might shift the T_{reg}-Th17 balance in favor of Th17 cells *in vivo*.

Materials and Methods

Thymocyte transduction and culture

Thymocytes were harvested from 3-6 week old C57Bl/6J female donor mice by first mechanically dissociating the tissue into a single cell suspension. Cells were then bound to CD4 and CD8 microbeads (Miltenyi) and passed through an LD column (Miltenyi) to isolate double negative cells according to the manufacturer's instructions. Resulting double negative cells were cultured on OP9-DL4 bone marrow stromal cells for 1 day, then transduced twice with retroviral vectors with approximately 18 hours between transductions. Thymocytes were transduced by spinoculation (centrifugation at 2000 rpm for 60 minutes) with addition of 8μg/ml polybrene (Chemicon) to the transduction solution. After transduction, thymocytes were maintained on OP9-DL4 cell culture for an additional 7-8 days prior to injection into mice to allow for expansion of cell numbers.

Retroviruses were generated using Phoenix-Eco packaging cells (Orbigen). Phoenix cells were cultured in DMEM containing glucose, L-glutamine, and sodium pyruvate (Corning), with 50 ml of fetal bovine serum added to every 500 ml of DMEM. Phoenix cells were transfected with pMIG plasmids containing wild type *hIL-7Rα*, mutant *hIL-7Rα*, cDNAs of, *hIL-7Rα* mutant were subcloned into pMIG vector by gateway cloning or PCR cloning methods by Wenqing Li. The *hIL-7Rα* mutant sequence was c.731_732insTTGTCCCAC, based on the mutation in subject P2 and was confirmed by sequencing previously by our laboratory (Zenatti et al., 2011). Thymocytes for the IL-17 reporter experiment were performed using a transgenic mouse designed to have IL-17a expression linked to TdTomato and IL-17f expression linked to GFP using bacterial artificial chromosome technology (Shen et al., 2014).

Transfection was performed using lipofectamine (Invitrogen) and OPTI-MEM I reducing serum medium (Invitrogen) 48-72 hours prior to thymocyte transduction.

Phoenix cell supernatants containing retroviruses were filtered using a 0.45 µm syringe filter (Millex) prior to transduction of thymocytes. OP9-DL4 cells were cultured according to published guidelines used for culture of OP9-DL1 cells and were cultured in MEM-alpha medium (Gibco). For 500 ml of media, the following additives were included: 50 ml fetal bovine serum (GE life Sciences), 3 ml fresh (frozen to maintain freshness) L-glutamine (Sigma), 0.5 ml 2-mercaptoethanol (Gibco), and 2.5 ml penicillin/ streptomycin (Gibco). When thymocytes were added to culture, growth was supported by the addition of 5 ng/ml mIL-7 and 5 ng/ml hFLT-3L (Peprotech) (Holmes and Zuniga-Pflucker, 2009).

Animal Experiments

Transduced cells were injected into sub-lethally irradiated, 6-15 week old, female *Rag1*$^{-/-}$ mice via tail vein in a concentration and volume of 5 x10^5 cells/ 200 µl/ mouse. Recipient mice were prophylactically treated for 3 days with SMZ antibiotics (0.08mg/ml in drinking water) either immediately prior to irradiation. Animals were monitored by a single, experienced technician for consistency (T.B.) and euthanized at the onset of clinical signs. Clinical signs included hunching, dyspnea, reduced ambulation, rough hair coat, crusted skin (in the mutant *IL-7Rα*-only group), or moribund status. Peripheral blood was collected immediately prior to euthanasia. Animals that required euthanasia for causes not related to development of experiment-associated disease (i.e. tail caught in caging, inner ear infection, fighting-associated skin lesions) were censored from experimental results. Technicians performing monitoring were not blinded to experimental groups.

Passage of untouched (Invitrogen trademark term) $CD4^+$ and $CD8^+$ inflammatory cells was performed using fresh spleens from mice injected with mutant IL-7Rα-only cells that had developed clinical disease. Spleens were mechanically dissociated, red blood cells were lysed, and cells were then depleted of lineage-expressing cells using the Invitrogen Dynabeads untouched mouse CD4 and untouched CD8 kits according to manufacturer's instructions (Invitrogen). These kits include magnetic beads bound to CD11b, CD16/32, Ter-119, and CD45R as well as CD8 and CD4, respectively. Untouched cells were suspended at 4-5 x 10^5 cells/ 200 µl PBS (dependent on cell yield), and injected into sub-lethally-irradiated *Rag1*$^{-/-}$ recipients.

Serum Cytokines

Serum from mice was submitted for the mouse cytokine array/ chemokine array 31-plex to Eve technologies (Calgary, Canada). Analysis of cytokine levels was performed using a laser bead multiplex technology, assessing levels of the following cytokines: Eotaxin, G-CSF, GM-CSF, IFNγ, IL-1α, IL-1β, IL-2, IL-3, IL-4, IL-5, IL-6, IL-7, IL-9, IL-10, IL-12 (p40), IL-12 (p70), IL-13, IL-15, IL-17A, IP-10, KC, LIF, LIX, MCP-1, M-CSF, MIG, MIP-1alpha, MIP-1beta, MIP-2, RANTES, TNFα, and VEGF.

Flow Cytometry

Thymus, spleen, and bone marrow were manually dissociated to single cell suspensions. Liver was dissociated using a Stomacher tissue lyser. Lungs were digested in a solution of 0.25 WU/mL TM liberase (Roche) in 2% glucose PBS. After placing dissected lobes in 3 ml of digestion solution in a C tube (Miltenyi), dissociation was performed using the Miltenyi gentleMACS Lung1 program. Dissociated lungs were incubated for 30 minutes at 37 degrees Celsius. Then, tissues were further dissociated

using the Lung 2 program. Red blood cell lysis was applied to these tissues as well as to peripheral blood using ACK Lysing Buffer (Lonza). Resultant suspensions were stained with Zombie Red live/dead fixable stain (Biolegend) for 15 minutes at room temperature. Then, CD16/32 Fc receptor block (93) was applied at a 1:400 dilution for 10-15 minutes (Biolegend). Cocktails of fluorochrome-conjugated antibodies were applied to cells for 15 minutes on ice, including the following antibodies: anti-Thy1.2 APC-Cy7 (30-H12), anti-CD4 PE-C7 (GK1.5), anti-CD8 Brilliant Violet 421 (53-6.7), anti-CD44 PerCP-Cy5.5 (IM7), anti-CD25 Brilliant Violet 650 (PC61), anti-TCRβ Alexa Fluor 700 (H57-597), anti-CD3 Brilliant Violet 421 (17A2), anti-Ly6G Pe-Cy7 (1A8) from Biolegend; anti-CD11b PerCP-Cy5.5 (M1/70), anti-B220 APC (RA3-6B2) from BD Biosciences. Fluorescence minus one (FMO) labeling was used for controls (Figure 2). Cells were then

Figure 2: Gating strategy for flow cytometric analyses. Cells were gated to exclude debris using FSC-A v. SSC-A, then doublet exclusion was performed using FSC-A v. FSC-H. Next, a live-dead stain was used to exclude dead cells. For assessment of CD4 and CD8 populations (A), live cells were assessed for GFP+ populations. GFP+ cells were analyzed based on Thy1.2+ expression. Thy1.2+ cells were gated based on CD8 and CD4 expression. CD8 single positive cells were analyzed for TCRβ expression. Fluorescence minus one (FMO) controls are shown below each gate. The FMO for GFP and Thy1.2 is blue, and the labeled populations are red. The CD4 FMO is blue, and the CD8 FMO is red. The TCRβ FMO is blue, and the labeled population is red (A). Gating for human IL-7Rα and GFP on the cell line is shown in B. Cells were gated to exclude debris using FSC-A v. SSC-A, then assessed for expression of hIL-7Rα. Unstained cells as a labeling control are shown below in blue, and the labeled population is red (B). Gating for CD11b expression of Hoxa-IL-7Rα-GOF cells is shown in C. Cells were gated to exclude debris using FSC-A v. SSC-A, then doublet exclusion was performed using FSC-A v. FSC-H. Next, a live-dead stain was used to exclude dead cells. Live cells were assessed for GFP+ populations. GFP+ cells were assessed for CD11b expression (C). FMO control is shown below in blue with CD11b labeled populations in red. Gating for Treg cells (D) began with FSC-A v. SSC-A, then FSC-A v. FSC-H, and selection of live cells. CD4+ populations were then gated, and expression of FoxP3 and CD25 were assessed. CD4 FMO is in blue, and GFP FMO is in red. FoxP3 FMO is in blue, and CD25 FMO is in red.

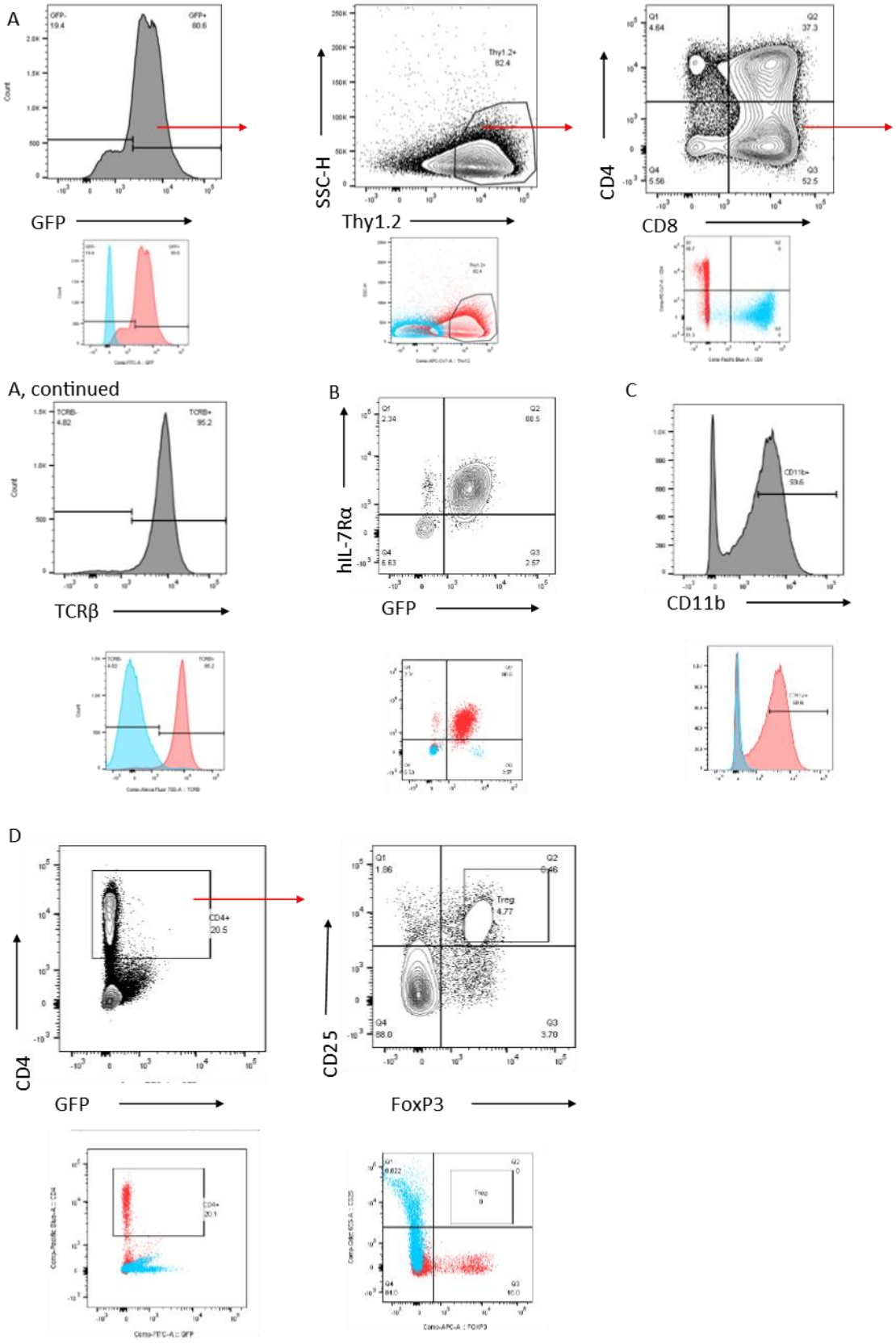
A
GFP
SSC-H
Thy1.2
CD4
CD8
A, continued
TCRβ
B
hIL-7Rα
GFP
C
CD11b
D
CD4
GFP
CD25
FoxP3
Treg

fixed in stabilizing fixative (BD Biosciences) for 30 minutes. Fixative was removed, and flow cytometric analysis was performed on an LSRIISORP cytometer with FACS DIVA software. Data analysis was performed using FlowJo (Tree Star, Inc.). Flow cytometry was performed on fresh tissues for intracellular staining and for those experiments assessing IL-17 expression linked to TdTomato.

Intracellular labeling was performed using either BD biosciences intracellular labeling kit (IL-17-producing cells) or Biolegend TruNuclear Fixation kit (T_{reg} cells). The following antibodies were used: anti-FOXP3 AlexaFluor 647 (150D), anti-CD25 Brilliant Violet 650 (PC61), anti-CD4 Brilliant Violet 421 (GK1.5), anti-IL-17a Brilliant Violet 650, anti-TCRγδ Pe-Cy7, anti-CD4 APC, anti-CD8 APC, and anti-CD45 PerCP (Biolegend). For IL-17 labeling, cells were processed, then stimulated with PMA (50 ng/ml) and Ionomycin (1μg/ml; Sigma) for 4 hours at 37 degrees Celsius in the presence of GolgiStop protein transport inhibitor (BD Biosciences) prior to labeling for intracellular IL-17.

Histopathology, Immunohistochemistry, and Digital Slide Analysis

Tissues were fixed in 10% neutral buffered formalin and transferred to 70% ethanol after complete fixation. Samples were trimmed, paraffin-embedded, sectioned, and stained with hematoxylin and eosin according to standard histotechnological procedures.

Immunohistochemistry was performed by the Pathology/ Histotechnology Laboratory using previously optimized protocols. Immunohistochemistry utilized anti-GFP antibody (Abcam ab6556) at 1:1000 dilution with proteolytic digestion using proteinase K (DAKO) incubated overnight at 4 degrees C; anti-CD3 antibody (Bio-Rad

#MCA1477) at 1:100 dilution incubated for 60 minutes with heat-induced epitope retrieval using citrate (Leica Biosystems) for 20 minutes; and anti-ki67 antibody (Abcam #ab16667) at 1:100 dilution incubated for 30 minutes with heat-induced epitope retrieval using citrate for 20 minutes. For all protocols, DAB (Sigma & Leica Biosystems) was used as the chromogen, and hematoxylin (Leica Biosystems) was used as a counterstain.

Slides were digitalized using an Aperio AT2 slide scanner (Leica) at a magnification of 20x. Digital slides were viewed in ImageScope (Aperio), and digital slides were used to generate images of the tissues. Digital image analysis of ki67 labeling was performed using an optimized Aperio Nuclear v9 algorithm.

Ligation-Mediated PCR

Oncogenes were transfected using retroviral vector and thus each original cell carried a unique molecular barcode that could be used to assess clonality by identifying the frequency of retroviral integration as described previously (De Ravin et al., 2016; Maldarelli et al., 2014). The integration sites were cloned from 5LTR-genomic junction using primers specific for the vector used in this study (MFGS5LTR, 5'ATGGCGTTACTTAAGCTAGCTTG 3', MFGS5LTRnest, CAAACCTACAGGTGGGGTCTTTC 3'). Integration site junctions were mapped to mouse genome build mm10. Frequency of each clone was calculated as the percentage of read numbers for each integration sites out of total mapped reads.

Statistics

For most studies, statistics were performed using GraphPad Prism version 6.00 for Windows (GraphPad Software, La Jolla, CA). To compare more than two groups,

Kruskall-Wallis analysis was performed, and the Mann-Whitney test was used to compare two groups. Survival curve analysis was performed using the Log-rank test. For the limiting dilution studies, extreme limiting dilution analysis was performed using software from the Walter and Eliza Hall Institute of Medical Research, available at the following website: http://bioinf.wehi.edu.au/software/elda/ (Hu and Smyth, 2009).

Results

Establishing techniques: CD4-CD8 depleted thymocytes yielded the best culture and transduction results

Initially, we compared two cell culture systems: the OP9-DL4 stromal cell system, and the DL4 protein cell-free system. Using the OP9-DL4 stromal cells, primary murine thymocytes and bone marrow cells survived and thrived. In comparison, cells did not grow well on the cell-free DL4 protein culture system, and most cells died in culture. From this, we decided to proceed with experiments using the OP9-DL4 cell culture system.

In addition to comparing culture systems, we also compared several techniques for depleting primary murine cells of mature cell populations. We performed one replicate of these experiments (results are shown), and therein it is unknown how robust the following data are. Isolating immature cells seemed vital to addressing our experimental questions because ALL likely arises from an immature cell population. Since T-ALL arises from thymic populations, it seemed that the ideal preparation would yield a pure population of immature thymocytes ($CD4^-CD8^-$ cells). To deplete mature cell populations, we used cocktails of antibody-conjugated magnetic beads. The lineage

depletion cocktail included anti-CD5, anti-CD45R, anti-CD11b, anti-Gr-1, anti-7-4, and anti-TER-119 to remove mature T-cells, B-cells, myeloid cells, and erythroid cells from the depleted populations. Beads conjugated to anti-CD4 and anti-CD8 were also used for some preparations. Cells expressing surface markers were bound by these beads, then removed by filtering over a magnetic column. With this technique, only cells that did not express the surface markers remained in suspension.

We compared lineage-depleted bone marrow cells (bone marrow cells depleted of cells using only the lineage cocktail of magnetic beads described above), lineage-depleted thymocytes (thymocytes depleted of cells using only the lineage cocktail of magnetic beads described above), CD4-CD8 depleted thymocytes (thymocytes depleted of cells using anti-$CD4^+$ and anti-$CD8^+$ magnetic beads), and lineage-CD4-CD8-depleted thymocytes (thymocytes depleted of cells using the lineage cocktail of magnetic beads as well as anti-$CD4^+$ and anti-$CD8^+$ magnetic beads). Comparing thymocyte preparations immediately after depletion, both lineage-depleted and CD4-CD8 depleted preparations yielded adequate numbers of cells (approximately 1% of thymocytes); the lineage-CD4-CD8 depletion yielded very few cells (data not shown). Further evaluating thymocyte preparations, there were similar percentages of $CD11b^-lineage^-$ cells in each of the three preparations (Figure 3A). However, the CD4-CD8 depletion yielded higher levels $CD4^-CD8^-$ cells (expected to be mostly immature T-cells) than either of the other preparations (Figure 3B). This preparation also had moderate enrichment of $CD11b^+$ myeloid cells, considered a less-than-ideal contaminating population (Figure 3C).

We then followed the maturation of the different cell preparations on the OP9-DL4 stromal cells over time. CD4 and CD8 were used as markers of T-cell maturation.

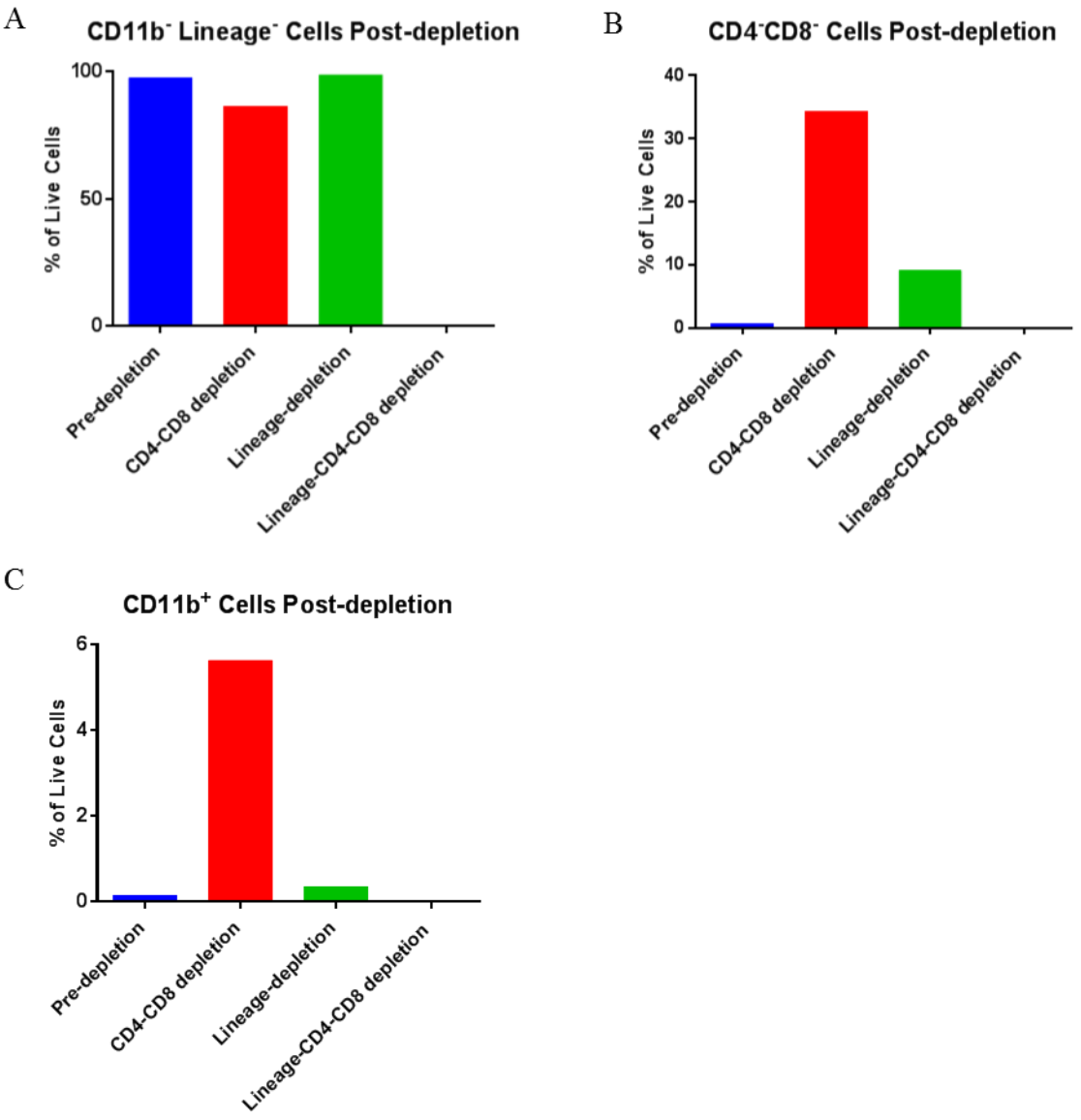

Figure 3: CD4-CD8 depleted cells yielded the highest percentage of CD4-CD8- immature thymocytes. Comparison of thymocyte depletion techniques immediately after depletion showed that the percentage of CD11b-lineage- cells was similar across techniques (A). The CD4-CD8 cell depletion yielded over 30% CD4-CD8- cells in comparison to fewer cells with lineage depletion and lineage-CD4-CD8 depletion (B). There was a modest enrichment of CD11b+ myeloid cells in the CD4-CD8 depletion (C). Data are from a single experiment, N=1 for each group.

When evaluating lineage$^-$ bone marrow cells, we compared cells grown in the absence of activating cytokines with those grown in the presence of activating cytokines required for transduction (IL-6, SCF, and FLT-3L). After 16 days, bone marrow cells without activating cytokines matured into mixed populations containing CD11b$^+$, lineage$^+$, and lineage$^-$ cells (Figure 4A). A few CD4$^+$ and CD4$^+$CD8$^+$ lymphoid cells developed. The addition of activating cytokines caused an increase in the percentage of CD11b$^+$ populations and a reduction in lymphocyte populations (Figure 4B). Based on the large number of CD11b$^+$ myeloid cells and few lymphocytes, we concluded that bone marrow cells would not be a good starting cell preparation.

In comparison, thymocyte preparations appeared to be excellent starting cell preparations. The CD4-CD8 depletion yielded relatively pure populations of ideal CD4$^-$CD8$^-$ cells. Lineage depletion yielded mixed populations of CD4$^-$CD8$^-$ and CD4$^+$CD8$^+$ cells. There were too few cells in the lineage-CD4-CD8 depleted preparation to assess immunophenotype at the time of harvest (Figure 5A). Though the immunophenotype of the starting populations varied, after 4 days on OP9-DL4 stromal cells in the presence of IL-7 and FLT-3L, the three preparations had become more uniform with mixed populations of predominantly CD4$^-$CD8$^-$ and CD4$^+$CD8$^+$ cells, similar to the populations seen in the thymus. These cell populations remained consistent after 16 days of culture on OP9-DL4 (Figure 5A). The enhancement of CD11b$^+$ cells seen in the CD4-CD8 depleted cells did not persist. Assessing the maturational stages DN cells in the three thymocyte preparations, the majority of cells in each of the preparations were in the DN3 stage (CD25$^+$CD44$^-$), and this remained consistent over time (Figure 5B).

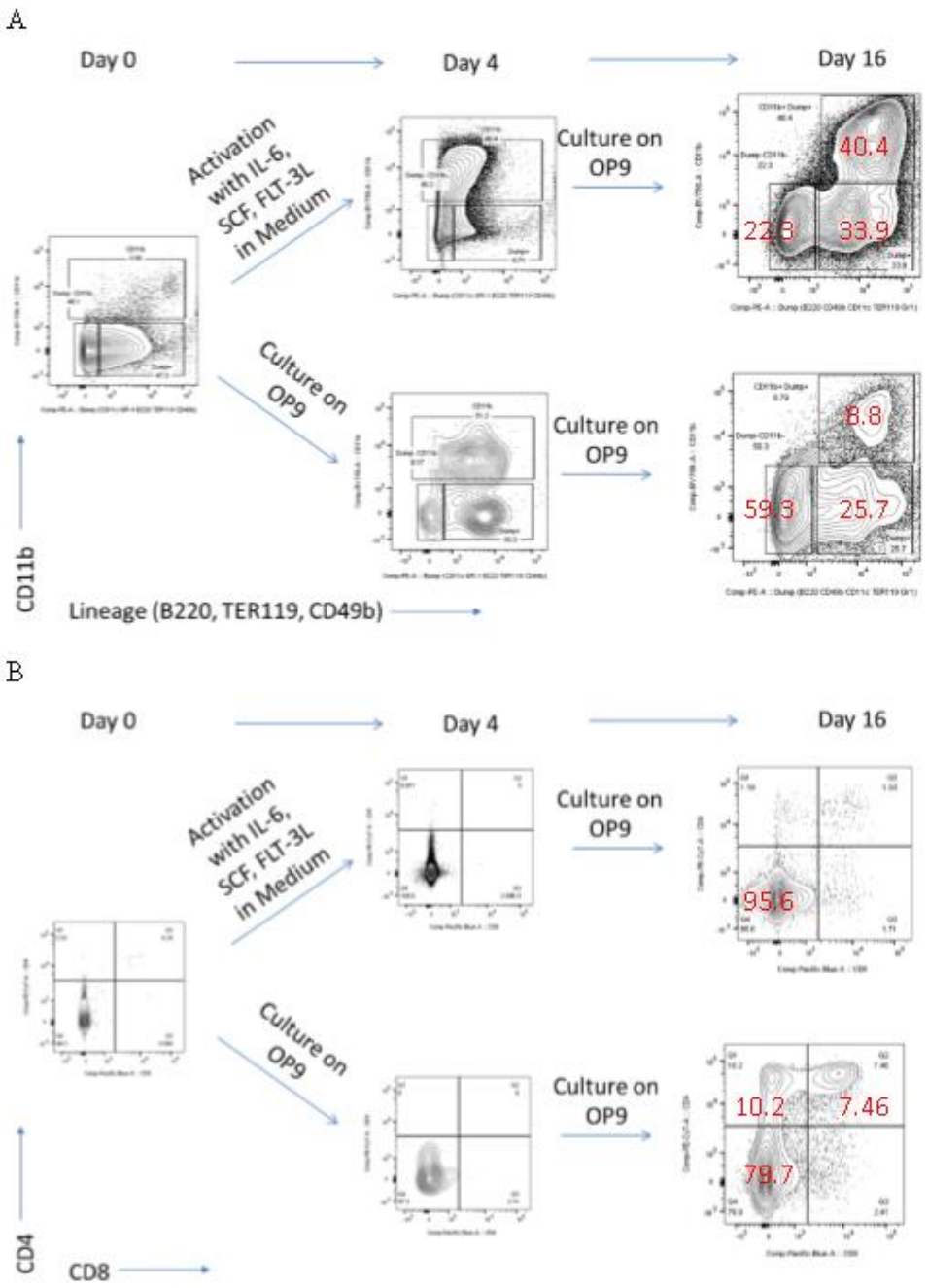

Figure 4: Lineage- bone marrow cells develop into myeloid and lineage+ populations when cultured in activating cytokines. After 16 days in culture, cells grown in the absence of activating cytokines have low percentages of CD11b+ and lineage+ cells, but the addition of activating cytokines markedly increases these undesirable populations (A). Cells do not appreciably differentiate to express CD4 or CD8 (B). Data are from a single experiment, N=1 for each group. Population percentages are in red, and this convention will be continued throughout the text.

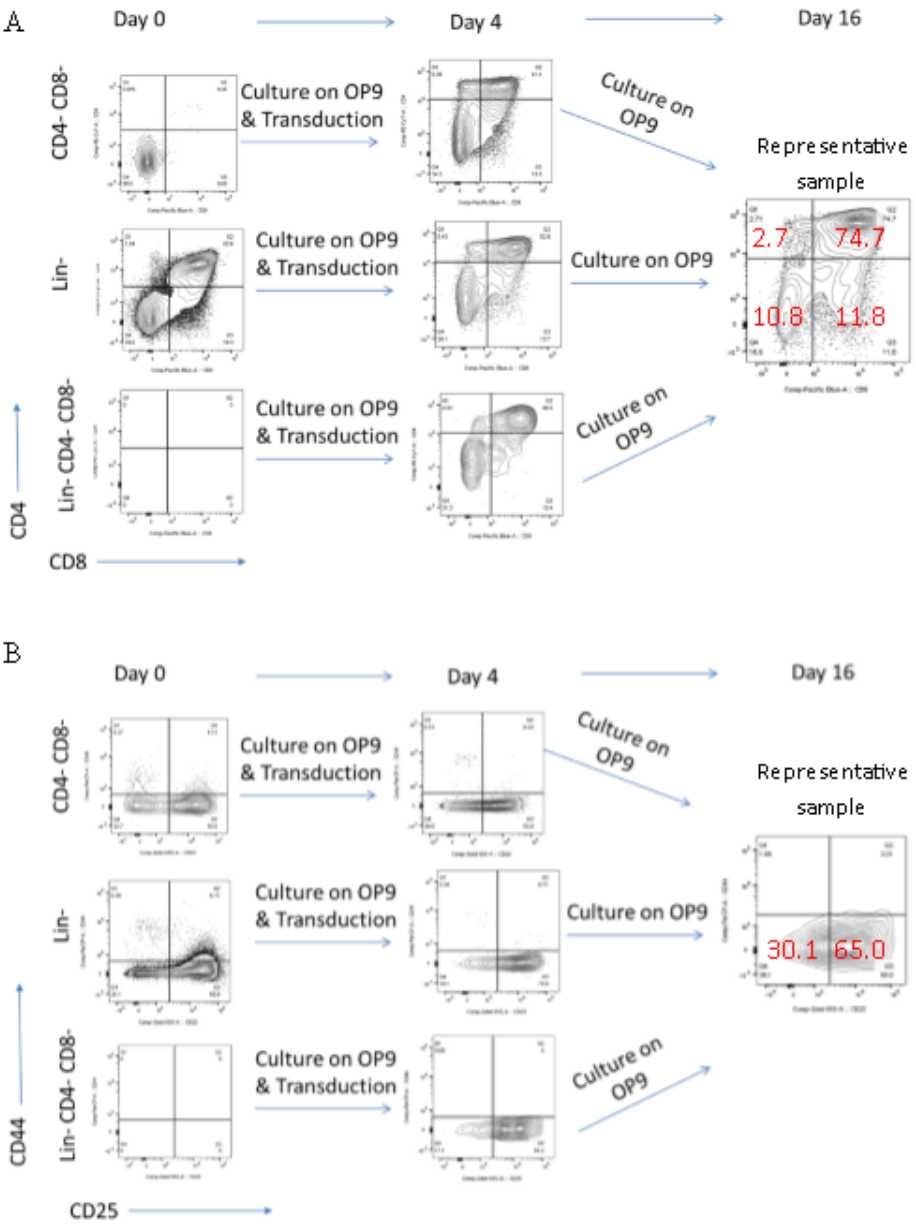

Figure 5: After culture on OP9-DL4 cells, the three thymocyte depletion preparations show similar maturation. Immediately after depletion, the three preparations yielded markedly different populations. The CD4-CD8 depletion was composed of a nearly pure population of ideal $CD4^{-}CD8^{-}$ cells. The lineage-depleted preparation was more mixed. There were too few cells in the lineage-CD4-CD8 depletion to assess phenotype (A). After 16 days in culture, the three thymocyte preparations developed into similar populations consisting predominantly of $CD4^{+}CD8^{+}$ and $CD4^{-}CD8^{-}$ cells (A). The majority of DN cells were in the DN3 stage immediately post-depletion and after culture on OP9-DL4 cells (B). Data are from a single experiment, N=1 for each group.

Since our experimental design required successful transduction with retroviral vectors, we next compared transduction of the three thymocyte depletion preparations using a GFP-containing retroviral vector. The percentage of live cells was relatively similar across preparations, though the lineage-CD4-CD8 preparation had the lowest percentage of live cells (Figure 6A). Similarly, the percentage of GFP^+ cells was similar across transductions, with a slight increase in the number of GFP^+ populations in the lineage-CD4-CD8 preparation, suggesting that transduction efficacy was not significantly affected by preparation (Figure 6B and D). However, the lineage-CD4-CD8 cells appeared to have a slight increase in the percentage of $CD11b^+$ cells as compared to the other cell preparations (Figure 6C). Based on these data, we determined that the ideal starting preparation was the CD4-CD8 depletion because it yielded relatively high numbers of cells, the resulting cells were nearly pure populations of $CD4^-CD8^-$ thymocytes, and these cells could be successfully transduced. Thymocytes depleted of $CD4^+$ and $CD8^+$ cells were therefore used for all subsequent experiments, and the preparation consistently yielded nearly pure populations of $CD4^-CD8^-$ thymocytes, with depletion success checked after each depletion to ensure consistent starting populations.

Mutant *IL-7Rα* enables IL-7-independent growth of primary murine thymocytes *in vitro*

We evaluated the effects of *IL-7Rα-GOF* mutation (also referred to as *mutIL-7Rα*) on cell growth and development *in vitro* by transducing CD4-CD8 depleted thymocytes with retroviral vectors containing the *IL-7Rα-GOF* or wild type *IL-7Rα* (*wtIL-7Rα)*.

A

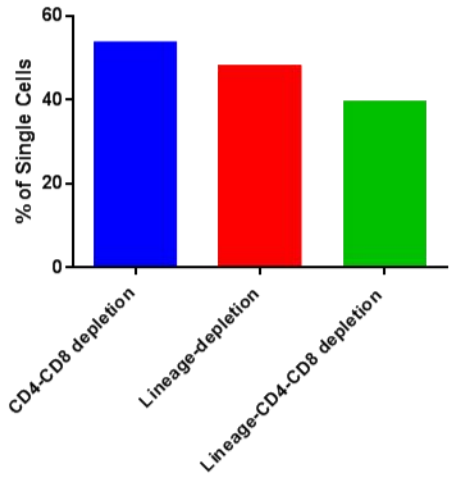

B

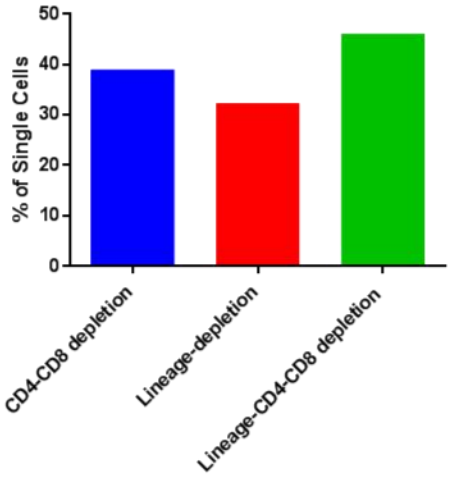

C

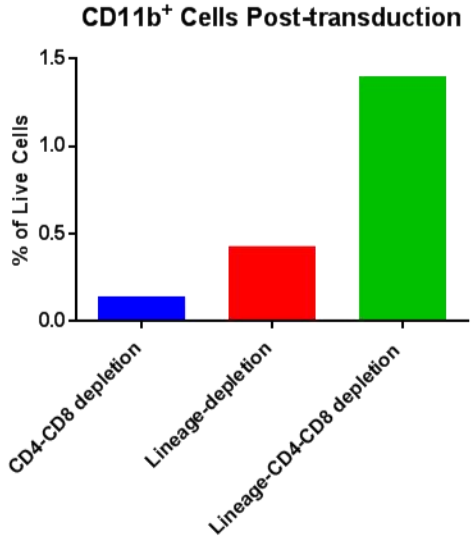

Figure 6: Depleted thymocytes can be successfully transduced using retroviral vectors. Survival of cells after transduction was similar across thymocyte depletion preparations (A). Transduction was successful as indicated by GFP expression in over 30% of cells (B). Transduction led to a slight enhancement of CD11b+ cells in the Lineage-CD4-CD8 depleted preparation (C). Evaluation of cultured CD4-CD8 depleted thymocytes using light microscopy showed healthy cells growing on OP9-DL4 stromal cells, and GFP expression by these cells could be visualized using a fluorescent microscope (D).

D

Transduced thymocytes by light microscopy

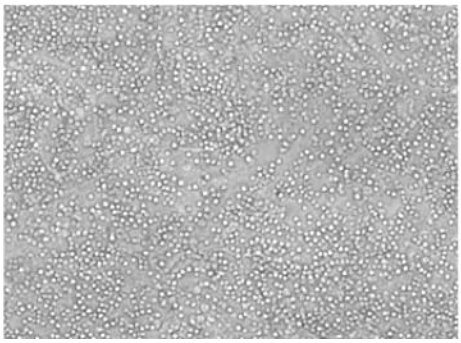

Transduced thymocytes by fluorescent microscopy

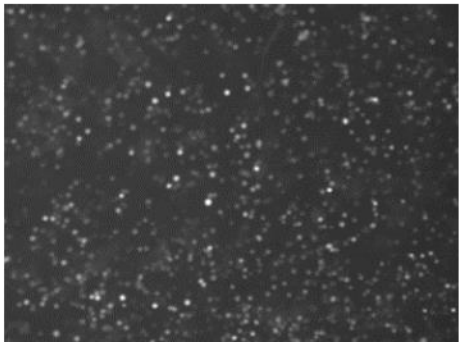

Removal of IL-7 from the culture media caused non-transduced thymocytes and *wtIL-7Rα* thymocytes to die after several days in culture (Figure 7A). In comparison,

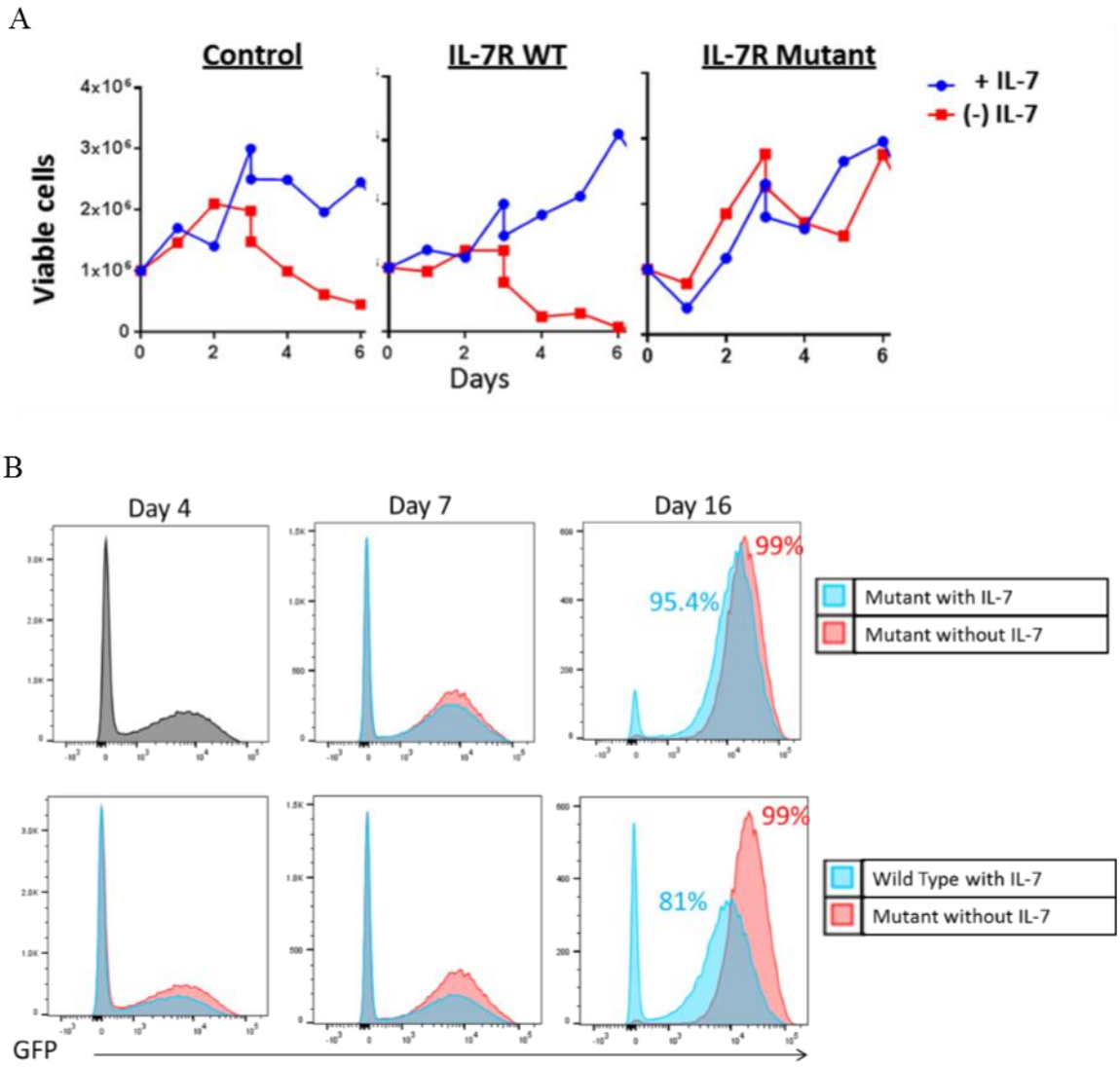

Figure 7: Transduction of thymocytes with *IL-7Rα-GOF* enables IL-7 independent growth and confers growth advantage. When IL-7 is removed from the culture media, non-transduced thymocytes and thymocytes transduced with *wtIL-7Rα* die after several days in culture. In contrast, thymocytes transduced with *IL-7Rα-GOF* survive in the absence of IL-7 (A). Transduction with *IL-7Rα-GOF* yields 95.4% GFP^+ cells in IL-7 replete media and 99% GFP^+ cells in IL-7 depleted media (B). In comparison, GFP^+ cells composed only 81% of the population of thymocytes transduced with *wtIL-7Rα* after 16 days in culture (B).

thymocytes transduced with *IL-7Rα-GOF* survived longer in culture media lacking IL-7 (Figure 7A). Removal of IL-7 from the culture media resulted in an increase in the percentage of GFP^+ (transduced) cells after 16 days in culture with 95.4% GFP^+ in IL-7 containing media and 99% GFP^+ in media without IL-7 (Figure 7B). Transduction with *IL-7Rα-GOF* conferred greater growth advantage than transduction with *wtIL-7Rα* where only 81% were GFP^+ after 16 days, and the mean fluorescence intensity was higher in cells transduced with *IL-7Rα-GOF* than with *wild type IL-7Rα* (Figure 7B).

Mutant *IL-7Rα-GOF* rescues cells from IL-7 starvation-induced DN3-DN4 shift *in vitro*

Next, we compared the effects of IL-7 removal on the DN cell populations. In non-transduced and *wtIL-7Rα* transduced thymocytes, removal of IL-7 led to a striking shift in the double negative cell population from DN3 stage ($CD25^+CD44^-$) to the more mature DN4 stage ($CD25^-CD44^-$). Thymocytes transduced with *IL-7Rα-GOF* did not undergo the same maturational shift when IL-7 was removed from culture, presumably because they continued to have IL-7 signaling support due to *IL-7Rα-GOF* constitutive signaling (Figure 8A).

Mutant *IL-7Rα-GOF* causes an increase in $CD8^+$ cells *in vitro*

Analysis of the development of non-transduced cells showed that the cells developed from a $CD4^-CD8^-$ (DN) population to populations containing a mixture of predominantly DN or $CD4^+CD8^+$ (DP) cells after 4 days on OP9-DL4 stromal cells. This is similar to the developmental stages seen in the normal thymus. By Day 16, there were fewer DP non-transduced cells than at Day 4 or Day 7 and higher percentages of $CD4^+$ and DN (Figure 9A). Thymocytes transduced with *wtIL-7Rα* followed a similar pattern of

development, with a slight increase in the $CD8^+$ population at each time point; whether this was statistically significant is not known due to the low number of experimental replicates (Figure 9A). In comparison, cells transduced with *IL-7Rα-GOF* showed a notable increase in the $CD8^+$ population with fewer DP cells and very few $CD4^+$ cells (Figure 9A&B). This $CD8^+$ population was present with or without IL-7 in the culture media (Figure 9C). To assess whether the $CD8^+$ population seen in *IL-7Rα-GOF* transduced thymocytes were immature or mature, we assessed expression of TCRβ.

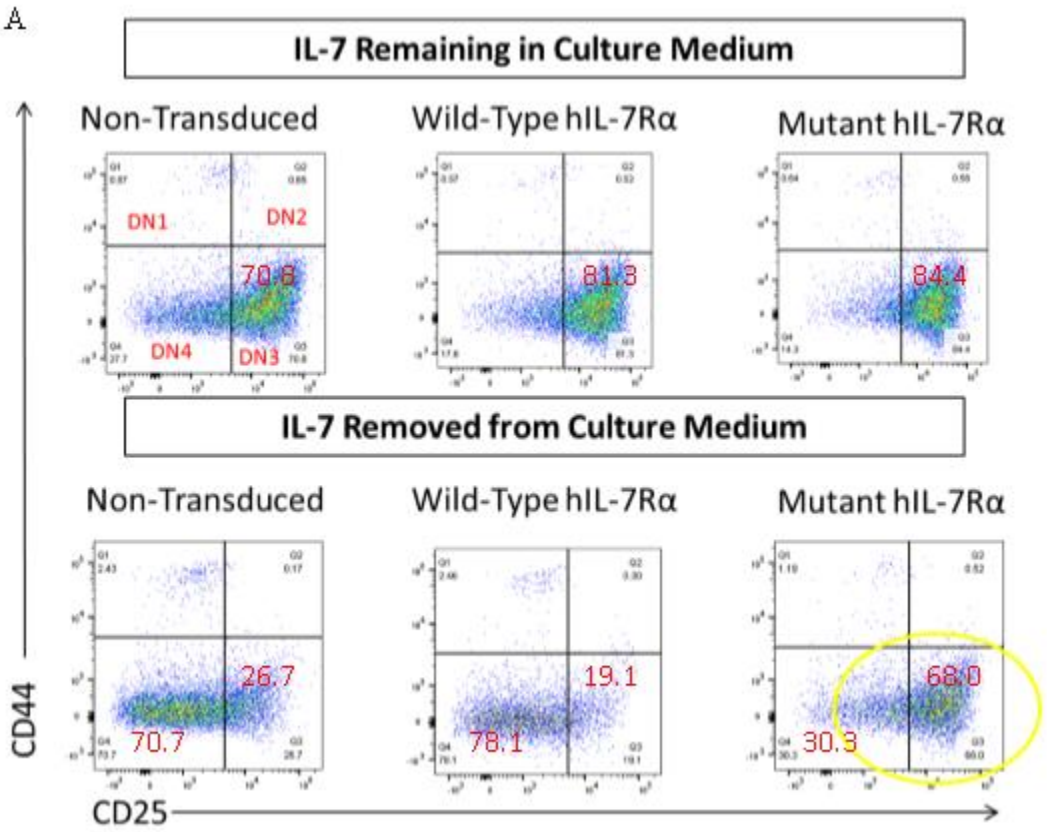

Figure 8: Transduction of thymocytes with *IL-7Rα-GOF* prevents DN3 to DN4 shift when IL-7 is removed from media. Removal of IL-7 from the culture media induced a rapid shift from predominantly DN3 stage to DN4 stage in non-transduced cells and cells transduced with *wtIL-7Rα*. In comparison, thymocytes transduced with *IL-7Rα-GOF* did not undergo this shift as highlighted by the yellow circle.

A

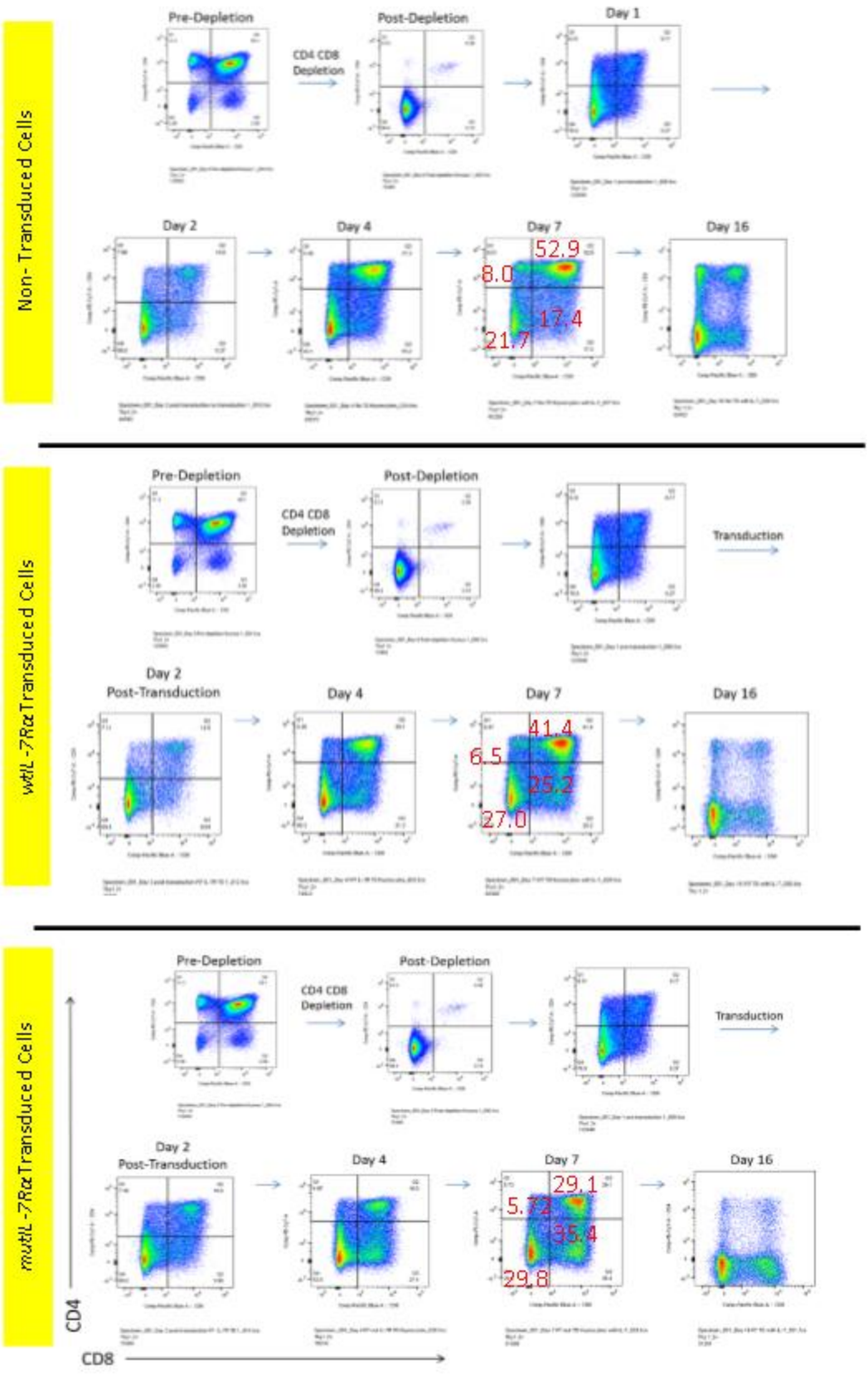
Non-Transduced Cells
Pre-Depletion
CD4 CD8 Depletion
Post-Depletion
Day 1
Day 2
Day 4
Day 7
Day 16
52.9
8.0
17.4
21.7
wtIL-7Rα Transduced Cells
Pre-Depletion
CD4 CD8 Depletion
Post-Depletion
Transduction
Day 2 Post-Transduction
Day 4
Day 7
Day 16
41.4
6.5
25.2
27.0
mutIL-7Rα Transduced Cells
Pre-Depletion
CD4 CD8 Depletion
Post-Depletion
Transduction
Day 2 Post-Transduction
Day 4
Day 7
Day 16
29.1
5.72
35.4
29.8
CD4
CD8

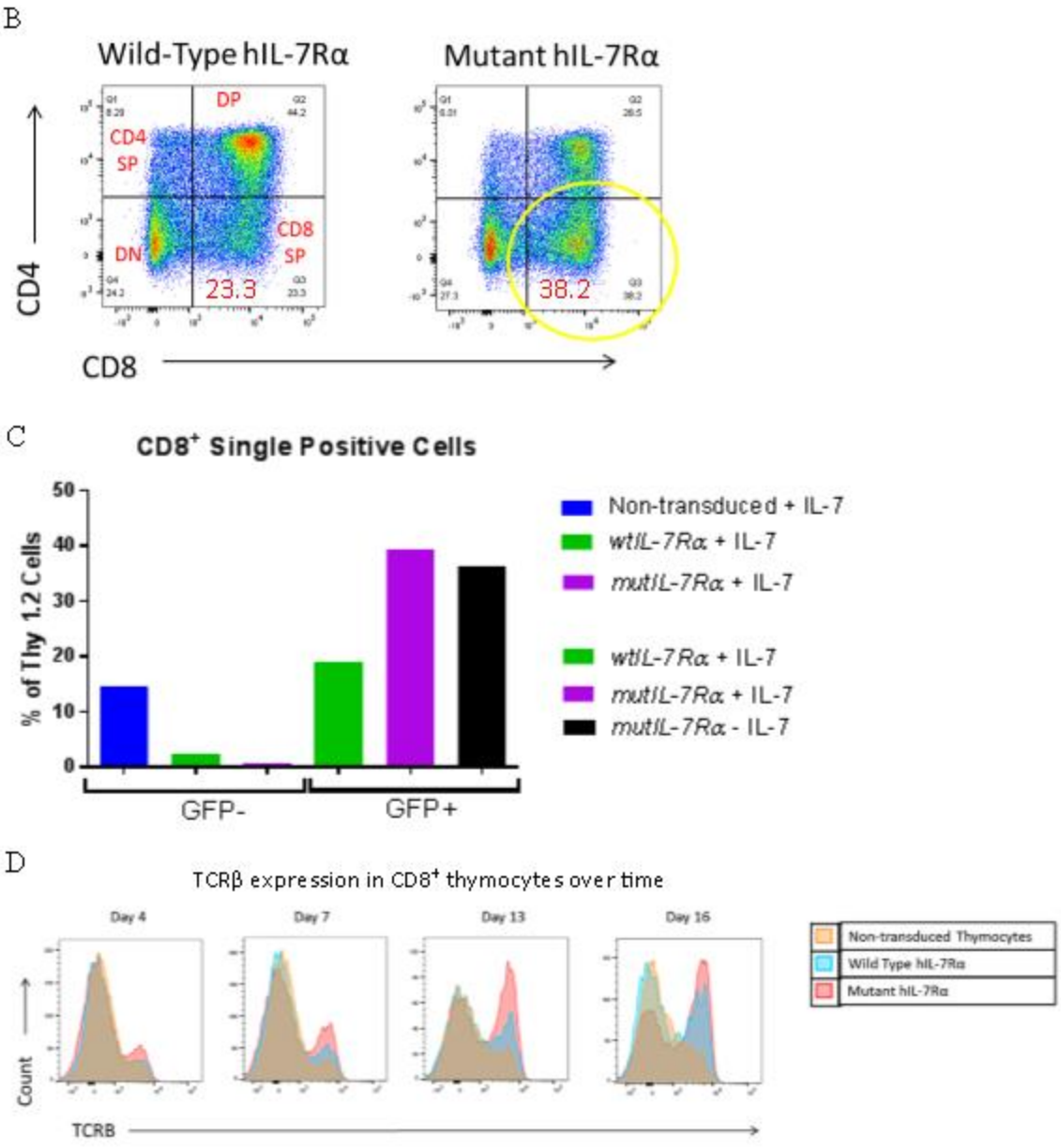

Figure 9: Transduction of thymocytes with *IL-7Rα-GOF* and culture on OP9-DL4 caused an increase in $CD8^+$ cells. Assessing maturation of thymocytes on OP9-DL4 at multiple time-points showed that non-transduced cells matured from predominantly DN populations to predominantly DP populations over 7 days with an enhancement of DN populations by day 16 (A). Thymocytes transduced with *wtIL-7Rα* developed similarly, with a slight enhancement of $CD8^+$ populations (A). In contrast, thymocytes transduced with *IL-7Rα-GOF* had a marked increase in percentage of $CD8^+$ cells as highlighted by the yellow circle (A&B). This population was present with or without IL-7 in the culture media (C). By day 16, many of the $CD8^+$ cells expressed TCRβ, suggesting maturity (D).

Many of the $CD8^+$ cells expressed TCRβ after 16 days on culture, consistent with a mature phenotype (Figure 9D).

Mutant *IL-7Rα* thymocytes cause inflammation in recipient mice

After evaluating the effects of *IL-7Rα-GOF* on growth and development of thymocytes *in vitro*, we next explored the effects of the mutant *in vivo*. To do this, transduced thymocytes were cultured for 8-9 days on OP9-DL4 stromal cells. After this, thymocytes were injected into sub-lethally irradiated *Rag1-/-* mice to enable engraftment of cells in the absence of a significant immune response. Mice injected with non-transduced cells, GFP vector-transduced cells, and *wtIL-7Rα* transduced cells did not consistently develop disease, though one animal injected with GFP vector-transduced cells did develop leukemia 110 days after injection, presumably due to retroviral integration activating an oncogene. In contrast, mice injected with *IL-7Rα-GOF* developed clinical disease necessitating euthanasia an average of 43 days after injection (Figure 10A). Clinical disease varied between experiments. Typically, disease onset was manifest as skin crusting, dyspnea, hunching, and/or reduced ambulation.

Mice injected with *IL-7Rα-GOF* thymocytes consistently developed inflammation in the liver and lungs and, more variably, skin. In some animals, inflammation was also present in the gastrointestinal tract, kidney, skeletal muscle, and cardiac muscle. Grossly, inflammatory infiltrates were visible as variably-sized white to yellow foci scattered throughout the affected lungs and liver. Skin of the ears, face, tail, and footpads was crusted and thickened with loss of facial hair in more severe cases (Figure 10B). Histologically, inflammation consisted of a mixed population of mononuclear cells including lymphocytes and macrophages intermingled with neutrophils. Cutaneous

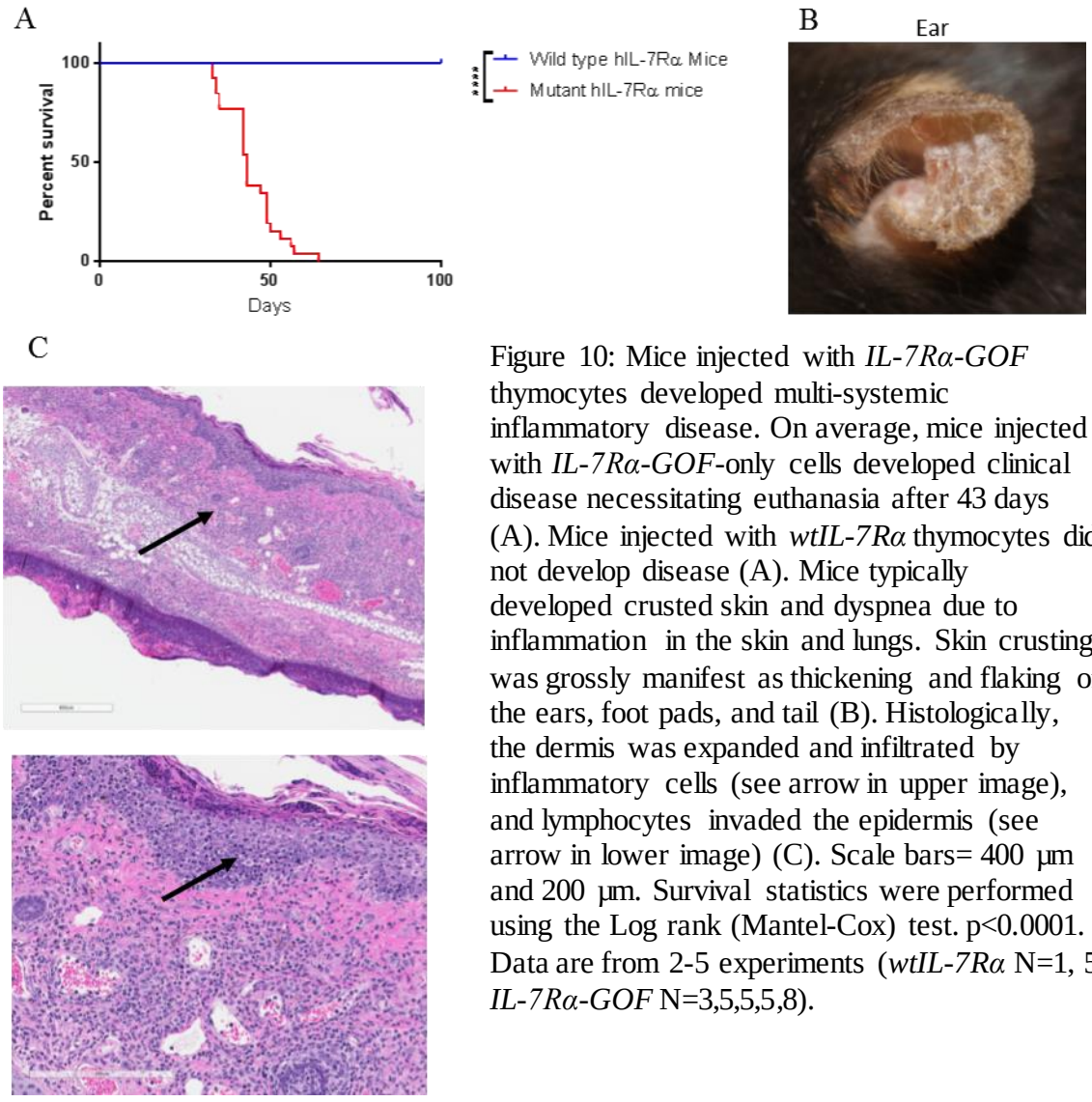

Figure 10: Mice injected with *IL-7Rα-GOF* thymocytes developed multi-systemic inflammatory disease. On average, mice injected with *IL-7Rα-GOF*-only cells developed clinical disease necessitating euthanasia after 43 days (A). Mice injected with *wtIL-7Rα* thymocytes did not develop disease (A). Mice typically developed crusted skin and dyspnea due to inflammation in the skin and lungs. Skin crusting was grossly manifest as thickening and flaking of the ears, foot pads, and tail (B). Histologically, the dermis was expanded and infiltrated by inflammatory cells (see arrow in upper image), and lymphocytes invaded the epidermis (see arrow in lower image) (C). Scale bars= 400 µm and 200 µm. Survival statistics were performed using the Log rank (Mantel-Cox) test. $p<0.0001$. Data are from 2-5 experiments (*wtIL-7Rα* N=1, 5; *IL-7Rα-GOF* N=3,5,5,5,8).

inflammation consisted of intense dermal infiltrates with less severe epidermal infiltration. In some areas, inflammation was associated with individual keratinocytes apoptosis. The epidermal surface was variably covered with thick, serocellular crusts (Figure 10C). In the lungs, inflammation was peribronchiolar and perivascular, and there was concurrent eosinophilic crystalline pneumonia in many cases. Inflammatory cells

variably infiltrated bronchiolar epithelium. In the liver, inflammation was centered on the portal triads, inducing biliary hyperplasia, periportal fibrosis, and variable degrees of hepatocellular loss. Similarly, biliary epithelium was variably infiltrated by inflammatory cells. Inflammation in the muscle and kidney was minimal and consisted predominantly of mononuclear cells. Spleens were variably infiltrated by mononuclear cells and neutrophils. Overall, the inflammatory lesions seen in mice injected with *IL-7Rα-GOF* cells were similar to the lesions associated with graft-versus-host disease (Diana Haines, personal communication).

Examination of GFP-immunolabeled skin, liver, and lung showed that the *IL-7Rα-GOF* (GFP^+) cells were present in areas of inflammation and were admixed with many GFP^- mononuclear cells and neutrophils (Figure 11A). Flow cytometry on the thymus, spleen, bone marrow, and peripheral blood showed that a majority of GFP^+ cells were $Thy1.2^+$. Of these, cell populations consisted predominantly of $CD4^+$ and $CD8^+$ populations (Figure 12A).

Mutant *IL-7Rα*-associated inflammation induces increases in serum cytokines and chemokines

Consistent with the inflammation seen in multiple tissues, analysis of serum cytokines showed significant increases in many inflammatory cytokines in mice injected with *IL-7Rα-GOF* compared to mice injected with *wtIL-7Rα* and C57BL/6 mice. The most prominently elevated serum cytokines/chemokines included IL-5, IL-6, CXCL10, CCL2, CCL3, CCL4, and CXCL9. Significant elevations in serum IFNγ, IL-10, IL-12 p70, IL-13, IL-17, and TNFα were also present (Figure 13). Slight (though significant) elevations were present in serum IL-1b, IL-3, and IL-9 (data not shown). There was no

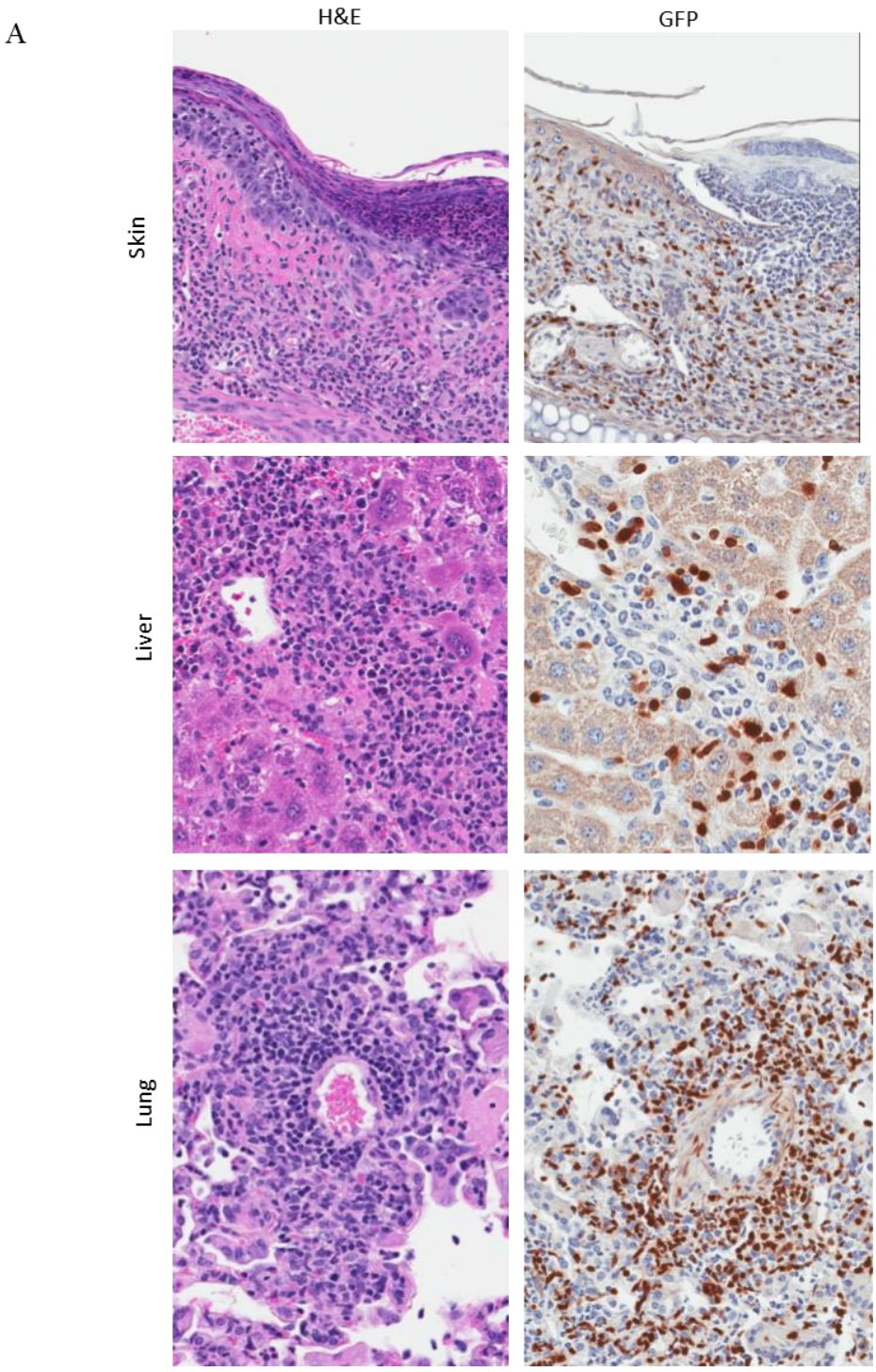

Figure 11: Immunohistochemistry showed that inflammation consisted of GFP^+ transduced cells and non-transduced cells. Examination of H&E and GFP-immunolabeled skin, liver, and lung showed many GFP^+ cells admixed with GFP^- mononuclear cells and neutrophils.

A

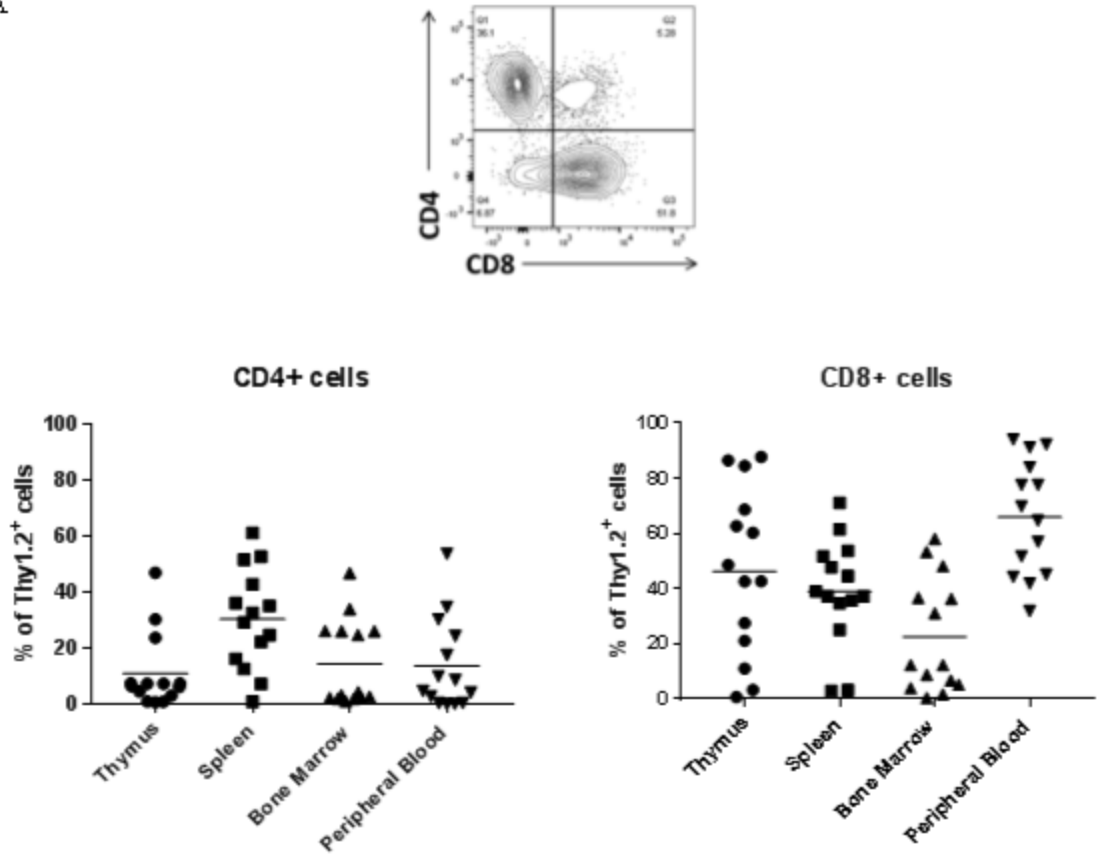

Figure 12: Cells transduced with *IL-7Rα-GOF* were predominantly CD4+ and CD8+ T-cells. Flow cytometry showed that the Thy1.2+ cell populations were a mixture of CD4+ and CD8+ populations.

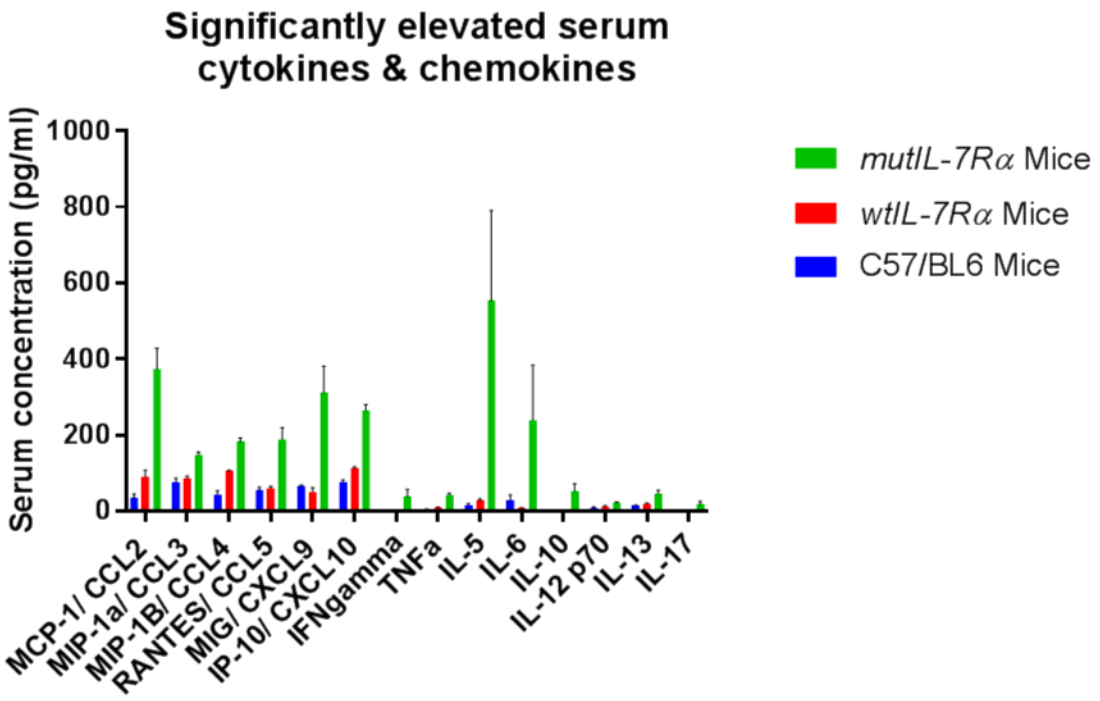

Figure 13: Serum cytokines and chemokines were elevated in *IL-7Rα-GOF* mice. Analysis of serum cytokine levels by laser bead multiplexing showed that many cytokines and chemokines were elevated in mice injected with *IL-7Rα-GOF* thymocytes compared to mice injected with *wtIL-7Rα* thymocytes or naïve C57BL/6 mice. The graph shows cytokines/ chemokines that were significantly elevated in *IL-7Rα-GOF* mice. Each analysis was performed with two technical replicates, and the average of the two values is shown. Statistics were performed using the Mann-Whitney test to compare *IL-7Rα-GOF* mice to controls.

significant difference between groups in levels of eotaxin, G-CSF, VEGF, IL-2, LIX, LIF, IL-15, IL-7, GM-CSF, IL-4, KC, or M-CSF. Animals injected with *wtIL-7Rα* had significant, though slight, increases in IL-1a, MIP-2, and IL-12 p40 (data not shown).

Mutant *IL-7Rα* cells are variably oligoclonal

Clonality of transduced cells was assessed using ligation-mediated PCR to identify retroviral integration sites in the splenic DNA from mice injected with *IL-7Rα-*

GOF cells. This showed that the transduced cells were relatively oligoclonal (Figure 14A).

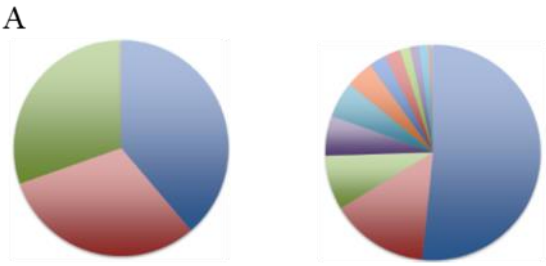

Figure 14: Populations of *IL-7Rα-GOF* cells have variable clonality.Assessment of clonality using ligation-mediated PCR to identify retroviral integration sites showed that cell populations in the two examined animals were relatively oligoclonal (A). Each pie chart represents a single mouse, and each pie wedge represents a unique retroviral integration site. A single clone may have more than one integration site. Numbers below the pie charts indicate the ear tag number of the individual animal.

Neither $CD4^+$ nor $CD8^+$ cells induce inflammation in recipient mice

In an effort to identify the cell population responsible for inciting inflammation in recipient mice, "untouched" $CD4^+$ and "untouched" $CD8^+$ cells were purified from the spleens of affected mice using magnetic beads to bind and remove lineage positive cells. The term "untouched" refers to the Invitrogen kit (described in the materials and methods) that isolates lineage negative cells by binding lineage positive cells to magnetic beads (negative selection); lineage negative cells, therefore, remain "untouched" by magnetic beads. (Lineage markers included CD11b, CD16/32, CD45R, Ter-119, and either CD4 or CD8 to remove myeloid cells, B-cells, erythroid cells, and mature T-cells.) Animals injected with $CD4^+$ or $CD8^+$ cells did not develop disease in a time frame

consistent with disease induced by *IL-7Rα-GOF* cells in donor animals (Figure 15A&B). This suggested either that the $CD4^+$ and $CD8^+$ cell populations were not responsible for the inflammatory lesion, or that the inflammatory lesion was not able to be passaged.

Inflammation is not driven by dysregulation of T_{reg} or Th17 populations

We hypothesized that *IL-7Rα-GOF* inflammation might be driven by dysregulation of the T_{reg}-Th17 balance. To address this hypothesis, we analyzed the populations of T_{reg} and Th17 cells in inflamed tissues. Populations of $CD4^+CD25^+FOXP3^+$ T_{reg} cells did not appear to be decreased in the bone marrow, spleen, liver, or thymus of recipient animals (Figure 16).

Intracellular labeling for IL-17a in PMA/ionomycin-stimulated cells from a single mouse injected with *IL-7Rα-GOF* cells did not identify $CD4^+$IL-$17a^+$ (Th17 cells) populations in the spleen, bone marrow, liver, or thymus (Figure 17). In the lungs of this mouse, there was a population of $CD4^-$IL-$17a^+$ cells. These were not consistent with Th17 cells (which are $CD4^{+)}$, but could represent T_c17 cells which are $CD8^+$ IL-17-producing cells (Figure 17). Given that there were many dead cells in the pulmonary tissue preparation, and intracellular labeling is notoriously prone to background labeling, this population could also have been a labeling artefact.

Because intracellular labeling for IL-17 was not conclusive, we next transduced the thymocytes from an IL-17 reporter mouse with *IL-7Rα-GOF* to better determine whether the mutant signaling was inducing IL-17 production (Shen et al., 2014). This transgenic mouse was designed to link IL-17a expression with TdTomato expression and IL-17f expression with GFP expression. Therefore, IL-17 producing cells can be

A

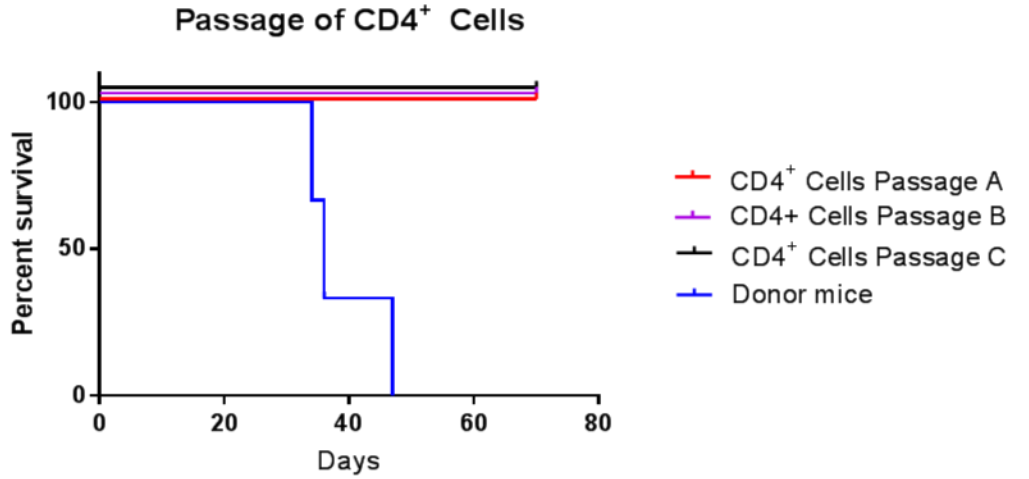

B

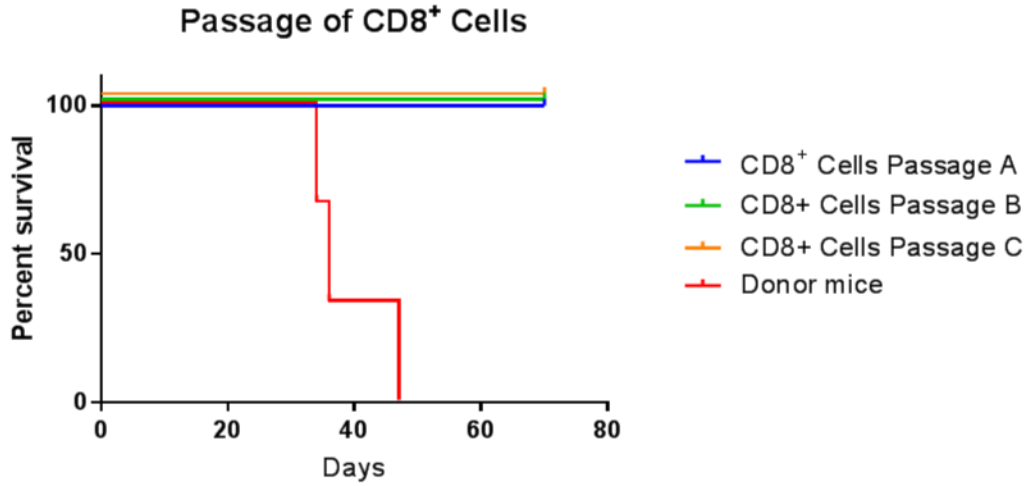

Figure 15: Injection of untouched CD4+ and CD8+ cells did not cause inflammation. CD4+ and CD8+ cells from mice injected with *IL-7Rα-GOF* were isolated using magnetic beads and injected into recipient Rag1-/- mice. Mice did not develop clinical disease in the same period as donor mice (A&B). N=1-2 mice/ passage.

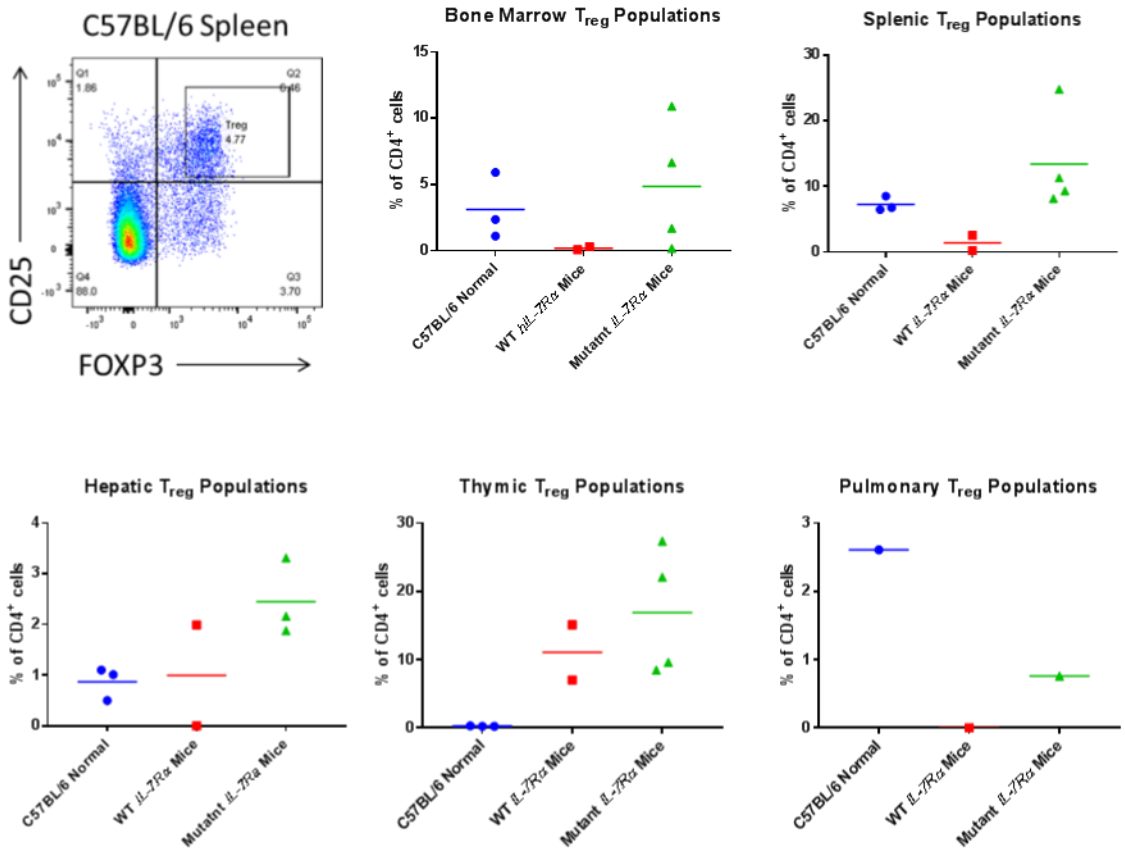

Figure 16: Populations of Treg cells are not reduced in *IL-7Rα-GOF* mice. Flow cytometry showed that CD4+CD25+FOXP3+ Treg cells in the bone marrow, spleen, liver, and lung were present in higher percentages in mice injected with *IL-7Rα-GOF* thymocytes than animals injected with wtIL-7Rα thymocytes. Data are from a single experiment. C57BL/6 N= 3, wtIL-7Rα N=2, and *IL-7Rα-GOF* N=4 (3 livers); lung N=1.

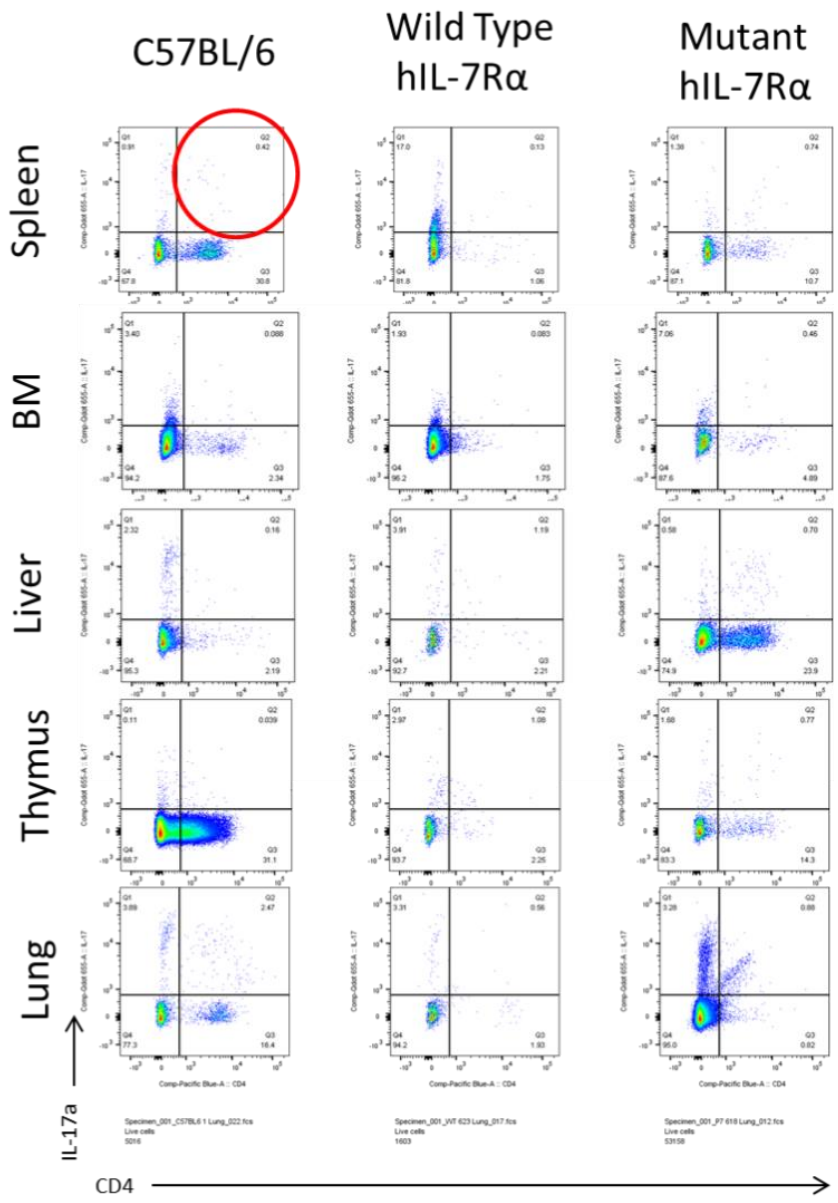

Figure 17: Populations of IL-17 producing cells identified by intracellular labeling were not increased in *IL-7Rα-GOF* mice. Cells from the spleen, bone marrow, liver, thymus, and lung were harvested and stimulated with PMA/ionomycin in the presence of a protein transport inhibitor to trap cytokines produced upon stimulation. Flow cytometry on these cells did not show significant populations of CD4+IL-17a+ cells in any of the examined tissues as highlighted by the red circle. The lungs of the mouse injected with *IL-7Rα-GOF* thymocytes contained a potential small population of IL-17a+ cells that may or may not have been artefact. Data are from a single experiment. C57BL/6 N= 1, wtIL-7Rα N=1, and *IL-7Rα-GOF* N=1

identified directly based on GFP and/or TdTomato expression rather than performing PMA/ionomycin-stimulation and intracellular labeling. It was hoped that this approach would minimize flow cytometry artefacts. Analysis of cells from the blood, spleen, liver, lung (shown), bone marrow, and thymus (not shown) of mice injected with *IL-7Rα-GOF* transduced into IL-17 reporter mouse thymocytes did not reveal significant populations of GFP$^+$ or TdTomato$^+$ populations (Figure 18). This indicated that *IL-7Rα-GOF* did not

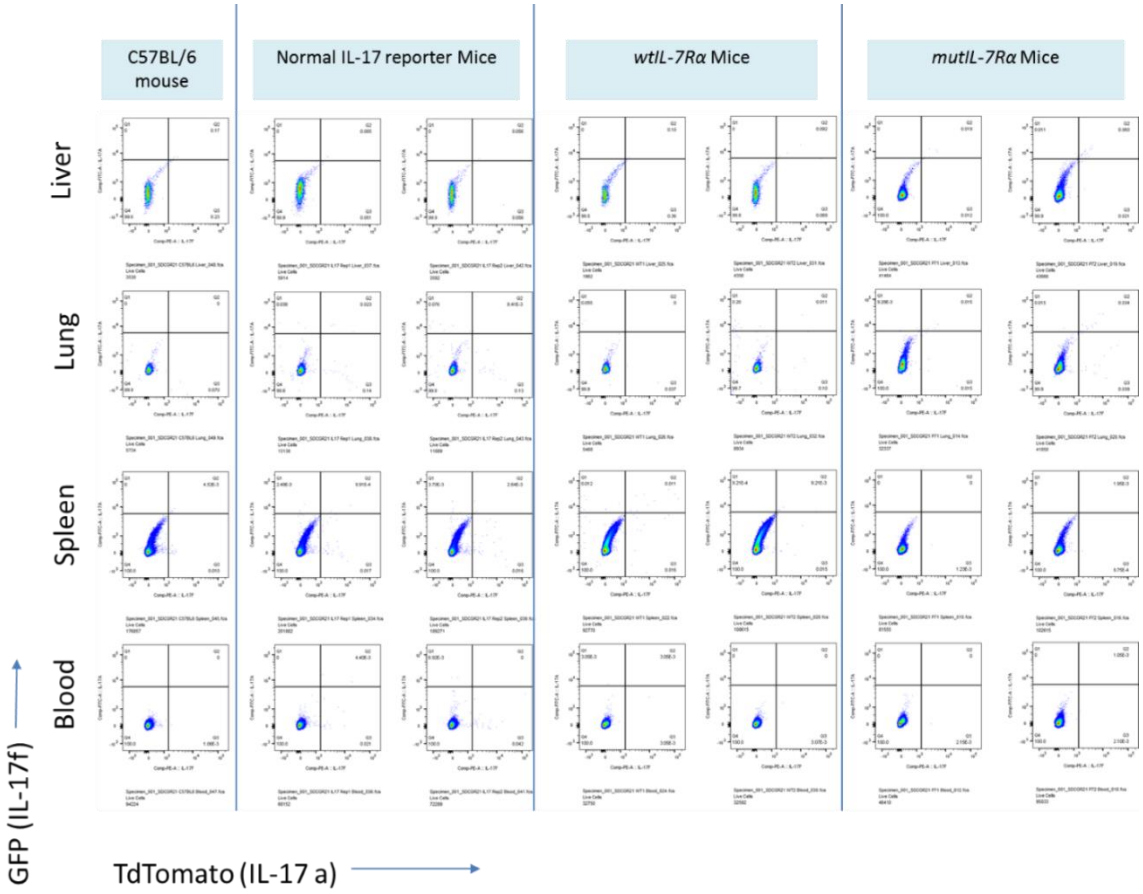

Figure 18: Use of IL-17 reporter mouse thymocytes does not demonstrate IL-17+ cell populations. Thymocytes from a transgenic mouse engineered to link IL-17a expression with TdTomato expression and IL-17f expression with GFP expression did not show TdTomato+ or GFP+ cell populations in tissues of mice injected with *IL-7Rα-GOF* thymocytes. N=1-2 mice as shown.

induce appreciable production of IL-17 in transduced thymocytes. The origin of the increased levels of IL-17 in the serum of some mice is unknown.

Discussion

***In vitro* experiments**

Experiments to establish culture techniques demonstrated that CD4-CD8 depleted thymocytes cultured on OP9-DL4 stromal cells were the best cell preparation, though there was a slight increase in the $CD11b^+$ population immediately after harvest. This population was lost after culture on the OP9-DL4 stromal cells, suggesting that $CD11b^+$ cells do not significantly contaminate transduced populations. Transduction of these cells using the OP9-DL4 stromal system for activation was successful, yielding consistent rates of 30-40% transduced cells. Cells transduced with *IL-7Rα-GOF* out-competed non-transduced cells in culture over time, suggesting that the mutation conferred a growth advantage.

The DN3 to DN4 maturational shift seen with IL-7 removal may occur because DN3 cells are IL-7-dependent while DP cells are not (Hong et al., 2012; Van de Wiele et al., 2004). Removal of IL-7 likely drives rapid maturation of cells from DN3 through DN4 to the DP stage to enable survival. Consistent with this, removal of IL-7 resulted in death of non-transduced and *wtIL-7Rα* cells over several days. Transduction with *IL-7Rα-GOF* prevented this maturational shift and enabled IL-7 independent growth. This suggests that constitutive signaling by the mutant receptor is able to replace exogenous IL-7 signaling for survival in primary murine thymocytes.

Culturing thymocytes transduced with *IL-7Rα-GOF* on OP9-DL4 stromal cells consistently yielded a population of $CD8^+TCR\beta^+$ cells that were more prevalent than in

wtIL-7Rα or non-transduced thymocytes. This expansion of $CD8^+$ cells was likely due to constitutive IL-7 signaling, since this is known to promote differentiation of DP cells into $CD8^+$ cells, in part due to silencing of CD4 genes (Hong et al., 2012; Yu et al., 2003). The expression of TCRβ by $CD8^+$ cells suggests maturity, and OP9-DL1 cells have been shown to support maturation of conventional $CD8^+$ cells (Dervovic et al., 2013).

***In vivo* experiments**

Mutant *IL-7Rα* transduced thymocytes consistently induced inflammation in recipient mice, while *wtIL-7Rα* transduced thymocytes did not. This is in contrast to studies performed in our laboratory and others. In our laboratory, previous work has shown that transduction of bone marrow cells leads to myeloproliferation. These cells were not cultured on the OP9-DL4 stromal cell system prior to injection into mice. Similarly, work by another group has failed to show an inflammatory phenotype associated with *IL-7Rα-GOF* transduction. In these studies, bone marrow cells and T-cell progenitor cells were transduced with *IL-7Rα-GOF* then injected into irradiated BALB/c mice. T-cell progenitors were generated by culturing $lineage^-kit^+$ stem cells on OP9-DL1 cells prior to transduction. Mice injected with transduced bone marrow cells developed rapid-onset myeloproliferative disease, and mice injected with transduced lymphoid progenitor cells did not develop disease (Yokoyama et al., 2013). These differences may be due to variations in starting cells, cell culture techniques, or recipient mice.

The inflammation was morphologically consistent with graft-versus-host disease, but it was not clear why the mutant receptor would preferentially induce this lesion. We hypothesized that the inflammation induced by *IL-7Rα-GOF* might be mediated by IL-17 signaling. We based this hypothesis on several factors. Several reports suggested

that IL-7 signaling could skew the balance between T_{reg} populations and T_h17 populations, leading to reduced T_{reg} cells and increased T_h17 cells (Diller et al., 2016; Joller et al., 2014). Furthermore, the morphology of the inflammation was consistent with an IL-17-induced lesion, as there was a marked neutrophilic component. Lastly, serum cytokine levels of IL-17 were significantly increased in mice injected with *IL-7Rα-GOF* thymocytes. However, experimental data did not support this hypothesis, as *IL-7Rα-GOF* mice did not have decreased populations of T_{reg} cells or increased populations of IL-17-producing cells. The mechanism by which *IL-7Rα-GOF* cells induce inflammation remains unknown.

Chapter 4: *TLX3* expression and *Hoxa* overexpression do not cause T-ALL in collaboration with mutant *IL-7Rα-GOF*

Introduction

The second aim of this project focused on providing experimental support of patient data that suggested oncogenic collaboration between mutant *IL-7Rα-GOF* and candidate genes to generate T-ALL. At the initiation of the project, we defined a list of criteria that we expected would occur when experimental evidence indicated that a combination of mutations was adequate to drive neoplastic transformation. These included: 1) rapid-onset disease, 2) lesions consistent with leukemia/lymphoma, 3) T-cell origin of leukemic cells, 4) polyclonal cell populations, 5) serial passage success, and 6) high leukemia-initiating cell frequency. Chapter 2 contains a review of genes known or suspected to collaborate with mutant *IL-7Rα* to cause ALL. Here, we review and provide additional details about the potential *IL-7Rα* collaborators *TLX3* and *HOXA* and describe the results of experiments combining these genetic lesions with IL-7Rα mutation.

TLX3 (HOX11L2)

Approximately 15-25% of pediatric T-ALL patients have the cryptic translocation t(5;14)(q35;q32.2) that results in the aberrant expression of *TLX3* in T-cells (Ballerini et al., 2002; Bernard et al., 2001; Cave et al., 2004; MacLeod et al., 2003; Noronha et al., 2016). Overexpression of the gene has been shown in up to 60% of pediatric T-ALL patients (Mauvieux et al., 2002). Overexpression of *TLX3* has been related to poor prognosis in some reports, but not in others, and expression levels can be used as a marker to assess minimal residual disease (Ballerini et al., 2002; Ballerini et al., 2008; Cave et al., 2004; Ma et al., 2014). In affected patients, fluorescent *in situ* hybridization is

required to identify the translocation, as conventional cytogenetic analysis does not detect it (Helias et al., 2002). This translocation juxtaposes *BCL11B* and *TLX3*, leading to ectopic expression of *TLX3* in T-cells (MacLeod et al., 2003; Su et al., 2006b).

In addition to the t(5;14)(q35;q32.2) translocation that was initially described, additional chromosomal translocations leading to overexpression of *TLX3* have been identified including t(5;7)(q35;q21), t(2;5)(p21;q35), and t(5;10)(q35;q21) translocations (Su et al., 2004). Genes affected by these translocations include *BCL11B*, which is vital to alpha/beta T-cell development, and *CDK6*, a gene which is involved in T-cell development (Su et al., 2004). Previous work has assessed the transforming capacity of *TLX3 in vivo* by transducing murine bone marrow cells with retroviral vectors expressing *TLX3*. Cells transduced solely with *TLX3* did not survive *in vivo*, suggesting that *TLX3* requires collaborating mutations to generate T-ALL (Su et al., 2006a). Potential collaborating genetic aberrations include *PHF6* mutation, *WT1* deletion, *FBXW7* deletion, and other recurrent deletions (Van Vlierberghe et al., 2008a; Van Vlierberghe et al., 2010).

HOXA

Similar to *TLX3*, the *HOXA* gene cluster is affected by dysregulating translocations in a subset of T-ALL, but the frequency of *HOXA* patients is lower, representing less than 10% of patients (Meijerink, 2010). The *HOXA* gene cluster contains eleven members, *HOXA1*, *HOXA2*, *HOXA3*, *HOXA4*, *HOXA5*, *HOXA6*, *HOXA7*, *HOXA9*, *HOXA10*, *HOXA11*, *HOXA13* (Speleman et al., 2005). Several translocations affecting the *HOXA* gene cluster have been identified. The recurrent translocation inv(7)(p15q34) juxtaposes the *HOXA* gene cluster with the *TCRβ* locus,

leading to increased expression of the *HOXA* genes *HOXA10* and *HOXA11* (Speleman et al., 2005). Juxtaposition of the *HOXA* gene cluster with the *TCRβ* locus has also been seen in other cases, and this may cause overexpression of some or all *HOXA* genes (Cauwelier et al., 2007; Speleman et al., 2005). In addition, *HOXA* gene cluster dysregulation may occur in *MLL* and *CALM-AF10* cases of T-ALL (Bergeron et al., 2006; Soulier et al., 2005). Similar to *TLX3*, a *BCL11B-HOXA13* fusion has also been identified which leads to *HOXA13* overexpression (Su et al., 2006a). In addition, the *SET-NUP214* fusion causes activation of *HOXA* cluster genes by binding to *HOXA* promoter regions (Van Vlierberghe et al., 2008b). *Hoxa9* has been shown to collaborate with *Meis1a* to generate acute myeloid leukemia (Kroon et al., 1998). In T-ALL, a *Hoxa9*-overexpressing transgenic mouse has been shown to develop T-ALL with spontaneous *NOTCH1* mutations (Beachy et al., 2013).

Materials and Methods

Thymocyte transduction and culture

Thymocytes were harvested from 3-6 week old C57Bl/6J female donor mice by first mechanically dissociating the tissue into a single cell suspension. Cells were then bound to CD4 and CD8 microbeads (Miltenyi) and passed through an LD column (Miltenyi) to isolate double negative cells according to the manufacturer's instructions. Resulting double negative cells were cultured on OP9-DL4 bone marrow stromal cells for 1 day, then transduced twice with retroviral vectors with approximately 18 hours between transductions. Thymocytes were transduced by spinoculation (centrifugation at 2000 rpm

for 60 minutes) with addition of 8µg/ml polybrene (Chemicon) to the transduction solution. After transduction, thymocytes were maintained on OP9-DL4 cell culture for an additional 7-8 days prior to injection into mice to allow for expansion of cell numbers.

Retroviruses were generated using Phoenix-Eco packaging cells (Orbigen). Phoenix cells were cultured in DMEM containing glucose, L-glutamine, and sodium pyruvate (Corning), with 50 ml of fetal bovine serum added to every 500 ml of DMEM. Phoenix cells were transfected with pMIG plasmids containing mutant *hIL-7Rα* or *hTLX3* (Dharmacon, Lafayette, CO). cDNAs of *hIL-7Rα* mutant and *hTLX3* were subcloned into pMIG vector by gateway cloning or PCR cloning methods by Wenqing Li. The *hIL-7Rα* mutant sequence was c.731_732insTTGTCCCAC, based on the mutation in subject P2 and was confirmed by sequencing previously by our laboratory (Zenatti et al., 2011). Thymocytes for the *Hoxa* experiments were isolated from the thymus of a *NUP98-HOXD13* transgenic mouse (Lin et al., 2005).

Transfection was performed using lipofectamine (Invitrogen) and OPTI-MEM I reducing serum medium (Invitrogen) 48-72 hours prior to thymocyte transduction. Phoenix cell supernatants containing retroviruses were filtered using a 0.45 µm syringe filter (Millex) prior to transduction of thymocytes. OP9-DL4 cells were cultured according to published guidelines used for culture of OP9-DL1 cells and were cultured in MEM-alpha medium (Gibco). For 500 ml of media, the following additives were included: 50 ml fetal bovine serum (GE life Sciences), 3 ml fresh (frozen to maintain freshness) L-glutamine (Sigma), 0.5 ml 2-mercaptoethanol (Gibco), and 2.5 ml penicillin/ streptomycin (Gibco). When thymocytes were added to culture, growth was supported by

the addition of 5 ng/ml mIL-7 and 5 ng/ml hFLT-3L (Peprotech) (Holmes and Zuniga-Pflucker, 2009).

Animal Experiments

Transduced cells were injected into sub-lethally irradiated, 6-15 week old, female *Rag1*$^{-/-}$ mice via tail vein in a concentration and volume of 5 x10^5 cells/ 200 µl/ mouse. Recipient mice were prophylactically treated for 3 days with SMZ antibiotics (0.08mg/ml in drinking water) either immediately prior to irradiation (initial experiments and limiting dilution experiments) or immediately following irradiation (serial passage experiments). Animals were monitored by a single, experienced technician for consistency (T.B.) and euthanized at the onset of clinical signs. Clinical signs included hunching, dyspnea, reduced ambulation, rough hair coat, crusted skin (in the mutant *IL-7Rα*-only group), or moribund status. Peripheral blood was collected immediately prior to euthanasia. Animals that required euthanasia for causes not related to development of experiment-associated disease (i.e. tail caught in caging, inner ear infection, fighting-associated skin lesions) were censored from experimental results. Technicians performing monitoring were not blinded to experimental groups.

Flow Cytometry

Thymus, spleen, and bone marrow were manually dissociated to single cell suspensions. Liver was dissociated using a Stomacher tissue lyser. Lungs were digested in a solution of 0.25 WU/mL TM liberase (Roche) in 2% glucose PBS. After placing dissected lobes in 3 ml of digestion solution in a C tube (Miltenyi), dissociation was performed using the Miltenyi gentleMACS Lung1 program. Dissociated lungs were incubated for 30 minutes at 37 degrees Celsius. Then, tissues were further dissociated

using the Lung 2 program. Red blood cell lysis was applied to these tissues as well as to peripheral blood using ACK Lysing Buffer (Lonza). Resultant suspensions were stained with Zombie Red live/dead fixable stain (Biolegend) for 15 minutes at room temperature. Then, CD16/32 Fc receptor block (93) was applied at a 1:400 dilution for 10-15 minutes (Biolegend). Cocktails of fluorochrome-conjugated antibodies were applied to cells for 15 minutes on ice, including the following antibodies: anti-Thy1.2 APC-Cy7 (30-H12), anti-CD4 PE-C7 (GK1.5), anti-CD8 Brilliant Violet 421 (53-6.7), anti-CD44 PerCP-Cy5.5 (IM7), anti-CD25 Brilliant Violet 650 (PC61), anti-TCRβ Alexa Fluor 700 (H57-597), anti-CD3 Brilliant Violet 421 (17A2), anti-Ly6G Pe-Cy7 (1A8) from Biolegend; anti-CD11b PerCP-Cy5.5 (M1/70), anti-B220 APC (RA3-6B2) from BD Biosciences. Fluorescence minus one (FMO) labeling was used for controls (Figure 2). Cells were then fixed in stabilizing fixative (BD Biosciences) for 30 minutes. Fixative was removed, and flow cytometric analysis was performed on an LSRIISORP cytometer with FACS DIVA software. Data analysis was performed using FlowJo, and gating strategy is included in the materials and methods in Chapter 2 (Tree Star, Inc.).

Histopathology, Immunohistochemistry, and Digital Slide Analysis

Tissues were fixed in 10% neutral buffered formalin and transferred to 70% ethanol after complete fixation. Samples were trimmed, paraffin-embedded, sectioned, and stained with hematoxylin and eosin according to standard histotechnological procedures.

Immunohistochemistry was performed by the Pathology/ Histotechnology Laboratory using previously optimized protocols. Immunohistochemistry utilized anti-GFP antibody (Abcam ab6556) at 1:1000 dilution with proteolytic digestion using

proteinase K (DAKO) incubated overnight at 4 degrees C; anti-CD3 antibody (Bio-Rad #MCA1477) at 1:100 dilution incubated for 60 minutes with heat-induced epitope retrieval using citrate (Leica Biosystems) for 20 minutes; and anti-ki67 antibody (Abcam #ab16667) at 1:100 dilution incubated for 30 minutes with heat-induced epitope retrieval using citrate for 20 minutes. For all protocols, DAB (Sigma & Leica Biosystems) was used as the chromogen, and hematoxylin (Leica Biosystems) was used as a counterstain.

Slides were digitalized using an Aperio AT2 slide scanner (Leica) at a magnification of 20x. Digital slides were viewed in ImageScope (Aperio), and digital slides were used to generate images of the tissues. Digital image analysis of ki67 labeling was performed using an optimized Aperio Nuclear v9 algorithm.

Ligation-Mediated PCR

Oncogenes were transfected using retroviral vector and thus each original cell carried a unique molecular barcode that could be used to assess clonality by identifying the frequency of retroviral integration as described previously (De Ravin et al., 2016; Maldarelli et al., 2014). The integration sites were cloned from 5LTR-genomic junction using primers specific for the vector used in this study (MFGS5LTR, 5'ATGGCGTTACTTAAGCTAGCTTG 3', MFGS5LTRnest, CAAACCTACAGGTGGGGTCTTTC 3'). Integration site junctions were mapped to mouse genome build mm10. Frequency of each clone was calculated as the percentage of read numbers for each integration sites out of total mapped reads.

Statistics

For most studies, statistics were performed using GraphPad Prism version 6.00 for Windows (GraphPad Software, La Jolla, CA). To compare more than two groups,

Kruskall-Wallis analysis was performed, and the Mann-Whitney test was used to compare two groups. Survival curve analysis was performed using the Log-rank test. For the limiting dilution studies, extreme limiting dilution analysis was performed using software from the Walter and Eliza Hall Institute of Medical Research, available at the following website: http://bioinf.wehi.edu.au/software/elda/ (Hu and Smyth, 2009).

Results

Combination of TLX3 expression and mutant *IL-7Rα-GOF*

TLX3 drives the immunophenotype of cultured TLX3-IL-7Rα-GOF cells

Combination of human *TLX3* expression and mutant *IL-7Rα-GOF* was achieved by transduction of primary immature $CD4^-CD8^-$ thymocytes from C57BL/6 donors with retroviral vectors containing either human *TLX3* or mutant human *IL-7Rα-GOF*. After transduction, cells were cultured on the OP9-DL4 stromal cell system for 8 days with hFLT3-L and mIL-7 then injected into sub-lethally-irradiated *Rag1*$^{-/-}$ mice. In the *TLX3*-only and *TLX3-IL-7Rα-GOF* cells, GFP was included in the TLX3 plasmid; the *IL-7Rα-GOF* plasmid did not include GFP. In the *IL-7Rα-GOF-only* cells, the *IL-7Rα-GOF* plasmid included GFP.

Analysis of cells at the time of injection showed that cultured cells transduced with both the *TLX3* and *IL-7Rα-GOF* plasmids had a moderate percentage of GFP^+ cells as compared to *TLX3*-only cells (Figure 19A). There were very few *TLX3*-only transduced cells, suggesting that these cells did not survive and/or proliferate well in culture. Therein, addition of *IL-7Rα-GOF* appeared to improve *in vitro* survival of *TLX3*-transduced cells. In each group, almost all of the cells expressed Thy1.2, consistent with

T-cell lineage. Within the GFP^+ populations, *TLX3-IL-7Rα-GOF* cells and *TLX3*-only cells were both predominantly immature $CD4^-CD8^-$, whereas the *IL-7Rα-GOF*-only cells were a mixture of predominantly $CD4^-CD8^-$ and $CD8^+$ cells (Figure 19B). In the *TLX3-IL-7Rα-GOF* group, GFP^- cells may have contained a subset of cells that had been solely transduced with *IL-7Rα-GOF*, as the immunophenotype of these cells was similar to that of the *IL-7Rα-GOF*-only group with a mixture of $CD4^-CD8^-$ and $CD8^+$ (Figure 19C).

TLX3-IL-7Rα-GOF combination is not sufficient to generate T-ALL

Survival analysis of recipient mice showed that mice injected with *IL-7Rα-GOF*-only cells developed clinical signs necessitating euthanasia more rapidly than *TLX3-IL-7Rα-GOF* mice. Mice injected with *TLX3*-only cells did not develop clinical disease (Figure 20A). Sick animals showed signs of dyspnea, hunching, decreased ambulation, and occasional skin crusting. In the *TLX3-IL-7Rα-GOF* group, one (#612) of five mice developed an enlarged inguinal lymph node. This node slowly enlarged over the course of several weeks, and at the time of euthanasia, the axillary lymph node had also become enlarged. At euthanasia, both nodes were approximately 1 cm in diameter. Analysis of

Figure 19: *TLX3* expression drives the immunophenotype of transduced cells. At the time of injection into mice, there were few successfully transduced *TLX3*-only cells, as indicated by a low percentage of GFP+ cells, though cells that were transduced expressed Thy1.2 indicating T-cell lineage. A higher percentage of cells were successfully transduced in the *IL-7Rα-GOF*-only cells and the *TLX3-IL-7Rα-GOF* cells (where GFP was linked to the *TLX3* plasmid) (A). *TLX3-IL-7Rα-GOF* cells had an immunophenotype that was more similar to *TLX3*-only cells than to *IL-7Rα-GOF*-only cells, as both *TLX3-IL-7Rα-GOF* cells and *TLX3*-only cells were predominantly CD4-CD8-, while *IL-7Rα-GOF*-only cells were a mixture of predominantly CD4-CD8– and CD8+ cells (B). The GFP– cells in the *TLX3-IL-7Rα-GOF* group likely contained *IL-7Rα-GOF*-only cells, as the population had a similar immunophenotype to the *IL-7Rα-GOF*-only cells (C). Data are representative of one experiment. N=1

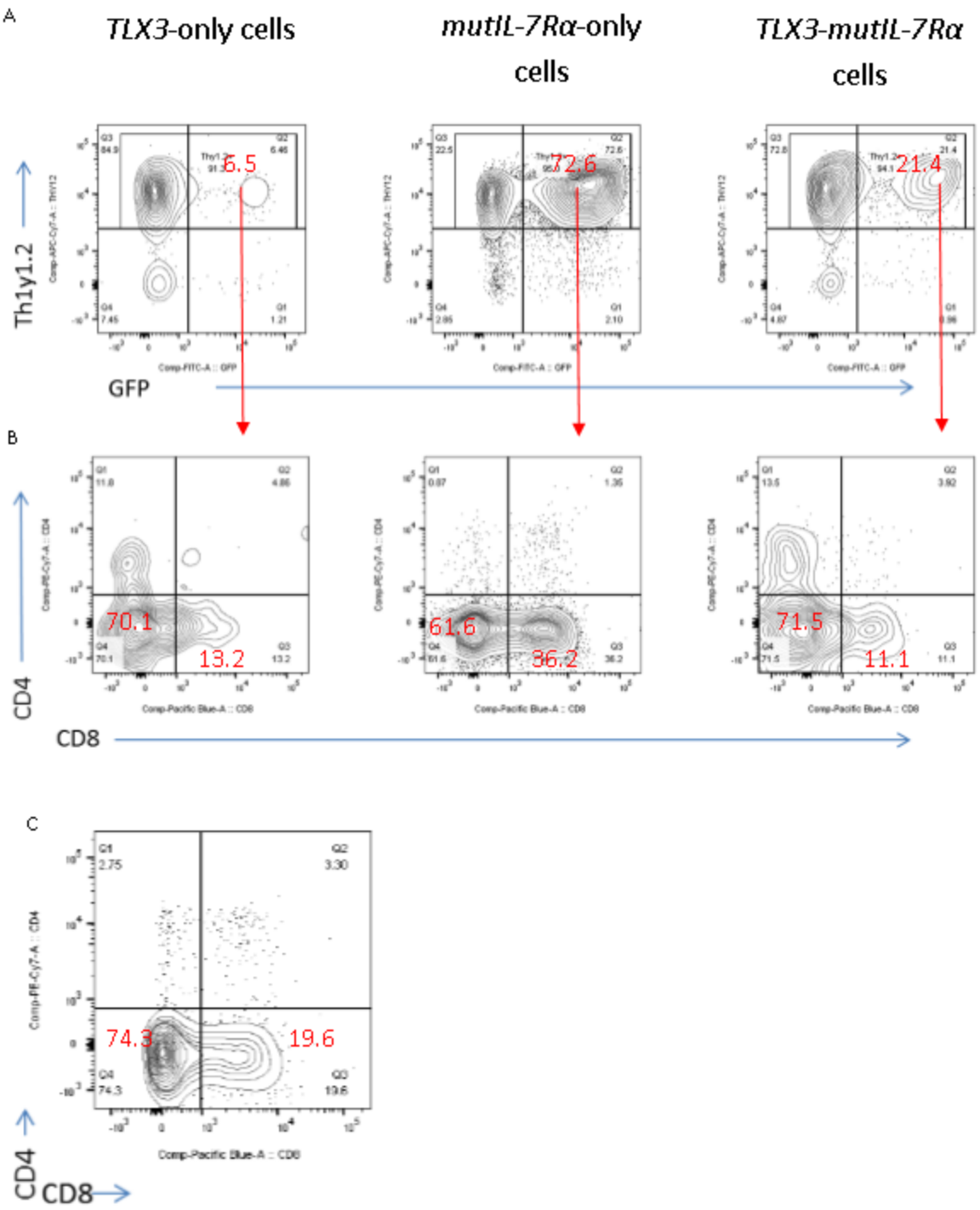
A
TLX3-only cells
mutIL-7Rα-only cells
TLX3-mutIL-7Rα cells
Th1y1.2
GFP
6.5
72.6
21.4
B
CD4
CD8
70.1
13.2
61.6
36.2
71.5
11.1
C
74.3
19.6
CD4
CD8

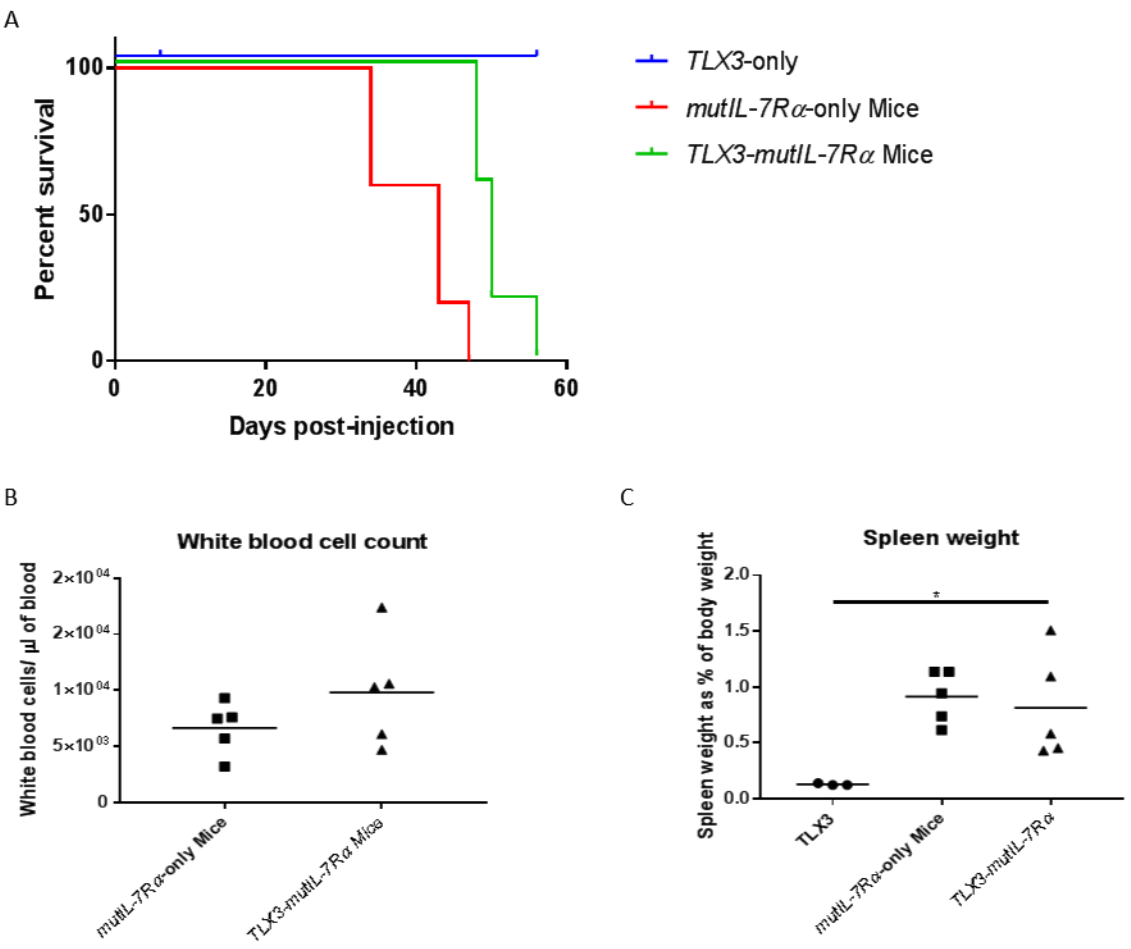

Figure 20: The combination of *TLX3* and *IL7-Rα-GOF* was not sufficient to cause T-ALL. Mice injected with *TLX3-IL-7Rα-GOF* cells developed clinical signs necessitating euthanasia after mice injected with *IL-7Rα-GOF*-only cells (A). The combination of mutations did not cause leukocytosis (B) or splenomegaly (C) relative to the *IL-7Rα-GOF*-only cells. Survival statistical analysis was performed using the Log-rank (Mantel-Cox) test. Organ weight statistics were performed using the Mann-Whitney test to compare *TLX3-IL-7Rα-GOF* mice with control groups. ($p<0.05$=*; $p<0.005$=**) *TLX3*-only N= 3; *IL-7Rα-GOF*-only N=5; *TLX3-IL-7Rα-GOF* N= 5

tissues from each group at the time of euthanasia showed that there was not a significant difference between *TLX3-IL-7Rα-GOF* mice and *IL-7Rα-GOF*-only mice in regards to white blood cell counts or splenic weight (Figures 20B-C). Histologic examination of

tissues from mice injected with *TLX3-IL-7Rα-GOF* cells showed inflammatory lesions similar to the lesions in *IL-7Rα-GOF*-only mice, as described in Chapter 3 (Figure 21). These inflammatory lesions were presumably caused by the *IL-7Rα-GOF*-only cells that were injected as part of the mixed *TLX3-IL-7Rα-GOF* cell population.

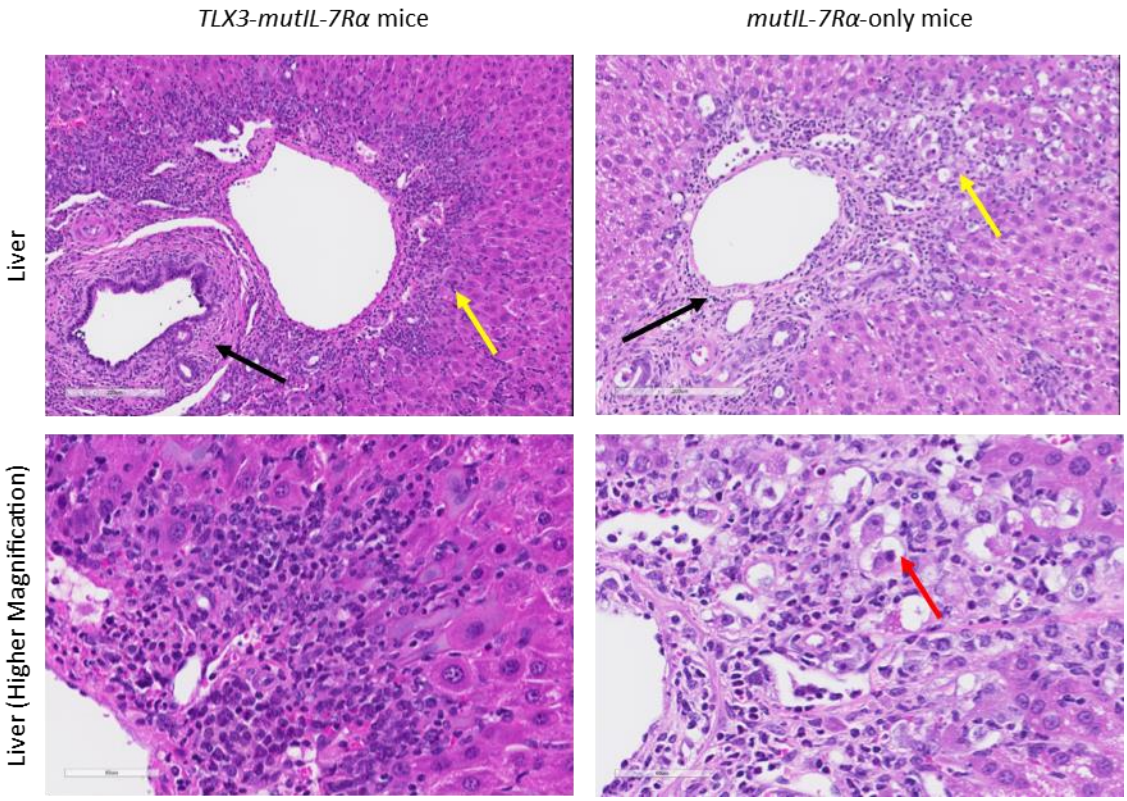

Figure 21: Mice injected with *TLX3-IL-7Rα-GOF* cells developed an inflammatory lesion similar to the mice injected with *IL-7Rα-GOF*-only cells. This was presumably because some of the injected cells were transduced only with *IL-7Rα-GOF* rather than with the combination of mutations. Associated with inflammatory infiltrates were biliary hyperplasia (yellow arrows), periportal fibrosis (black arrows), and hepatocellular apoptosis (red arrow). H&E staining; Scale bars = 200 μm (upper) and 60 μm (lower). Data are representative of one experiment.

TLX3-IL-7Rα-GOF cells are present at low frequency in tissues

Analysis of tissues from four mice injected with *TLX3-IL-7Rα-GOF* cells showed there were relatively few GFP^+ cells within the thymus, bone marrow, and peripheral

blood. Larger percentages of GFP$^+$ cells were present in the spleen of some mice, though there was variability between animals. In the tissues examined, the majority of GFP$^+$ cells were Thy1.2$^-$, suggesting loss of the T-cell phenotype (Figure 22).

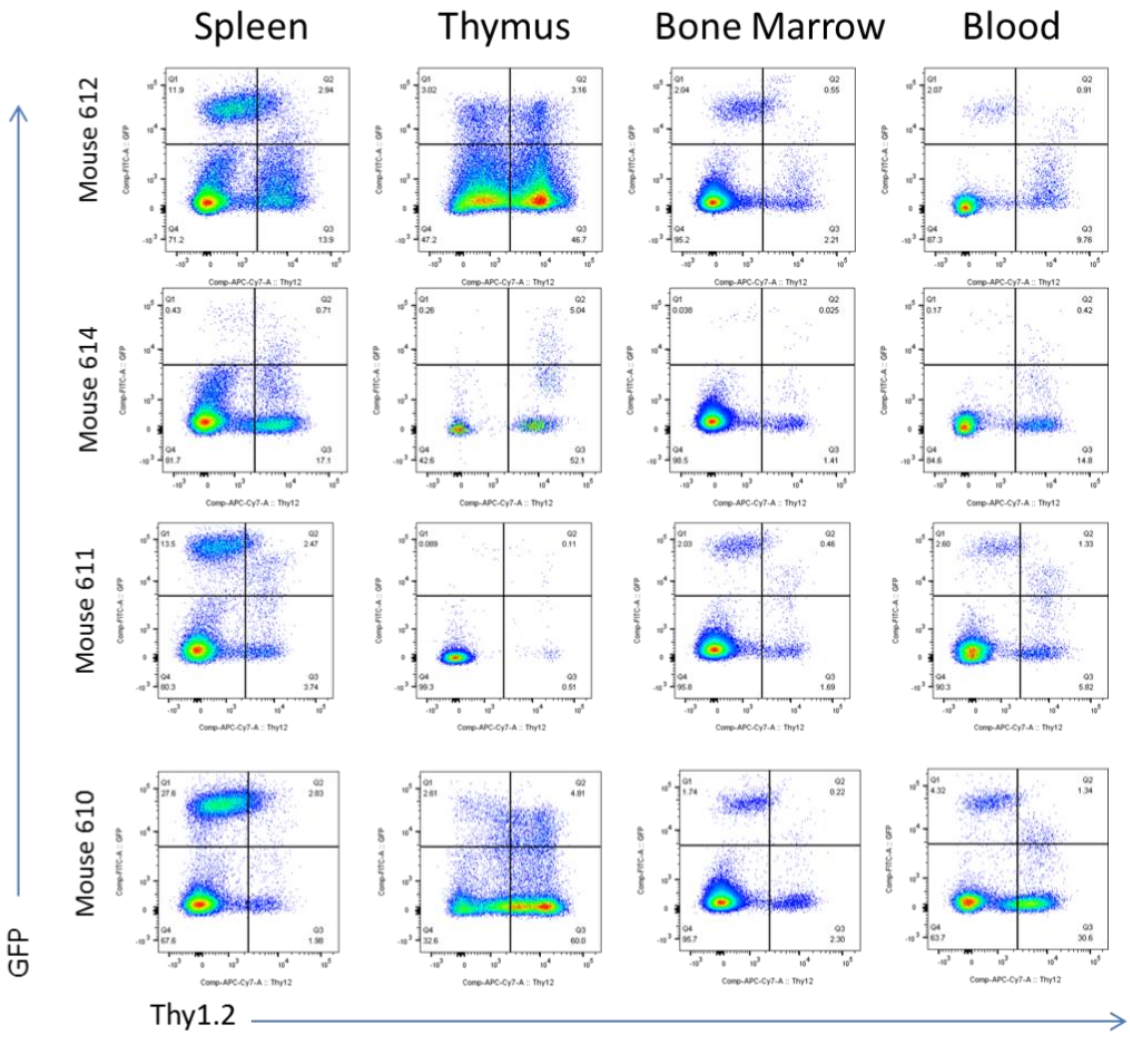

Figure 22: GFP+ cells are present in low percentages in *TLX3-IL-7Rα-GOF* mice. In mice that had developed clinical signs necessitating euthanasia, there were relatively few GFP+ cells in the thymus, bone marrow, and blood of mice injected with *TLX3-IL-7Rα-GOF* cells. The number of GFP+ cells in the spleen was more variable between mice, and the GFP+ cells that were present in the spleen were not Thy1.2+, suggesting they were not T-cells. N=4 mice.

TLX3-IL-7Rα-GOF cells cause low-penetrance T-cell lymphoma

Histologic assessment of the lymph nodes from the single mouse that developed lymphadenopathy (#612) showed that the normal nodal architecture was replaced by sheets of neoplastic round cells (Figure 23A) that expressed GFP and CD3 (Figure 23B). By flow cytometry, the majority of the GFP^+ cells were $Thy1.2^+$ but lacked expression of CD4 and CD8 (Figure 23C), consistent with an immature T-cell phenotype.

Combination of *Hoxa* overexpression and mutant *IL-7Rα*

Hoxa drives the immunophenotype of cultured Hoxa-IL-7Rα-GOF cells

To evaluate the combination of mutant *IL-7Rα* and *Hoxa* overexpression, cells were cultured in a manner similar to the *TLX3-IL-7Rα-GOF* cells prior to injection into *Rag1*$^{-/-}$ recipient mice. However, while *TLX3-IL-7Rα-GOF* cells were sourced from the DN thymocytes of a C57BL/6J donor mouse, the *Hoxa-IL-7Rα-GOF* cells were sourced from a *NUP98-D13* transgenic mouse donor provided by the laboratory of Peter Aplan. This mouse is known to have overexpression of the *Hoxa* gene cluster and is prone to developing myeloproliferative disease (Lin et al., 2005). Therefore, all cells in the *Hoxa*-only and *Hoxa-IL-7Rα-GOF* groups had overexpression of the *Hoxa* cluster, and this was not linked to GFP expression. GFP was included in the *IL-7Rα-GOF* plasmid in both the *IL-7Rα-GOF*-only and *Hoxa-IL-7Rα-GOF* groups. Flow cytometric analysis of the cultured cells injected into recipient mice showed that almost all cells expressed Thy1.2, consistent with T-cell lineage (Figure 24). In both the *Hoxa*-only and *Hoxa-IL-7Rα-GOF* groups, cells were predominantly $CD4^-CD8^-$. The *IL-7Rα-GOF*-only cells were $CD4^-$

CD8^{-} and CD8^{+}, similar to the immunophenotype seen in other replications of this transduction.

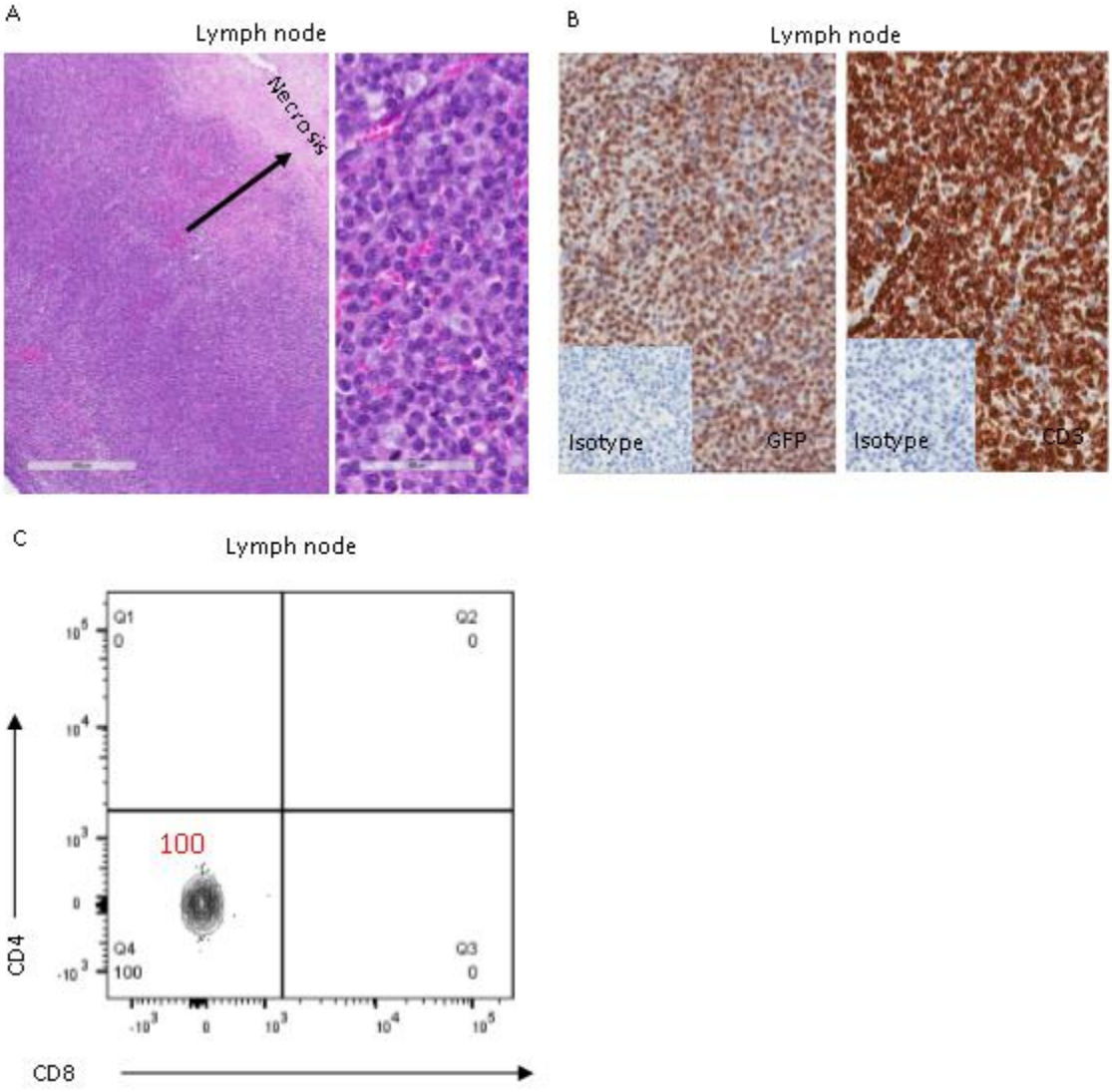

Figure 23: One of five mice (612) injected with *TLX3-IL-7Rα-GOF* cells developed T-cell lymphoma. Histology of enlarged lymph nodes showed infiltration by sheets of monomorphic, neoplastic round cells, and there were large areas of necrosis (A). Scale bar= 500 µm (left) and 60 µm (right). Immunohistochemistry showed that neoplastic cells demonstrated strong immunoreactivity on labeling with anti-GFP antibody and anti-CD3 antibody (B). Flow cytometry showed that GFP+Thy1.2+ cells were CD4-CD8- (C).

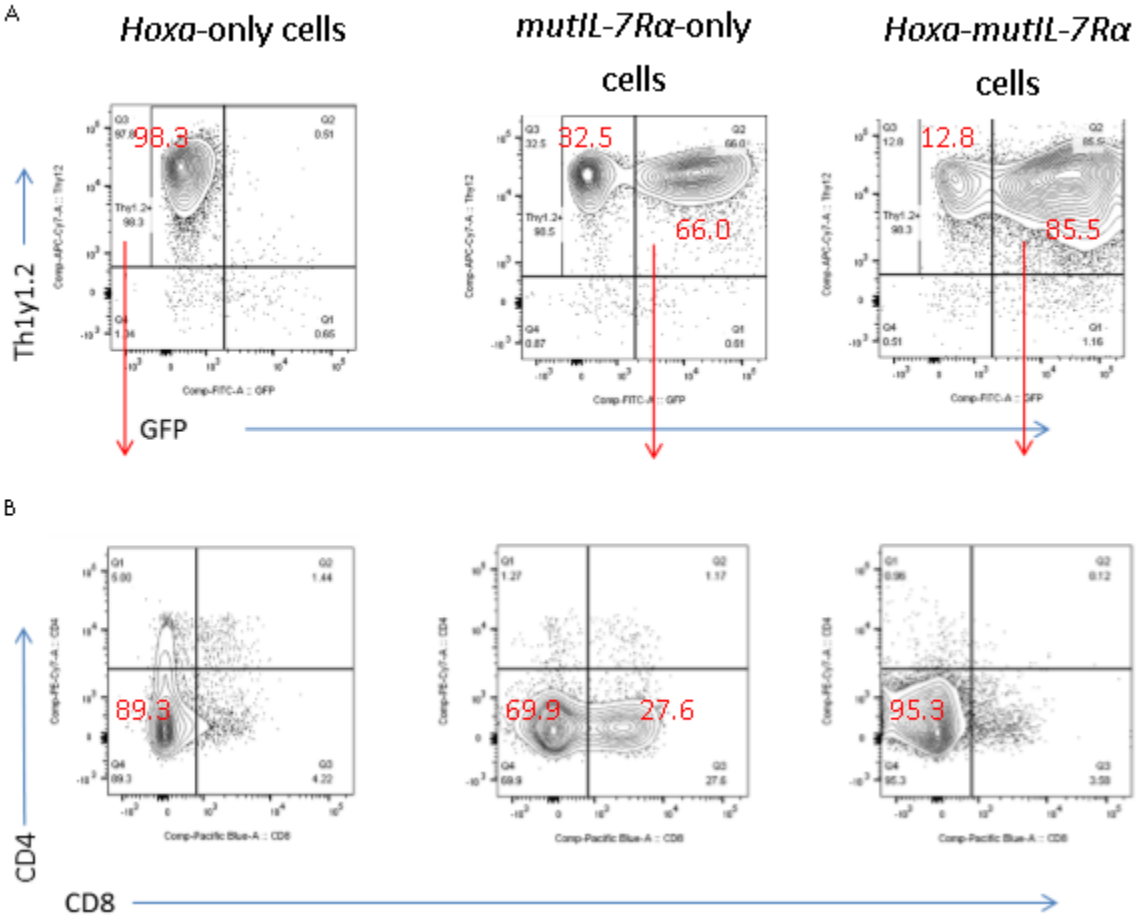

Figure 24: *Hoxa* overexpression drives the immunophenotype of transduced cells. At the time of injection into mice, most *Hoxa*-only cells were Thy1.2+, suggesting T-cell lineage commitment (A), though most cells lacked CD4 or CD8 expression, suggesting immaturity (B). These cells were derived from the *NUP98-HOXD13* transgenic mouse that was engineered to overexpress the *Hoxa* gene cluster, so GFP was linked with *IL-7Rα-GOF* expression rather than *Hoxa* overexpression. Cells transduced with *IL-7Rα-GOF*-only showed high percentages of transduced, GFP+ cells that were Thy1.2+ (A). Thy1.2+ cells were a mixture of predominantly CD4-CD8– and CD8+ cells (B). The immunophenotype of *Hoxa-IL-7Rα-GOF* cells was more similar to *Hoxa*-only cells and was predominantly Thy1.2+ (A) and CD4-CD8- (B). Data are from a single experiment. N=1 for each group.

Hoxa-IL-7Rα-GOF combination generates full-penetrance myeloid leukemia

Mice injected with *Hoxa-IL-7Rα-GOF* cells developed clinical disease necessitating euthanasia at a time-point similar to, though slightly earlier than, those injected with *IL-7Rα-GOF*-only cells. Disease onset was rapid with full penetrance (Figure 25A). Sick animals showed signs of hunching, decreased ambulation, enlarged abdomens, and, in the *IL-7Rα-GOF-only* group, skin crusting. *IL-7Rα-GOF*-only mice developed inflammatory lesions consistent with those described in Chapter 3, and *Hoxa*-only mice did not develop disease.

Hoxa-IL-7Rα-GOF mice developed a marked leukocytosis composed of cells morphologically consistent with neutrophils in varying stages of development. There were many cells with band neutrophil morphology as well as earlier stages of development (Figure 25B). Animals developed splenomegaly, lymphadenopathy, and hepatomegaly (Figures 25C and D). Histologic examination showed infiltration of the liver, spleen, lymph nodes, dural space, and lung with sheets of cells that were morphologically similar to those seen in the peripheral blood, consistent with varying stages of neutrophil maturation (Figure 26A and B). By flow cytometry, the thymus, spleen, bone marrow, and peripheral blood contained high percentages of GFP^+ cells. Most of these cells expressed the myeloid marker CD11b, consistent with the myeloid morphology (Figure 27A&B). Few GFP^+ cells in the spleen, bone marrow, and peripheral blood expressed Thy1.2, with a slightly higher percentage of $Thy1.2^+$ cells in the thymus (Figure 27C). Most of the $Thy1.2^+$ cells were $CD4^-CD8^-$, consistent with an immature T-cell phenotype (Figure 27D). Immunohistochemistry showed that neoplastic cells expressed GFP and, surprisingly, CD3 (Figure 27E). Though the expression of CD3 was

consistent with an early T-cell precursor-like ALL, the myeloid morphology of these cells was not consistent with this disease (Peter Aplan, personal communication).

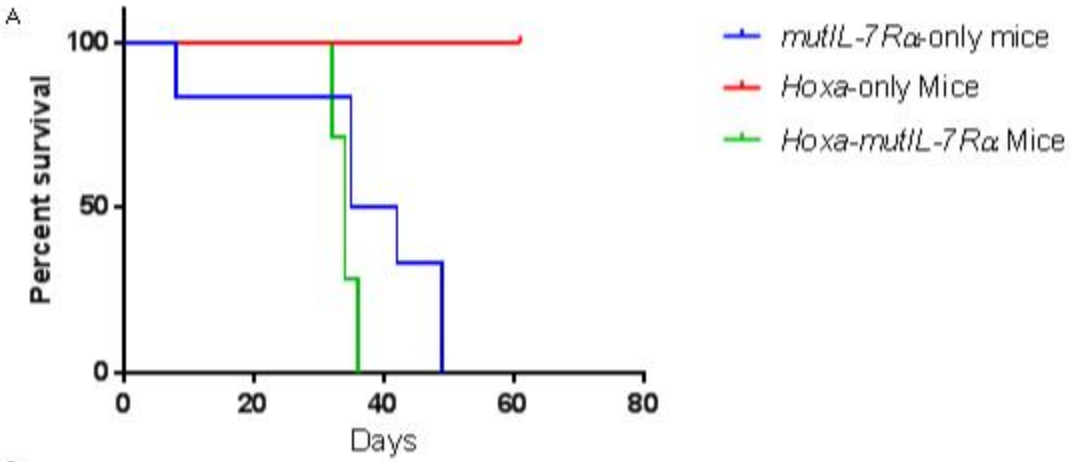
A
100
50
0
Percent survival
0
20
40
60
80
Days
mutIL-7Rα-only mice
Hoxa-only Mice
Hoxa-mutIL-7Rα Mice

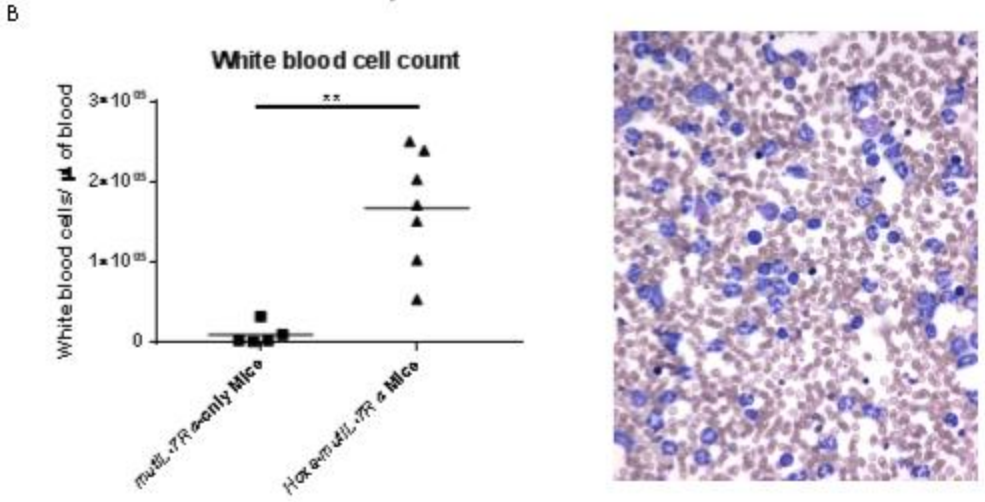
B
White blood cell count
White blood cells/ µl of blood
3×10^05
2×10^05
1×10^05
0
**
mutIL-7Rα-only Mice
Hoxa-mutIL-7Rα Mice

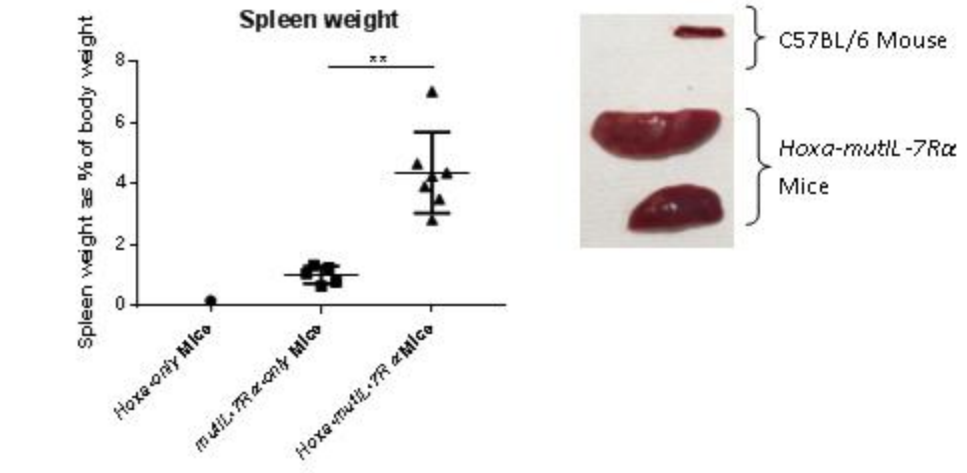
C
Spleen weight
Spleen weight as % of body weight
8
6
4
2
0
**
Hoxa-only Mice
mutIL-7Rα-only Mice
Hoxa-mutIL-7Rα Mice
C57BL/6 Mouse
Hoxa-mutIL-7Rα
Mice

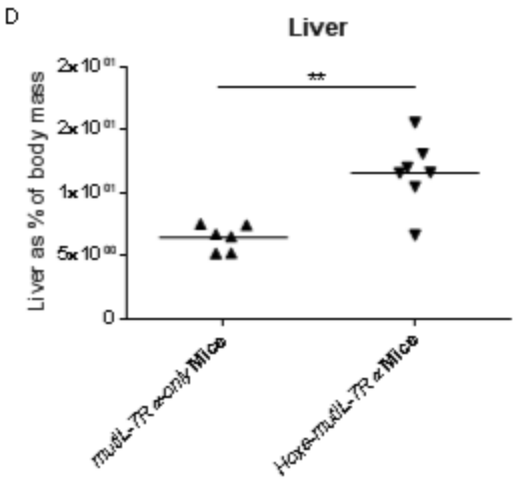

Figure 25: The combination of *Hoxa* overexpression and *IL7-Rα-GOF* generated high-penetrance, rapid-onset myeloid leukemia. Mice injected with *Hoxa-IL-7Rα-GOF* cells developed clinical signs necessitating euthanasia at a similar time point as mice injected with *IL-7Rα-GOF*-only cells (A). The *Hoxa-IL-7Rα-GOF* cells caused leukocytosis composed of cells that were morphologically consistent with neutrophils in varying stages of maturity (B). Mice also developed enlargement of the spleen (C) and liver (D) relative to *IL-7Rα-GOF*-only mice. Data are from a single experiment. Survival statistical analysis was performed using the Log-rank (Mantel-Cox) test. Organ weight statistics were performed using the Mann-Whitney test to compare *Hoxa-IL-7Rα-GOF* mice with control groups. (*Hoxa* only N= 2; *IL-7Rα-GOF*-only N=6*; Hoxa-IL-7Rα-GOF* N= 7)

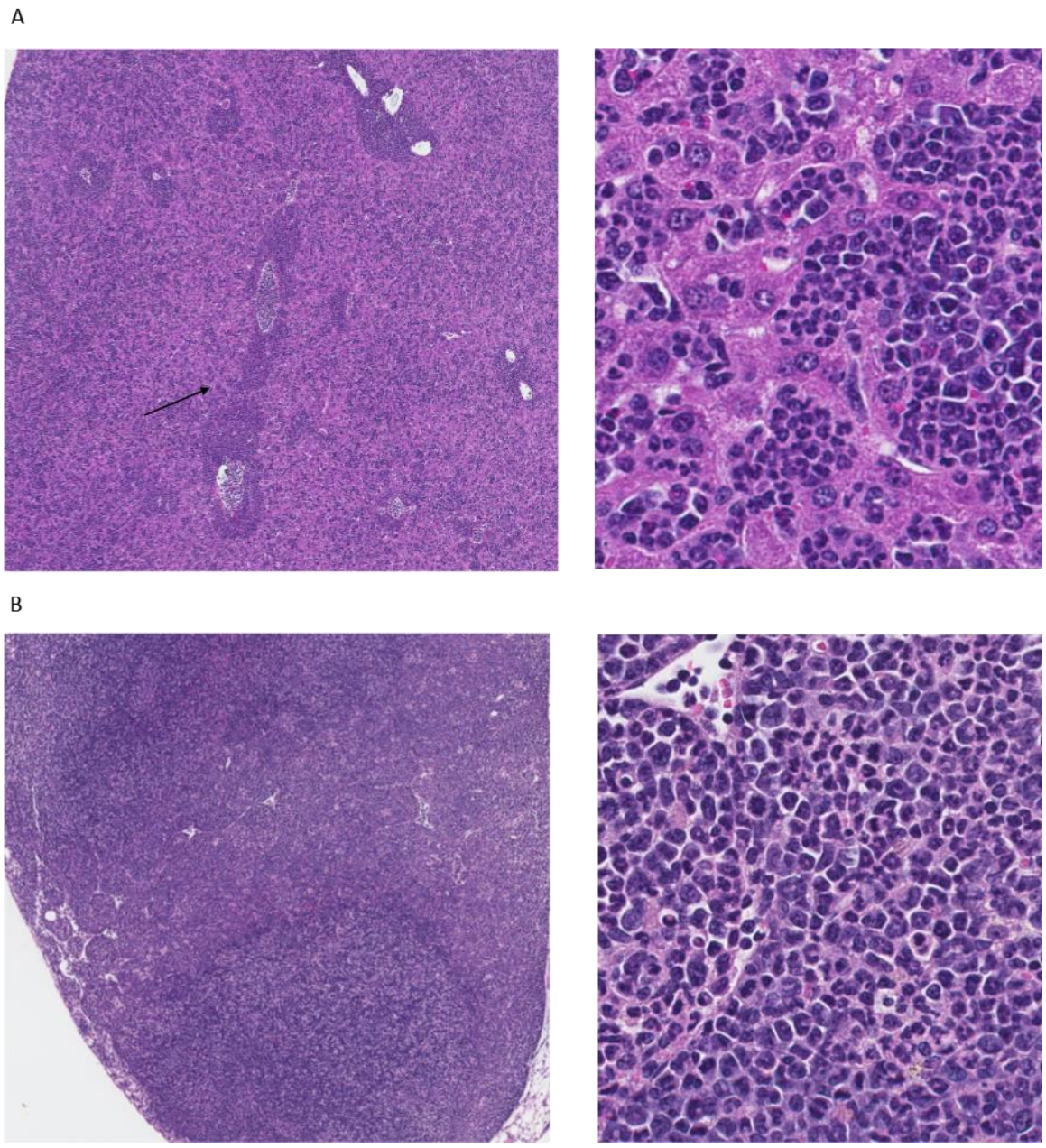

Figure 26: Multiple tissues were infiltrated and effaced by *Hoxa-IL-7Rα-GOF* cells. Here, *Hoxa-IL-7Rα-GOF* cells infiltrate the liver, forming sheets of neoplastic cells that disrupt the normal hepatic architecture (A, left panel, arrow). At higher magnification, the cells distend hepatic sinusoids and are morphologically similar to those seen in the peripheral blood, consistent with neutrophils in varying stages of maturation (right panel). Similar infiltrates are seen in the lymph nodes at low (left panel) and high (right panel) magnification (B). Data are representative of a single experiment. N=7

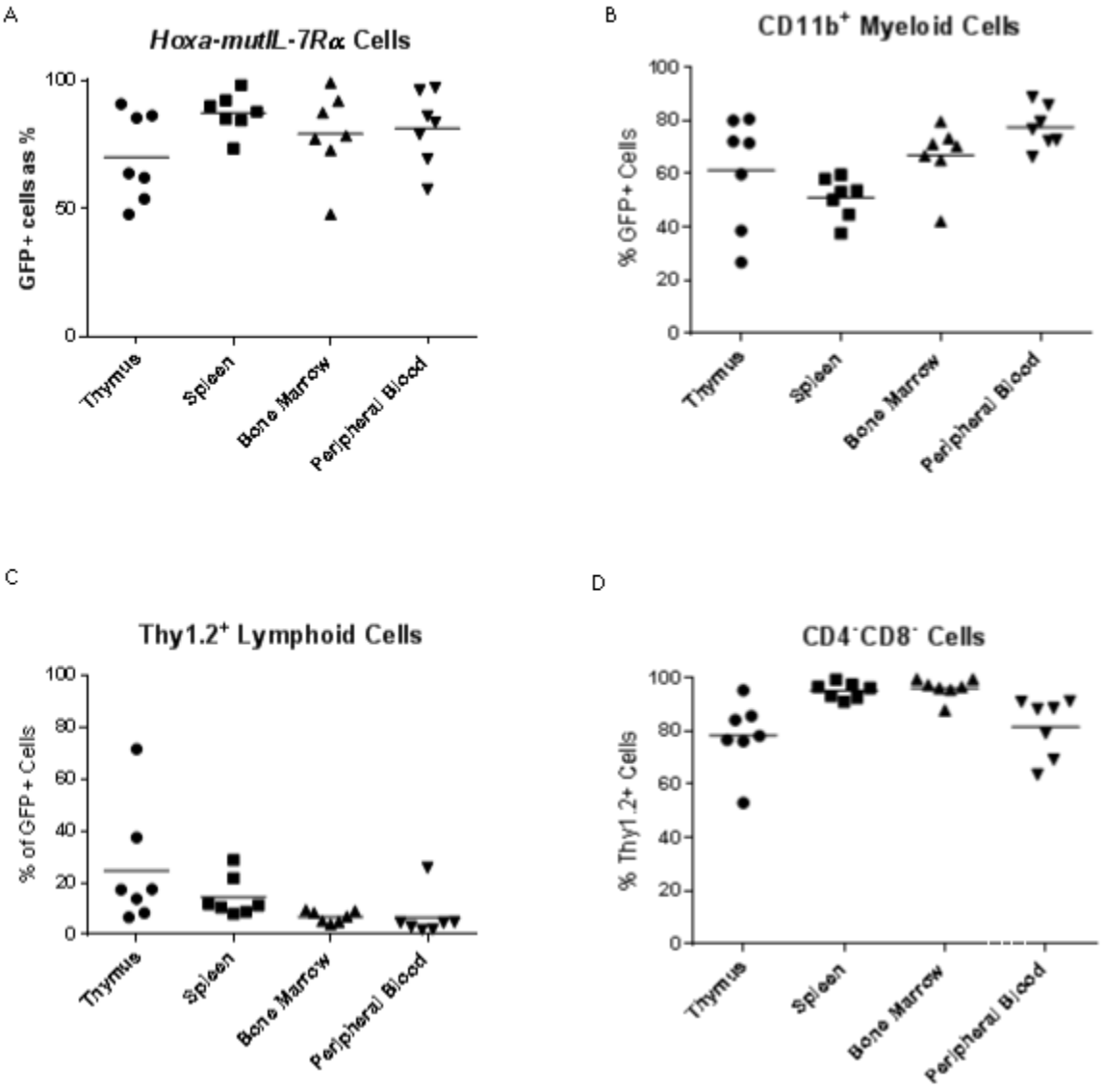
A
Hoxa-mutIL-7Rα Cells
GFP+ cells as %
100
50
0
Thymus
Spleen
Bone Marrow
Peripheral Blood
B
CD11b+ Myeloid Cells
% GFP+ Cells
100
80
60
40
20
0
Thymus
Spleen
Bone Marrow
Peripheral Blood
C
Thy1.2+ Lymphoid Cells
% of GFP + Cells
100
80
60
40
20
0
Thymus
Spleen
Bone Marrow
Peripheral Blood
D
CD4-CD8- Cells
% Thy1.2+ Cells
100
80
60
40
20
0
Thymus
Spleen
Bone Marrow
Peripheral Blood

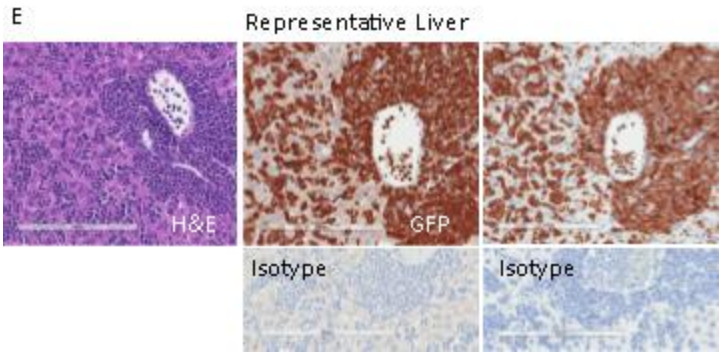

Figure 27: *Hoxa-IL-7Rα-GOF* cells are GFP+CD11b+CD3+ cells. Flow cytometry on selected tissues from mice injected with *Hoxa-IL-7Rα-GOF* cells demonstrated that a high percentage of cells in the thymus, spleen, bone marrow, and peripheral blood were GFP+ suggesting a high degree of infiltration of these tissues by transduced neoplastic cells (A). The majority of these cells expressed the myeloid marker CD11b, consistent with their morphology (B). Far fewer cells expressed the T-cell marker Thy1.2 (C), and of these, most lack CD4 and CD8 expression, suggesting an immature stage of development (D). Immunohistochemistry showed that most infiltrating cells expressed GFP and the T-cell marker CD3 (E). Data are representative of a single experiment. N=7

Hoxa-IL-7Rα-GOF cells were oligoclonal

Analysis of the DNA from spleens of mice injected with *Hoxa-IL-7Rα-GOF* cells using ligation-mediated PCR to identify retroviral insertion sites demonstrated that the cell populations were oligoclonal with few major dominant clones in each mouse. There were three mice with a major dominant clone with a retroviral insertion in the *Irs2* gene, and two mice with major dominant clones with a retroviral insertion in the *Itgb7* gene (Figure 28).

Figure 28: *Hoxa-IL-7Rα-GOF* cell populations were oligoclonal.
Each pie chart represents a single animal, and each wedge is a unique retroviral integration site as identified by ligation-mediated PCR on splenic DNA. In this diagram, the gene affected by the retroviral integration is listed for the major dominant clones. Three animals had a major dominant clone with an integration site affecting the *Irs2* gene, and two animals had an integration site affecting the *Itgb7* gene.

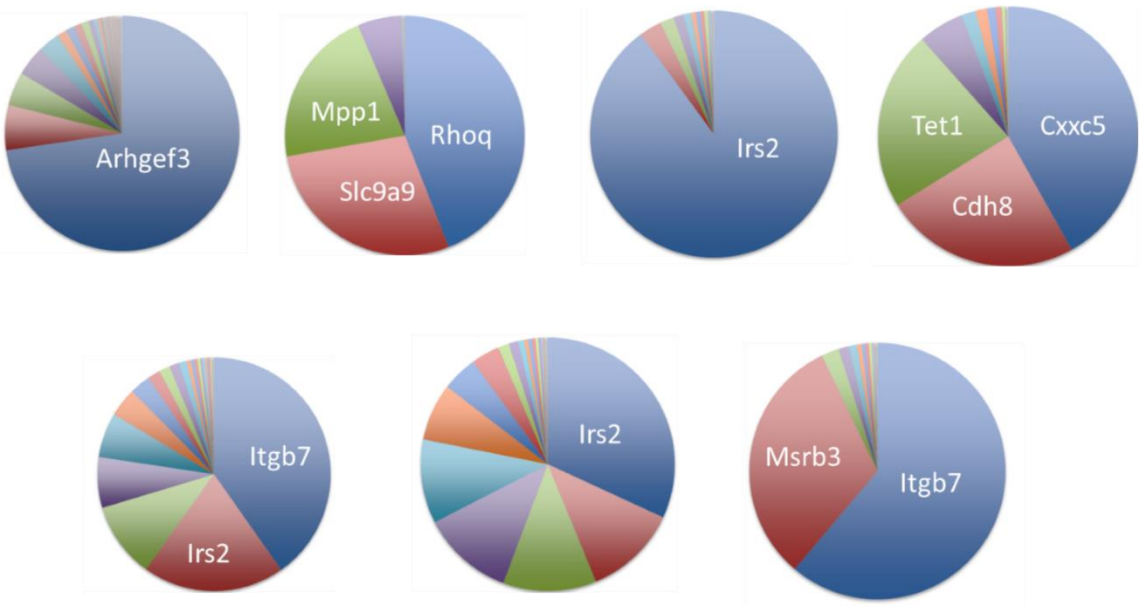

Discussion

Neither *TLX3-IL-7Rα-GOF* cells nor *Hoxa-IL-7Rα-GOF* met the stated project goal of identifying a genetic combination that was sufficient to induce T-ALL. However, both combinations yielded interesting results. In both *TLX3-IL-7Rα-GOF* cells and *Hoxa-IL-7Rα-GOF* cells, expression of the homeobox transcription factor caused cultured thymocytes to have an immature DN phenotype at the time of injection. This suggests that aberrant expression of these homeobox transcription factors may block T-cell differentiation at an early stage of development in culture. This is consistent with some studies showing that overexpression of *HOX* due to juxtaposition with the *TCRβ* locus

can cause maturation arrest (Cauwelier et al., 2007; Speleman et al., 2005). T-cells from pediatric patients with TLX3 and HOXA subtypes of T-ALL also show maturation arrest (Meijerink, 2010). In TLX3 subtypes, maturation block is caused, at least in part, to blockade of Vα-Jα rearrangement by *ETS1* (Dadi et al., 2012).

TLX3-only cells did not seem to survive well *in vitro*, and dual transduction with *IL-7Rα-GOF* appeared to improve survival rates. After injection, there were few *TLX3-IL-7Rα-GOF* cells in the examined tissues of most mice, and most mice eventually developed inflammatory disease necessitating euthanasia. This inflammation was presumably due to injection of a subpopulation of *IL-7Rα-GOF*-only cells as part of the mixed population of transduced cells. From these experiments, it seems that combination of *TLX3* expression and *IL-7Rα-GOF* is inadequate to drive leukemogenesis in this experimental system. Previous studies have shown that *TLX3*-transduced cells do not survive when injected into mice (Su et al., 2006a).

However, one of the five mice injected with *TLX3-IL-7Rα-GOF* cells developed T-cell lymphoma. This suggests that the presence of one or more additional genetic lesion(s) may be sufficient to drive transformation when combined with *TLX3* expression and *IL-7Rα-GOF*. Neoplastic cells expressed CD3 by immunohistochemistry and Thy1.2 by flow cytometry, though cells were $CD4^-CD8^-$, suggesting an immature T-cell phenotype. Alternatively, it is possible that cells were committed to the γδ TCR lineage rather than the αβ TCR lineage, since some cases of human TLX3 leukemia/lymphoma express γδ TCR (Meijerink, 2010). We did not assess the lymphoma for γδ TCR expression.

In comparison to the *TLX3-IL-7Rα-GOF* cells, *Hoxa*-only cells seemed to survive better in culture. This could be due to the method of inducing gene overexpression, as *Hoxa*-only cells were derived from the *NUP98-D13* transgenic mouse while *TLX3* expression was induced by transduction with a retroviral vector (Lin et al., 2005). The *NUP98-HOXD13* transgenic has been shown to have activation of the *Hoxa* gene cluster, including *Hoxa7*, *Hoxa9*, and *Hoxa10*, and mice consistently develop myelodysplastic syndrome and acute leukemia over the course of up to 14 months (Choi et al., 2009; Lin et al., 2005). Thymocytes from these animals have a partial differentiation block at the DN2 to DN3 transition and may also develop into precursor T-cell lymphoblastic leukemia/lymphoma (Choi et al., 2009). However, similar to *TLX3*-only cells, *Hoxa*-only cells did not cause clinical disease in injected mice. This is consistent with published data demonstrating that bone marrow cells transduced with *Hoxa9* and *HOXA13* do not survive *in vivo* once injected into mice (Kroon et al., 1998; Su et al., 2006a).

The effects of combining *Hoxa* overexpression and *IL-7Rα-GOF* were more striking than the *TLX3-IL-7Rα-GOF* combination. Every mouse injected with *Hoxa-IL-7Rα-GOF* cells developed myeloid leukemia. This is may be an artefact of the experimental conditions, as, to our knowledge, there are not cases of human myeloid leukemia with mutations in the *IL-7Rα-GOF* gene. The *NUP98-HOXD13* mouse is known to develop varying stages of myeloid disorders, and it is also possible that myeloid precursor cells were transduced as part of the culture system, since these cells were not depleted from the thymus with the depletion strategy used, though $CD11b^+$ cells are present at very low rates after days in culture (see Chapter 3).

In each case of *Hoxa-IL-7Rα-GOF* myeloid leukemia, the resulting disease was oligoclonal, suggesting that growth advantage may be conferred by additional genetic lesions (either additional acquired mutations or gene activation/ suppression due to retroviral integration). Mice were injected from the same pool of transduced cells, and three mice shared major dominant clones with *Irs2* gene retroviral integration sites while two had integrations into the *Itgb7* gene. These clones likely had proliferative advantage prior to injection into the mice. *Itgb7* encodes the integrin subunit beta 7, and it is involved in cell adhesion and extracellular matrix signaling (Neri et al., 2011). *Irs2* encodes the insulin receptor substrate 2 which is involved in signaling by insulin as well as insulin-like growth factor 1 (Uddin et al., 1997). This is particularly interesting, as insulin-like growth factor 1 appears to be a target of *HOXA9*, and Igf1 signaling is important in leukemia induced by *HOXA* expression (Steger et al., 2015). Given this, it seems likely that the activation of the *Irs2* gene by retroviral integration conferred significant growth advantage to *Hoxa-IL-7Rα-GOF* cells.

The fact that *Hoxa-IL-7Rα-GOF* leukemic cells expressed CD3 was interesting. Typically, CD3 expression is associated with T-cell lineage commitment, and cells expressing CD3 would not be expected to co-express the myeloid marker CD11b (as was the case in the *Hoxa-IL-7Rα-GOF* leukemias). However, there is a subset of ALL cases, early T-cell precursor ALL (ETP-ALL), that is defined by shared expression of T-cell markers and myeloid markers; this is particularly relevant because some cases of ETP-ALL have been shown to have *HOXA* overexpression and *IL-7Rα* mutation (Zhang et al., 2012). It is tempting to classify the *Hoxa-IL-7Rα-GOF* leukemias as ETP-ALL-like lesions. Similar murine lesions have been published as ETP-ALL, but human cases of the

disease are composed of small round cells rather than cells with distinct myeloid morphology (Peter Aplan, personal communication) (Treanor et al., 2014). Therefore, it seems most conservative to conclude that the combination of *Hoxa* expression and mutant *IL-7Rα-GOF* induces a myeloid leukemia with features suggestive of ETP-ALL-like disease. However, additional genetic lesion(s) are likely necessary to drive T-cell lineage commitment that more closely mimics the morphology of human disease.

In conclusion, the combination of *TLX3* and *IL-7Rα-GOF* was not sufficient to cause T-ALL, but led to development of a T-cell lymphoma in one mouse. The combination of *Hoxa* overexpression and *IL-7Rα-GOF* caused a full-penetrance, rapid-onset myeloid leukemia with some features similar to ETP-ALL.

Chapter 5: Mutant *NRAS* and mutant *IL-7Rα-GOF* are sufficient to induce T-ALL

Introduction

Review of patient data suggested that *TLX3* expression, *HOXA* overexpression, and mutant *NRAS* were each excellent candidates for collaboration with mutant IL-7Rα in the generation of T-ALL (Chapter 2). However, experiments showed that neither *TLX3* expression nor *Hoxa* overexpression collaborated with mutant *IL-7Rα* to generate T-ALL (Chapter 4). We continued our search for potential collaborators by investigating the effects of combining mutant *NRAS* with mutant human *IL-7Rα*.

To review, NRAS functions as a GTPase, mediating the effects of growth factor receptors by activating multiple intracellular signaling pathways. Mutations in *RAS* proteins are common in many human cancers and enable activation of intracellular signaling pathways without growth factor binding to receptors (Ward et al., 2012). Rates of *NRAS* mutation in T-ALL are variable, with some reports as low as 4% and others as high as 25% (Kalender Atak et al., 2012; Kawamura et al., 1999; Oshima et al., 2016; Perentesis et al., 2004). Downs syndrome-associated ALL had higher rates of *NRAS* or *KRAS* mutation (Nikolaev et al., 2014). *RAS* pathway mutations were more frequent in high-risk, relapsed ALL where the mutations show heterogeneous clonal evolution (Oshima et al., 2016). Such relapsed cases represent patients that might currently benefit most from targeted therapies.

NRAS mutation seemed a possible collaborator with mutant *IL-7Rα* because 41.6% of T-ALL patients with mutations in N-Ras/K-Ras/NF1 pathway had concurrent

mutations in the IL-7Rα signaling pathway (Cante-Barrett et al., 2016a). In addition, concurrent mutations in both pathways had been identified in Philadelphia chromosome-like BCP-ALL and in the T-ALL cell line DND41 (Atak et al., 2013; Roberts et al., 2014). To compliment the proliferative and survival benefits conferred by mutant *IL-7Rα*, mutant *NRAS* might be expected to enhance self-renewal (Li et al., 2013). Here we provide evidence that a combination of gain-of-function mutations in *IL-7Rα* and *NRAS* were sufficient to drive transformation of immature primary murine thymocytes.

Materials and Methods

Thymocyte transduction and culture

Thymocytes were harvested from 3-6 week old C57Bl/6J female donor mice by first mechanically dissociating the tissue into a single cell suspension. Cells were then bound to CD4 and CD8 microbeads (Miltenyi) and passed through an LD column (Miltenyi) to isolate double negative cells according to the manufacturer's instructions. Resulting double negative cells were cultured on OP9-DL4 bone marrow stromal cells for 1 day, then transduced twice with retroviral vectors with approximately 18 hours between transductions. Thymocytes were transduced by spinoculation (centrifugation at 2000 rpm for 60 minutes) with addition of 8μg/ml polybrene (Chemicon) to the transduction solution. After transduction, thymocytes were maintained on OP9-DL4 cell culture for an additional 7-8 days prior to injection into mice to allow for expansion of cell numbers.

Retroviruses were generated using Phoenix-Eco packaging cells (Orbigen). Phoenix cells were cultured in DMEM containing glucose, L-glutamine, and sodium pyruvate (Corning), with 50 ml of fetal bovine serum added to every 500 ml of DMEM. Phoenix cells were transfected with pMIG plasmids containing wild type *hIL-7Rα*,

mutant *hIL-7Rα*, mutant *NRAS* G13D (sourced from Dominic Esposito, Protein Expression Lab, NCI), cDNAs of *NRAS* G13D mutant and *hIL-7Rα* mutant were subcloned into pMIG vector by gateway cloning or PCR cloning methods by Wenqing Li. The *hIL-7Rα* mutant sequence was c.731_732insTTGTCCCAC, based on the mutation in subject P2 and was confirmed by sequencing previously by our laboratory (Zenatti et al., 2011).

Transfection was performed using lipofectamine (Invitrogen) and OPTI-MEM I reducing serum medium (Invitrogen) 48-72 hours prior to thymocyte transduction. Phoenix cell supernatants containing retroviruses were filtered using a 0.45 μm syringe filter (Millex) prior to transduction of thymocytes. OP9-DL4 cells were cultured according to published guidelines used for culture of OP9-DL1 cells and were cultured in MEM-alpha medium (Gibco). For 500 ml of media, the following additives were included: 50 ml fetal bovine serum (GE life Sciences), 3 ml fresh (frozen to maintain freshness) L-glutamine (Sigma), 0.5 ml 2-mercaptoethanol (Gibco), and 2.5 ml penicillin/ streptomycin (Gibco). When thymocytes were added to culture, growth was supported by the addition of 5 ng/ml mIL-7 and 5 ng/ml hFLT-3L (Peprotech) (Holmes and Zuniga-Pflucker, 2009).

Animal Experiments

Transduced cells were injected into sub-lethally irradiated, 6-15 week old, female *Rag1*$^{-/-}$ mice via tail vein in a concentration and volume of 5 x10^5 cells/ 200 μl/ mouse. Recipient mice were prophylactically treated for 3 days with SMZ antibiotics (0.08mg/ml in drinking water) either immediately prior to irradiation (initial experiments and limiting dilution experiments) or immediately following irradiation (serial passage experiments).

Animals were monitored by a single, experienced technician for consistency (T.B.) and euthanized at the onset of clinical signs. Clinical signs included hunching, dyspnea, reduced ambulation, rough hair coat, crusted skin (in the mutant *IL-7Rα*-only group), or moribund status. Peripheral blood was collected immediately prior to euthanasia. Animals that required euthanasia for causes not related to development of experiment-associated disease (i.e. tail caught in caging, inner ear infection, fighting-associated skin lesions) were censored from experimental results. Technicians performing monitoring were not blinded to experimental groups.

Leukemia serial passage experiments were performed using fresh spleen cells from mice that were euthanized with clinical disease. Fresh spleens were mechanically dissociated, red blood cells were lysed using ACK lysis buffer (Lonza), and the single-cell suspensions were re-suspended in PBS at a concentration of 5×10^5 cells/ 200 µl/ mouse then injected immediately into sub-lethally irradiated $Rag^{-/-}$ mice.

Limiting dilution experiments were performed by injecting serial dilutions of mutant *NRAS*- mutant *IL7Rα* transduced thymocytes into irradiated *Rag1*$^{-/-}$ mice. Each mouse was injected with 200µl of cell suspension containing unsorted cells (5×10^5, 5×10^4, 5×10^3, 5×10^2, or 5×10^1 cells, depending on the group). Animals were euthanized at the onset of clinical signs, and presence of leukemia/lymphoma was confirmed on necropsy by assessing mass of spleen and liver, identification of gross lesions consistent with lymphoma, and/or diagnosis of leukocytosis by cell counting and peripheral blood smear analysis. To calculate the number of leukemia-initiating cells in the injected cell population, the number of live, GFP^+ cells injected per group was first calculated based on flow cytometry analysis of the injected cells.

Flow Cytometry

Thymus, spleen, and bone marrow were manually dissociated to single cell suspensions. Red blood cell lysis was applied to these tissues as well as to peripheral blood using ACK Lysing Buffer (Lonza). Resultant suspensions were stained with Zombie Red live/dead fixable stain (Biolegend) for 15 minutes at room temperature. Then, CD16/32 Fc receptor block (93) was applied at a 1:400 dilution for 10-15 minutes (Biolegend). Cocktails of fluorochrome-conjugated antibodies were applied to cells for 15 minutes on ice, including the following antibodies: anti-Thy1.2 APC-Cy7 (30-H12), anti-CD4 PE-C7 (GK1.5), anti-CD8 Brilliant Violet 421 (53-6.7), anti-CD44 PerCP-Cy5.5 (IM7), anti-CD25 Brilliant Violet 650 (PC61), anti-TCRβ Alexa Fluor 700 (H57-597), anti-CD3 Brilliant Violet 421 (17A2), anti-Ly6G Pe-Cy7 (1A8) from Biolegend; anti-CD11b PerCP-Cy5.5 (M1/70), anti-B220 APC (RA3-6B2) from BD Biosciences. Fluorescence minus one (FMO) labeling was used for controls (Figure 2). Cells were then fixed in stabilizing fixative (BD Biosciences) for 30 minutes. Fixative was removed, and flow cytometric analysis was performed on an LSRIISORP cytometer with FACS DIVA software. Data analysis was performed using FlowJo, and gating strategy is included in the materials and methods in Chapter 2 (Tree Star, Inc.).

Histopathology, Immunohistochemistry, and Digital Slide Analysis

Tissues were fixed in 10% neutral buffered formalin and transferred to 70% ethanol after complete fixation. Samples were trimmed, paraffin-embedded, sectioned, and stained with hematoxylin and eosin according to standard histotechnological procedures.

Immunohistochemistry was performed by the Pathology/ Histotechnology Laboratory using previously optimized protocols. Immunohistochemistry utilized anti-GFP antibody (Abcam ab6556) at 1:1000 dilution with proteolytic digestion using proteinase K (DAKO) incubated overnight at 4 degrees C; anti-CD3 antibody (Bio-Rad #MCA1477) at 1:100 dilution incubated for 60 minutes with heat-induced epitope retrieval using citrate (Leica Biosystems) for 20 minutes; and anti-ki67 antibody (Abcam #ab16667) at 1:100 dilution incubated for 30 minutes with heat-induced epitope retrieval using citrate for 20 minutes. For all protocols, DAB (Sigma & Leica Biosystems) was used as the chromogen, and hematoxylin (Leica Biosystems) was used as a counterstain. In some cases, isotype controls were performed using the same tissue as was labeled originally, and in other cases, isotype controls were performed on standard tissues and/or cell pellets.

Slides were digitalized using an Aperio AT2 slide scanner (Leica) at a magnification of 20x. Digital slides were viewed in ImageScope (Aperio), and digital slides were used to generate images of the tissues. Digital image analysis of ki67 labeling was performed using an optimized Aperio Nuclear v9 algorithm.

Ligation-Mediated PCR

Oncogenes were transfected using retroviral vector and thus each original cell carried a unique molecular barcode that could be used to assess clonality by identifying the frequency of retroviral integration as described previously (De Ravin et al., 2016; Maldarelli et al., 2014). The integration sites were cloned from 5LTR-genomic junction using primers specific for the vector used in this study (MFGS5LTR, 5'ATGGCGTTACTTAAGCTAGCTTG 3', MFGS5LTRnest,

CAAACCTACAGGTGGGGTCTTTC 3'). Integration site junctions were mapped to mouse genome build mm10. Frequency of each clone was calculated as the percentage of read numbers for each integration sites out of total mapped reads.

Transcriptome Analysis

RNA for transcriptome analysis was isolated from cell-sorted, GFP^+, transduced and cultured thymocytes using the RNeasy Plus Mini and Micro Kit (Qiagen) with the QIAshredder (Qiagen) according to manufacturer's instructions. Resulting RNA samples were flash-frozen in liquid nitrogen.

RNA samples were sequenced using paired-end sequencing (ACGT Inc.). A standard Illumina TruSeq protocol was used, and the read length was 150bp. Bioinformatics analysis was performed using an in-house RNASeq pipeline, CCBR Pipeliner (https://github.com/CCBR/Pipeliner). The raw RNA-Seq fastq reads were aligned to mouse genome (mm10) using STAR (v. 2.4.0h) on 2-pass mode with mouse gencode (release 4) gtf (Dobin et al., 2013). Genes were subsequently counted using Rsubread and further normalized using TMM (edgeR) and analyzed for gene expression changes using limma-voom with quantile normalization (Law et al., 2014; Liao et al., 2013). Heatmaps of gene expression and principal component analysis were generated using Partek software. For pathway analysis, gene lists were imported into Metacore pathway analysis tool (Thomson Reuters) to analyze gene enrichment and pathway activation.

TCR Clonality Assessment

T-cell receptor clonality of a subset of *mutNRAS-mutIL7Rα* leukemias was performed by real time PCR to assess VDJ rearrangement using degenerate 5' V primer

and C primers that annealed to both Cβ1 and Cβ2. PCR products were then sequenced using Sanger sequencing. For those samples with chromatograms indicating multiple sequences, the PCR product was sub-cloned into a plasmid vector, introduced into bacteria, and 10 resultant bacterial colonies were sequenced and the populations were compared to assess degree of clonality. For samples without evidence of VDJ recombination, DJ recombination was assessed by real time PCR. Primer sequences are as follows (Table 2).

Primer Name	Primer Sequence
5'TCRVB	TAAGCGGCCGCATGKDYTGGTAYMRRCAG
3'TCRCB	CCCACCAGCTCAGCTCCACGTGG
5'TCRBD1.1	CTTATCTGGTGGTTTCTTCCAGC
3'TCRBJ1S4.2	TTTACATACCCAGGACAGACAGC
3'TCRBJ1S6.1	AGACCATGGTCATCCAACACAGGC
5'TCRBD2.2	TGTATCACGATGTAACATTGTGG
3'TCRBJ2S4.2	TACTGGGTGTCTTGGTTCACAGC
3'TCRBJ2S7.2	TTGAGAGCTGTCTCCTACTATCG
5' Mouse Beta-actin	GTGGGCCGCTCTAGGCACCAA
3' Mouse Beta-actin	CTCTTTGATGTCACGCACGATTTC
mouse SCID Primer 1	CTAGGCCACAGAATTGAAAGATCT
mouse SCID Primer 2	GTAGGTGGAAATTCTAGCATCATCC

Table 2: Primers used for TCRβ clonality assessment.

Statistics

For most studies, statistics were performed using GraphPad Prism version 6.00 for Windows (GraphPad Software, La Jolla, CA). To compare more than two groups, Kruskall-Wallis analysis was performed, and the Mann-Whitney test was used to compare two groups. Survival curve analysis was performed using the Log-rank test. For the limiting dilution studies, extreme limiting dilution analysis was performed using software from the Walter and Eliza Hall Institute of Medical Research, available at the following website: http://bioinf.wehi.edu.au/software/elda/ (Hu and Smyth, 2009).

Results

Mutant *NRAS* combined with mutant *IL-7Rα-GOF* is sufficient to generate T-cell acute lymphoblastic leukemia

To assess collaboration between human *IL-7Rα-GOF* mutation and *NRAS* mutation c.38G>A (G13D), we used the same approach as with *TLX3*, transducing C57BL/6J $CD4^-CD8^-$ immature thymocytes with retroviral vectors encoding the mutated genes. Mice injected with *mutNRAS-IL-7Rα-GOF* cells developed clinical signs necessitating euthanasia more rapidly than those injected with *TLX3-IL-7Rα-GOF* cells, *Hoxa- IL-7Rα-GOF* cells or control groups (Figure 29A). *MutNRAS-IL-7Rα-GOF* mice developed full-penetrance disease with splenomegaly and lymphoblastic leukocytosis (Figures 29 B&C).

By flow cytometry, the thymus, spleen, bone marrow, and peripheral blood contained high percentages of GFP^+ (*mutNRAS*) cells (Figure 30A). Histologically, the spleen, liver, and lungs were infiltrated by large numbers of small, round, GFP^+CD3^+

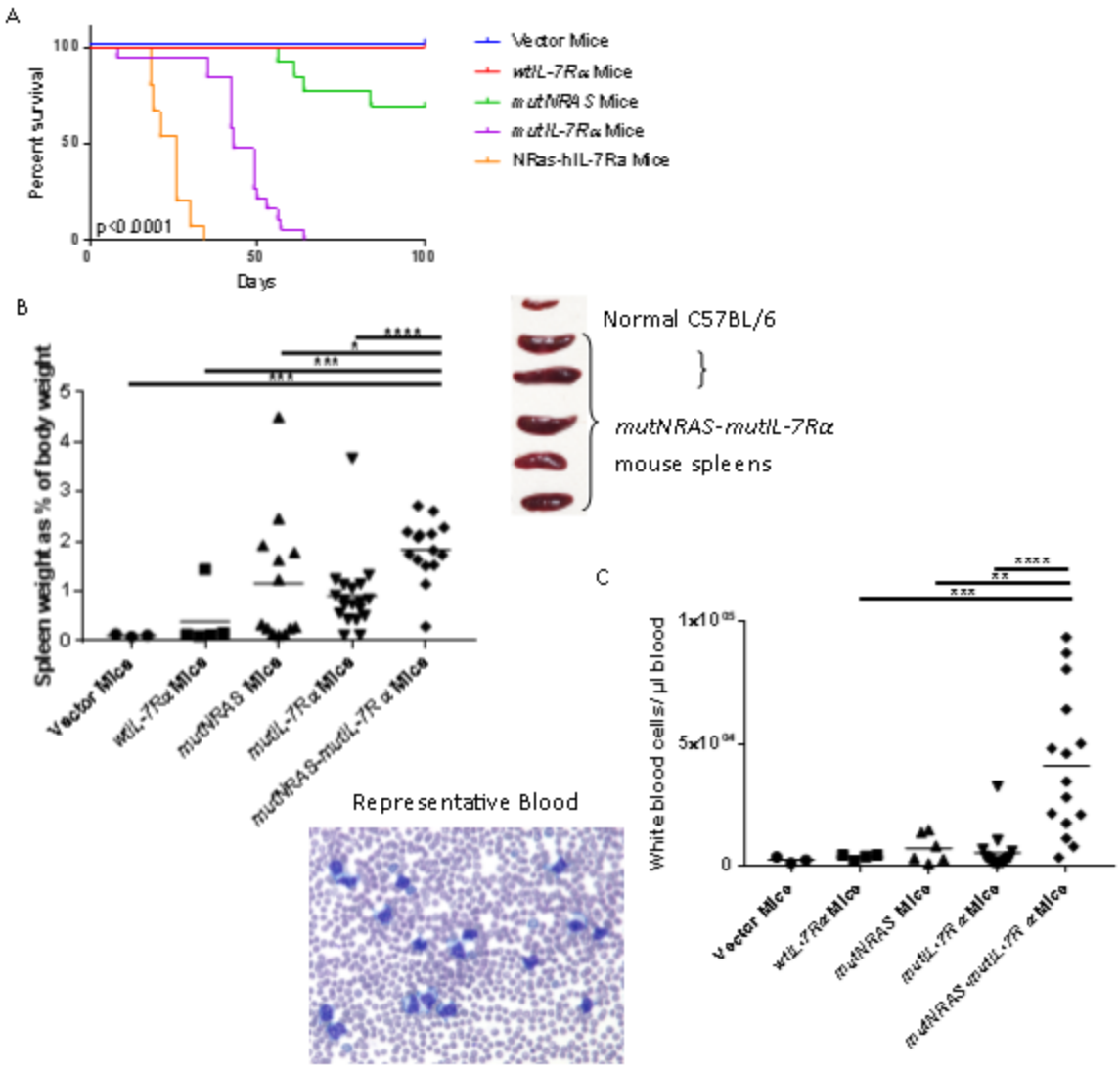

Figure 29: Mutant *IL-7Rα-GOF* combined with mutant *NRAS* was sufficient to generate rapid-onset leukemia. Mice injected with *mutNRAS-IL-7Rα-GOF* cells developed clinical signs requiring euthanasia more rapidly than control mice (A). The spleens of mice injected with *mutNRAS-IL-7Rα-GOF* cells were significantly larger than those of controls (B). *mutNRAS-IL-7Rα-GOF* mice developed a lymphoblastic leukocytosis (C). Bars represent mean values. Survival statistical analysis used the Log-rank (Mantel-Cox) test comparing all groups as well as *mutNRAS-IL-7Rα-GOF* to individual controls. Other statistical comparisons used the Mann-Whitney test comparing *mutNRAS-IL-7Rα-GOF* cells to individual control groups. $p<0.05$=*; $p<0.005$=**; $p\leq0.0005$=***; $p<0.0001$=****. Survival and organ weight data include results from 1-3 independent experiments (Vector N=3; Wild type N=1, 4; *mutNRAS* N= 1, 8, 4; *IL-7Rα-GOF* N= 3, 8, 5; *mutNRAS-IL-7Rα-GOF* N= 2, 8, 5).

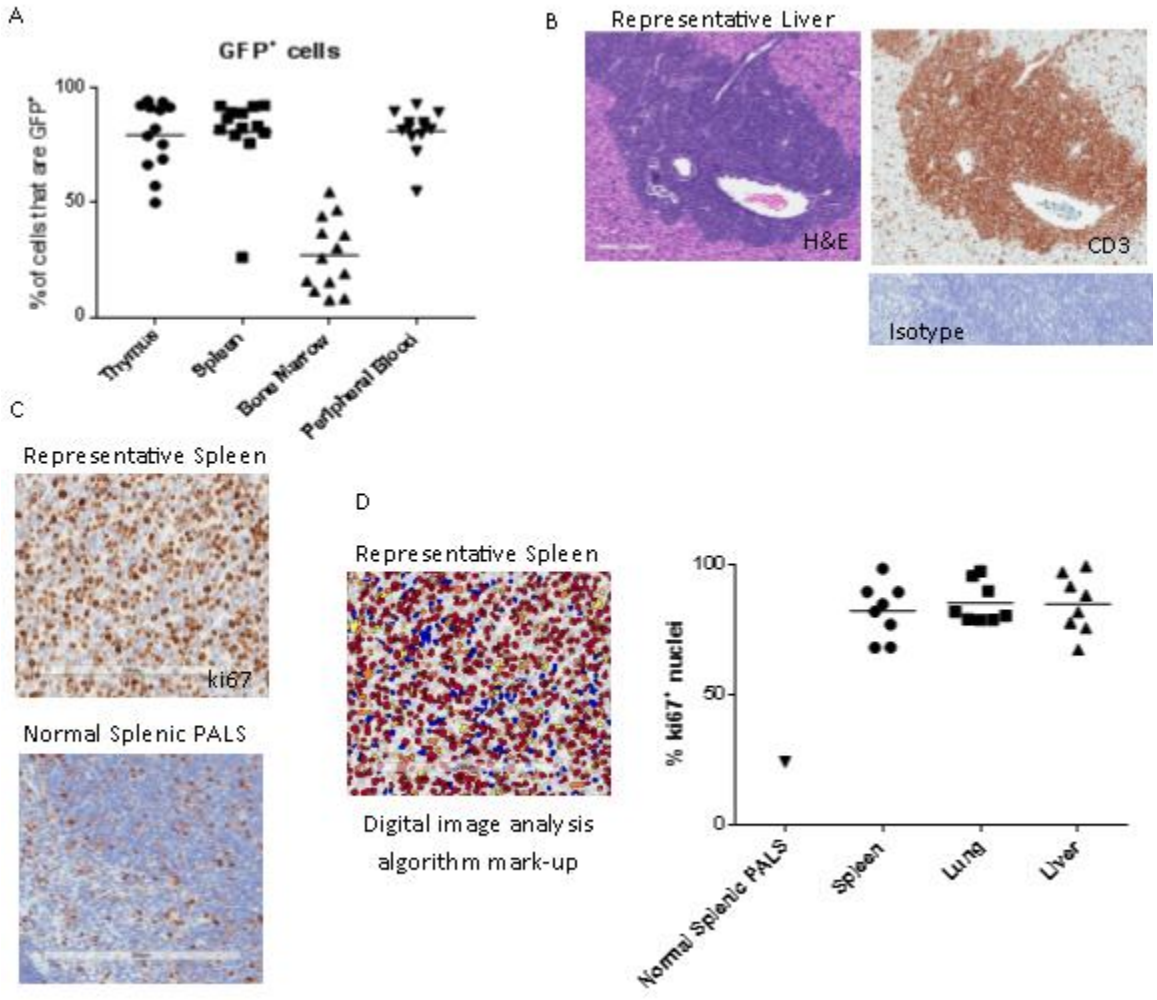

Figure 30: *MutNRAS-IL-7Rα-GOF* cells were GFP+CD3+ cells. *MutNRAS-IL-7Rα-GOF* cells extensively infiltrated thymus, spleen, bone marrow, peripheral blood, and liver (A&B) and were GFP+ by flow cytometry (A) and immunohistochemistry (B). Immunohistochemistry showed cells were CD3+ (B) and highly-proliferative based anti-ki67 immunolabeling (C). Quantifying ki67+ nuclei using digital image analysis showed that 67-99% of nuclei were positive in splenic, pulmonic, and hepatic leukemic infiltrates of *mutNRas-IL-7Rα-GOF* mice as compared to 24% positive nuclei in the periarteriolar lymphoid sheath (PALS) of a normal C57BL/6 mouse (D). Bars represent mean values. Scale bars = 200 μm

mononuclear cells that formed sheets replacing the normal parenchyma, morphologically consistent with neoplastic infiltrates (Figure 30B). The majority of these cells were in

active cell cycling based on expression of ki67 (Figure 30 C&D).

MutNRAS-IL-7Rα-GOF cells were predominantly a mixed immunophenotype with Thy1.2^{+}CD4^{+}CD8^{+} or Thy1.2^{+}CD8^{+}TCRβ^{+} expression (Figure 31A-D), consistent with origination from multiple clones (gating strategy and flow cytometry labeling controls are in materials and methods). Several control mice injected with *mutNRAS*-only cells developed later-onset T-cell lymphoma (Figure 32A-C). Immunophenotype of one *mutNRAS*-only lymphoma was similar to that of *mutNRAS-IL-7Rα-GOF* leukemia (Figure 32 D&E). Control mice injected with *IL-7Rα-GOF*-only cells developed inflammatory disease as described in Chapter 3. One animal injected with GFP vector-transduced cells developed gross lesions consistent with leukemia/lymphoma at 110 days post-injection, and this animal was censored due to the late onset of disease, as the disease was presumably due to retroviral activation of an oncogene or an acquired mutation in an injected thymocyte.

While morphology suggested *mutNRAS-IL-7Rα-GOF* cells were neoplastic, we attempted to verify this by performing serial passage experiments, transferring cells from four individual donor animals through 3 consecutive groups of sub-lethally irradiated *Rag1*$^{-/-}$ recipient mice. Supportive of neoplastic properties, cells from donor mice induced full-penetrance, rapid-onset disease necessitating euthanasia in two passage attempts (Figure 33A). A third passage attempt with frozen cells from the initiating donor gave low-penetrance disease at the first passage but full-penetrance disease subsequently, and a fourth attempt failed after the first passage (data not shown). While serial passage induced disease in recipient mice, degree of splenomegaly and leukocytosis varied between passages (Figure 33B&C). Serial passages A and B were continued through 8

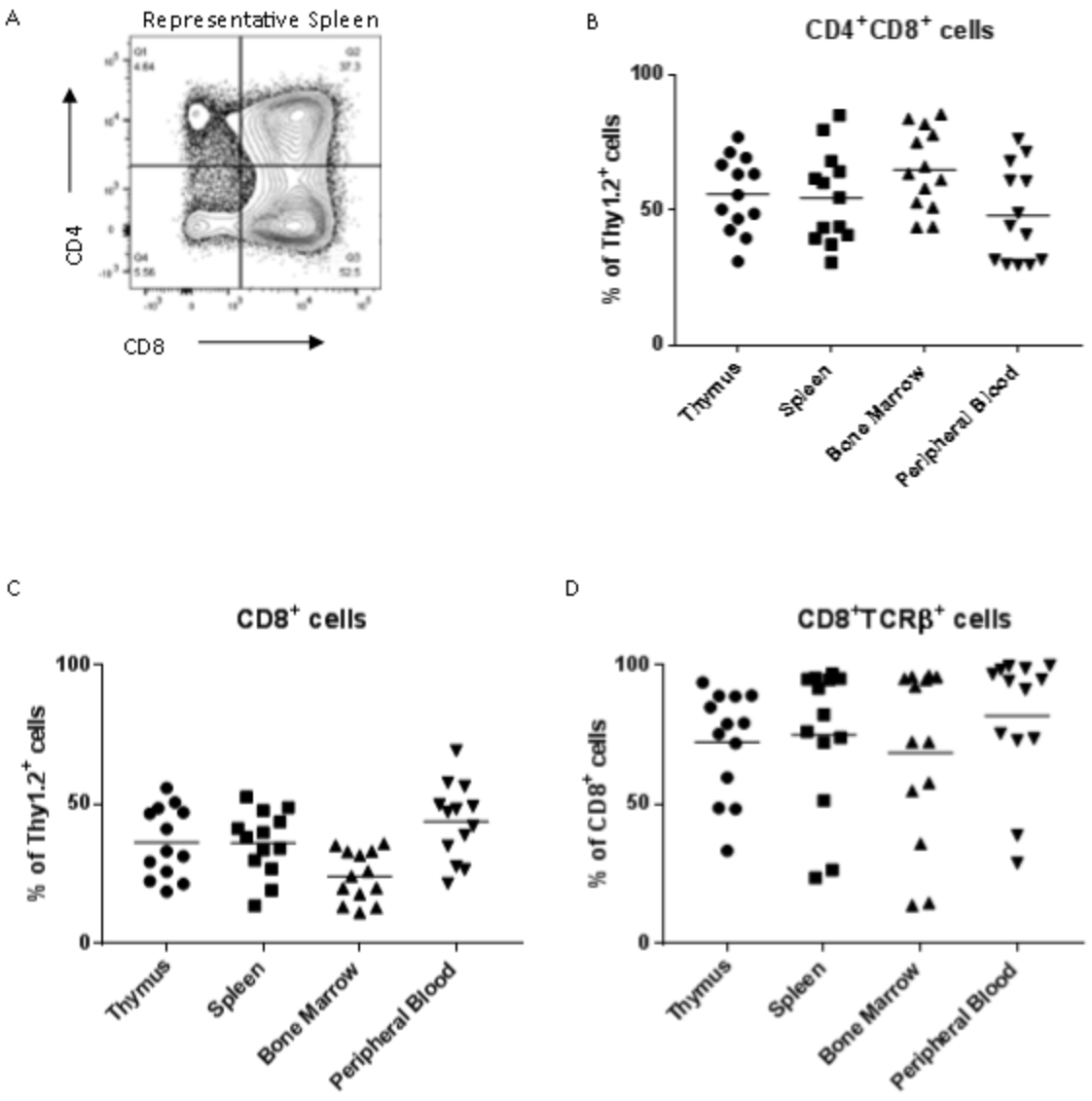

Figure 31: *MutNRAS-IL-7Rα-GOF* cells were CD4+CD8+ and CD8+ T-cells. Flow cytometric analysis of mutNRas-IL-7Rα-GOF cells showed predominant populations of CD4+ CD8+ cells and CD8+ cells in the thymus, spleen, bone marrow, and peripheral blood of affected mice (A-C). Most CD8+ cells expressed TCRβ, suggesting maturity (D). Bars represent mean values. Flow data include values from 2 independent experiments (N=8 & 5).

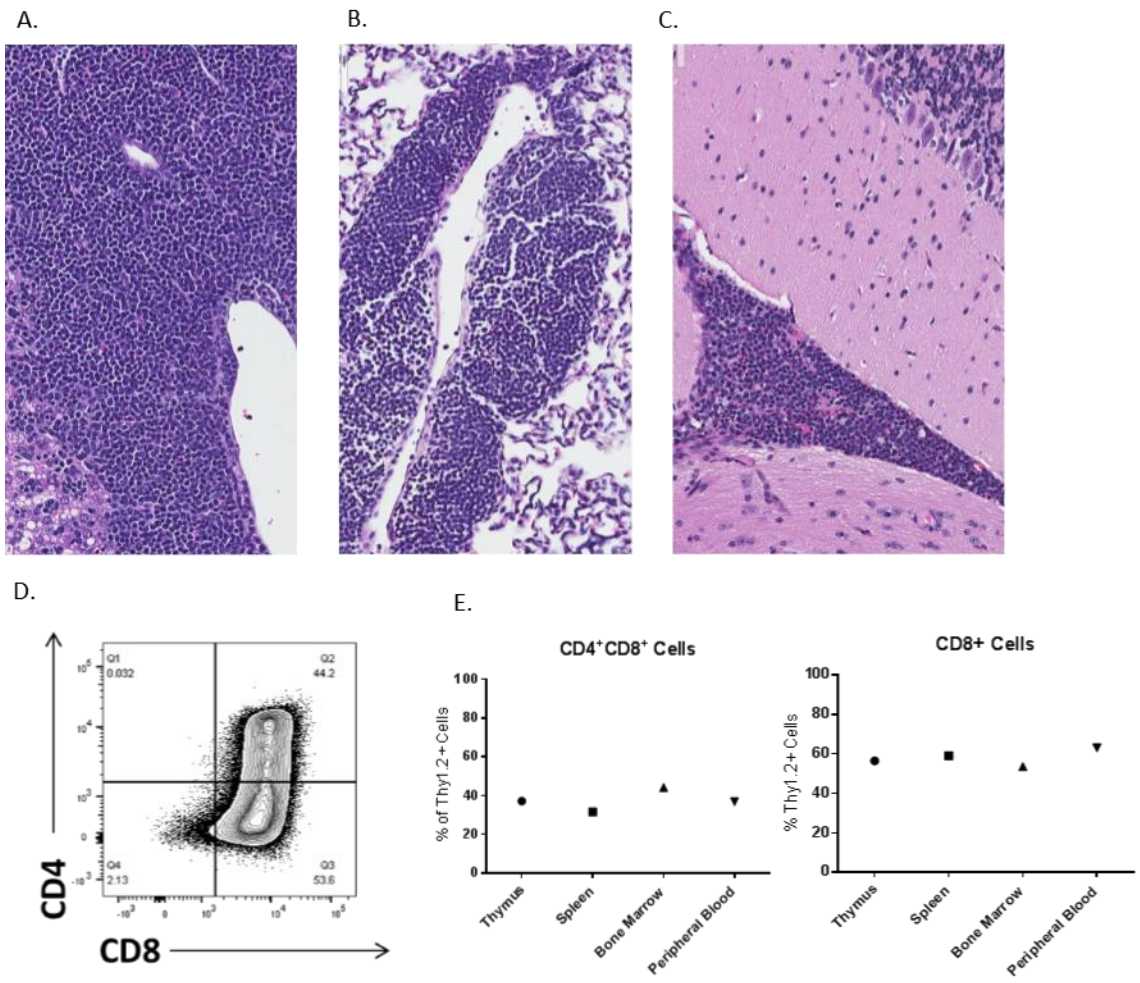

Figure 32: A few mice injected with *mutNRAS*-only cells developed late-onset T-cell lymphoma. Neoplastic cells infiltrated multiple organs including liver (A), lung (B), and meninges (C). By flow cytometry, neoplastic populations were composed of populations of CD4+ CD8+ double positive and CD8+ single positive cells (D & E). Histologic results are representative of 2 mice. Flow cytometry results represent 1 mouse.

A

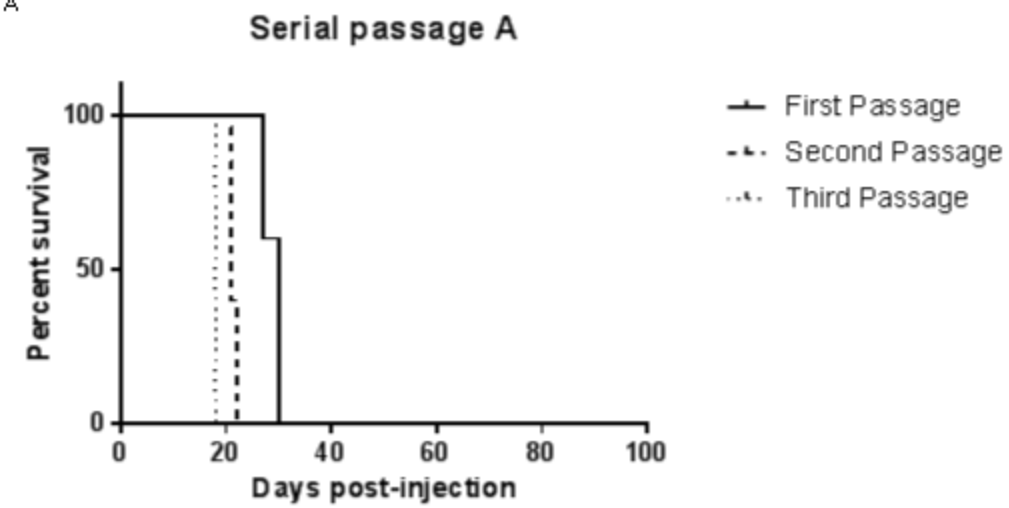
Serial passage A
Percent survival
100
50
0
0
20
40
60
80
100
Days post-injection
First Passage
Second Passage
Third Passage

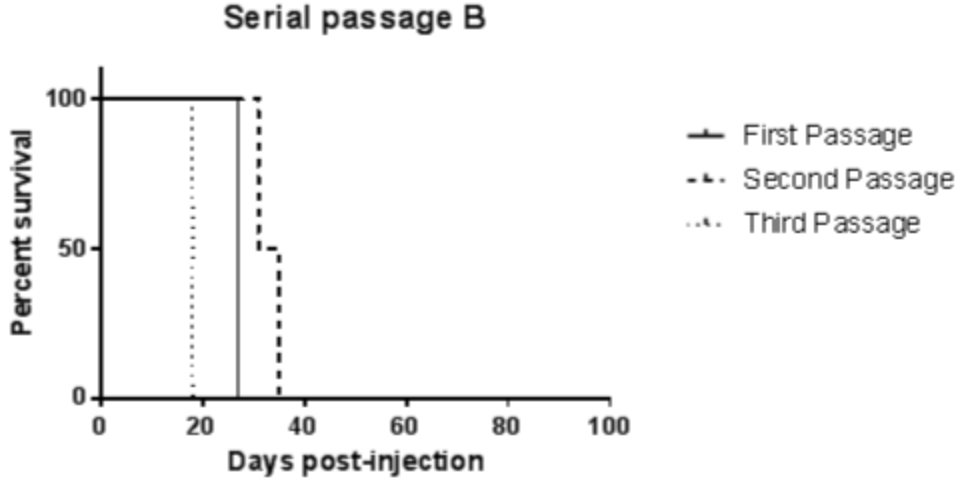
Serial passage B
Percent survival
100
50
0
0
20
40
60
80
100
Days post-injection
First Passage
Second Passage
Third Passage

B

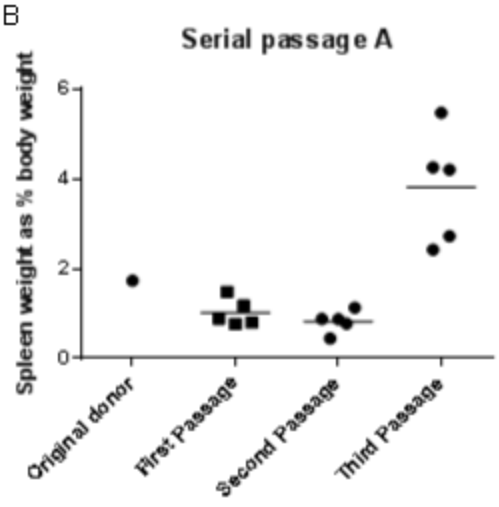
Serial passage A
Spleen weight as % body weight
6
4
2
0
Original donor
First Passage
Second Passage
Third Passage

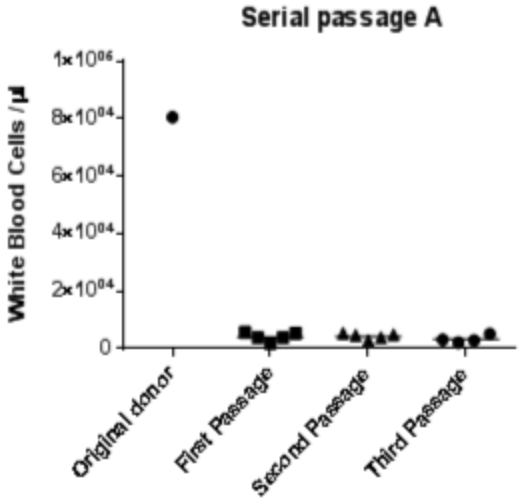
Serial passage A
White Blood Cells / µl
1x10^06
8x10^04
6x10^04
4x10^04
2x10^04
0
Original donor
First Passage
Second Passage
Third Passage

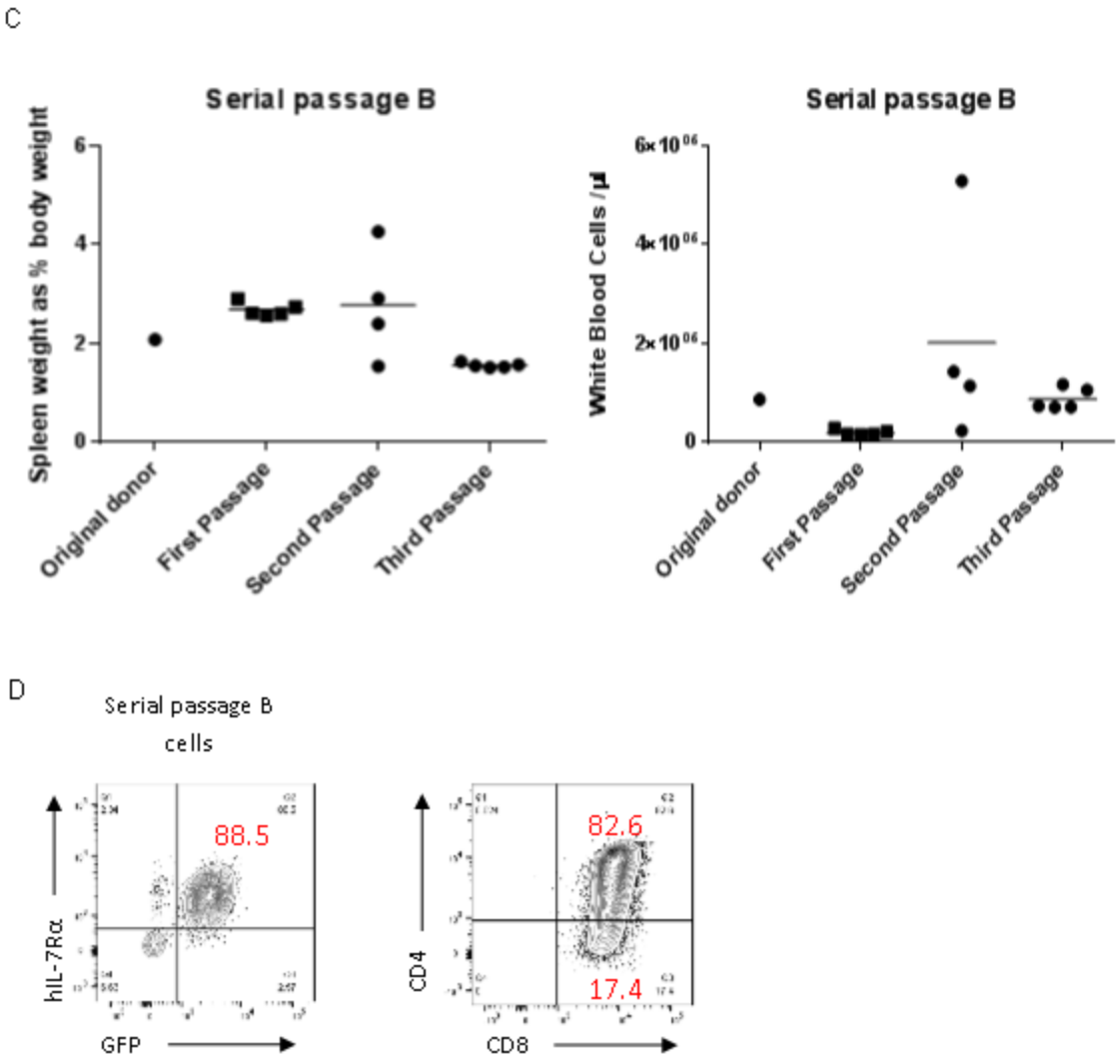

Figure 33. Splenic cells from donors injected with *mutNRas-IL-7Rα-GOF* cells caused rapid-onset disease in serial recipients. Of four independent passage experiments, three generated successful passage through three sequential groups of recipients (two shown, N=5 recipients/group) (A). Passaged cells continued to cause splenomegaly and variable leukocytosis (B-C). Cells from passage B continued to express human IL-7Rα and GFP as a marker of successful transduction with *IL-7Rα-GOF* and *mutNRAS*, respectively and maintained an immunophenotype similar to the original donor (D). Bars represent mean values.

and 9 passages, respectively, to generate cell lines. The resultant cell line from serial passage B continued to express human IL-7Rα and GFP (*mutNRAS*) and maintained an

immunophenotype similar to the original donor animal (Figure 33D). This cell line would not grow in culture, similar to patient T-ALL cells which must be passaged as xenografts in mice. We used these cells in the following drug study.

To determine the leukemia-initiating cell frequency of *mutNRAS-IL-7Rα-GOF* cells, we injected groups of mice with serial dilutions of newly transduced cells (Figure 34A). Using these results, we performed extreme limiting dilution analysis statistics and calculated the number of leukemia-initiating cells to be approximately 1 in 614 (Figure 34B) (Hu and Smyth, 2009). Animals receiving fewer cells developed disease later than those injected with larger numbers of cells (Figure 34C). Calculation of leukemia-initiating cell frequency was based on the number of live, GFP^+ cells injected into mice, and it did not take into account the percentage of those cells expressing human IL-7Rα (typically ~40%). Given this, the leukemia-initiating cell frequency may actually be higher.

MutNRAS-IL-7Rα-GOF cells are polyclonal

While *mutNRAS-IL-7Rα-GOF* cells appeared to be neoplastic and disease onset was rapid, it seemed possible that additional genetic lesions could have occurred *in vitro* or *in vivo* to drive leukemia formation. If the *mutNRAS-IL-7Rα-GOF* combination was sufficient to generate leukemia absent other mutations, we expected the resulting leukemias to be polyclonal since they would have originated from many different cells, each of which had been transduced with the combination of mutant genes. If additional

A

Number of Live, GFP+ cells Injected	Number of Mice in Group	Number of Mice developing Leukemia/lymphoma
202000	4	4
20200	5	5
2020	5	5
202	5	1
20	5	0

B

Confidence intervals for leukemia -initiating cell frequency		
Lower	Estimate	Upper
1714	614	220

C

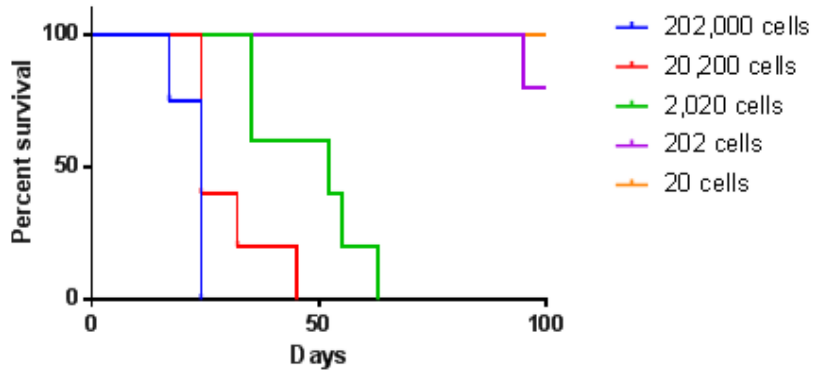

Figure 34. Limiting dilution demonstrated that leukemia-initiating cells were present at an approximate ratio of 1 in 614. Mice injected with as few as 202 cells developed leukemia/lymphoma (A). Based on these data, limiting dilution statistics indicate that the leukemia-initiating cell frequency was approximately 1 in 614 (B). Mice injected with fewer cells survived longer (C). Survival analysis by Log-rank (Mantel-Cox) test $p<0.0001$. Data are from 1 experiment (N= 4-5 recipients/group).

mutations were necessary to cause leukemia, we expected leukemic cells to be oligoclonal or monoclonal, with all leukemic cells derived from those few cells where the requisite additional mutations occurred. To assess clonality, we performed ligation-mediated PCR to identify the retroviral integration sites within the genome. This showed that the *mutNRAS-IL-7Rα-GOF* leukemias were highly polyclonal in comparison to a *mutNRAS*- only lymphoma and the *Hoxa- IL-7Rα-GOF* leukemias which were oligoclonal (Figure 35A and Figure 28). The *mutNRAS*-only cells had a major dominant clone with an integration site in the *Notch1* gene that was predicted to be an activating insertion in the 5' regulatory region. Whether there were additional genetic mutations in this lymphoma is unknown. While *mutNRAS-IL-7Rα-GOF* cell populations were polyclonal, assessment of the top 20 integration sites from each mouse suggested that some animals injected with cells from the same pool of transduced cells shared major clones, indicating differential growth of clones both *in vitro* and *in vivo*. T-cell receptor clonality assessment showed variations in the degree of clonality between animals (Figure 35B), and assessment of TCR clonality on samples from the limiting dilution experiment showed overgrowth of one or a few dominant clones (data not shown). To determine whether retroviral insertion site could be conferring growth advantage to major clones, we assessed the genes impacted by integration. On average, 5 of the 20 top integration sites in each animal impacted genes that were known tumor suppressors and/or oncogenes (Bushman, 2016; Zhao et al., 2016). These data confirm that the combination of mutant *IL-7Ra* and *NRAS*, while sufficient to induce T-ALL, can also be conferred growth advantage by additional genetic lesions. This is consistent with the observation that human T-ALL cases typically have more than two mutations.

A

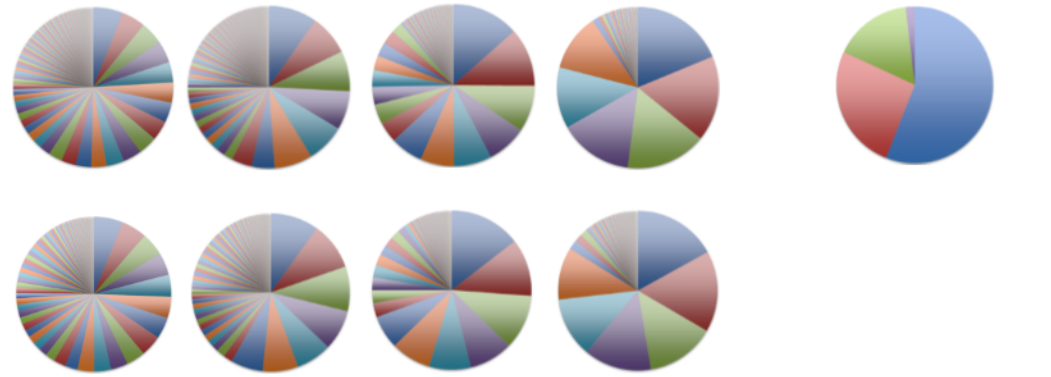

B

mutNRAS-mutIL-7Rα mouse number	% Population composed of a single clone (VDJ recombination analysis)	Clonality based on DJ recombination analysis		
		D1J1	D2J2	Clonal Recombination
1372	No Recombination	Germline/ Polyclonal	Germline/ Polyclonal	-
1363	No Recombination	Clonal	Polyclonal	D1-J1S1 and D1-J1S5
1227	No Recombination	Clonal	Germline	D1-J1S1
994	No Recombination	Clonal	Polyclonal	D1-J1S1
882	30	Not performed		
884	60	Not performed		
872	60, 20, 20	Not performed		
875	30, 30, 20	Not performed		
973	80	Not performed		
999	71, 29	Not performed		

Figure 35. *MutNRAS-IL-7Ra-GOF* cell populations were polyclonal, though some clones were more dominant than others. Splenic DNA was analyzed for unique retroviral integration sites using ligation-mediated PCR. Each circle represents the DNA from a single spleen, and each wedge of the circle represents a unique retroviral integration site. A single clone may have more than one integration site. Cell populations from the *mutNRas-IL-7Rα-GOF* leukemias included multiple clones with unique integration sites. In comparison, cell populations from the *mutNRas*-only lymphoma were relatively oligoclonal (A). Analysis of T-cell receptor clonality of a different subset of *mutNRas-IL-7Ra-GOF* leukemias showed variable clonality between populations, with some leukemias having a major dominant clone and others having more clonal variation (B).

***MutNRAS-IL-7Rα-GOF* cell transcriptome is more similar to *IL-7Rα-GOF*-only cells than *mutNRAS*-only cells**

Continuing to investigate the effects of combining mutant *NRAS* and mutant *IL-7Rα*, we performed transcriptome analysis on RNA isolated from cultured, transduced thymocytes analyzed at the time-point when the cells would have typically been injected into mice. Consistent with previous experiments, transduced genes conferred different immunophenotypes in cultured cells. Based on flow cytometry, *mutNRAS-IL-7Rα-GOF* cells and *IL-7Rα-GOF*-only cells were predominantly $CD4^-CD8^-$ and $CD8^+$ while *mutNRAS*-only cells were predominantly $CD4^-CD8^-$ and $CD4^+$ (Figure 36A). Principal component analysis showed that each group of cells clustered together, suggesting sufficiently unique sets of genes separating each group (Figure 36B). Volcano plot analysis showed greater numbers of genes that were significantly, differentially expressed when comparing *mutNRAS*-only cells and *mutNRAS-IL-7Rα-GOF* cells than when comparing *IL-Rα-GOF*-only cells and *mutNRAS-IL-7Rα-GOF* cells (Figure 36C). Similarly, hierarchical clustering of the transcriptome showed that the overall pattern of

Figure 36: The transcriptional activity of *mutNRAS-IL-7Rα-GOF* cells was more similar to the *IL-7Rα-GOF* cells than *mutNRAS* cells. Cultured *mutNRAS-IL-7Rα-GOF* cells and *IL-7Rα-GOF*-only cells were predominantly CD4-CD8– and CD8+. *MutNRAS*-only cells were predominantly CD4-CD8– and CD4+ (A). Each group of cells clustered separately on principle component analysis (B). Volcano plots show genes that were significantly ($p<0.05$) and differentially (fold change > 2) as red dots. These show greater significant, differential gene expression when comparing *mutNRAS* cells with *mutNRAS-IL-7Rα-GOF* cells than when comparing *IL-7Rα-GOF* cells with *mutNRAS-IL-7Rα-GOF* cells (C). Hierarchical clustering of gene expression similarly showed that the transcriptome of mutNRAS-IL-7Rα-GOF cells appeared more similar to *IL-7Rα-GOF* cells than *mutNRAS* cells (D).

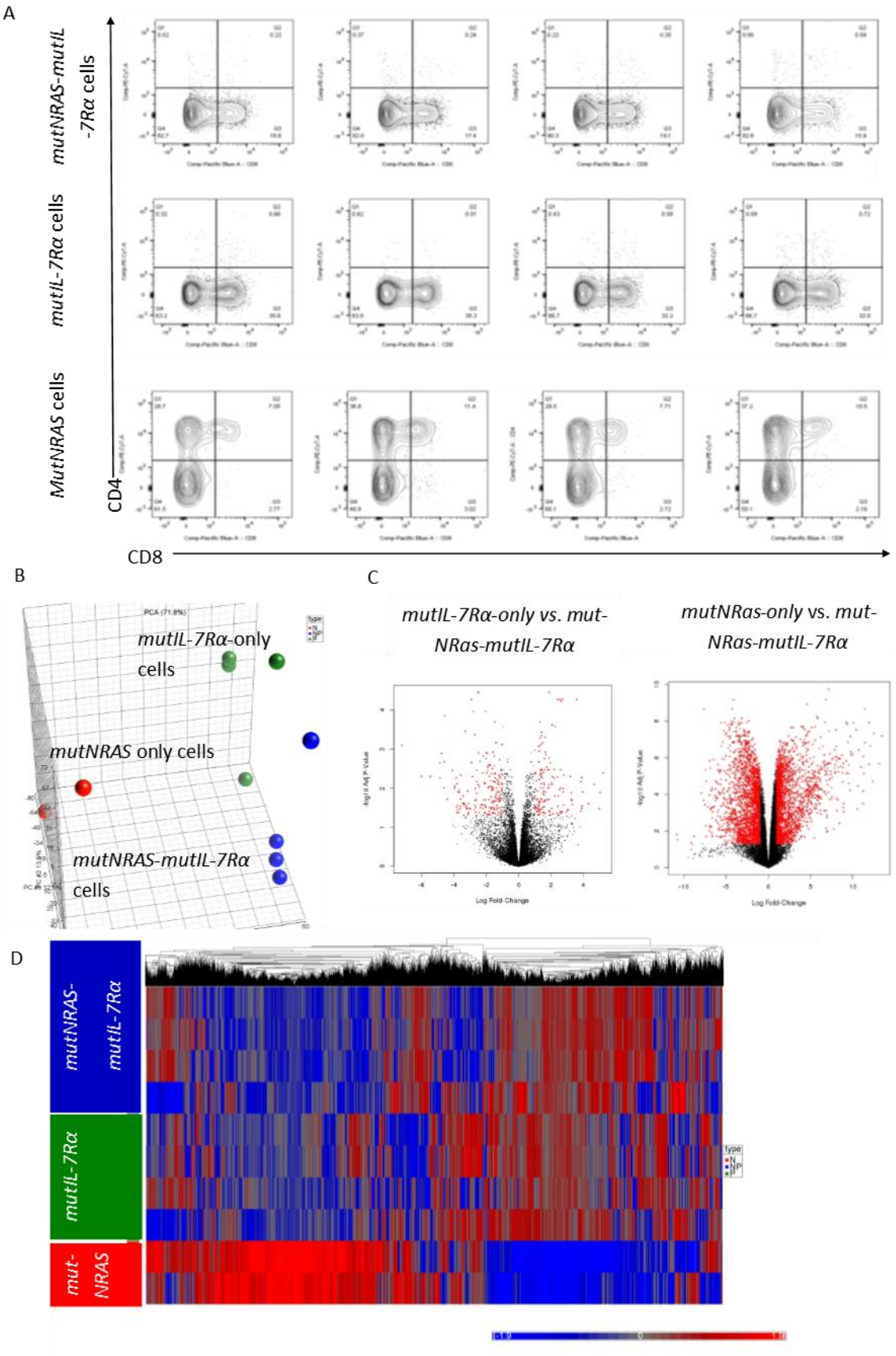
A
mutNRAS-mutIL-7Rα cells
mutIL-7Rα cells
MutNRAS cells
CD4
CD8
B
PCA (71.8%)
mutIL-7Rα-only cells
mutNRAS only cells
mutNRAS-mutIL-7Rα cells
C
mutIL-7Rα-only vs. mut-NRas-mutIL-7Rα
mutNRas-only vs. mut-NRas-mutIL-7Rα
Log Fold Change
D
mutNRAS-mutIL-7Rα
mutIL-7Rα
mut-NRAS

gene expression was similar between *mutNRAS-IL-7Rα-GOF* cells and *IL-7Rα-GOF*-only cells, while *mutNRAS*-only cells had a markedly different gene expression pattern (Figure 36D). This could be due, at least in part, to the similar immunophenotype between *IL-7Rα-GOF*-only cells and *mutNRAS-IL-7Rα-GOF* cells. Within each mutation combination group, there was marked variation between group members. If such variability in gene expression is true for patient samples as well, this could have implications for the development of precision medicine/ targeted therapy. To attempt to determine whether the combination of mutant *NRAS* and mutant *IL-7Rα-GOF* led to dysregulation of oncogenes or tumor suppressor genes, we mined the transcriptome data using lists of known oncogenes and tumor suppressors (Bushman, 2016; Zhao et al., 2016). Hierarchical clustering of the resultant data did not demonstrate coordinated, differential expression of oncogenes or tumor suppressor genes that could explain why *mutNRAS-IL-7Rα-GOF* cells were leukemogenic.

Treatment of *mutNRAS-IL-7Rα-GOF* leukemia reduced disease progression and prolonged survival

To see if targeted therapy would successfully treat *mutNRAS-IL-7Rα-GOF* leukemia, we injected mice with the *mutNRAS-IL-7Rα-GOF* cell line (described in Figure 33) that had been developed by serial passage in mice. We then treated the mice with the MEK inhibitor Trametinib to target the NRAS signaling pathway and the JAK1 inhibitor Ruxolitinib to target the IL-7Rα signaling pathway (Cante-Barrett et al., 2016; Zenatti et al., 2011). Dual treatment significantly reduced disease progression, leading to lowered white blood cell counts, spleen weights, and liver weights at time-matched euthanasia

(Figure 37A-C). Neoplastic infiltrates into the liver and lungs were significantly decreased in treated mice analyzed at time-matched euthanasia (Figure 37D-G). Treated mice survived significantly longer than untreated animals (Figure 37H). Drug treatments were limited by humane considerations to a total of thirty gavages, and additional treatments may have further improved outcomes.

Figure 37: Targeted therapy combining the JAK1 inhibitor Ruxolitinib with the MEK inhibitor Trametinib reduced disease progression and prolonged survival. Mice were treated with Trametinib (0.39 mg/ kg once a day) and Ruxolitinib (150 mg/kg twice a day) by gavage for 10 days. Dual therapy significantly reduced the white blood cell count (A), spleen weight (B), and liver weight (C) when mice were compared at time-matched euthanasia. Histologic analysis of liver (D) and lung (E) showed reduced CD3+ leukemic infiltrates. Digital image analysis of CD3-immunolabeled slides showed significant reductions in percent of CD3+ pixels in liver (F) and lung (G). Red dots indicate animals whose tissues are depicted in D&E. Drug-treated mice survived longer than vehicle-treated mice (H). Time-matched euthanasia data statistical analysis used the Mann-Whitney test comparing the dual therapy-treated mice to controls, and survival analysis used the Log-rank (Mantel-Cox) test. ($p<0.05$=*; $p<0.005$=**; $p\leq0.0005$=***). Data were from a single experiment. Vehicle-only N=12; Ruxolitinib-only N= 9; Trametinib-only N= 10; Dual treatment N=13.

A.

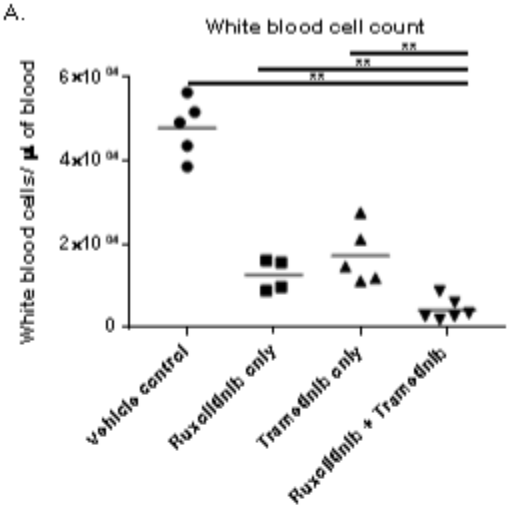
White blood cell count
White blood cells/ µl of blood
6x10 04
4x10 04
2x10 04
0
**
**
**
Vehicle control
Ruxolitinib only
Trametinib only
Ruxolitinib + Trametinib

B.

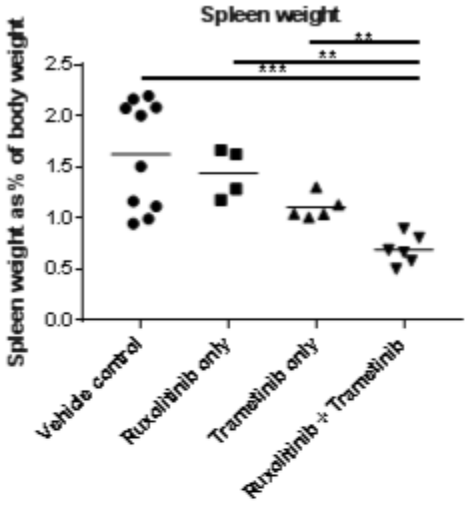
Spleen weight
Spleen weight as % of body weight
2.5
2.0
1.5
1.0
0.5
0.0
**
**
***
Vehicle control
Ruxolitinib only
Trametinib only
Ruxolitinib + Trametinib

C.

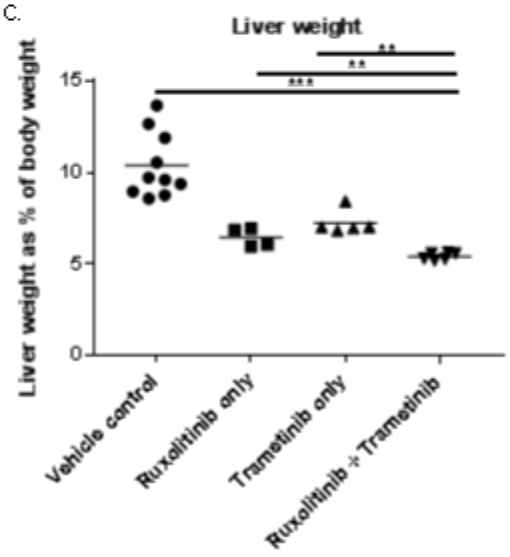
Liver weight
Liver weight as % of body weight
15
10
5
0
**
**
***
Vehicle control
Ruxolitinib only
Trametinib only
Ruxolitinib + Trametinib

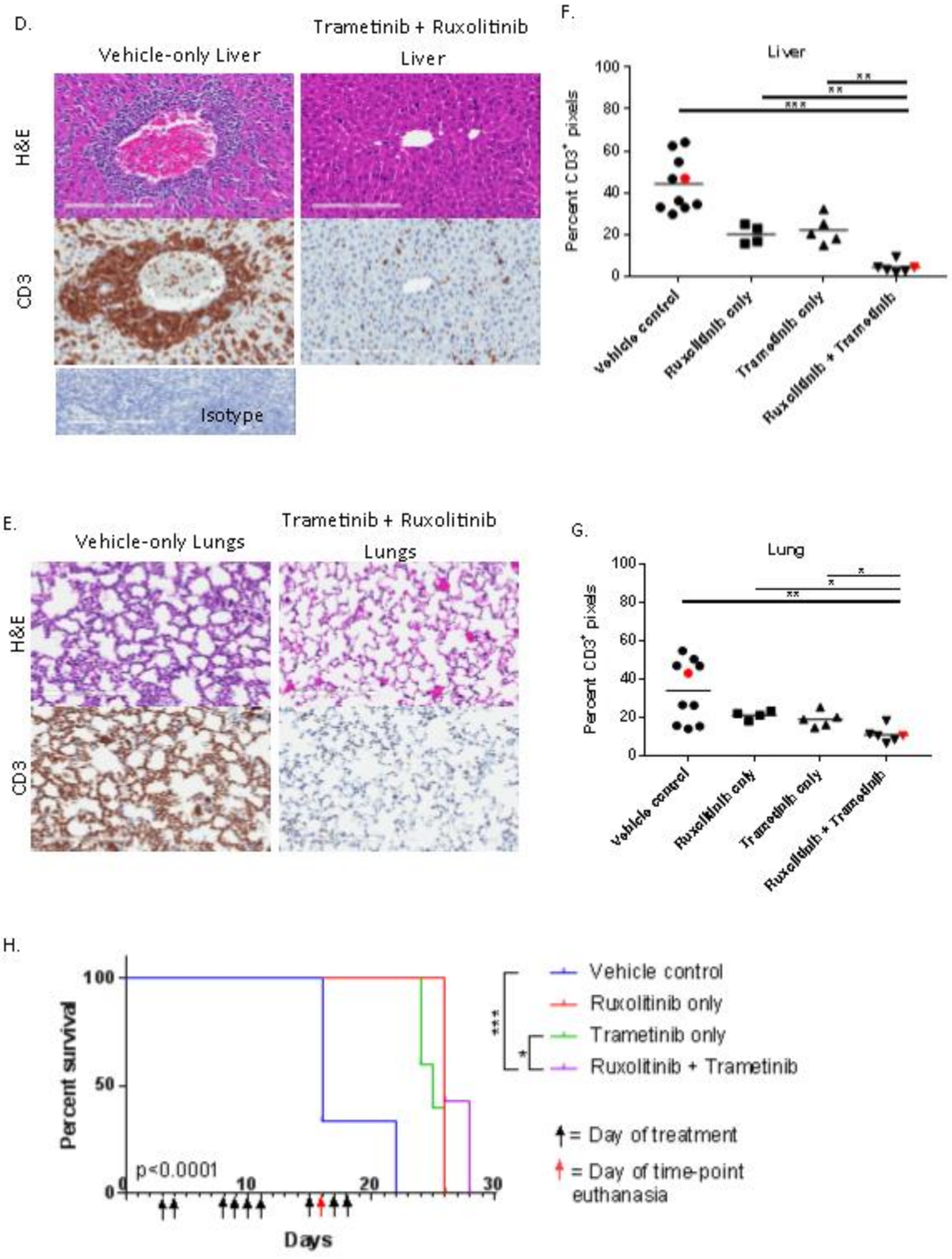
D.
Vehicle-only Liver
Trametinib + Ruxolitinib Liver
H&E
CD3
Isotype
F.
Liver
Percent CD3+ pixels
Vehicle control
Ruxolitinib only
Trametinib only
Ruxolitinib + Trametinib
E.
Vehicle-only Lungs
Trametinib + Ruxolitinib Lungs
G.
Lung
H.
Percent survival
p<0.0001
Days
Vehicle control
Ruxolitinib only
Trametinib only
Ruxolitinib + Trametinib
= Day of treatment
= Day of time-point euthanasia

Discussion

Combination of mutant *IL-7Rα-GOF* with *TLX3* expression or *Hoxa* overexpression was not sufficient to induce T-ALL in our experimental system (Chapter 4). However, mutant *IL-7Rα-GOF* combined with mutant *NRAS* induced rapid-onset, full-penetrance T-ALL. We believe this combination of mutations is sufficient to drive T-ALL because the disease onset was rapid and fully-penetrant, the leukemia-initiating cell frequency was relatively high, and the resultant leukemias were highly polyclonal. The data also revealed that additional genetic lesions can confer growth advantage, as some clones out-competed others, even over the short disease course. This may help to explain why more than two genetic lesions are typically present in human ALL cases.

Having found that combination of mutant *NRas* and mutant *IL-7Rα-GOF* was sufficient to generate T-ALL, we designed a drug study to examine the effects of targeting both signaling pathways on leukemia progression and animal survival. Targeting mutated *RAS* is notoriously difficult, and targeting the downstream effector pathways Raf/MEK/ERK and PI3K/AKT/mTOR is currently more feasible (Ward et al., 2012). The mutant *IL-7Rα* pathway also signals through PI3K/AKT/mTOR as well as JAK1/STAT5, and it can be targeted at multiple levels (Cramer et al., 2016; Zenatti et al., 2011). Therefore, an optimal therapeutic approach would include blockade of the Raf/MEK/ERK, PI3K/AKT/mTOR, and JAK1/STAT5 pathways. However, we were limited in the number of times we could gavage animals due to humane considerations. Therein, we treated animals for 10 days with drugs to target both MEK and JAK1.Though this was not an ideal treatment protocol, dual therapy significantly reduced disease progression and prolonged survival. It seems possible that additional blockade of

the PI3K/AKT/mTOR pathway and longer treatment could have further improved treatment outcomes. These data build on earlier work in patient cells that suggested MEK and PI3K/AKT/mTOR blockade could be useful in targeting *mutNRas-IL-7Rα-GOF* leukemia (Cante-Barrett et al., 2016a).

In conclusion, our data suggest that combined mutations in *IL-7Rα* and *NRas* were sufficient to drive T-ALL formation. Treatment of the resultant leukemia by blocking both pathways reduced leukemia progression and prolonged animal survival. For pediatric patients with this gene signature, these experiments could help to inform the development of targeted therapies.

Chapter 6: Conclusions and future directions

Our laboratory has a long-term interest in the role of IL-7 signaling in T-cell development, and the laboratory has been instrumental in determining some of the basic mechanisms of IL-7 effects on T-cell survival and proliferation. Recently, our laboratory and others have identified mutations in *IL-7Rα* in a subset of pediatric T-ALL, B-ALL, and ETP-ALL. These mutations were the driving force behind development of this project. Studies of cell lines had shown that the mutations enabled homodimerization of the receptor and constitutive signaling in the absence of JAK3 and γ_c. However, little was known about how the mutant signaling might affect normal, immature T-cell development. Furthermore, while the mutation in *IL-7Rα* was likely oncogenic, it did not appear to be sufficient to drive leukemia formation on its own, suggesting that collaborative genetic lesions were necessary for leukemogenesis.

Based on this, we designed a project with two specific aims in mind. The first was to evaluate the effect of mutant *IL-7Rα* signaling on T-cell development and differentiation. The second was to explore genetic mutations that may complement mutated *IL-7Rα* and lead to leukemia formation. To address these specific aims, we designed an experimental approach that relied heavily on *in vivo* experiments. This yielded striking results, though it incurred higher costs in many respects than an *in vitro* approach. Going forward, the experimental strategy used in this project seems best used to assess candidate collaborations that, like those we explored, are well-founded in patient data.

Mutant IL-7Rα-GOF effects on T-cell development

To address our first specific aim, *in vitro* studies on the developmental effects of mutant *IL-7Rα-GOF* signaling showed that mutant signaling induced an increased maturation of $CD8^+$ cells from immature thymocytes. Though this was interesting, it was not unexpected, since IL-7 signaling was already known to support CD8 differentiation and to block CD4 differentiation (Hong et al., 2012). *In vivo* studies, on the other hand, yielded novel and surprising results. Mice injected with thymocytes transduced with *IL-7Rα-GOF* developed fairly rapid-onset, full-penetrance, multi-systemic inflammation morphologically consistent with graft-versus-host disease. Animals injected with *wtIL-7Rα* transduced thymocytes did not develop disease. Inflammation was most severe in the lungs, liver, and skin of affected animals, inflammatory infiltrates were composed of mixed populations of transduced cells as well as non-transduced cells, and there was a marked neutrophilic component. Flow cytometry indicated that transduced cells were predominantly $CD4^+$ and $CD8^+$ cells. Affected mice had elevations of multiple serum cytokines and chemokines.

Based on the literature and the morphology of the inflammation, we hypothesized that mutant signaling was dysregulating the balance between T_{reg} and Th17 cell populations. However, analysis of tissues from affected animals did not support this hypothesis. Therefore, the mechanism by which *IL-7Rα-GOF* cells induce inflammation remains unknown. To our knowledge, there is not a human correlate to this condition, so insights gained by further study of this lesion may not yield information relevant to human health.

Mutant IL-7Rα-GOF as a leukemogenic collaborator

Our experimental goal for our second specific aim was to identify gene(s) that collaborated with mutant human *IL-7Rα* to drive T-ALL. We chose candidate collaborators with two factors in mind: patient data and presumed collaborative role. *TLX3* expression, *HOXA* overexpression, and *NRAS* mutation were all known to occur together with mutant *IL-7Rα* in patients (as reviewed in Chapter 2) (Cante-Barrett et al., 2016a; Zenatti et al., 2011). As to collaborative role, modeling leukemic evolution suggests leukemogenesis requires induction of aberrant self-renewal and proliferation/ survival signaling (Tremblay and Curtis, 2014). A successful collaborator, then, would be expected to enable self-renewal, since mutant *IL-7Rα* is thought to support proliferation and survival of T-ALL cells (Li et al., 2010; Li et al., 2006). Consistent with this, *TLX3* expression and *HOXA* overexpression have both been postulated to play a role in driving self-renewal (Tremblay and Curtis, 2014). *NRAS* mutations have been shown to support enhanced self-renewal (Li et al., 2013). Therefore, all three genes appear to be excellent candidates for collaboration based on these criteria.

However, when mutant *IL-7Rα-GOF* was combined with expression of human *TLX3*, only one of five mice injected developed T-cell lymphoma. This suggested that the combination of *TLX3* expression and mutant *IL-7Rα-GOF* required additional genetic lesion/s to cause cancer. Combination of mutant *IL-7Rα* with overexpression of the *Hoxa* gene cluster yielded rapid-onset, fully-penetrant myeloid leukemia. To our knowledge, mutations in *IL-7Rα* have not been identified in human cases of myeloid leukemia. These experiments suggested that the combination of mutant *IL-7Rα* and *Hoxa* gene overexpression has a potent capacity to drive myeloid leukemia formation, but additional

genetic lesion/s are necessary for commitment to the T-cell lineage. Taken together, our experiments showed that neither *TLX3* expression nor *Hoxa* gene cluster overexpression was sufficient to drive T-ALL formation when combined with mutant *IL-7Rα-GOF*.

However, when we combined mutant *IL-7Rα-GOF* with mutant *NRAS*, recipient mice developed rapid-onset, full-penetrance leukemia composed of mixed populations of T-cells. Cells were polyclonal, consistent with our experimental model, serial passage was successful, and the leukemia-initiating cell frequency was relatively high. Based on this, we concluded that the combination of mutant *IL-7Rα-GOF* and mutant *NRAS* was sufficient to drive T-ALL formation. While it was exciting to find a combination of mutations that caused T-ALL, it was even more exciting to find that treating the two signaling pathways in leukemic mice significantly decreased disease burden and prolonged survival. This suggests that blocking these two signaling pathways might be important in the development of targeted therapies for pediatric leukemia.

Candidate collaborations for future investigations

This project identified one collaborative partnership that was sufficient to induce T-ALL and two other partnerships that may be nearly sufficient. As gene sequencing becomes ever cheaper and easier, we will soon have a plethora of patient data to inform future studies of genes that might collaborate with mutant *IL-7Rα-GOF* and its signaling pathway members to generate leukemia. At this point, there remain several potential candidate combinations that could induce T-ALL. These may be excellent candidates for future experiments.

To begin, results from studies with *TLX3* expression and *Hoxa* overexpression suggested that an additional genetic lesion might be adequate to drive T-ALL formation.

In the case of *TLX3*, a candidate collaborator is unknown. However, it appears that *Hoxa* overexpression may be adequate to induce leukemia, just not T-cell leukemia. An ideal candidate for T-ALL collaboration, then, would be *NOTCH1* mutation, as *NOTCH* signaling drives commitment to the T-cell lineage (Holmes and Zuniga-Pflucker, 2009). *NOTCH1* is mutated in over half of T-ALL patients, and 4/5 patients with mutated *IL-7Rα* in the HOXA subgroup had *NOTCH1* mutations (Weng et al., 2004; Zenatti et al., 2011).

In addition, there is ample patient data to support that mutations in epigenetic regulators act in collaboration with mutant *IL-7Rα-GOF* to cause leukemia formation, particularly *PHF6* mutations (see Chapter 2). A model of clonal evolution suggests that this combination of mutations might require at least a third mutation that induced aberrant self-renewal to generate fulminant leukemia (Tremblay and Curtis, 2014). Of particular interest, polycomb repressor complex 2 (*PRC2*) has been shown to regulate *HOXA* gene expression, suggesting that loss of *PRC2* combined with mutant *IL-7Rα-GOF* and *HOXA* overexpression might yield interesting results (Nagel et al., 2010). However, work performed in our laboratory by Gisele Rodrigues suggested that it was quite difficult to knockdown the epigenetic regulator *PHF6*.

Work in our laboratory has also shown that mutant *IL-7Rα-GOF* transduction of the immortalized cell line D1 leads to leukemia when injected into mice. This cell line is known to have a mutation in the tumor suppressor p53. p53 is typically thought of as a cell cycle regulator, though it has been shown to enable self-renewal in murine nephrons (Li et al., 2015). It seems possible that loss of p53 might play a similar role as loss of Arf in collaborating with mutant *IL-7Rα* (Treanor et al., 2014). To our knowledge, there are

not current patient data to corroborate such a collaboration. Mutations in *TP53* (the gene that encodes p53) seem to be more prevalent in relapsed pediatric ALL where concurrent mutations have been identified (Hof et al., 2011; Richter-Pechanska et al., 2017). This suggests that experimental combination of mutant *IL-7Rα* and p53 deletion in primary thymocytes could yield interesting results.

While there are multiple genetic lesions with data to support potential collaboration with mutant *IL-7Rα*, there are other genetic lesions that patient data suggest are not common collaborators. In one patient study, *TAL1/LMO2* mutations were mutually exclusive of *IL-7R-JAK* mutations (Vicente et al., 2015). Another study showed that only 1/17 patients with *IL-7Rα* mutation was in the TAL1/LMO2 subtype (Zenatti et al., 2011) Thus, patient data suggest that a combination of mutant *IL-7Rα-GOF* and *TAL1/LMO2* mutation should not be first on the list of new potential collaborations to assess.

More confounding is the question of whether or not additional mutations in the *IL-7Rα* signaling pathway might collaborate with the mutant receptor to drive leukemia. Dogma would suggest that such a combination would be redundant, and one study of patient samples showed that mutations in the IL-7Rα signaling pathway were mutually exclusive (Cante-Barrett et al., 2016a). However, other sets of patient data support multiple concurrent mutations in the IL-7Rα signaling pathways in T-ALL, B-ALL, and ETP-ALL. These include one case with concurrent *IL-7Rα* mutation and *SH2B3* deletion in B-ALL and fairly frequent concurrence between *IL-7Rα* mutation and *JAK3* mutation in T-ALL and ETP-ALL (Roberts et al., 2012; Vicente et al., 2015; Zhang et al., 2012). Interestingly, a top retroviral integration site in one of the *mutNRas-IL-7Rα-GOF*

leukemias in our study was in the *JAK3* gene, suggesting that *JAK3* activation conferred additional growth advantage to this clone. While it isn't consistent with dogma, it seems that combination of mutant *IL-7Rα-GOF* and mutant *JAK3* might act collaboratively. A potential collaboration might be more likely because, while wild type *IL-7Rα* signals through *JAK3* activation, mutant *IL-7Rα-GOF* signaling is independent of JAK3.

We need to identify collaborators to improve T-ALL therapy

Parsing potential collaborations from patient and experimental data is a start. But searching individual reports of patient data for evidence of collaborative mutations is not enough. As technology continues to advance, it will become ever easier to identify genetic lesions in individual ALL cases. With this will come ever-growing data sets. These sets offer immense opportunity to identify leukemogenic collaborations using bioinformatics approaches. To do this, many data sets need to be made available for analysis through shared outlets such as COSMIC (http://cancer.sanger.ac.uk/cosmic) or cBioportal (http://www.cbioportal.org/). Such sharing of data can enable efficient identification of potential collaborative mutations. Based on these data, experimental approaches can be used to further examine the collaboration, as was done in this project.

We must continue to focus on understanding networks of collaborative mutations. Once we know which combination of mutations are vital to the development of leukemia, we can tailor treatment protocols to target these signaling pathways. Each leukemia is unique, and perhaps someday, each patient's treatment protocol will also be unique.

Bibliography

Agnusdei, V., S. Minuzzo, C. Frasson, A. Grassi, F. Axelrod, S. Satyal, A. Gurney, T. Hoey, E. Seganfreddo, G. Basso, S. Valtorta, R.M. Moresco, A. Amadori, and S. Indraccolo. 2014. Therapeutic antibody targeting of Notch1 in T-acute lymphoblastic leukemia xenografts. *Leukemia* 28:278-288.

Anderson, F.W., T.R. Johnson, and R. de Vries. 2017. Global Health Ethics: The Case of Maternal and Neonatal Survival. *Best Pract Res Clin Obstet Gynaecol*.

Argiropoulos, B., and R.K. Humphries. 2007. Hox genes in hematopoiesis and leukemogenesis. *Oncogene* 26:6766-6776.

Asnafi, V., S. Le Noir, L. Lhermitte, C. Gardin, F. Legrand, X. Vallantin, J.V. Malfuson, N. Ifrah, H. Dombret, and E. Macintyre. 2010. JAK1 mutations are not frequent events in adult T-ALL: a GRAALL study. *Brit J Haematol* 148:179-179.

Atak, Z.K., V. Gianfelici, G. Hulselmans, K. De Keersmaecker, A.G. Devasia, E. Geerdens, N. Mentens, S. Chiaretti, K. Durinck, A. Uyttebroeck, P. Vandenberghe, I. Wlodarska, J. Cloos, R. Foa, F. Speleman, J. Cools, and S. Aerts. 2013. Comprehensive Analysis of Transcriptome Variation Uncovers Known and Novel Driver Events in T-Cell Acute Lymphoblastic Leukemia. *Plos Genet* 9.

Bailey, Z.D., N. Krieger, M. Agenor, J. Graves, N. Linos, and M.T. Bassett. 2017. Structural racism and health inequities in the USA: evidence and interventions. *Lancet* 389:1453-1463.

Bains, T., M.C. Heinrich, M.M. Loriaux, C. Beadling, D. Nelson, A. Warrick, T.L. Neff, J.W. Tyner, J. Dunlap, C.L. Corless, and G. Fan. 2012. Newly described activating JAK3 mutations in T-cell acute lymphoblastic leukemia. *Leukemia* 26:2144-2146.

Ballerini, P., A. Blaise, M. Busson-Le Coniat, X.Y. Su, J. Zucman-Rossi, M. Adam, J. van den Akker, C. Perot, B. Pellegrino, J. Landman-Parker, L. Douay, R. Berger, and O.A. Bernard. 2002. HOX11L2 expression defines a clinical subtype of pediatric T-ALL associated with poor prognosis. *Blood* 100:991-997.

Ballerini, P., J. Landman-Parker, J.M. Cayuela, V. Asnafi, M. Labopin, V. Gandemer, Y. Perel, G. Michel, T. Leblanc, C. Schmitt, S. Fasola, A. Hagemejier, F. Sigaux, M.F. Auclerc, L. Douay, G. Leverger, and A. Baruchel. 2008. Impact of genotype on survival of children with T-cell acute lymphoblastic leukemia treated according to the French protocol FRALLE-93: the effect of TLX3/HOX11L2 gene expression on outcome. *Haematologica* 93:1658-1665.

Bandapalli, O.R., S. Schuessele, J.B. Kunz, T. Rausch, A.M. Stutz, N. Tal, I. Geron, N. Gershman, S. Izraeli, J. Eilers, N. Vaezipour, R. Kirschner-Schwabe, J. Hof, A. von Stackelberg, M. Schrappe, M. Stanulla, M. Zimmermann, R. Koehler, S. Avigad, R. Handgretinger, V. Frismantas, J.P. Bourquin, B. Bornhauser, J.O. Korbel, M.U. Muckenthaler, and A.E. Kulozik. 2014. The activating STAT5B N642H mutation is a common abnormality in pediatric T-cell acute lymphoblastic leukemia and confers a higher risk of relapse. *Haematologica* 99:e188-192.

Barata, J.T., A.A. Cardoso, L.M. Nadler, and V.A. Boussiotis. 2001. Interleukin-7 promotes survival and cell cycle progression of T-cell acute lymphoblastic leukemia cells by down-regulating the cyclin-dependent kinase inhibitor p(27kip1). *Blood* 98:1524-1531.

Barata, J.T., T.D. Keenan, A. Silva, L.M. Nadler, V.A. Boussiotis, and A.A. Cardoso. 2004a. Common gamma chain-signaling cytokines promote proliferation of T-cell acute lymphoblastic leukemia. *Haematologica* 89:1459-1467.

Barata, J.T., A. Silva, J.G. Brandao, L.M. Nadler, A.A. Cardoso, and V.A. Boussiotis. 2004b. Activation of PI3K is indispensable for interleukin 7-mediated viability, proliferation, glucose use, and growth of T cell acute lymphoblastic leukemia cells. *Journal of Experimental Medicine* 200:659-669.

Baxter, C., and S. Abdool Karim. 2016. Combination HIV prevention options for young women in Africa. *Afr J AIDS Res* 15:109-121.

Beachy, S.H., M. Onozawa, D. Silverman, Y.J. Chung, M.M. Rivera, and P.D. Aplan. 2013. Isolated Hoxa9 overexpression predisposes to the development of lymphoid but not myeloid leukemia. *Exp Hematol* 41:518-529 e515.

Bercovich, D., I. Ganmore, L.M. Scott, G. Wainreb, Y. Birger, A. Elimelech, C. Shochat, G. Cazzaniga, A. Biondi, G. Basso, G. Cario, M. Schrappe, M. Stanulla, S. Strehl, O.A. Haas, G. Mann, V. Binder, A. Borkhardt, H. Kempski, J. Trka, B. Bielorei, S. Avigad, B. Stark, O. Smith, N. Dastugue, J.P. Bourquin, N.B. Tal, A.R. Green, and S. Izraeli. 2008. Mutations of JAK2 in acute lymphoblastic leukaemias associated with Down's syndrome. *Lancet* 372:1484-1492.

Bergeron, J., E. Clappier, B. Cauwelier, N. Dastugue, C. Millien, E. Delabesse, K. Beldjord, F. Speleman, J. Soulier, E. Macintyre, and V. Asnafi. 2006. HOXA cluster deregulation in T-ALL associated with both a TCRD-HOXA and a CALM-AF10 chromosomal translocation. *Leukemia* 20:1184-1187.

Bernard, O.A., M. Busson-LeConiat, P. Ballerini, M. Mauchauffe, V. Della Valle, R. Monni, F. Nguyen Khac, T. Mercher, V. Penard-Lacronique, P. Pasturaud, L. Gressin, R. Heilig, M.T. Daniel, M. Lessard, and R. Berger. 2001. A new recurrent and specific cryptic translocation, t(5;14)(q35;q32), is associated with expression of the Hox11L2 gene in T acute lymphoblastic leukemia. *Leukemia* 15:1495-1504.

Bertin, R., C. Acquaviva, D. Mirebeau, C. Guidal-Giroux, E. Vilmer, and H. Cave. 2003. CDKN2A, CDKN2B, and MTAP gene dosage permits precise characterization of mono- and bi-allelic 9p21 deletions in childhood acute lymphoblastic leukemia. *Genes Chromosomes Cancer* 37:44-57.

Borowski, A., T. Vetter, M. Kuepper, A. Wohlmann, S. Krause, T. Lorenzen, J.C. Virchow, W. Luttmann, and K. Friedrich. 2013. Expression analysis and specific blockade of the receptor for human thymic stromal lymphopoietin (TSLP) by novel antibodies to the human TSLPR alpha receptor chain. *Cytokine* 61:546-555.

Brandimarte, L., V. Pierini, D. Di Giacomo, C. Borga, F. Nozza, P. Gorello, M. Giordan, G. Cazzaniga, G. Te Kronnie, R. La Starza, and C. Mecucci. 2013. New MLLT10 gene recombinations in pediatric T-acute lymphoblastic leukemia. *Blood* 121:5064-5067.

Bray, S.J. 2016. Notch signalling in context. *Nat Rev Mol Cell Biol* 17:722-735.

Breit, S., M. Stanulla, T. Flohr, M. Schrappe, W.D. Ludwig, G. Tolle, M. Happich, M.U. Muckenthaler, and A.E. Kulozik. 2006. Activating NOTCH1 mutations predict favorable early treatment response and long-term outcome in childhood precursor T-cell lymphoblastic leukemia. *Blood* 108:1151-1157.

Brown, V.I., J.J. Fang, K. Alcorn, R. Barr, J.M. Kim, R. Wasserman, and S.A. Grupp. 2003. Rapamycin is active against B-precursor leukemia in vitro and in vivo, an effect that is modulated by Il-7-mediated signalling. *P Natl Acad Sci USA* 100:15113-15118.

Bugarin, C., J. Sarno, C. Palmi, A.M. Savino, G. te Kronnie, M. Dworzak, A. Shumich, B. Buldini, O. Maglia, S. Sala, I. Bronzini, J.P. Bourquin, E. Mejstrikova, O. Hrusak, D. Luria, G. Basso, S. Izraeli, A. Biondi, G. Cazzaniga, G. Gaipa, and I.B.s. group. 2015. Fine tuning of surface CRLF2 expression and its associated signaling profile in childhood B-cell precursor acute lymphoblastic leukemia. *Haematologica* 100:e229-232.

Buontempo, F., E. Orsini, L.R. Martins, I. Antunes, A. Lonetti, F. Chiarini, G. Tabellini, C. Evangelisti, C. Evangelisti, F. Melchionda, A. Pession, A. Bertaina, F. Locatelli, J.A. McCubrey, A. Cappellini, J.T. Barata, and A.M. Martelli. 2014. Cytotoxic activity of the casein kinase 2 inhibitor CX-4945 against T-cell acute lymphoblastic leukemia: targeting the unfolded protein response signaling. *Leukemia* 28:543-553.

Cani, A., C. Simioni, A.M. Martelli, G. Zauli, G. Tabellini, S. Ultimo, J.A. McCubrey, S. Capitani, and L.M. Neri. 2015. Triple Akt inhibition as a new therapeutic strategy in T-cell acute lymphoblastic leukemia. *Oncotarget* 6:6597-6610.

Cante-Barrett, K., J.A. Spijkers-Hagelstein, J.G. Buijs-Gladdines, J.C. Uitdehaag, W.K. Smits, J. van der Zwet, R.C. Buijsman, G.J. Zaman, R. Pieters, and J.P. Meijerink. 2016a. MEK and PI3K-AKT inhibitors synergistically block activated IL7 receptor signaling in T-cell acute lymphoblastic leukemia. *Leukemia* 1832-1834.

Cante-Barrett, K., J.C. Uitdehaag, and J.P. Meijerink. 2016b. Structural modeling of JAK1 mutations in T-cell acute lymphoblastic leukemia reveals a second contact site between pseudokinase and kinase domains. *Haematologica* 101:e189-191.

Cao, X., E.W. Shores, J. Hu-Li, M.R. Anver, B.L. Kelsall, S.M. Russell, J. Drago, M. Noguchi, A. Grinberg, E.T. Bloom, and et al. 1995. Defective lymphoid development in mice lacking expression of the common cytokine receptor gamma chain. *Immunity* 2:223-238.

Carrasco Salas, P., L. Fernandez, M. Vela, D. Bueno, B. Gonzalez, J. Valentin, P. Lapunzina, and A. Perez-Martinez. 2016. The role of CDKN2A/B deletions in pediatric acute lymphoblastic leukemia. *Pediatr Hematol Oncol* 33:415-422.

Castro, M.C., M.E. Wilson, and D.E. Bloom. 2017. Disease and economic burdens of dengue. *Lancet Infect Dis* 17:e70-e78.

Cauwelier, B., H. Cave, C. Gervais, M. Lessard, C. Barin, C. Perot, J. Van den Akker, F. Mugneret, C. Charrin, M.P. Pages, M.J. Gregoire, P. Jonveaux, M. Lafage-Pochitaloff, M.J. Mozzicconacci, C. Terre, I. Luquet, P. Cornillet-Lefebvre, B. Laurence, G. Plessis, C. Lefebvre, D. Leroux, H. Antoine-Poirel, C. Graux, L. Mauvieux, P. Heimann, C. Chalas, E. Clappier, B. Verhasselt, Y. Benoit, B.D. Moerloose, B. Poppe, N. Van Roy, K.D. Keersmaecker, J. Cools, F. Sigaux, J. Soulier, A. Hagemeijer, A.D. Paepe, N. Dastugue, R. Berger, and F. Speleman.

2007. Clinical, cytogenetic and molecular characteristics of 14 T-ALL patients carrying the TCRbeta-HOXA rearrangement: a study of the Groupe Francophone de Cytogenetique Hematologique. *Leukemia* 21:121-128.

Cave, H., S. Suciu, C. Preudhomme, B. Poppe, A. Robert, A. Uyttebroeck, M. Malet, P. Boutard, Y. Benoit, L. Mauvieux, P. Lutz, F. Mechinaud, N. Grardel, F. Mazingue, M. Dupont, G. Margueritte, M.P. Pages, Y. Bertrand, E. Plouvier, G. Brunie, C. Bastard, D. Plantaz, I. Vande Velde, A. Hagemeijer, F. Speleman, M. Lessard, J. Otten, E. Vilmer, N. Dastugue, and C.L.G. Eortc. 2004. Clinical significance of HOX11L2 expression linked to t(5;14)(q35;q32), of HOX11 expression, and of SIL-TAL fusion in childhood T-cell malignancies: results of EORTC studies 58881 and 58951. *Blood* 103:442-450.

Chao, M.M., M.A. Todd, U. Kontny, K. Neas, M.J. Sullivan, A.G. Hunter, D.J. Picketts, and C.P. Kratz. 2010. T-cell acute lymphoblastic leukemia in association with Borjeson-Forssman-Lehmann syndrome due to a mutation in PHF6. *Pediatr Blood Cancer* 55:722-724.

Chapiro, E., L. Russell, E. Lainey, S. Kaltenbach, C. Ragu, V. Della-Valle, K. Hanssens, E.A. Macintyre, I. Radford-Weiss, E. Delabesse, H. Cave, T. Mercher, C.J. Harrison, F. Nguyen-Khac, P. Dubreuil, and O.A. Bernard. 2010. Activating mutation in the TSLPR gene in B-cell precursor lymphoblastic leukemia. *Leukemia* 24:642-645.

Chen, I.M., R.C. Harvey, C.G. Mullighan, J. Gastier-Foster, W. Wharton, H. Kang, M.J. Borowitz, B.M. Camitta, A.J. Carroll, M. Devidas, D.J. Pullen, D. Payne-Turner, S.K. Tasian, S. Reshmi, C.E. Cottrell, G.H. Reaman, W.P. Bowman, W.L. Carroll, M.L. Loh, N.J. Winick, S.P. Hunger, and C.L. Willman. 2012. Outcome modeling with CRLF2, IKZF1, JAK, and minimal residual disease in pediatric acute lymphoblastic leukemia: a Children's Oncology Group study. *Blood* 119:3512-3522.

Chen, Y., S.K. Chauhan, X. Tan, and R. Dana. 2016. Interleukin-7 and -15 maintain pathogenic memory Th17 cells in autoimmunity. *J Autoimmun*

Chiang, M.Y., L.W. Xu, O. Shestova, G. Histen, S. L'Heureux, C. Romany, M.E. Childs, P.A. Gimotty, J.C. Aster, and W.S. Pear. 2008. Leukemia-associated NOTCH1 alleles are weak tumor initiators but accelerate K-ras-initiated leukemia. *J Clin Invest* 118:3181-3194.

Chiarini, F., C. Grimaldi, F. Ricci, P.L. Tazzari, C. Evangelisti, A. Ognibene, M. Battistelli, E. Falcieri, F. Melchionda, A. Pession, P. Pagliaro, J.A. McCubrey, and A.M. Martelli. 2010. Activity of the Novel Dual Phosphatidylinositol 3-Kinase/Mammalian Target of Rapamycin Inhibitor NVP-BEZ235 against T-Cell Acute Lymphoblastic Leukemia. *Cancer Res* 70:8097-8107.

Choi, C.W., Y.J. Chung, C. Slape, and P.D. Aplan. 2009. A NUP98-HOXD13 fusion gene impairs differentiation of B and T lymphocytes and leads to expansion of thymocytes with partial TCRB gene rearrangement. *J Immunol* 183:6227-6235.

Corcoran, A.E., F.M. Smart, R.J. Cowling, T. Crompton, M.J. Owen, and A.R. Venkitaraman. 1996. The interleukin-7 receptor alpha chain transmits distinct signals for proliferation and differentiation during B lymphopoiesis. *EMBO J* 15:1924-1932.

Cramer, S.D., P.D. Aplan, and S.K. Durum. 2016. Therapeutic targeting of IL-7Ralpha signaling pathways in ALL treatment. *Blood* 473-478.

Crawley, J.B., J. Willcocks, and B.M.J. Foxwell. 1996. Interleukin-7 induces T cell proliferation in the absence of ErK/MAP kinase activity. *European journal of immunology* 26:2717-2723.

Cullion, K., K.M. Draheim, N. Hermance, J. Tammam, V.M. Sharma, C. Ware, G. Nikov, V. Krishnamoorthy, P.K. Majumder, and M.A. Kelliher. 2009. Targeting the Notch1 and mTOR pathways in a mouse T-ALL model. *Blood* 113:6172-6181.

Cumming, C., L. Troeung, J.T. Young, E. Kelty, and D.B. Preen. 2016. Barriers to accessing methamphetamine treatment: A systematic review and meta-analysis. *Drug Alcohol Depend* 168:263-273.

Cuschieri, S., J. Vassallo, N. Calleja, N. Pace, J. Abela, B.A. Ali, F. Abdullah, E. Zahra, and J. Mamo. 2016. The diabesity health economic crisis-the size of the crisis in a European island state following a cross-sectional study. *Arch Public Health* 74:52.

Dadi, H., S. Ke, and C.M. Roifman. 1994. Activation of phosphatidylinositol-3 kinase by ligation of the interleukin-7 receptor is dependent on protein tyrosine kinase activity. *Blood* 84:1579-1586.

Dadi, S., S. Le Noir, D. Payet-Bornet, L. Lhermitte, J. Zacarias-Cabeza, J. Bergeron, P. Villarese, E. Vachez, W.A. Dik, C. Millien, I. Radford, E. Verhoeyen, F.L. Cosset, A. Petit, N. Ifrah, H. Dombret, O. Hermine, S. Spicuglia, A.W. Langerak, E.A. Macintyre, B. Nadel, P. Ferrier, and V. Asnafi. 2012. TLX Homeodomain Oncogenes Mediate T Cell Maturation Arrest in T-ALL via Interaction with ETS1 and Suppression of TCR alpha Gene Expression. *Cancer Cell* 21:563-576.

De Ravin, S.S., X.L. Wu, S. Moir, S. Anaya-O'Brien, N. Kwatemaa, P. Littel, N. Theobald, U. Choi, L. Su, M. Marquesen, D. Hilligoss, J. Lee, C.M. Buckner, K.A. Zarember, G. O'Connor, D. McVicar, D. Kuhns, R.E. Throm, S. Zhou, L.D. Notarangelo, I.C. Hanson, M.J. Cowan, E. Kang, C. Hadigan, M. Meagher, J.T. Gray, B.P. Sorrentino, and H.L. Malech. 2016. Lentiviral hematopoietic stem cell gene therapy for X-linked severe combined immunodeficiency. *Sci Transl Med* 8.

DeAngelo, D.J., A. Spencer, K.N. Bhalla, H.M. Prince, T. Fischer, T. Kindler, F.J. Giles, J.W. Scott, K. Parker, A. Liu, M. Woo, P. Atadja, K.K. Mishra, and O.G. Ottmann. 2013. Phase Ia/II, two-arm, open-label, dose-escalation study of oral panobinostat administered via two dosing schedules in patients with advanced hematologic malignancies. *Leukemia* 27:1628-1636.

Dervovic, D.D., H.C. Liang, J.L. Cannons, A.R. Elford, M. Mohtashami, P.S. Ohashi, P.L. Schwartzberg, and J.C. Zuniga-Pflucker. 2013. Cellular and molecular requirements for the selection of in vitro-generated CD8 T cells reveal a role for Notch. *J Immunol* 191:1704-1715.

Dickey, L.M., and A.A. Singh. 2017. Social Justice and Advocacy for Transgender and Gender-Diverse Clients. *Psychiatr Clin North Am* 40:1-13.

Diller, M.L., R.R. Kudchadkar, K.A. Delman, D.H. Lawson, and M.L. Ford. 2016. Balancing Inflammation: The Link between Th17 and Regulatory T Cells. *Mediators Inflamm* 2016:6309219.

DiSanto, J.P., W. Muller, D. Guy-Grand, A. Fischer, and K. Rajewsky. 1995. Lymphoid development in mice with a targeted deletion of the interleukin 2 receptor gamma chain. *Proc Natl Acad Sci U S A* 92:377-381.

Dobin, A., C.A. Davis, F. Schlesinger, J. Drenkow, C. Zaleski, S. Jha, P. Batut, M. Chaisson, and T.R. Gingeras. 2013. STAR: ultrafast universal RNA-seq aligner. *Bioinformatics* 29:15-21.

Dondorp, A.M., F.M. Smithuis, C. Woodrow, and L.V. Seidlein. 2017. How to Contain Artemisinin- and Multidrug-Resistant Falciparum Malaria. *Trends Parasitol*

Dorritie, K.A., J.A. McCubrey, and D.E. Johnson. 2014. STAT transcription factors in hematopoiesis and leukemogenesis: opportunities for therapeutic intervention. *Leukemia* 28:248-257.

Evangelisti, C., F. Ricci, P. Tazzari, G. Tabellini, M. Battistelli, E. Falcieri, F. Chiarini, R. Bortul, F. Melchionda, P. Pagliaro, A. Pession, J.A. McCubrey, and A.M. Martelli. 2011. Targeted inhibition of mTORC1 and mTORC2 by active-site mTOR inhibitors has cytotoxic effects in T-cell acute lymphoblastic leukemia. *Leukemia* 25:781-791.

Ferrando, A.A., and A.T. Look. 2000. Clinical implications of recurring chromosomal and associated molecular abnormalities in acute lymphoblastic leukemia. *Semin Hematol* 37:381-395.

Flex, E., V. Petrangeli, L. Stella, S. Chiaretti, T. Hornakova, L. Knoops, C. Ariola, V. Fodale, E. Clappier, F. Paoloni, S. Martinelli, A. Fragale, M. Sanchez, S. Tavolaro, M. Messina, G. Cazzaniga, A. Camera, G. Pizzolo, A. Tornesello, M. Vignetti, A. Battistini, H. Cave, B.D. Gelb, J.C. Renauld, A. Biondi, S.N. Constantinescu, R. Foa, and M. Tartaglia. 2008. Somatically acquired JAK1 mutations in adult acute lymphoblastic leukemia. *Journal of Experimental Medicine* 205:751-758.

Frei, E., 3rd. 1984. Acute leukemia in children. Model for the development of scientific methodology for clinical therapeutic research in cancer. *Cancer-Am Cancer Soc* 53:2013-2025.

Freyer, D.R., M. Devidas, M. La, W.L. Carroll, P.S. Gaynon, S.P. Hunger, and N.L. Seibel. 2011. Postrelapse survival in childhood acute lymphoblastic leukemia is independent of initial treatment intensity: a report from the Children's Oncology Group. *Blood* 117:3010-3015.

Garcia-Peydro, M., V.G. de Yebenes, and M.L. Toribio. 2006. Notch1 and IL-7 receptor interplay maintains proliferation of human thymic progenitors while suppressing non-T cell fates. *J Immunol* 177:3711-3720.

Gehre, N., A. Nusser, L. von Muenchow, R. Tussiwand, C. Engdahl, G. Capoferri, N. Bosco, R. Ceredig, and A.G. Rolink. 2015. A stromal cell free culture system generates mouse pro-T cells that can reconstitute T-cell compartments in vivo. *European journal of immunology* 45:932-942.

Gerby, B., C.S. Tremblay, M. Tremblay, S. Rojas-Sutterlin, S. Herblot, J. Hebert, G. Sauvageau, S. Lemieux, E. Lecuyer, D.F.T. Veiga, and T. Hoang. 2014. SCL, LMO1 and Notch1 Reprogram Thymocytes into Self-Renewing Cells. *Plos Genet* 10.

Giri, J.G., M. Ahdieh, J. Eisenman, K. Shanebeck, K. Grabstein, S. Kumaki, A. Namen, L.S. Park, D. Cosman, and D. Anderson. 1994. Utilization of the beta and gamma chains of the IL-2 receptor by the novel cytokine IL-15. *EMBO J* 13:2822-2830.

Gonzalez-Garcia, S., M. Garcia-Peydro, J. Alcain, and M.L. Toribio. 2012. Notch1 and IL-7 receptor signalling in early T-cell development and leukaemia. *Curr Top Microbiol Immunol* 360:47-73.

Gonzalez-Garcia, S., M. Garcia-Peydro, E. Martin-Gayo, E. Ballestar, M. Esteller, R. Bornstein, J.L. de la Pompa, A.A. Ferrando, and M.L. Toribio. 2009. CSL-MAML-dependent Notch1 signaling controls T lineage-specific IL-7R{alpha} gene expression in early human thymopoiesis and leukemia. *J Exp Med* 206:779-791.

Goossens, S., E. Radaelli, O. Blanchet, K. Durinck, J. Van der Meulen, S. Peirs, T. Taghon, C.S. Tremblay, M. Costa, M. Farhang Ghahremani, J. De Medts, S. Bartunkova, K. Haigh, C. Schwab, N. Farla, T. Pieters, F. Matthijssens, N. Van Roy, J.A. Best, K. Deswarte, P. Bogaert, C. Carmichael, A. Rickard, S. Suryani, L.S. Bracken, R. Alserihi, K. Cante-Barrett, L. Haenebalcke, E. Clappier, P. Rondou, K. Slowicka, D. Huylebroeck, A.W. Goldrath, V. Janzen, M.P. McCormack, R.B. Lock, D.J. Curtis, C. Harrison, G. Berx, F. Speleman, J.P. Meijerink, J. Soulier, P. Van Vlierberghe, and J.J. Haigh. 2015. ZEB2 drives immature T-cell lymphoblastic leukaemia development via enhanced tumour-initiating potential and IL-7 receptor signalling. *Nature communications* 6:5794.

Grimaldi, C., F. Chiarini, G. Tabellini, F. Ricci, P.L. Tazzari, M. Battistelli, E. Falcieri, R. Bortul, F. Melchionda, I. Iacobucci, P. Pagliaro, G. Martinelli, A. Pession, J.T. Barata, J.A. McCubrey, and A.M. Martelli. 2012. AMP-dependent kinase/mammalian target of rapamycin complex 1 signaling in T-cell acute lymphoblastic leukemia: therapeutic implications. *Leukemia* 26:91-100.

Gutierrez, A., T. Sanda, R. Grebliunaite, A. Carracedo, L. Salmena, Y. Ahn, S. Dahlberg, D. Neuberg, L.A. Moreau, S.S. Winter, R. Larson, J. Zhang, A. Protopopov, L. Chin, P.P. Pandolfi, L.B. Silverman, S.P. Hunger, S.E. Sallan, and A.T. Look. 2009. High frequency of PTEN, PI3K, and AKT abnormalities in T-cell acute lymphoblastic leukemia. *Blood* 114:647-650.

Gutierrez, A., and L. Silverman. 2015. Acute lymphoblastic leukemia. In Nathan and Oski's Hematology and Oncology of Infancy and Childhood. S. Orkin, D. Fisher, D. Ginsburg, A. Look, S. Lux, and D. Nathan, editors. Elsevier Saunders, Philadelphia. 1527-1554.

Hall, C.P., C.P. Reynolds, and M.H. Kang. 2015. Modulation of glucocorticoid resistance in pediatric T-cell Acute Lymphoblastic Leukemia by increasing BIM expression with the PI3K/mTOR inhibitor BEZ235. *Clin Cancer Res*

Hanahan, D., and R.A. Weinberg. 2011. Hallmarks of cancer: the next generation. *Cell* 144:646-674.

Harrison, C.J. 2001. The detection and significance of chromosomal abnormalities in childhood acute lymphoblastic leukaemia. *Blood Rev* 15:49-59.

Harvey, R.C., C.G. Mullighan, I.M. Chen, W. Wharton, F.M. Mikhail, A.J. Carroll, H. Kang, W. Liu, K.K. Dobbin, M.A. Smith, W.L. Carroll, M. Devidas, W.P. Bowman, B.M. Camitta, G.H. Reaman, S.P. Hunger, J.R. Downing, and C.L. Willman. 2010. Rearrangement of CRLF2 is associated with mutation of JAK

kinases, alteration of IKZF1, Hispanic/Latino ethnicity, and a poor outcome in pediatric B-progenitor acute lymphoblastic leukemia. *Blood* 115:5312-5321.

Hebert, J., J.M. Cayuela, J. Berkeley, and F. Sigaux. 1994. Candidate tumor-suppressor genes MTS1 (p16INK4A) and MTS2 (p15INK4B) display frequent homozygous deletions in primary cells from T- but not from B-cell lineage acute lymphoblastic leukemias. *Blood* 84:4038-4044.

Helias, C., V. Leymarie, N. Entz-Werle, A. Falkenrodt, D. Eyer, J.A. Costa, D. Cherif, P. Lutz, and M. Lessard. 2002. Translocation t(5;14)(q35;q32) in three cases of childhood T cell acute lymphoblastic leukemia: a new recurring and cryptic abnormality. *Leukemia* 16:7-12.

Higashiguchi, T., H. Arai, L.H. Claytor, M. Kuzuya, J. Kotani, S.D. Lee, J.P. Michel, T. Nogami, and N. Peng. 2017. Taking action against malnutrition in Asian healthcare settings: an initiative of a Northeast Asia Study Group. *Asia Pac J Clin Nutr* 26:202-211.

Hof, J., S. Krentz, C. van Schewick, G. Korner, S. Shalapour, P. Rhein, L. Karawajew, W.D. Ludwig, K. Seeger, G. Henze, A. von Stackelberg, C. Hagemeier, C. Eckert, and R. Kirschner-Schwabe. 2011. Mutations and deletions of the TP53 gene predict nonresponse to treatment and poor outcome in first relapse of childhood acute lymphoblastic leukemia. *J Clin Oncol* 29:3185-3193.

Holmes, R., and J.C. Zuniga-Pflucker. 2009. The OP9-DL1 system: generation of T-lymphocytes from embryonic or hematopoietic stem cells in vitro. *Cold Spring Harb Protoc* 2009:pdb prot5156.

Holmfeldt, L., and C.G. Mullighan. 2010. PHF6 mutations in T-lineage acute lymphoblastic leukemia. *Pediatr Blood Cancer* 55:595-596.

Homminga, I., R. Pieters, A.W. Langerak, J.J. de Rooi, A. Stubbs, M. Verstegen, M. Vuerhard, J. Buijs-Gladdines, C. Kooi, P. Klous, P. van Vlierberghe, A.A. Ferrando, J.M. Cayuela, B. Verhaaf, H.B. Beverloo, M. Horstmann, V. de Haas, A.S. Wiekmeijer, K. Pike-Overzet, F.J. Staal, W. de Laat, J. Soulier, F. Sigaux, and J.P. Meijerink. 2011. Integrated transcript and genome analyses reveal NKX2-1 and MEF2C as potential oncogenes in T cell acute lymphoblastic leukemia. *Cancer Cell* 19:484-497.

Homminga, I., R. Pieters, and J.P. Meijerink. 2012. NKL homeobox genes in leukemia. *Leukemia* 26:572-581.

Hong, C., M.A. Luckey, and J.H. Park. 2012. Intrathymic IL-7: the where, when, and why of IL-7 signaling during T cell development. *Semin Immunol* 24:151-158.

Hong, D.S., U. Banerji, B. Tavana, G.C. George, J. Aaron, and R. Kurzrock. 2013. Targeting the molecular chaperone heat shock protein 90 (HSP90): Lessons learned and future directions. *Cancer Treat Rev* 39:375-387.

Hu, Y., and G.K. Smyth. 2009. ELDA: extreme limiting dilution analysis for comparing depleted and enriched populations in stem cell and other assays. *J Immunol Methods* 347:70-78.

Huether, R., L. Dong, X. Chen, G. Wu, M. Parker, L. Wei, J. Ma, M.N. Edmonson, E.K. Hedlund, M.C. Rusch, S.A. Shurtleff, H.L. Mulder, K. Boggs, B. Vadordaria, J. Cheng, D. Yergeau, G. Song, J. Becksfort, G. Lemmon, C. Weber, Z. Cai, J. Dang, M. Walsh, A.L. Gedman, Z. Faber, J. Easton, T. Gruber, R.W. Kriwacki, J.F. Partridge, L. Ding, R.K. Wilson, E.R. Mardis, C.G. Mullighan, R.J.

Gilbertson, S.J. Baker, G. Zambetti, D.W. Ellison, J. Zhang, and J.R. Downing. 2014. The landscape of somatic mutations in epigenetic regulators across 1,000 paediatric cancer genomes. *Nature communications* 5:3630.

Hunger, S.P., and C.G. Mullighan. 2015. Redefining ALL classification: toward detecting high-risk ALL and implementing precision medicine. *Blood* 125:3977-3987.

Iacovelli, S., M.R. Ricciardi, M. Allegretti, S. Mirabilii, R. Licchetta, P. Bergamo, C. Rinaldo, A. Zeuner, R. Foa, M. Milella, J.A. McCubrey, A.M. Martelli, and A. Tafuri. 2015. Co-targeting of Bcl-2 and mTOR pathway triggers synergistic apoptosis in BH3 mimetics resistant acute lymphoblastic leukemia. *Oncotarget* 6:32089-32103.

Janes, M.R., C. Vu, S. Mallya, M.P. Shieh, J.J. Limon, L.S. Li, K.A. Jessen, M.B. Martin, P. Ren, M.B. Lilly, L.S. Sender, Y. Liu, C. Rommel, and D.A. Fruman. 2013. Efficacy of the investigational mTOR kinase inhibitor MLN0128/INK128 in models of B-cell acute lymphoblastic leukemia. *Leukemia* 27:586-594.

Jeong, E.G., M.S. Kim, H.K. Nam, C.K. Min, S. Lee, Y.J. Chung, N.J. Yoo, and S.H. Lee. 2008. Somatic mutations of JAK1 and JAK3 in acute leukemias and solid cancers. *Clin Cancer Res* 14:3716-3721.

Jiang, Q., W.Q. Li, R.R. Hofmeister, H.A. Young, D.R. Hodge, J.R. Keller, A.R. Khaled, and S.K. Durum. 2004. Distinct regions of the interleukin-7 receptor regulate different Bcl2 family members. *Mol Cell Biol* 24:6501-6513.

Johnson, S.E., N. Shah, A.A. Bajer, and T.W. LeBien. 2008. IL-7 activates the phosphatidylinositol 3-kinase/AKT pathway in normal human thymocytes but not normal human B cell precursors. *J Immunol* 180:8109-8117.

Joller, N., E. Lozano, P.R. Burkett, B. Patel, S. Xiao, C. Zhu, J. Xia, T.G. Tan, E. Sefik, V. Yajnik, A.H. Sharpe, F.J. Quintana, D. Mathis, C. Benoist, D.A. Hafler, and V.K. Kuchroo. 2014. Treg cells expressing the coinhibitory molecule TIGIT selectively inhibit proinflammatory Th1 and Th17 cell responses. *Immunity* 40:569-581.

Kalender Atak, Z., K. De Keersmaecker, V. Gianfelici, E. Geerdens, R. Vandepoel, D. Pauwels, M. Porcu, I. Lahortiga, V. Brys, W.G. Dirks, H. Quentmeier, J. Cloos, H. Cuppens, A. Uyttebroeck, P. Vandenberghe, J. Cools, and S. Aerts. 2012. High accuracy mutation detection in leukemia on a selected panel of cancer genes. *PLoS One* 7:e38463.

Kamijo, T., F. Zindy, M.F. Roussel, D.E. Quelle, J.R. Downing, R.A. Ashmun, G. Grosveld, and C.J. Sherr. 1997. Tumor suppression at the mouse INK4a locus mediated by the alternative reading frame product p19ARF. *Cell* 91:649-659.

Karawajew, L., V. Ruppert, C. Wuchter, A. Kosser, M. Schrappe, B. Dorken, and W.D. Ludwig. 2000. Inhibition of in vitro spontaneous apoptosis by IL-7 correlates with bcl-2 up-regulation, cortical/mature immunophenotype, and better early cytoreduction of childhood T-cell acute lymphoblastic leukemia. *Blood* 96:297-306.

Kawamura, M., H. Ohnishi, S.X. Guo, X.M. Sheng, M. Minegishi, R. Hanada, K. Horibe, T. Hongo, Y. Kaneko, F. Bessho, M. Yanagisawa, T. Sekiya, and Y. Hayashi. 1999. Alterations of the p53, p21, p16, p15 and RAS genes in childhood T-cell acute lymphoblastic leukemia. *Leuk Res* 23:115-126.

Khaled, A.R., D.V. Bulavin, C. Kittipatarin, W.Q. Li, M. Alvarez, K. Kim, H.A. Young, A.J. Fornace, and S.K. Durum. 2005. Cytokine-driven cell cycling is mediated through Cdc25A. *J Cell Biol* 169:755-763.

Khaled, A.R., K. Kim, R. Hofmeister, K. Muegge, and S.K. Durum. 1999. Withdrawal of IL-7 induces Bax translocation from cytosol to mitochondria through a rise in intracellular pH. *Proc Natl Acad Sci U S A* 96:14476-14481.

Kim, K., A.R. Khaled, D. Reynolds, H.A. Young, C.K. Lee, and S.K. Durum. 2003. Characterization of an interleukin-7-dependent thymic cell line derived from a p53(-/-) mouse. *J Immunol Methods* 274:177-184.

Kimura, Y., T. Takeshita, M. Kondo, N. Ishii, M. Nakamura, J. Van Snick, and K. Sugamura. 1995. Sharing of the IL-2 receptor gamma chain with the functional IL-9 receptor complex. *Int Immunol* 7:115-120.

King, K., M. Paterson, and S.K. Green. 2013. Global justice and the proposed ban on thimerosal-containing vaccines. *Pediatrics* 131:154-156.

Kleppe, M., I. Lahortiga, T. El Chaar, K. De Keersmaecker, N. Mentens, C. Graux, K. Van Roosbroeck, A.A. Ferrando, A.W. Langerak, J.P. Meijerink, F. Sigaux, T. Haferlach, I. Wlodarska, P. Vandenberghe, J. Soulier, and J. Cools. 2010. Deletion of the protein tyrosine phosphatase gene PTPN2 in T-cell acute lymphoblastic leukemia. *Nature genetics* 42:530-535.

Kondo, M., T. Takeshita, N. Ishii, M. Nakamura, S. Watanabe, K. Arai, and K. Sugamura. 1993. Sharing of the interleukin-2 (IL-2) receptor gamma chain between receptors for IL-2 and IL-4. *Science* 262:1874-1877.

Kontro, M., H. Kuusanmaki, S. Eldfors, T. Burmeister, E.I. Andersson, O. Bruserud, T.H. Brummendorf, H. Edgren, B.T. Gjertsen, M. Itala-Remes, S. Lagstrom, O. Lohi, T. Lundan, J.M.L. Marti, M.M. Majumder, A. Parsons, T. Pemovska, H. Rajala, K. Vettenranta, O. Kallioniemi, S. Mustjoki, K. Porkka, and C.A. Heckman. 2014. Novel activating STAT5B mutations as putative drivers of T-cell acute lymphoblastic leukemia. *Leukemia* 28:1738-1742.

Koppikar, P., N. Bhagwat, O. Kilpivaara, T. Manshouri, M. Adli, T. Hricik, F. Liu, L.M. Saunders, A. Mullally, O. Abdel-Wahab, L. Leung, A. Weinstein, S. Marubayashi, A. Goel, M. Gonen, Z. Estrov, B.L. Ebert, G. Chiosis, S.D. Nimer, B.E. Bernstein, S. Verstovsek, and R.L. Levine. 2012. Heterodimeric JAK-STAT activation as a mechanism of persistence to JAK2 inhibitor therapy. *Nature* 489:155-159.

Koyama, D., J. Kikuchi, N. Hiraoka, T. Wada, H. Kurosawa, S. Chiba, and Y. Furukawa. 2014. Proteasome inhibitors exert cytotoxicity and increase chemosensitivity via transcriptional repression of Notch1 in T-cell acute lymphoblastic leukemia. *Leukemia* 28:1216-1226.

Kraszewska, M.D., M. Dawidowska, N.S. Larmonie, M. Kosmalska, L. Sedek, M. Szczepaniak, W. Grzeszczak, A.W. Langerak, T. Szczepanski, M. Witt, and G. Polish Pediatric Leukemia Lymphoma Study. 2012. DNA methylation pattern is altered in childhood T-cell acute lymphoblastic leukemia patients as compared with normal thymic subsets: insights into CpG island methylator phenotype in T-ALL. *Leukemia* 26:367-371.

Kroon, E., J. Krosl, U. Thorsteinsdottir, S. Baban, A.M. Buchberg, and G. Sauvageau. 1998. Hoxa9 transforms primary bone marrow cells through specific collaboration with Meis1a but not Pbx1b. *EMBO J* 17:3714-3725.

Lacronique, V., A. Boureux, V. DellaValle, H. Poirel, C.T. Quang, M. Mauchauffe, C. Berthou, M. Lessard, R. Berger, J. Ghysdael, and O.A. Bernard. 1997. A TEL-JAK2 fusion protein with constitutive kinase activity in human leukemia. *Science* 278:1309-1312.

Law, C.W., Y. Chen, W. Shi, and G.K. Smyth. 2014. voom: Precision weights unlock linear model analysis tools for RNA-seq read counts. *Genome Biol* 15:R29.

Lawrence, H.J., C.D. Helgason, G. Sauvageau, S. Fong, D.J. Izon, R.K. Humphries, and C. Largman. 1997. Mice bearing a targeted interruption of the homeobox gene HOXA9 have defects in myeloid, erythroid, and lymphoid hematopoiesis. *Blood* 89:1922-1930.

Levy, D.S., J.A. Kahana, and R. Kumar. 2009. AKT inhibitor, GSK690693, induces growth inhibition and apoptosis in acute lymphoblastic leukemia cell lines. *Blood* 113:1723-1729.

Li, Q., N. Bohin, T. Wen, V. Ng, J. Magee, S.C. Chen, K. Shannon, and S.J. Morrison. 2013. Oncogenic Nras has bimodal effects on stem cells that sustainably increase competitiveness. *Nature* 504:143.

Li, W.Q., T. Guszczynski, J.A. Hixon, and S.K. Durum. 2010. Interleukin-7 Regulates Bim Proapoptotic Activity in Peripheral T-Cell Survival. *Mol Cell Biol* 30:590-600.

Li, W.Q., Q. Jiang, E. Aleem, P. Kaldis, A.R. Khaled, and S.K. Durum. 2006. IL-7 promotes T cell proliferation through destabilization of p27Kip1. *J Exp Med* 203:573-582.

Li, W.Q., Q. Jiang, A.R. Khaled, J.R. Keller, and S.K. Durum. 2004. Interleukin-7 inactivates the pro-apoptotic protein Bad promoting T cell survival. *J Biol Chem* 279:29160-29166.

Li, Y., J. Liu, W. Li, A. Brown, M. Baddoo, M. Li, T. Carroll, L. Oxburgh, Y. Feng, and Z. Saifudeen. 2015. p53 Enables metabolic fitness and self-renewal of nephron progenitor cells. *Development* 142:1228-1241.

Liao, Y., G.K. Smyth, and W. Shi. 2013. The Subread aligner: fast, accurate and scalable read mapping by seed-and-vote. *Nucleic Acids Res* 41:e108.

Lin, Y.W., C. Slape, Z. Zhang, and P.D. Aplan. 2005. NUP98-HOXD13 transgenic mice develop a highly penetrant, severe myelodysplastic syndrome that progresses to acute leukemia. *Blood* 106:287-295.

Liu, X., S. Leung, C. Wang, Z. Tan, J. Wang, T.B. Guo, L. Fang, Y. Zhao, B. Wan, X. Qin, L. Lu, R. Li, H. Pan, M. Song, A. Liu, J. Hong, H. Lu, and J.Z. Zhang. 2010. Crucial role of interleukin-7 in T helper type 17 survival and expansion in autoimmune disease. *Nat Med* 16:191-197.

Liu, Y.J., V. Soumelis, N. Watanabe, T. Ito, Y.H. Wang, W. Malefyt Rde, M. Omori, B. Zhou, and S.F. Ziegler. 2007. TSLP: an epithelial cell cytokine that regulates T cell differentiation by conditioning dendritic cell maturation. *Annu Rev Immunol* 25:193-219.

Liu, Z., F. Li, B. Zhang, S. Li, J. Wu, and Y. Shi. 2015. Structural basis of plant homeodomain finger 6 (PHF6) recognition by the retinoblastoma binding protein

4 (RBBP4) component of the nucleosome remodeling and deacetylase (NuRD) complex. *J Biol Chem* 290:6630-6638.

Loh, M.L., S.K. Tasian, K.R. Rabin, P. Brown, D. Magoon, J.M. Reid, X. Chen, C.H. Ahern, B.J. Weigel, and S.M. Blaney. 2015. A phase 1 dosing study of ruxolitinib in children with relapsed or refractory solid tumors, leukemias, or myeloproliferative neoplasms: A Children's Oncology Group phase 1 consortium study (ADVL1011). *Pediatr Blood Cancer* 62:1717-1724.

Lonetti, A., I.L. Antunes, F. Chiarini, E. Orsini, F. Buontempo, F. Ricci, P.L. Tazzari, P. Pagliaro, F. Melchionda, A. Pession, A. Bertaina, F. Locatelli, J.A. McCubrey, J.T. Barata, and A.M. Martelli. 2014. Activity of the pan-class I phosphoinositide 3-kinase inhibitor NVP-BKM120 in T-cell acute lymphoblastic leukemia. *Leukemia* 28:1196-1206.

Ma, J., J. Hua, Y. Sha, and Y. Xie. 2014. The effect of TLX3 expression on the prognosis of pediatric T cell acute lymphocytic leukemia--a systematic review. *Tumour Biol* 35:8439-8443.

Macchi, P., A. Villa, S. Giliani, M.G. Sacco, A. Frattini, F. Porta, A.G. Ugazio, J.A. Johnston, F. Candotti, J.J. O'Shea, and et al. 1995. Mutations of Jak-3 gene in patients with autosomal severe combined immune deficiency (SCID). *Nature* 377:65-68.

MacLeod, R.A., S. Nagel, M. Kaufmann, J.W. Janssen, and H.G. Drexler. 2003. Activation of HOX11L2 by juxtaposition with 3'-BCL11B in an acute lymphoblastic leukemia cell line (HPB-ALL) with t(5;14)(q35;q32.2). *Genes Chromosomes Cancer* 37:84-91.

Makrynikola, V., A. Kabral, and K. Bradstock. 1991. Effects of interleukin 7 on the growth of clonogenic cells in T-cell acute lymphoblastic leukaemia. *Leuk Res* 15:879-882.

Maldarelli, F., X. Wu, L. Su, F.R. Simonetti, W. Shao, S. Hill, J. Spindler, A.L. Ferris, J.W. Mellors, M.F. Kearney, J.M. Coffin, and S.H. Hughes. 2014. Specific HIV integration sites are linked to clonal expansion and persistence of infected cells. *Science* 345:179-183.

Mansour, M.R., C. Reed, A.R. Eisenberg, J.C. Tseng, J.C. Twizere, S. Daakour, A. Yoda, S.J. Rodig, N. Tal, C. Shochat, A. Berezovskaya, D.J. DeAngelo, S.E. Sallan, D.M. Weinstock, S. Izraeli, A.L. Kung, A. Kentsis, and A.T. Look. 2015. Targeting oncogenic interleukin-7 receptor signalling with N-acetylcysteine in T cell acute lymphoblastic leukaemia. *Brit J Haematol* 168:230-238.

Maude, S.L., S. Dolai, C. Delgado-Martin, T. Vincent, A. Robbins, A. Selvanathan, T. Ryan, J. Hall, A.C. Wood, S.K. Tasian, S.P. Hunger, M.L. Loh, C.G. Mullighan, B.L. Wood, M.L. Hermiston, S.A. Grupp, R.B. Lock, and D.T. Teachey. 2015. Efficacy of JAK/STAT pathway inhibition in murine xenograft models of early T-cell precursor (ETP) acute lymphoblastic leukemia. *Blood* 125:1759-1767.

Maude, S.L., S.K. Tasian, T. Vincent, J.W. Hall, C. Sheen, K.G. Roberts, A.E. Seif, D.M. Barrett, I.M. Chen, J.R. Collins, C.G. Mullighan, S.P. Hunger, R.C. Harvey, C.L. Willman, J.S. Fridman, M.L. Loh, S.A. Grupp, and D.T. Teachey. 2012. Targeting JAK1/2 and mTOR in murine xenograft models of Ph-like acute lymphoblastic leukemia. *Blood* 120:3510-3518.

Mauvieux, L., V. Leymarie, C. Helias, C. Gervais, N. Perrusson, A. Falkenrodt, B. Lioure, P. Lutz, and M. Lessard. 2002. High incidence of HOX11L2 expression in children with T-ALL. *Blood* 100:753a-753a.

Mavrakis, K.J., J. Van Der Meulen, A.L. Wolfe, X. Liu, E. Mets, T. Taghon, A.A. Khan, M. Setty, P. Rondou, P. Vandenberghe, E. Delabesse, Y. Benoit, N.B. Socci, C.S. Leslie, P. Van Vlierberghe, F. Speleman, and H.G. Wendel. 2011. A cooperative microRNA-tumor suppressor gene network in acute T-cell lymphoblastic leukemia (T-ALL). *Nature genetics* 43:673-678.

Mazzucchelli, R.I., A. Riva, and S.K. Durum. 2012. The human IL-7 receptor gene: Deletions, polymorphisms and mutations. *Semin Immunol* 24:225-230.

McBryde, E.S., M.T. Meehan, T.N. Doan, R. Ragonnet, B.J. Marais, V. Guernier, and J.M. Trauer. 2017. The risk of global epidemic replacement with drug-resistant Mycobacterium tuberculosis strains. *Int J Infect Dis* 56:14-20.

Meijerink, J.P. 2010. Genetic rearrangements in relation to immunophenotype and outcome in T-cell acute lymphoblastic leukaemia. *Best Pract Res Clin Haematol* 23:307-318.

Mendenhall, E., B.A. Kohrt, S.A. Norris, D. Ndetei, and D. Prabhakaran. 2017. Non-communicable disease syndemics: poverty, depression, and diabetes among low-income populations. *Lancet* 389:951-963.

Mets, E., G. Van Peer, J. Van der Meulen, M. Boice, T. Taghon, S. Goossens, P. Mestdagh, Y. Benoit, B. De Moerloose, N. Van Roy, B. Poppe, J. Vandesompele, H.G. Wendel, P. Van Vlierberghe, F. Speleman, and P. Rondou. 2014. MicroRNA-128-3p is a novel oncomiR targeting PHF6 in T-cell acute lymphoblastic leukemia. *Haematologica* 99:1326-1333.

Meyer, S.C., and R.L. Levine. 2014. Molecular Pathways: Molecular Basis for Sensitivity and Resistance to JAK Kinase Inhibitors. *Clin Cancer Res* 20:2051-2059.

Montecino-Rodriguez, E., H. Leathers, and K. Dorshkind. 2006. Identification of a B-1 B cell-specified progenitor. *Nat Immunol* 7:293-301.

Mullighan, C.G. 2013. Genomic characterization of childhood acute lymphoblastic leukemia. *Semin Hematol* 50:314-324.

Mullighan, C.G., J.R. Collins-Underwood, L.A. Phillips, M.G. Loudin, W. Liu, J. Zhang, J. Ma, E. Coustan-Smith, R.C. Harvey, C.L. Willman, F.M. Mikhail, J. Meyer, A.J. Carroll, R.T. Williams, J. Cheng, N.A. Heerema, G. Basso, A. Pession, C.H. Pui, S.C. Raimondi, S.P. Hunger, J.R. Downing, W.L. Carroll, and K.R. Rabin. 2009a. Rearrangement of CRLF2 in B-progenitor- and Down syndrome-associated acute lymphoblastic leukemia. *Nature genetics* 41:1243-1246.

Mullighan, C.G., and J.R. Downing. 2009. Genome-wide profiling of genetic alterations in acute lymphoblastic leukemia: recent insights and future directions. *Leukemia* 23:1209-1218.

Mullighan, C.G., and S.P. Hunger. 2013. Therapy of pediatric ALL: from Bowie to Obama. *Blood* 122:2531-2532.

Mullighan, C.G., J. Zhang, R.C. Harvey, J.R. Collins-Underwood, B.A. Schulman, L.A. Phillips, S.K. Tasian, M.L. Loh, X. Su, W. Liu, M. Devidas, S.R. Atlas, I.M. Chen, R.J. Clifford, D.S. Gerhard, W.L. Carroll, G.H. Reaman, M. Smith, J.R. Downing, S.P. Hunger, and C.L. Willman. 2009b. JAK mutations in high-risk

childhood acute lymphoblastic leukemia. *Proc Natl Acad Sci U S A* 106:9414-9418.

Nagel, S., C. Pommerenke, M. Scherr, C. Meyer, M. Kaufmann, K. Battmer, R.A. MacLeod, and H.G. Drexler. 2017. NKL homeobox gene activities in hematopoietic stem cells, T-cell development and T-cell leukemia. *PLoS One* 12:e0171164.

Nagel, S., L. Venturini, V.E. Marquez, C. Meyer, M. Kaufmann, M. Scherr, R.A. MacLeod, and H.G. Drexler. 2010. Polycomb repressor complex 2 regulates HOXA9 and HOXA10, activating ID2 in NK/T-cell lines. *Mol Cancer* 9:151.

Neri, L.M., A. Cani, A.M. Martelli, C. Simioni, C. Junghanss, G. Tabellini, F. Ricci, P.L. Tazzari, P. Pagliaro, J.A. McCubrey, and S. Capitani. 2014. Targeting the PI3K/Akt/mTOR signaling pathway in B-precursor acute lymphoblastic leukemia and its therapeutic potential. *Leukemia* 28:739-748.

Neri, P., L. Ren, A.K. Azab, M. Brentnall, K. Gratton, A.C. Klimowicz, C. Lin, P. Duggan, P. Tassone, A. Mansoor, D.A. Stewart, L.H. Boise, I.M. Ghobrial, and N.J. Bahlis. 2011. Integrin beta7-mediated regulation of multiple myeloma cell adhesion, migration, and invasion. *Blood* 117:6202-6213.

Nguyen, K., M. Devidas, S.C. Cheng, M. La, E.A. Raetz, W.L. Carroll, N.J. Winick, S.P. Hunger, P.S. Gaynon, M.L. Loh, and G. Children's Oncology. 2008. Factors influencing survival after relapse from acute lymphoblastic leukemia: a Children's Oncology Group study. *Leukemia* 22:2142-2150.

Nikolaev, S.I., M. Garieri, F. Santoni, E. Falconnet, P. Ribaux, M. Guipponi, A. Murray, J. Groet, E. Giarin, G. Basso, D. Nizetic, and S.E. Antonarakis. 2014. Frequent cases of RAS-mutated Down syndrome acute lymphoblastic leukaemia lack JAK2 mutations. *Nature communications* 5:4654.

Noguchi, M., H. Yi, H.M. Rosenblatt, A.H. Filipovich, S. Adelstein, W.S. Modi, O.W. McBride, and W.J. Leonard. 1993. Interleukin-2 receptor gamma chain mutation results in X-linked severe combined immunodeficiency in humans. *Cell* 73:147-157.

Noronha, E.P., F.G. Andrade, C. Zampier, C.F. de Andrade, E. Terra-Granado, M.S. Pombo-de-Oliveira, and L. Brazilian Study Group for Childhood. 2016. Immunophenotyping with CD135 and CD117 predicts the FLT3, IL-7R and TLX3 gene mutations in childhood T-cell acute leukemia. *Blood Cells Mol Dis* 57:74-80.

Nosaka, T., J.M. van Deursen, R.A. Tripp, W.E. Thierfelder, B.A. Witthuhn, A.P. McMickle, P.C. Doherty, G.C. Grosveld, and J.N. Ihle. 1995. Defective lymphoid development in mice lacking Jak3. *Science* 270:800-802.

Ntziachristos, P., A. Tsirigos, P. Van Vlierberghe, J. Nedjic, T. Trimarchi, M.S. Flaherty, D. Ferres-Marco, V. da Ros, Z. Tang, J. Siegle, P. Asp, M. Hadler, I. Rigo, K. De Keersmaecker, J. Patel, T. Huynh, F. Utro, S. Poglio, J.B. Samon, E. Paietta, J. Racevskis, J.M. Rowe, R. Rabadan, R.L. Levine, S. Brown, F. Pflumio, M. Dominguez, A. Ferrando, and I. Aifantis. 2012. Genetic inactivation of the polycomb repressive complex 2 in T cell acute lymphoblastic leukemia. *Nat Med* 18:298-301.

Opferman, J.T., A. Letai, C. Beard, M.D. Sorcinelli, C.C. Ong, and S.J. Korsmeyer. 2003. Development and maintenance of B and T lymphocytes requires antiapoptotic MCL-1. *Nature* 426:671-676.

Orkin, S., D. Fisher, D. Ginsburg, A. Look, S. Lux, and D. Nathan. 2015. Nathan and Oski's Hematology and Oncology of Infancy and Childhood. In S. Orkin, D. Fisher, D. Ginsburg, A. Look, S. Lux, and D. Nathan, editors. Elsevier Inc., Philadelphia. 1525-2255.

Oshima, K., H. Khiabanian, A.C. da Silva-Almeida, G. Tzoneva, F. Abate, A. Ambesi-Impiombato, M. Sanchez-Martin, Z. Carpenter, A. Penson, A. Perez-Garcia, C. Eckert, C. Nicolas, M. Balbin, M.L. Sulis, M. Kato, K. Koh, M. Paganin, G. Basso, J.M. Gastier-Foster, M. Devidas, M.L. Loh, R. Kirschner-Schwabe, T. Palomero, R. Rabadan, and A.A. Ferrando. 2016. Mutational landscape, clonal evolution patterns, and role of RAS mutations in relapsed acute lymphoblastic leukemia. *Proc Natl Acad Sci U S A*.

Ott, C.J., N. Kopp, L. Bird, R.M. Paranal, J. Qi, T. Bowman, S.J. Rodig, A.L. Kung, J.E. Bradner, and D.M. Weinstock. 2012. BET bromodomain inhibition targets both c-Myc and IL7R in high-risk acute lymphoblastic leukemia. *Blood* 120:2843-2852.

Palmi, C., E. Vendramini, D. Silvestri, G. Longinotti, D. Frison, G. Cario, C. Shochat, M. Stanulla, V. Rossi, A.M. Di Meglio, T. Villa, E. Giarin, G. Fazio, A. Leszl, M. Schrappe, G. Basso, A. Biondi, S. Izraeli, V. Conter, M.G. Valsecchi, G. Cazzaniga, and G. Te Kronnie. 2012. Poor prognosis for P2RY8-CRLF2 fusion but not for CRLF2 over-expression in children with intermediate risk B-cell precursor acute lymphoblastic leukemia. *Leukemia* 26:2245-2253.

Palomero, T., W.K. Lim, D.T. Odom, M.L. Sulis, P.J. Real, A. Margolin, K.C. Barnes, J. O'Neil, D. Neuberg, A.P. Weng, J.C. Aster, F. Sigaux, J. Soulier, A.T. Look, R.A. Young, A. Califano, and A.A. Ferrando. 2006. NOTCH1 directly regulates c-MYC and activates a feed-forward-loop transcriptional network promoting leukemic cell growth. *Proc Natl Acad Sci U S A* 103:18261-18266.

Park, J.H., S. Adoro, T. Guinter, B. Erman, A.S. Alag, M. Catalfamo, M.Y. Kimura, Y. Cui, P.J. Lucas, R.E. Gress, M. Kubo, L. Hennighausen, L. Feigenbaum, and A. Singer. 2010. Signaling by intrathymic cytokines, not T cell antigen receptors, specifies CD8 lineage choice and promotes the differentiation of cytotoxic-lineage T cells. *Nat Immunol* 11:257-264.

Park, S.Y., K. Saijo, T. Takahashi, M. Osawa, H. Arase, N. Hirayama, K. Miyake, H. Nakauchi, T. Shirasawa, and T. Saito. 1995. Developmental defects of lymphoid cells in Jak3 kinase-deficient mice. *Immunity* 3:771-782.

Perentesis, J.P., S. Bhatia, E. Boyle, Y. Shao, X.O. Shu, M. Steinbuch, H.N. Sather, P. Gaynon, W. Kiffmeyer, J. Envall-Fox, and L.L. Robinson. 2004. RAS oncogene mutations and outcome of therapy for childhood acute lymphoblastic leukemia. *Leukemia* 18:685-692.

Peschon, J.J., P.J. Morrissey, K.H. Grabstein, F.J. Ramsdell, E. Maraskovsky, B.C. Gliniak, L.S. Park, S.F. Ziegler, D.E. Williams, C.B. Ware, J.D. Meyer, and B.L. Davison. 1994. Early lymphocyte expansion is severely impaired in interleukin 7 receptor-deficient mice. *J Exp Med* 180:1955-1960.

Piovan, E., J. Yu, V. Tosello, D. Herranz, A. Ambesi-Impiombato, A.C. Da Silva, M. Sanchez-Martin, A. Perez-Garcia, I. Rigo, M. Castillo, S. Indraccolo, J.R. Cross,

E. de Stanchina, E. Paietta, J. Racevskis, J.M. Rowe, M.S. Tallman, G. Basso, J.P. Meijerink, C. Cordon-Cardo, A. Califano, and A.A. Ferrando. 2013. Direct reversal of glucocorticoid resistance by AKT inhibition in acute lymphoblastic leukemia. *Cancer Cell* 24:766-776.

Plummer, M., C. de Martel, J. Vignat, J. Ferlay, F. Bray, and S. Franceschi. 2016. Global burden of cancers attributable to infections in 2012: a synthetic analysis. *Lancet Glob Health* 4:e609-616.

Puel, A., S.F. Ziegler, R.H. Buckley, and W.J. Leonard. 1998. Defective IL7R expression in T(-)B(+)NK(+) severe combined immunodeficiency. *Nature genetics* 20:394-397.

Pui, C.H., D. Campana, D. Pei, W.P. Bowman, J.T. Sandlund, S.C. Kaste, R.C. Ribeiro, J.E. Rubnitz, S.C. Raimondi, M. Onciu, E. Coustan-Smith, L.E. Kun, S. Jeha, C. Cheng, S.C. Howard, V. Simmons, A. Bayles, M.L. Metzger, J.M. Boyett, W. Leung, R. Handgretinger, J.R. Downing, W.E. Evans, and M.V. Relling. 2009. Treating childhood acute lymphoblastic leukemia without cranial irradiation. *N Engl J Med* 360:2730-2741.

Qin, H., M. Cho, W. Haso, L. Zhang, S. Tasian, H. Oo, G. Negri, Y. Lin, J. Zou, B. Mallon, S. Maude, D. Teachey, D. Barrett, R. Orentas, M. Daugaard, P. Sorensen, S. Grupp, and T. Fry. 2015. Eradication of B-ALL using chimeric antigen receptor-expressing T cells targeting the TSLPR oncoprotein. *Blood* Jul 30;126:629-639.

Rampal, R., and M.E. Figueroa. 2016. Wilms tumor 1 mutations in the pathogenesis of acute myeloid leukemia. *Haematologica* 101:672-679.

Remke, M., S. Pfister, C. Kox, G. Toedt, N. Becker, A. Benner, W. Werft, S. Breit, S. Liu, F. Engel, A. Wittmann, M. Zimmermann, M. Stanulla, M. Schrappe, W.D. Ludwig, C.R. Bartram, B. Radlwimmer, M.U. Muckenthaler, P. Lichter, and A.E. Kulozik. 2009. High-resolution genomic profiling of childhood T-ALL reveals frequent copy-number alterations affecting the TGF-beta and PI3K-AKT pathways and deletions at 6q15-16.1 as a genomic marker for unfavorable early treatment response. *Blood* 114:1053-1062.

Rich, B.E., J. Campostorres, R.I. Tepper, R.W. Moreadith, and P. Leder. 1993. Cutaneous Lymphoproliferation and Lymphomas in Interleukin-7 Transgenic Mice. *Journal of Experimental Medicine* 177:305-316.

Richie, E.R., A. Schumacher, J.M. Angel, M. Holloway, E.M. Rinchik, and T. Magnuson. 2002. The Polycomb-group gene eed regulates thymocyte differentiation and suppresses the development of carcinogen-induced T-cell lymphomas. *Oncogene* 21:299-306.

Richter-Pechanska, P., J.B. Kunz, J. Hof, M. Zimmermann, T. Rausch, O.R. Bandapalli, E. Orlova, G. Scapinello, J.C. Sagi, M. Stanulla, M. Schrappe, G. Cario, R. Kirschner-Schwabe, C. Eckert, V. Benes, J.O. Korbel, M.U. Muckenthaler, and A.E. Kulozik. 2017. Identification of a genetically defined ultra-high-risk group in relapsed pediatric T-lymphoblastic leukemia. *Blood Cancer J* 7:e523.

Roberts, K.G., Y. Li, D. Payne-Turner, R.C. Harvey, Y.L. Yang, D. Pei, K. McCastlain, L. Ding, C. Lu, G. Song, J. Ma, J. Becksfort, M. Rusch, S.C. Chen, J. Easton, J. Cheng, K. Boggs, N. Santiago-Morales, I. Iacobucci, R.S. Fulton, J. Wen, M. Valentine, C. Cheng, S.W. Paugh, M. Devidas, I.M. Chen, S. Reshmi, A. Smith,

E. Hedlund, P. Gupta, P. Nagahawatte, G. Wu, X. Chen, D. Yergeau, B. Vadodaria, H. Mulder, N.J. Winick, E.C. Larsen, W.L. Carroll, N.A. Heerema, A.J. Carroll, G. Grayson, S.K. Tasian, A.S. Moore, F. Keller, M. Frei-Jones, J.A. Whitlock, E.A. Raetz, D.L. White, T.P. Hughes, J.M. Guidry Auvil, M.A. Smith, G. Marcucci, C.D. Bloomfield, K. Mrozek, J. Kohlschmidt, W. Stock, S.M. Kornblau, M. Konopleva, E. Paietta, C.H. Pui, S. Jeha, M.V. Relling, W.E. Evans, D.S. Gerhard, J.M. Gastier-Foster, E. Mardis, R.K. Wilson, M.L. Loh, J.R. Downing, S.P. Hunger, C.L. Willman, J. Zhang, and C.G. Mullighan. 2014. Targetable kinase-activating lesions in Ph-like acute lymphoblastic leukemia. *N Engl J Med* 371:1005-1015.

Roberts, K.G., R.D. Morin, J. Zhang, M. Hirst, Y. Zhao, X. Su, S.C. Chen, D. Payne-Turner, M.L. Churchman, R.C. Harvey, X. Chen, C. Kasap, C. Yan, J. Becksfort, R.P. Finney, D.T. Teachey, S.L. Maude, K. Tse, R. Moore, S. Jones, K. Mungall, I. Birol, M.N. Edmonson, Y. Hu, K.E. Buetow, I.M. Chen, W.L. Carroll, L. Wei, J. Ma, M. Kleppe, R.L. Levine, G. Garcia-Manero, E. Larsen, N.P. Shah, M. Devidas, G. Reaman, M. Smith, S.W. Paugh, W.E. Evans, S.A. Grupp, S. Jeha, C.H. Pui, D.S. Gerhard, J.R. Downing, C.L. Willman, M. Loh, S.P. Hunger, M.A. Marra, and C.G. Mullighan. 2012. Genetic alterations activating kinase and cytokine receptor signaling in high-risk acute lymphoblastic leukemia. *Cancer Cell* 22:153-166.

Rodon, J., R. Dienstmann, V. Serra, and J. Tabernero. 2013. Development of PI3K inhibitors: lessons learned from early clinical trials. *Nat Rev Clin Oncol* 10:143-153.

Rodriguez-Perea, A.L., E.D. Arcia, C.M. Rueda, and P.A. Velilla. 2016. Phenotypical characterization of regulatory T cells in humans and rodents. *Clin Exp Immunol* 185:281-291.

Roifman, C.M., J.Y. Zhang, D. Chitayat, and N. Sharfe. 2000. A partial deficiency of interleukin-7R alpha is sufficient to abrogate T-cell development and cause severe combined immunodeficiency. *Blood* 96:2803-2807.

Rozendo, C.A., A.S. Salas, and B. Cameron. 2017. A critical review of social and health inequalities in the nursing curriculum. *Nurs Educ Today* 50:62-71.

Rubenstein, L.S., J.J. Amon, M. McLemore, P. Eba, K. Dolan, R. Lines, and C. Beyrer. 2016. HIV, prisoners, and human rights. *Lancet* 388:1202-1214.

Russell, L.J., M. Capasso, I. Vater, T. Akasaka, O.A. Bernard, M.J. Calasanz, T. Chandrasekaran, E. Chapiro, S. Gesk, M. Griffiths, D.S. Guttery, C. Haferlach, L. Harder, O. Heidenreich, J. Irving, L. Kearney, F. Nguyen-Khac, L. Machado, L. Minto, A. Majid, A.V. Moorman, H. Morrison, V. Rand, J.C. Strefford, C. Schwab, H. Tonnies, M.J.S. Dyer, R. Siebert, and C.J. Harrison. 2009. Deregulated expression of cytokine receptor gene, CRLF2, is involved in lymphoid transformation in B-cell precursor acute lymphoblastic leukemia. *Blood* 114:2688-2698.

Russell, S.M., A.D. Keegan, N. Harada, Y. Nakamura, M. Noguchi, P. Leland, M.C. Friedmann, A. Miyajima, R.K. Puri, W.E. Paul, and et al. 1993. Interleukin-2 receptor gamma chain: a functional component of the interleukin-4 receptor. *Science* 262:1880-1883.

Russell, S.M., N. Tayebi, H. Nakajima, M.C. Riedy, J.L. Roberts, M.J. Aman, T.S. Migone, M. Noguchi, M.L. Markert, R.H. Buckley, J.J. O'Shea, and W.J. Leonard. 1995. Mutation of Jak3 in a patient with SCID: essential role of Jak3 in lymphoid development. *Science* 270:797-800.

Santos, F.P., and S. Verstovsek. 2011. JAK2 inhibitors: what's the true therapeutic potential? *Blood Rev* 25:53-63.

Schafer, V., J. Ernst, J. Rinke, N. Winkelmann, J.F. Beck, A. Hochhaus, B. Gruhn, and T. Ernst. 2016. EZH2 mutations and promoter hypermethylation in childhood acute lymphoblastic leukemia. *J Cancer Res Clin Oncol* 142:1641-1650.

Schluns, K.S., W.C. Kieper, S.C. Jameson, and L. Lefrancois. 2000. Interleukin-7 mediates the homeostasis of naive and memory CD8 T cells in vivo. *Nat Immunol* 1:426-432.

Schwartz, Y.B., and V. Pirrotta. 2008. Polycomb complexes and epigenetic states. *Curr Opin Cell Biol* 20:266-273.

Shandilya, J., and S.G. Roberts. 2015. A role of WT1 in cell division and genomic stability. *Cell Cycle* 14:1358-1364.

Shen, W., W. Li, J.A. Hixon, N. Bouladoux, Y. Belkaid, A. Dzutzev, and S.K. Durum. 2014. Adaptive immunity to murine skin commensals. *Proc Natl Acad Sci U S A* 111:E2977-2986.

Shepherd, C., L. Banerjee, C.W. Cheung, M.R. Mansour, S. Jenkinson, R.E. Gale, and A. Khwaja. 2013. PI3K/mTOR inhibition upregulates NOTCH-MYC signalling leading to an impaired cytotoxic response. *Leukemia* 27:650-660.

Shochat, C., N. Tal, O.R. Bandapalli, C. Palmi, I. Ganmore, G. te Kronnie, G. Cario, G. Cazzaniga, A.E. Kulozik, M. Stanulla, M. Schrappe, A. Biondi, G. Basso, D. Bercovich, M.U. Muckenthaler, and S. Izraeli. 2011. Gain-of-function mutations in interleukin-7 receptor-alpha (IL7R) in childhood acute lymphoblastic leukemias. *J Exp Med* 208:901-908.

Silva, A., A.B. Laranjeira, L.R. Martins, B.A. Cardoso, J. Demengeot, J.A. Yunes, B. Seddon, and J.T. Barata. 2011. IL-7 contributes to the progression of human T-cell acute lymphoblastic leukemias. *Cancer Res* 71:4780-4789.

Silva, A., J.A. Yunes, B.A. Cardoso, L.R. Martins, P.Y. Jotta, M. Abecasis, A.E. Nowill, N.R. Leslie, A.A. Cardoso, and J.T. Barata. 2008. PTEN posttranslational inactivation and hyperactivation of the PI3K/Akt pathway sustain primary T cell leukemia viability. *J Clin Invest* 118:3762-3774.

Silveira, A.B., A.B. Laranjeira, G.O. Rodrigues, P.C. Leal, B.A. Cardoso, J.T. Barata, R.A. Yunes, N.I. Zanchin, S.R. Brandalise, and J.A. Yunes. 2015. PI3K inhibition synergizes with glucocorticoids but antagonizes with methotrexate in T-cell acute lymphoblastic leukemia. *Oncotarget* 6:13105-13118.

Simioni, C., A. Cani, A.M. Martelli, G. Zauli, G. Tabellini, J. McCubrey, S. Capitani, and L.M. Neri. 2014. Activity of the novel mTOR inhibitor Torin-2 in B-precursor acute lymphoblastic leukemia and its therapeutic potential to prevent Akt reactivation. *Oncotarget* 5:10034-10047.

Simioni, C., L.M. Neri, G. Tabellini, F. Ricci, D. Bressanin, F. Chiarini, C. Evangelisti, A. Cani, P.L. Tazzari, F. Melchionda, P. Pagliaro, A. Pession, J.A. McCubrey, S. Capitani, and A.M. Martelli. 2012. Cytotoxic activity of the novel Akt inhibitor, MK-2206, in T-cell acute lymphoblastic leukemia. *Leukemia* 26:2336-2342.

Simon, C., J. Chagraoui, J. Krosl, P. Gendron, B. Wilhelm, S. Lemieux, G. Boucher, P. Chagnon, S. Drouin, R. Lambert, C. Rondeau, A. Bilodeau, S. Lavallee, M. Sauvageau, J. Hebert, and G. Sauvageau. 2012. A key role for EZH2 and associated genes in mouse and human adult T-cell acute leukemia. *Genes Dev* 26:651-656.

Soulier, J., E. Clappier, J.M. Cayuela, A. Regnault, M. Garcia-Peydro, H. Dombret, A. Baruchel, M.L. Toribio, and F. Sigaux. 2005. HOXA genes are included in genetic and biologic networks defining human acute T-cell leukemia (TALL). *Blood* 106:274-286.

Speleman, F., B. Cauwelier, N. Dastugue, J. Cools, B. Verhasselt, B. Poppe, N. Van Roy, J. Vandesompele, C. Graux, A. Uyttebroeck, M. Boogaerts, B. De Moerloose, Y. Benoit, D. Selleslag, J. Billiet, A. Robert, F. Huguet, P. Vandenberghe, A. De Paepe, P. Marynen, and A. Hagemeijer. 2005. A new recurrent inversion, inv(7)(p15q34), leads to transcriptional activation of HOXA10 and HOXA11 in a subset of T-cell acute lymphoblastic leukemias. *Leukemia* 19:358-366.

Springuel, L., T. Hornakova, E. Losdyck, F. Lambert, E. Leroy, S.N. Constantinescu, E. Flex, M. Tartaglia, L. Knoops, and J.C. Renauld. 2014. Cooperating JAK1 and JAK3 mutants increase resistance to JAK inhibitors. *Blood* 124:3924-3931.

Steger, J., E. Fuller, M.P. Garcia-Cuellar, K. Hetzner, and R.K. Slany. 2015. Insulin-like growth factor 1 is a direct HOXA9 target important for hematopoietic transformation. *Leukemia* 29:901-908.

Su, X., H. Drabkin, E. Clappier, E. Morgado, M. Busson, S. Romana, J. Soulier, R. Berger, O.A. Bernard, and C. Lavau. 2006a. Transforming potential of the T-cell acute lymphoblastic leukemia-associated homeobox genes HOXA13, TLX1, and TLX3. *Gene Chromosome Canc* 45:846-855.

Su, X.Y., M. Busson, V. Della Valle, P. Ballerini, N. Dastugue, P. Talmant, A.A. Ferrando, D. Baudry-Bluteau, S. Romana, R. Berger, and O.A. Bernard. 2004. Various types of rearrangements target TLX3 locus in T-cell acute lymphoblastic leukemia. *Gene Chromosome Canc* 41:243-249.

Su, X.Y., V. Della-Valle, I. Andre-Schmutz, C. Lemercier, I. Radford-Weiss, P. Ballerini, M. Lessard, M. Lafage-Pochitaloff, F. Mugneret, R. Berger, S.P. Romana, O.A. Bernard, and V. Penard-Lacronique. 2006b. HOX11L2/TLX3 is transcriptionally activated through T-cell regulatory elements downstream of BCL11B as a result of the t(5;14)(q35;q32). *Blood* 108:4198-4201.

Taghon, T., K. Thys, M. De Smedt, F. Weerkamp, F.J. Staal, J. Plum, and G. Leclercq. 2003. Homeobox gene expression profile in human hematopoietic multipotent stem cells and T-cell progenitors: implications for human T-cell development. *Leukemia* 17:1157-1163.

Tal, N., C. Shochat, I. Geron, D. Bercovich, and S. Izraeli. 2014. Interleukin 7 and thymic stromal lymphopoietin: from immunity to leukemia. *Cell Mol Life Sci* 71:365-378.

Tasian, S.K., M.Y. Doral, M.J. Borowitz, B.L. Wood, I.M. Chen, R.C. Harvey, J.M. Gastier-Foster, C.L. Willman, S.P. Hunger, C.G. Mullighan, and M.L. Loh. 2012. Aberrant STAT5 and PI3K/mTOR pathway signaling occurs in human CRLF2-rearranged B-precursor acute lymphoblastic leukemia. *Blood* 120:833-842.

Teachey, D.T., C. Sheen, J. Hall, T. Ryan, V.I. Brown, J. Fish, G.S. Reid, A.E. Seif, R. Norris, Y.J. Chang, M. Carroll, and S.A. Grupp. 2008. mTOR inhibitors are synergistic with methotrexate: an effective combination to treat acute lymphoblastic leukemia. *Blood* 112:2020-2023.

Todd MA1, Ivanochko D3,4, Picketts DJ5,6,7. 2015. PHF6 Degrees of Separation: The Multifaceted Roles of a Chromatin Adaptor Protein. *Genes (Basel)*

Todd, M.A., and D.J. Picketts. 2012. PHF6 interacts with the nucleosome remodeling and deacetylation (NuRD) complex. *J Proteome Res* 11:4326-4337.

Tosello, V., and A.A. Ferrando. 2013. The NOTCH signaling pathway: role in the pathogenesis of T-cell acute lymphoblastic leukemia and implication for therapy. *Ther Adv Hematol* 4:199-210.

Tosello, V., M.R. Mansour, K. Barnes, M. Paganin, M.L. Sulis, S. Jenkinson, C.G. Allen, R.E. Gale, D.C. Linch, T. Palomero, P. Real, V. Murty, X. Yao, S.M. Richards, A. Goldstone, J. Rowe, G. Basso, P.H. Wiernik, E. Paietta, R. Pieters, M. Horstmann, J.P. Meijerink, and A.A. Ferrando. 2009. WT1 mutations in T-ALL. *Blood* 114:1038-1045.

Touw, I., K. Pouwels, T. Vanagthoven, R. Vangurp, L. Budel, H. Hoogerbrugge, R. Delwel, R. Goodwin, A. Namen, and B. Lowenberg. 1990. Interleukin-7 Is a Growth-Factor of Precursor-B and Precursor-T Acute Lymphoblastic-Leukemia. *Blood* 75:2097-2101.

Treanor, L.M., E.J. Volanakis, S. Zhou, T. Lu, C.J. Sherr, and B.P. Sorrentino. 2011. Functional interactions between Lmo2, the Arf tumor suppressor, and Notch1 in murine T-cell malignancies. *Blood* 117:5453-5462.

Treanor, L.M., S. Zhou, L. Janke, M.L. Churchman, Z. Ma, T. Lu, S.C. Chen, C.G. Mullighan, and B.P. Sorrentino. 2014. Interleukin-7 receptor mutants initiate early T cell precursor leukemia in murine thymocyte progenitors with multipotent potential. *J Exp Med* 211:701-713.

Tremblay, C.S., F.C. Brown, M. Collett, J. Saw, S.K. Chiu, S.E. Sonderegger, S.E. Lucas, R. Alserihi, N. Chau, M.L. Toribio, M.P. McCormack, M. Chircop, P.J. Robinson, S.M. Jane, and D.J. Curtis. 2016. Loss-of-function mutations of Dynamin 2 promote T-ALL by enhancing IL-7 signalling. *Leukemia*.

Tremblay, C.S., and D.J. Curtis. 2014. The clonal evolution of leukemic stem cells in T-cell acute lymphoblastic leukemia. *Current opinion in hematology* 21:320-325.

Uddin, S., E.N. Fish, D. Sher, C. Gardziola, O.R. Colamonici, M. Kellum, P.M. Pitha, M.F. White, and L.C. Platanias. 1997. The IRS-pathway operates distinctively from the Stat-pathway in hematopoietic cells and transduces common and distinct signals during engagement of the insulin or interferon-alpha receptors. *Blood* 90:2574-2582.

Uehira, M., H. Matsuda, I. Hikita, T. Sakata, H. Fujiwara, and H. Nishimoto. 1993. The development of dermatitis infiltrated by gamma delta T cells in IL-7 transgenic mice. *Int Immunol* 5:1619-1627.

van Bodegom, D., J. Zhong, N. Kopp, C. Dutta, M.S. Kim, L. Bird, O. Weigert, J. Tyner, A. Pandey, A. Yoda, and D.M. Weinstock. 2012. Differences in signaling through the B-cell leukemia oncoprotein CRLF2 in response to TSLP and through mutant JAK2. *Blood* 120:2853-2863.

Van de Wiele, C.J.V., J.H. Marino, B.W. Murray, S.S. Vo, M.E. Whetsell, and T.K. Teague. 2004. Thymocytes between the beta-selection and positive selection checkpoints are nonresponsive to IL-7 as assessed by STAT-5 phosphorylation. *Journal of Immunology* 172:4235-4244.

van der Plas, D.C., F. Smiers, K. Pouwels, L.H. Hoefsloot, B. Lowenberg, and I.P. Touw. 1996. Interleukin-7 signaling in human B cell precursor acute lymphoblastic leukemia cells and murine BAF3 cells involves activation of STAT1 and STAT5 mediated via the interleukin-7 receptor alpha chain. *Leukemia* 10:1317-1325.

van der Veer, A., E. Waanders, R. Pieters, M.E. Willemse, S.V. Van Reijmersdal, L.J. Russell, C.J. Harrison, W.E. Evans, V.H.J. van der Velden, P.M. Hoogerbrugge, F. Van Leeuwen, G. Escherich, M.A. Horstmann, L.M. Khankahdani, D. Rizopoulos, H.A. De Groot-Kruseman, E. Sonneveld, R.P. Kuiper, and M.L. Den Boer. 2013. Independent prognostic value of BCR-ABL1-like signature and IKZF1 deletion, but not high CRLF2 expression, in children with B-cell precursor ALL. *Blood* 122:2622-2629.

Van Vlierberghe, P., I. Homminga, L. Zuurbier, J. Gladdines-Buijs, E.R. van Wering, M. Horstmann, H.B. Beverloo, R. Pieters, and J.P. Meijerink. 2008a. Cooperative genetic defects in TLX3 rearranged pediatric T-ALL. *Leukemia* 22:762-770.

Van Vlierberghe, P., T. Palomero, H. Khiabanian, J. Van der Meulen, M. Castillo, N. Van Roy, B. De Moerloose, J. Philippe, S. Gonzalez-Garcia, M.L. Toribio, T. Taghon, L. Zuurbier, B. Cauwelier, C.J. Harrison, C. Schwab, M. Pisecker, S. Strehl, A.W. Langerak, J. Gecz, E. Sonneveld, R. Pieters, E. Paietta, J.M. Rowe, P.H. Wiernik, Y. Benoit, J. Soulier, B. Poppe, X.P. Yao, C. Cordon-Cardo, J. Meijerink, R. Rabadan, F. Speleman, and A. Ferrando. 2010. PHF6 mutations in T-cell acute lymphoblastic leukemia. *Nature genetics* 42:338-U395.

Van Vlierberghe, P., M. van Grotel, J. Tchinda, C. Lee, H.B. Beverloo, P.J. van der Spek, A. Stubbs, J. Cools, K. Nagata, M. Fornerod, J. Buijs-Gladdines, M. Horstmann, E.R. van Wering, J. Soulier, R. Pieters, and J.P. Meijerink. 2008b. The recurrent SET-NUP214 fusion as a new HOXA activation mechanism in pediatric T-cell acute lymphoblastic leukemia. *Blood* 111:4668-4680.

Venkitaraman, A.R., and R.J. Cowling. 1994. Interleukin-7 induces the association of phosphatidylinositol 3-kinase with the alpha chain of the interleukin-7 receptor. *European journal of immunology* 24:2168-2174.

Vicente, C., C. Schwab, M. Broux, E. Geerdens, S. Degryse, S. Demeyer, I. Lahortiga, A. Elliott, L. Chilton, R. La Starza, C. Mecucci, P. Vandenberghe, N. Goulden, A. Vora, A.V. Moorman, J. Soulier, C.J. Harrison, E. Clappier, and J. Cools. 2015. Targeted sequencing identifies associations between IL7R-JAK mutations and epigenetic modulators in T-cell acute lymphoblastic leukemia. *Haematologica* 100:1301-1310.

von Freeden-Jeffry, U., P. Vieira, L.A. Lucian, T. McNeil, S.E. Burdach, and R. Murray. 1995. Lymphopenia in interleukin (IL)-7 gene-deleted mice identifies IL-7 as a nonredundant cytokine. *J Exp Med* 181:1519-1526.

Wang, Q., H. Qiu, H. Jiang, L. Wu, S. Dong, J. Pan, W. Wang, N. Ping, J. Xia, A. Sun, D. Wu, Y. Xue, H.G. Drexler, R.A. Macleod, and S. Chen. 2011a. Mutations of PHF6 are associated with mutations of NOTCH1, JAK1 and rearrangement of

SET-NUP214 in T-cell acute lymphoblastic leukemia. *Haematologica* 96:1808-1814.

Wang, X., J. Zeng, M. Shi, S. Zhao, W. Bai, W. Cao, Z. Tu, Z. Huang, and W. Feng. 2011b. Targeted blockage of signal transducer and activator of transcription 5 signaling pathway with decoy oligodeoxynucleotides suppresses leukemic K562 cell growth. *DNA Cell Biol* 30:71-78.

Wang, Y.C., W. Fiskus, D.G. Chong, K.M. Buckley, K. Natarajan, R. Rao, A. Joshi, R. Balusu, S. Koul, J.G. Chen, A. Savoie, C. Ustun, A.P. Jillella, P. Atadja, R.L. Levine, and K.N. Bhalla. 2009. Cotreatment with panobinostat and JAK2 inhibitor TG101209 attenuates JAK2V617F levels and signaling and exerts synergistic cytotoxic effects against human myeloproliferative neoplastic cells. *Blood* 114:5024-5033.

Ward, A.F., B.S. Braun, and K.M. Shannon. 2012. Targeting oncogenic Ras signaling in hematologic malignancies. *Blood* 120:3397-3406.

Watanabe, T. 2017. Adult T-cell leukemia: molecular basis for clonal expansion and transformation of HTLV-1-infected T cells. *Blood* 129:1071-1081.

Weigert, O., A.A. Lane, L. Bird, N. Kopp, B. Chapuy, D. van Bodegom, A.V. Toms, S. Marubayashi, A.L. Christie, M. McKeown, R.M. Paranal, J.E. Bradner, A. Yoda, C. Gaul, E. Vangrevelinghe, V. Romanet, M. Murakami, R. Tiedt, N. Ebel, E. Evrot, A. De Pover, C.H. Regnier, D. Erdmann, F. Hofmann, M.J. Eck, S.E. Sallan, R.L. Levine, A.L. Kung, F. Baffert, T. Radimerski, and D.M. Weinstock. 2012. Genetic resistance to JAK2 enzymatic inhibitors is overcome by HSP90 inhibition. *J Exp Med* 209:259-273.

Weng, A.P., A.A. Ferrando, W. Lee, J.P.t. Morris, L.B. Silverman, C. Sanchez-Irizarry, S.C. Blacklow, A.T. Look, and J.C. Aster. 2004. Activating mutations of NOTCH1 in human T cell acute lymphoblastic leukemia. *Science* 306:269-271.

Wu, L., J. Li, H.L. Xu, B. Xu, X.H. Tong, J. Kwak-Kim, and Y.S. Liu. 2016. IL-7/IL-7R signaling pathway might play a role in recurrent pregnancy losses by increasing inflammatory Th17 cells and decreasing Treg cells. *Am J Reprod Immunol*

Yano, M., T. Imamura, D. Asai, N. Kiyokawa, K. Nakabayashi, K. Matsumoto, T. Deguchi, Y. Hashii, Y.K. Honda, D. Hasegawa, Y. Sasahara, M. Ishii, Y. Kosaka, K. Kato, M. Shima, H. Hori, K. Yumura-Yagi, J. Hara, M. Oda, K. Horibe, H. Ichikawa, and A. Sato. 2015. Identification of novel kinase fusion transcripts in paediatric B cell precursor acute lymphoblastic leukaemia with IKZF1 deletion. *Br J Haematol*.

Yano, M., T. Imamura, D. Asai, A. Moriya-Saito, S. Suenobu, D. Hasegawa, T. Deguchi, Y. Hashii, H. Kawasaki, H. Hori, Y. Kosaka, K. Kato, K. Horibe, K. Yumura-Yagi, J. Hara, K. Matsumoto, N. Kiyokawa, M. Oda, A. Sato, and Jacls. 2014. An Overall Characterization of Pediatric Acute Lymphoblastic Leukemia with CRLF2 Overexpression. *Gene Chromosome Canc* 53:815-823.

Yoda, A., Y. Yoda, S. Chiaretti, M. Bar-Natan, K. Mani, S.J. Rodig, N. West, Y. Xiao, J.R. Brown, C. Mitsiades, M. Sattler, J.L. Kutok, D.J. DeAngelo, M. Wadleigh, A. Piciocchi, P. Dal Cin, J.E. Bradner, J.D. Griffin, K.C. Anderson, R.M. Stone, J. Ritz, R. Foa, J.C. Aster, D.A. Frank, and D.M. Weinstock. 2010. Functional screening identifies CRLF2 in precursor B-cell acute lymphoblastic leukemia. *Proc Natl Acad Sci U S A* 107:252-257.

Yokoyama, K., N. Yokoyama, K. Izawa, A. Kotani, A. Harashima, K. Hozumi, and A. Tojo. 2013. In vivo leukemogenic potential of an interleukin 7 receptor alpha chain mutant in hematopoietic stem and progenitor cells. *Blood* 122:4259-4263.

Yoo, N.J., Y.R. Kim, and S.H. Lee. 2012. Somatic mutation of PHF6 gene in T-cell acute lymphoblatic leukemia, acute myelogenous leukemia and hepatocellular carcinoma. *Acta Oncol* 51:107-111.

You, D., J. Xin, A. Volk, W. Wei, R. Schmidt, G. Scurti, S. Nand, E.K. Breuer, P.C. Kuo, P. Breslin, A.R. Kini, M.I. Nishimura, N.J. Zeleznik-Le, and J. Zhang. 2015. FAK mediates a compensatory survival signal parallel to PI3K-AKT in PTEN-null T-ALL cells. *Cell Rep* 10:2055-2068.

Yu, Q., B. Erman, A. Bhandoola, S.O. Sharrow, and A. Singer. 2003. In vitro evidence that cytokine receptor signals are required for differentiation of double positive thymocytes into functionally mature CD8(+) T cells. *Journal of Experimental Medicine* 197:475-487.

Yuan, J.S., J.B. Tan, I. Visan, I.R. Matei, P. Urbanellis, K. Xu, J.S. Danska, S.E. Egan, and C.J. Guidos. 2011. Lunatic Fringe prolongs Delta/Notch-induced self-renewal of committed alphabeta T-cell progenitors. *Blood* 117:1184-1195.

Zenatti, P.P., D. Ribeiro, W. Li, L. Zuurbier, M.C. Silva, M. Paganin, J. Tritapoe, J.A. Hixon, A.B. Silveira, B.A. Cardoso, L.M. Sarmento, N. Correia, M.L. Toribio, J. Kobarg, M. Horstmann, R. Pieters, S.R. Brandalise, A.A. Ferrando, J.P. Meijerink, S.K. Durum, J.A. Yunes, and J.T. Barata. 2011. Oncogenic IL7R gain-of-function mutations in childhood T-cell acute lymphoblastic leukemia. *Nature genetics* 43:932-939.

Zhang, J., L. Ding, L. Holmfeldt, G. Wu, S.L. Heatley, D. Payne-Turner, J. Easton, X. Chen, J. Wang, M. Rusch, C. Lu, S.C. Chen, L. Wei, J.R. Collins-Underwood, J. Ma, K.G. Roberts, S.B. Pounds, A. Ulyanov, J. Becksfort, P. Gupta, R. Huether, R.W. Kriwacki, M. Parker, D.J. McGoldrick, D. Zhao, D. Alford, S. Espy, K.C. Bobba, G. Song, D. Pei, C. Cheng, S. Roberts, M.I. Barbato, D. Campana, E. Coustan-Smith, S.A. Shurtleff, S.C. Raimondi, M. Kleppe, J. Cools, K.A. Shimano, M.L. Hermiston, S. Doulatov, K. Eppert, E. Laurenti, F. Notta, J.E. Dick, G. Basso, S.P. Hunger, M.L. Loh, M. Devidas, B. Wood, S. Winter, K.P. Dunsmore, R.S. Fulton, L.L. Fulton, X. Hong, C.C. Harris, D.J. Dooling, K. Ochoa, K.J. Johnson, J.C. Obenauer, W.E. Evans, C.H. Pui, C.W. Naeve, T.J. Ley, E.R. Mardis, R.K. Wilson, J.R. Downing, and C.G. Mullighan. 2012. The genetic basis of early T-cell precursor acute lymphoblastic leukaemia. *Nature* 481:157-163.

Zhang, Q., D.M. Hossain, S. Nechaev, A. Kozlowska, W. Zhang, Y. Liu, C.M. Kowolik, P. Swiderski, J.J. Rossi, S. Forman, S. Pal, R. Bhatia, A. Raubitschek, H. Yu, and M. Kortylewski. 2013. TLR9-mediated siRNA delivery for targeting of normal and malignant human hematopoietic cells in vivo. *Blood* 121:1304-1315.

Ziegler, S.F., and D. Artis. 2010. Sensing the outside world: TSLP regulates barrier immunity. *Nat Immunol* 11:289-293.